Reconstructing past vegetation and modern human foraging strategies on the south coast of South Africa

Irene Esteban Alamá

UNIVERSITAT DE BARCELONA

RECONSTRUCTING PAST VEGETATION AND MODERN HUMAN FORAGING STRATEGIES ON THE SOUTH COAST OF SOUTH AFRICA

PhD dissertation by

IRENE ESTEBAN ALAMÁ

For the degree of
Doctor of Philosophy by the University of Barcelona

Doctoral Program "Societat i Cultura"

Specialization in Prehistory

Supervised by

Dr. Rosa María Albert Cristóbal
Catalan Institution for Research and Advanced Studies (ICREA)
Departament de Història i Arqueologia, Universitat de Barcelona

Dr. Dan Cabanes i Cruelles
Department of Anthropology, Schools of Arts and Sciences
Rutgers University

Barcelona, 2016

RECONSTRUCTING PAST VEGETATION AND MODERN HUMAN FORAGING STRATEGIES ON THE SOUTH COAST OF SOUTH AFRICA

PhD dissertation by

Irene Esteban Alamá

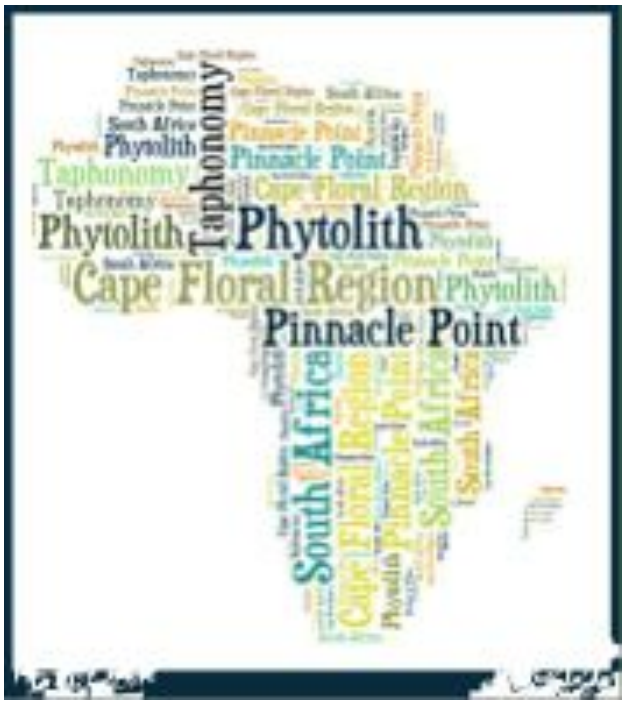

The PhD candidate

Irene Esteban Alamá

The supervisors

Rosa María Albert Dan Cabanes

Per a mons pares, Paqui i Ramón
la meua Nani i el Solet

“And those who were seen dancing were thought to be insane by those who could not hear the music.”

— Friedrich Nietzsche

Acknowledgements

Son muchas las personas a las que he de agradecer el haber estado a mi lado a lo largo de los cinco años de doctorado. He de decir que estos cinco años en Barcelona/Badalona, volviendo a casa, viajando, asistiendo a congresos, excavaciones, han sido simplemente maravisollos y todo gracias a:

Primero que todo, quiero agradecer a mis directores de tesis, la Dra. Rosa María Albert y el Dr. Dan Cabanes, por todo el apoyo y ayuda dada a lo largo de estos años. Varios estudiantes que he conocido a lo largo de estos años siempre me decían, "que suerte, tienes a los mejores", y así es. A Rosa le agradezco el haber confiado en mí para llevar a cabo la tesis doctoral en el proyecto de Mossel Bay. Durante todos estos años son muchas las cosas que hemos pasado y le agradezco toda la ayuda prestada, las largas correcciones, los consejos, etc. En suma, por todo lo que me ha enseñado, ya que gracias a ello hasta aquí he llegado.

I would particularly like to thank Prof. Curtis W. Marean, from Arizona State University, principal investigator of the project my thesis focus on, for his support and good advices when I needed some, for the many important suggestions and comments about my project and because he was always available when I needed him. I also thank Dr. Erich Fisher for his help and support along these years and for making lot of the figures of this thesis. To all the SACP4 team and to Jake, Tina, Kerstin, Lwando, Dicks, James and Ben, for the good time we have spent together. I thank to Jan Vlok for helping us in the collection of the modern plant and surface soil reference collections used in this thesis, those days in the field were so much fun. I also thanks to Dr Panagiotis Karkanas for his always-useful comments on my work in early phases.

Agradecer al catedrático Valentín Villaderde, de la Universitat de València, porque gracias a él descubrí, cuando todavía era una estudiante de carrera, que es la arqueología y la prehistoria con mi participación en la campaña del 2007 en el Abrigo de la Quebrada. Le agradezco además todo el apoyo y ayuda dada durante estos años. A Aleix, Cristina y Didac porque han sido grandes compañeros de excavaciones. Espero que podamos seguir trabajando juntos en nuestra futura carrera como investigadores.

The AESOP Project ("Erasmus Mundus Programme, Action 2 – STRABD 1, Lot 17, South Africa") let me the opportunity to conduct a doctoral mobility stay at the Evolutionary Studies Institute at the University of the Witwatersrand, Johannesburg. This scholarship has been a great support for the last period of my doctorate. Thanks to financial support of this scholarship I was able to only focus only on my thesis work and this was a significant advance in my research. I would like to thank all the people from the Evolutionary Studies Institute, who made my stay just amazing. Special mention deserve Marine, Gary, Kuda, May, Alice, Fernando, Julien, Paloma, Katja, Ely, Lea, Cory, Kathe, Merryl, Browyn, Tandi, Tammy, Jerome, Mike, Jennifer and Meriska. I would like to thank Prof. Marion Bamford for hosting me at the ESI, for all her support and help, and because she always gave me a good advice when I needed it.

I would also like to thank Katerina Kotina and Aleksei Oskolski from the Department of Botany of the University of Johannesburg for their help on the analysis of restio and wood anatomy. They did not know me at all, and they opened their lab to me, and didn't hesitate to offer me their good counsel.

A molts professors i investigadors del antic Departament de Prehistòria, Història Antiga i Arqueologia, i en especial a Mercé Bergada, Inés Domingo, Santiago Riera, Miguel Angel Cau, Alessandra Pecci, Evanthia Tsantini i Francesc Tusset, per el recolzament donant durant els meus anys al departament.

A mis compañeras de equipo, a Mónica, Ágata, Laia y Marta, porque siempre me han echado un cable cuando lo he necesitado, por todos los consejos y en suma, por todos los buenos momentos, porque no he podido tener mejores compañeras. A muchos estudiantes del departamento, con los que he pasado mucho de mi tiempo y en especial a Mar, Juanjo y Frans. A mis compañeros y amigos del Espai de Recerca ("la salita"), Andreas, Gustavo, José y Ana por todas las horas de trabajo juntos y todos los buenos momentos que hemos vivido.

Als meus companys de pis d'Heures, Maria, Xisca i Toni, perquè han segut la meua família a Barcelona, res haguera sigut igual sense ells.

A tots els meus amics. Als meus amics de la Universitat de València, i en especial a Sonia, Francesca, Sol, Ricardo, Tonio i Sandra, perquè estic feliç de poder dir que després de tants anys encara som amics, molt bons amics; perquè les paelles

nadalenques i estiuenques mai s'acaben. A tota la meua quadrilla de Sueca, i en especial a Nerea, Maria, Davit, Rubi, Cris i Olivia, perquè són els millors. A los marenyeros, por todos los años de amistad, por todos los buenos momentos, porque los veranos de mi vida no hubieran sido igual sin ellos. A todos mis amigos de Paterna, y a Gema, Javi y Leticia, porque siempre han tenido una sonrisa para mí, por su alegría al verme aún después de mis largas desapariciones. Als amics de Badalona, Sonia, Sergio y Aura, perquè han fet que els anys viscuts a Badalona siguen genials, per moltes més birres junts. Y la salsa, y a todos los salseros y salseras, als de Badalona and to those from Joburg.

A Albert, per tots els anys que hem estat junts, perquè sempre m'has volgut i m'has recolçat en allò que he fet. Perquè tot i que la vida ens ha separat al final del meu doctorat, gran part d'aquesta tesi ha sigut gràcies a tu.

A mi Fernanda, porque la conocí durante mi año de Máster, cuando nos juntábamos para nuestro cigarro y café con leche, y que desde entonces se convirtió en mi gran compañera y amiga, mi gran apoyo en Barcelona.

A Mónica, porque somos compañeras de equipo, de investigación y amigas. Porque la vida ha hecho que esté pasando los últimos meses de doctorado compartiendo piso contigo. Porque no he podido tener más suerte. Porque estos duros meses de escritura no hubieran sido lo mismo sin ti #gorditasfelices# #comonosgustaelvermut#

I a tota la meua família. Als mis tios, Juanvi, Amparo, Rosa y Juan; a mis primos, Laura, Juanra –a los bollitos y a Marta-, Juan y Borja; als meus yayos, Ramón y Ana, que mai arribaren a saber el que acabaria fent, i als meus abuelitos, Juan y Paquita perquè sempre m'han animat sense entendre molt be el que feia. A la meua Nani, que se'n va anar fa molt de temps, però que sempre la recordaré. Al meu Solet, perquè el trobí sense espera-m'ho, per totes les siestes que s'ha pegat en mi mentre jo escrivia, i per els seus sirocos, que m'ha tret un riure quan estava decaiguda.

Esta tesis esta dedicada a mis padres, Ramón y Paqui, porque su apoyo lo ha sido todo en mi vida y en mi tesis. Porque no les puedo querer más.

Badalona, 7 de Septiembre de 2016

Abstract

South Africa continues to receive substantial attention from scholars researching modern human origins. The importance of this region lies in the many caves and rock shelters containing well preserved evidence of human activity, cultural material complexity and a growing number of early modern human fossils dating to the Middle Stone Age (MSA). South Africa also hosts the world's smallest floral kingdom, now called the Greater Cape Floristic Region (GCFR), with high species richness and endemism. We use phytoliths –amorphous silica particles that formed in epidermal cells of plants–in order to study the evolution of plant exploitation strategies by first modern humans and also to reconstruct the paleoenvironmental conditions on the south coast of South Africa. A second main aim is to understand the response of GCFR environments to glacial-interglacial cycles and rainfall shifts and its implication with the evolution of first modern humans that inhabited the south coast of South Africa during marine isotope stages (MIS) 5 to 3.

In paleoanthropological research, improving our capacity to reconstruct past climatic and environmental conditions can help us to shed light on survival strategies of hunter-gatherers. To do this, one must use actualistic studies of modern assemblages from extant habitats to develop analogies for the past and improve paleoenvironmental reconstructions. Accordingly, this thesis contemplates fossil and modern material: i) archaeological sediment samples from Pinnacle Point 5-6 site (PP5-6) located on the south coast of South Africa; ii) modern plants from the GCFR and susceptible to have been exploited by first modern humans inhabiting the south coast; iii) modern surface soil samples from different GCFR vegetation types of the south coast of South Africa.

The modern plant reference collection is the first quantitative and morphological study conducted with different plant types and plant parts (wood and leaves of trees and shrubs, leaves, bulb scale leaves and edible part of the bulb of geophytes, restios–Restionaceae and grasses–Poaceae) from the GCFR on the south coast of South Africa. We observed that grasses are the highest phytolith producers among plant types. We reported through thin sections and SEM that the characteristic restio phytoliths belong to and characterize the Restionaceae family and have been detected in the parenchyma sheath of the culms. Geophytes did not produce diagnostic phytolith morphotypes that

can be used for taxonomic identification what might make difficult their identification in the fossil record.

The results of the modern surface soil samples showed that phytolith concentration relates mostly to vegetation types and the dominant vegetation rather than to the type of soils. More abundant phytoliths from Restionaceae and woody/shrubby vegetation are also noted from fynbos vegetation and grass phytoliths are a recurrent component in all the vegetation types in spite of being a minor component in the modern vegetation. The grass silica short cells (GSSCs) from these plants, however, suggest a mix of C_3 and C_4 grasses in most of the vegetation types with a major presence of the rondels ascribed to C_3 grasses. The exceptions are riparian, coastal thicket and coastal forest vegetation, which are characterized by the dominance of C_4 grass phytoliths.

The study of the modern plants and soils from the surrounding areas of Pinnacle Point were used as proxy for the reconstruction of past human foraging strategies and paleoenvironmental reconstruction through the phytolith record from PP5-6 site. The study of the archaeological sediment samples from this site indicated a wide range of plants used by first modern humans inhabiting the area including wood, leaves and fruits of trees and shrubs, grasses and restios. We reported for the first time the presence of restios in the South African archaeological record through the study of phytoliths. Changes in the plant and mineralogical component from MIS5 to 4 have been interpreted as the result of changes in the plant exploitation strategies. These changes are also associated to major changes observed in the cultural material that took place over MIS5 to 4 and that have also been link to climate shifts. From an environmental perspective, the combined study of modern plants and soils in comparison to the archaeological phytolith assemblage have been interpreted as indicative of the presence of a fynbos-thicket mosaic vegetation where C_3 grasses dominated although C_4 grasses were also well represented and this is also supported by previous archives recorded from the south coast.

Table of Contents

List of Figures

polyhedral from the leaves of *Vepris undulata*, h-i) EGM polyhedral from the leaves of *Tarchonanthus camphoratus*, j-k) EGM polyhedral from the leaves of *Grewia occidentalis*, l-m) EGM sinuate from the leaves of *Rhoicissus digitata*, n-o) EGM polyhedral from the leaves of *Pterocelastrus tricuspidatus*. Scale bar represents 10mm.

Figure 16. Box-plots showing those phytolith morphotypes that more abounded in the thirteen species of geophyte in the leaves, the bulb scale leaves and the edible part of the bulb (bulb). The sample mean (grey line), standard error ± (box), standard deviation (whiskers) and outliers (green dots) are given for each phytolith morphotype.

Figure 17. Microphotographs of two restio phytoliths identified in Restionaceae modern plants. Phytoliths are shown from three different points of view by its rotation on the slide. Pictures taken at 400x. a-c) spheroid showing protuberances, with granulate/verrucate decoration (*Thamnochortus insignis*); d-f) spheroids showing spiraling decoration with a double ring on the edges (*Elegia juncea*). Scale bar represents 10 mm.

Figure 18. Box-plots showing those phytolith morphotypes that more abounded in the four Restionaceae specimens. The sample mean (grey line), standard error ± (box), standard deviation (whiskers) and outliers (green dots) are given for each phytolith morphotype.

Figure 19. Thin section (a-d) and SEM (e-h) images of the X section of culms of *Thamnochortus insignis*.

Figure 20. Box-plots showing those phytolith morphotypes that more abounded in the seven C_3 species of Poaceae plants. The sample mean (grey line), standard error ± (box), standard deviation (whiskers) and outliers (green dots) are given for each phytolith morphotype.

Figure 21. Micrographs of common non-GSSCs (A) and GSSCs (B) morphotypes observed in C_3 grasses. Pictures taken at 400x. See Table 1 for detailed descriptions of the phytolith morphologies. A: a) elongate morphologies with sinuate decorated margins from *Stipagrostis zeyheri* (Aristidoideae); b) elongates

morphologies with echinate decorated margins from *Ehrharta bulbosa* (Ehrhartoideae); c) hair cell traichomes from *Ehrharta bulbosa* (Ehrhartoideae); d) papillae from *Festuca scabra* (Pooideae). B: a-c) GSSC bilobate tabular angulate lobes; d) GSSC rondel conical from *Stipa dregeana* (Pooideae); e) GSSC rondel conical with wavy top from *Stipagrostis zeyheri* (Aristidoideae); f) GSSC rondel keeled from *Tribolium uniolae* (Danthonioideae); g) GSSC bilobates with flattened-rounded lobes from *Pentachistis colorata* (Danthonioideae). Scale bar represents 10 mm.

Figure 22. Micrographs of common non-GSSCs (A) and GSSCs (B) morphotypes observed in C_4 grasses. Pictures taken at 400x. See Table 1 for detailed descriptions of the phytolith morphologies. A: a-b) elongate morphologies with sinuate decorated margins from *Setaria sphacelata* and *Tristachya leucothrix* (Panicoideae); c) Bulliform cell from *Stenotaphrum secundatum* (Panicoideae). B: a-b) GSSC bilobate tabular flattened lobes from *Panicum deustum* and *Heteropogon contortus* (Panicoideae); c-d) GSSC flattened-rounded lobes from *Stenotaphrum secundatum* (Panicoideae); e) GSSC tabular round lobes from *Setaria sphacelata* (Panicoideae); f) GSSC saddle from *Eragrostis curvula* (Chloridoideae); g-h) GSSC bilobate trapeziform with notched lobes from Panicum deustum and *Heteropogon contortus* (Panicoideae). Scale bar represents 10 mm.

Figure 23. Box-plots showing those phytolith morphotypes that more abounded in the eight C_4 grass species of Poaceae plants. The sample mean (grey line), standard error ± (box), standard deviation (whiskers) and outliers (green dots) are given for each phytolith morphotype.

Figure 24. Microphotographs of phytoliths identified in samples analyzed. Pictures taken at 400. a) prickle (RV10-04), b) bulliform cell (GF10-10), c) elongate with echinate margin (RV11-58), d-f) rondel GSSCs (SF11-42, SF11-43 and RV11-15), g-h) bilobates GSSCs (GF10-14, CF10-13), i) saddle GSSCs (CT06-05), j) epidermal ground mass polyhedral (STV11- 01), k) eudicot hair cell (SF11-37), l) sclerenchyma (RP11-59). Scale bar represents 10 mm (retrieved from Esteban et al., in press).

Figure 25. Ternary plot showing the grass silica short cells, grouped by the three fundamental categories: rondels, lobates and saddles, distribution among vegetation types. Rondel category includes also the oblong morphotypes. Legend: CT, coastal thicket; GF, grassy fynbos; LF, limestone fynbos; RP, riparian; RV, renosterveld; SF, sand fynbos; StT, subtropical thicket; STV, strandveld (retrieved from Esteban et al., in press).

Figure 26. Microphotographs of two restio phytoliths identified in modern soils. Phytoliths are shown from three different points of view by its rotation on the slide. Pictures taken at 400x. a-c) large spheroid showing protuberances, with granulate decoration (LF11-68); d-f) spheroids showing spiraling decoration (LF11- 85). Scale bar represents 10 mm (retrieved from Esteban et al., in press).

Figure 27. Box-plots showing the phytolith indices values among vegetation types. a) D/Pº index [∑(psilate and rugulate spheroids)/∑grass silica short cells] and the standard deviation among the different vegetation types; b) Fy index [∑(psilate and rugulate spheroids and restio phytoliths)/grass silica short cells] and the standard deviation among the different vegetation types; c) Iph index [GSSC saddles/∑(GSSC saddles and lobates)]; d) Ic index [GSSC rondels and oblongs/∑(GSSC rondels, lobates and saddles)]. The mean values (mid- line), standard error ± (box) and standard deviation (whiskers) are given for the four indices. Legend: LF, limestone fynbos; SF, sand fynbos; GF, grassy fynbos; RV, renosterveld; StT, subtropical thicket; CT, coastal thicket; STV, strandveld; RP, riparian. Different letters indicate means that are significantly different based on a Kruskal-Wallis test (retrieved from Esteban et al., in press).

Figure 28. Box-plots of the nine phytolith morphotypes pointed out by ANOVA and a post hoc Tukey Honest Significant Differences (HSD) as statistically significant different among vegetation types. The mean values (mid-line), standard error ± (box) and standard deviation (whiskers) are given for the nine phytolith morphotypes. Legend: CT, coastal thicket; GF, grassy fynbos; LF, limestone fynbos; RP, riparian; RV, renosterveld; SF, sand fynbos; StT, subtropical thicket; STV, strandveld. Different letters indicate means that are significantly different based on the post hoc Tukey (HSD) test (retrieved from Esteban et al., in press).

Figure 29. Box-plots of the eight phytolith morphotypes pointed out by ANOVA and a post hoc Tukey Honest Significant Differences (HSD) as statistically significant different among vegetation biomes. The mean values (mid-line), standard error ± (box) and standard deviation (whiskers) are given for the eight phytolith morphotypes. Different letters indicate means that are significantly different based on the post hoc Tukey (HSD) test (retrieved from Esteban et al., in press).

Figure 30. Scatterplot and trendline of the phytolith concentration per gram of sediment against a) number of phytolith morphotypes; b) percentage of weathered morphotypes; c) percentage of delicate morphologies.

Figure 31. Distribution of the phytolith concentration per gram of sediment among sample types from the different StratAggs studied.

Figure 32. Representative FTIR spectra of sediment samples from different StratAggs and sample types (hearth facies). a) white layer (162466) showing clay absorption peak at 1038 cm^{-1} characteristic of burned clay; b) white layer showing clay absorption peak at 1047 cm^{-1} characteristic of clay exposed to high temperatures; c) white layer showing three calcite absorption peaks at 1420, 874 and 712 cm^{-1}.

Figure 33. Photograph of the LBSR profile showing the sample location in two hearth layers (hearth 1: 356454, 356453, 356455; hearth 2: 356456, 162781, 356457, 356458) (figure by Erich Fisher).

Figure 34. Microphotograph from a white layer from LBSR showing high presence of irregular morphologies (sample 356475). Picture taken at 400.

Figure 35. Box-plots showing the plant types and plant parts distribution for the different StratAggs at PP5-6. The mean values (mid- line), standard error ± (box) and standard deviation (whiskers) are given for each of the plant groups with the exception of those from BBCSR StratAgg since only one sample was considered for morphological interpretation.

Figure 36. Box-plots showing the phytolith indices values among StratAggs of PP5-6. D/P^o index [(psilate and rugulate spheroids)/ ∑GSSCs]; Fy index [(psilate and

Figure 40. Box-Plots showing the distribution of grass, elongate without decoration margins, eudicot leaf and wood/bark phytoliths among the different StratAggs from PP13B (Albert and Marean, 2012) and PP5-6 sites. The mean values (mid- line), standard error ± (box) and standard deviation (whiskers) are given for the four plant types.

Figure 41. Phytolith diagram for the PP5-6 sequence showing the frequencies of the different plant type identified, the distribution of the GSSCs (rondels, lobates and saddles) expressed as the percentage of the total sum and the phytolith indices. GSSC Rondels account for both Rondel and Oblong supertypes. Values below 1% are represented by circles.

List of Tables

sediment (/g sed), percentage of weathered morphotypes, diatoms and sponge spicules, FT-IR results and the D/Pº, Fy, Ic, Iph and Fs indices. WM = weathered morphotypes. Clay (b=burned), (nb=not burned), (b?= probably burnt)..

Chapter VI. Discussion

Table 7. Table 7. Phytolith concentration per gram of original plant material of grass phytoliths (bulliform cells and GSSCs) by average in the wood/bark and the leaves of eudicot plants, in geophytes (leaves, bulb scale leaves and bulbs), restios and in grasses.

List of Appendices

I. Introducción

Las plantas constituyen uno de los recursos más utilizados en las actividades cotidianas de poblaciones cazadoras-recolectoras. Entre algunos de los usos más comunes destacan el de constituir la base de la alimentación, así como fuente importante de agua (plantas con órganos de reserva de agua, también conocidos como geófitos), combustible para los fuegos (madera), elaboración de herramientas para la caza y la pesca (arcos, flechas, redes, etc.) o utensilios con fines diversos como el almacenamiento y/o transporte de alimentos, la construcción de cabañas y esterillas para dormir, elaboración de medicinas y cosméticos, etc.

Aunque tradicionalmente se ha considerado el consumo de carne como la base fundamental de la dieta en poblaciones de cazadores-recolectores, actualmente no hay duda del papel fundamental que las plantas desempeñaron. Estudios sobre sociedades cazadoras-recolectoras actuales (!Kung, Hadza y Aka Pygmy en África; aborígenes australianos y de Papua Nueva Guinea) muestran como gran parte de su dieta está basada en el consumo de vegetales (Lee, 1968; Woodburn, 1968; Gould, 1980; Dwyer y Minnegal, 1990; Hladik et al., 1993; O'Dea, 1991; Milton, 2000). En el sur de África, la dieta de poblaciones Khoi-San, que han habitado la región desde hace al menos 120,000 años, se ha basado en su mayor parte en el consumo de vegetales (Fox y Norwood Young, 1982; Parsons, 1993).

Los patrones y estrategias de subsistencia de sociedades cazadoras-recolectoras están estrechamente relacionados con la disponibilidad de los recursos naturales (animales y plantas). Es generalmente aceptado que los cambios en el clima y el ambiente desempeñaron un papel importante a lo largo de la evolución del género *Homo* y sus ancestros. Por ello, entender la relación existente entre las plantas y los humanos en la prehistoria es fundamental para comprender cómo las poblaciones del pasado evolucionaron, vivieron y prosperaron.

Así, el estudio de restos vegetales preservados en yacimientos arqueológicos es de gran importancia para mejorar nuestro conocimiento sobre aquellas plantas utilizadas por antiguos cazadores-recolectores, para así obtener información sobre las diversas estrategias de explotación de recursos vegetales. Además, el estudio de restos vegetales procedentes de yacimientos arqueológicos también puede ofrecer información sobre las condiciones climáticas y ambientales del pasado, y la relación entre el entorno y las poblaciones humanas del pasado.

El presente trabajo de tesis se centra en conocer el uso que las poblaciones de primeros humanos modernos que habitaron la zona de Pinnacle Point (Mossel Bay, Sudáfrica) durante la Edad de Piedra Media africana (MSA- Middle Stone Age) harían de los recursos vegetales disponibles (Fig. 1), así como la reconstrucción de la vegetación y el clima existente durante el Pleistoceno Medio y el Pleistoceno Final a través del estudio de fitolitos.

Los fitolitos son microrestos minerales formados en las plantas vivas y que reproducen los tejidos intra- y extra-celulares, por lo que constituyen una herramienta de gran eficacia para la identificación de plantas en registros fósiles (Piperno, 1988, 2006 y referencias en ellos citadas). Además, debido a su naturaleza inorgánica, los fitolitos son resistentes a diversos procesos postdeposicionales que otros restos vegetales en contextos arqueológicos no pueden superar, pudiendo encontrarse en contextos de varios millones de años (Wolde Gabriel et al., 2009; McInerney et al., 2011; Strömberg y McInerney, 2011).

Pinnacle Point se localiza en la costa sur de Sudáfrica, en el área comprendida entre el río Breerivier, situado al oeste de Still Bay, y Brenton Lake, en las inmediaciones de Knysna. Se trata de una zona en la que se han identificado al menos unas 50 cuevas con restos paleoantropológicos. La elección de esta zona como objeto de nuestro trabajo de investigación se debe a diversos factores:

1) Larga ocupación humana que empieza durante el Pleistoceno Medio en la cueva Pinnacle Point 13B (PP13B) hace unos 170 ka (miles de años) y acaba en el período Holoceno en el complejo Pinnacle Point Shell Midden Complex (PPSMC) hace unos 0,9 ka (Marean et al., 2007; McGrath et al., 2015).

2) Pinnacle Point preserva las evidencias más antiguas de comportamiento humano moderno como son la explotación de recursos marinos de manera continua e intensa, así como el trabajo intencionado del ocre (Marean et al., 2007; Watts, 2010).

3) Como ya se ha apuntado, los recursos vegetales constituyen un recurso alimenticio esencial para la supervivencia de sociedades cazadoras recolectoras y que ha sido la base de la dieta de la población Khoi-San en Sudáfrica (Fox y Norwood Young, 1982; Parsons, 1993).

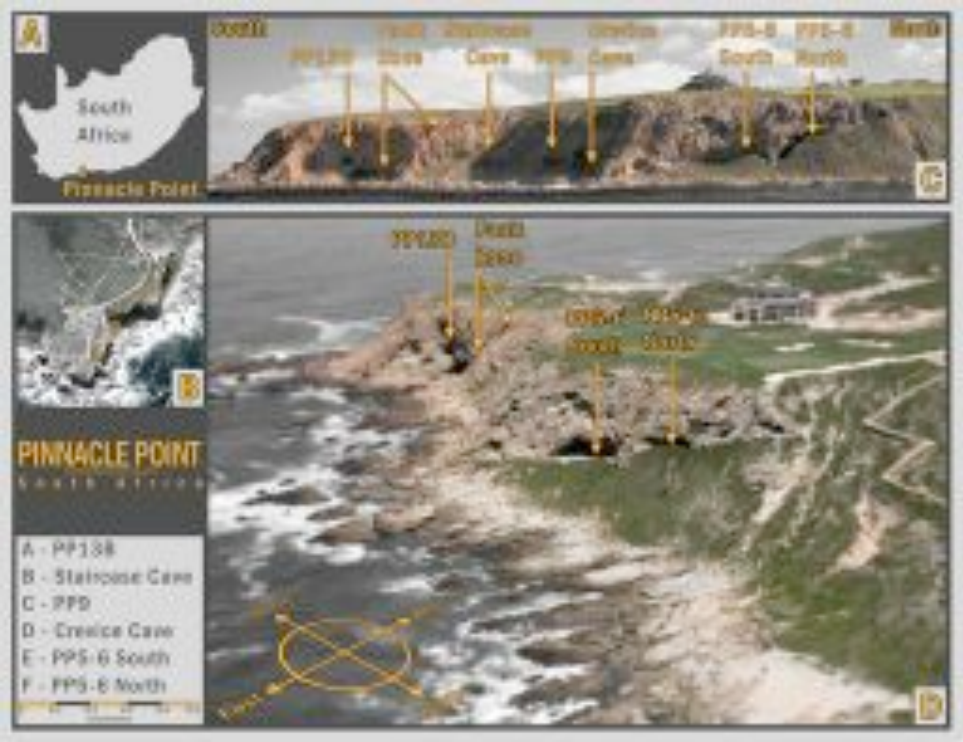

Figura 1. Localización del área de Pinnacle Point y de las principales cuevas. a) Mapa de Sudáfrica mostrando la localización de Pinnacle Point; b-d) Fotografías aéreas y panorámicas de Pinnacle Point mostrando la localización de diversas cuevas y abrigos rocosos con restos paleoantropológicos (Mapa sacado de Karkanas et al., 2015).

4) La costa sur de Sudáfrica se ubica en la Greater Cape Floristic Region (de aquí en adelante, GCFR), la cual presenta la flora extra-tropical de mayor diversidad en términos de riqueza y endemismo (Colville et al., 2014).

5) Gran variedad de tipos de vegetación presentes en nuestra área de estudio (Campbell et al., 1981) (Fig. 2), cada cual con características bióticas distintas, que ocurren dentro de lo que sería el área de explotación de recursos de cazadores-recolectores (10-15 km; Kelly, 1995; Marlowe, 2005). Esto les habría proporcionado una gran variedad de recursos vegetales entre los que encontraríamos una gran variedad de plantas comestibles (frutos, geófitos) (Marean et al., 2014; De Vynck et al., 2015).

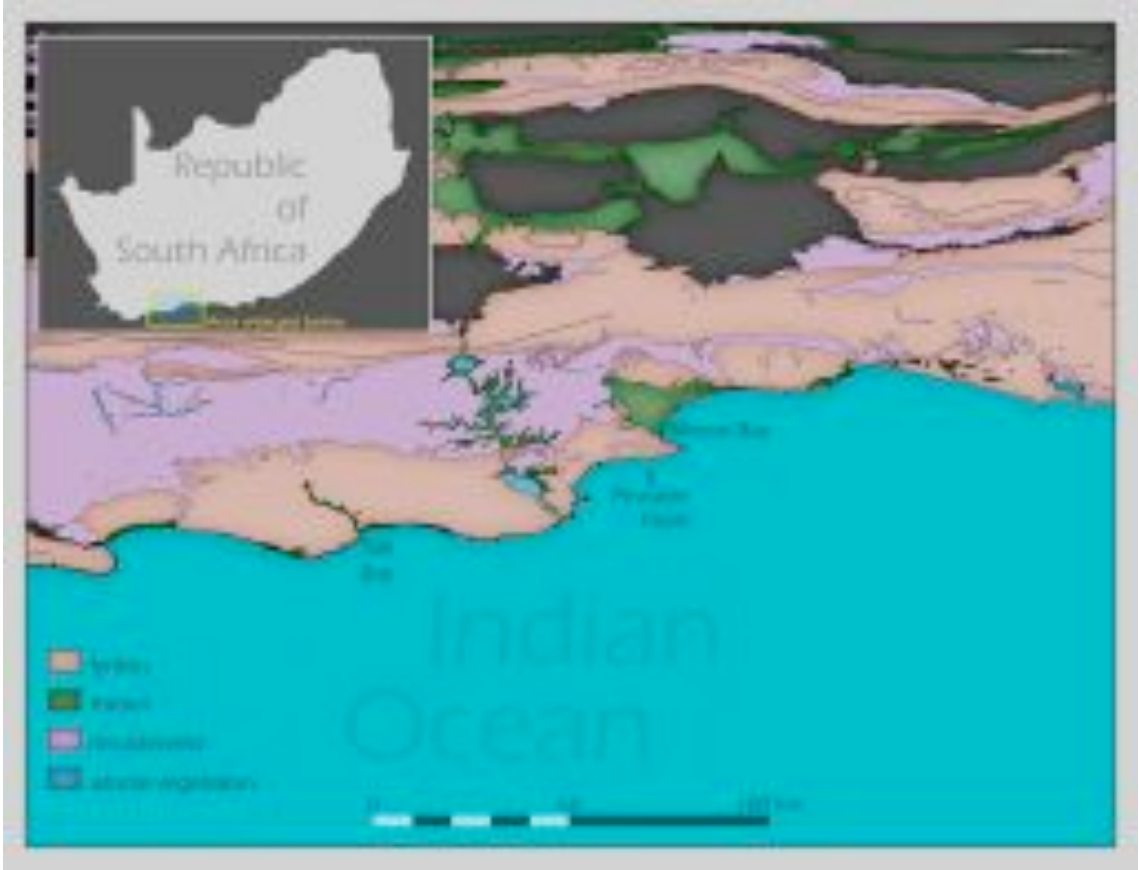

Figura 2. Mapa de nuestra área de estudio dónde se muestran los diversos biomas que componen la Greater Cape Floristic Region (Mapa por Erich Fisher).

6) La costa sur de Sudáfrica presenta, además, un ecosistema marino muy rico (Menge y Branch, 2001; De Vynck et al., 2015), y que los antiguos cazadores recolectores del MSA conocían y explotaban (Marean et al., 2007; Jerardino y Marean, 2010; Jerardino, 2016).

I. 1. Contextualización de la investigación

Esta tesis doctoral se enmarca dentro del proyecto de investigación de I+D "El impacto de los cambios paleoecológicos en la evolución humana y la explotación de los recursos marinos y vegetales en África: La Garganta de Olduvai y Mossel Bay" (HAR2010-15967), dirigido por la doctora Rosa María Albert, directora de esta tesis, y el South African Coast Paleoclimate, Paleoenvironment, Palaeoecology and Paleoanthropology Project (SACP4) liderado por el profesor Curtis W. Marean de la

Arizona State University. Ambos proyectos en colaboración tienen el objetivo común de reconocer las estrategias de supervivencia y el uso de los recursos vegetales, a partir de la reconstrucción del paisaje y la vegetación, durante la Edad de Piedra Media africana en la costa sur de Sudáfrica.

I. 2. Estructuración

Este trabajo de tesis presenta tres elementos de estudio, una parte arqueológica, que se centra en los depósitos arqueológicos del abrigo rocoso Pinnacle Point 5-6 (PP5-6), y una parte de estudios actualísticos. Estos últimos se componen de una colección de referencia de fitolitos de plantas y suelos modernos cuyo estudio será utilizado para establecer analogías con el registro arqueológico y así hacer inferencias sobre el pasado. Además, los procesos tafonómicos sufridos por el conjunto de fitolitos procedentes de los tres tipos de registros estudiados (plantas, suelos modernos y sedimentos arqueológicos) son también tenidos en cuenta. Para ello conocer la composición mineralógica de los sedimentos y su estado de preservación es fundamental, y para ello hemos utilizado espectroscopia de infrarrojos por derivada de Fourier (Fourier Transform Infrared Spectra– FTIR).

La tesis está estructurada en siete capítulos. El Capítulo 1, corresponde a la introducción, en la cuál nos encontramos, y donde se destacan los principales elementos en los que se ha basado este trabajo de investigación. El Capítulo 2 corresponde al marco teórico que está dedicado a la recopilación de datos para la contextualización de nuestro estudio. La redacción tanto de la introducción como del marco teórico se han llevado a cabo en lengua castellana, aunque se han mantenido muchos términos y sus siglas inglesas, sobre todo aquellos relativos a la vegetación y la geología de Sudáfrica. El resto de los capítulos han sido redactados en inglés. El Capítulo 3 corresponde a los objetivos generales y específicos que han centrado nuestro trabajo de investigación. El Capítulo 4 está dedicado a los materiales y métodos utilizados en este trabajo de tesis. El Capítulo 5 corresponde a los resultados, y ha sido dividido en tres secciones: en la primera sección se detallan los resultados del estudio de fitolitos de la colección de referencia de plantas modernas procedentes de las inmediaciones de Pinnacle Point. Todas las plantas proceden de la GCFR. La selección de plantas estudiadas se centró

principalmente en aquellas especies que por sus características y propiedades son susceptibles de haber sido utilizadas por poblaciones cazadoras-recolectoras del pasado. El estudio de colecciones de referencia es importante ya que permite la clasificación de fitolitos que posteriormente serán identificados en el estudio tanto de suelos modernos como de sedimentos arqueológicos, permitiendo así la identificación de ciertas plantas y partes de plantas presentes en estos contextos. En la segunda sección se detallan los resultados obtenidos del estudio de fitolitos de la colección de suelos modernos procedentes de distintos biomas y tipos de vegetación del GCFR y que se localizan en las inmediaciones de Pinnacle Point. La parte correspondiente a suelos modernos (Capítulo V.2. y VI.2.) ha sido recientemente publicada (Esteban, I., et al., Modern soil phytolith assemblages used as proxies for Paleoscape reconstruction on the south coast of South Africa, Quaternary International (2016), http://dx.doi.org/10.1016/j.quaint.2016.01.037 - Esteban et al., in press-a). El conjunto de fitolitos identificado se ha analizado en base a las plantas que dominan o deberían dominar en cada tipo de vegetación. Con ello se pretende, i) detectar la capacidad de identificar distintos tipos de vegetación a través del estudio de fitolitos, ii) evaluar los efectos postdeposicionales que pueden afectar estos microrestos una vez depositados en los suelos, y después de la descomposición de la materia orgánica, y iii) utilizarse como base análoga para la reconstrucción de la vegetación del pasado de nuestro conjunto fósil. En la tercera y última sección se presentan los resultados del conjunto de fitolitos procedente de distintos estratos arqueológicos del yacimiento de PP5-6. Este yacimiento, con 14 m de depósitos antropogénicos alternados con niveles geogénicos de desocupación humana, cubre un período de 60.000 años (~100-40ka), abarcando dos periodos interglaciares (estadios isotópicos marinos 5 y 3) y un periodo glaciar (estadio isotópico marino 4). El Capítulo 6 esta dedicado a la discusión de los resultados. Los resultados de la colección de plantas y suelos modernos se utilizan para la interpretación de los datos obtenidos del registro fósil. La interpretación de los resultados obtenidos del registro fósil se centra en tres ejes principales: i) patrones de explotación de recursos vegetales de los habitantes de PP5-6, ii) reconstrucción del paleoambiente, el paleoclima y la paleovegetación y iii) la relación entre el paleoambiente con la ocupación humana de Pinnacle Point durante el Pleistoceno Medio y Final. El último capítulo, el Capítulo 7, está dedicado a las conclusiones finales de la tesis y las perspectivas de futuro.

II. Marco Teórico

II. 1. Sudáfrica y los humanos anatómicamente modernos

El MSA abarca parte del Pleistoceno Medio y Pleistoceno Superior, desde hace unos 300 ka (Barham y Smart, 1996; Kuman et al., 1999; Deino y McBrearty, 2002; Tryon y McBrearty, 2002; Morgan y Renne, 2008; Johnson y McBrearty, 2010; Porat et al., 2010; Herries, 2011), hasta hace unos 40-30 ka (Beaumont, 1978; Villa et al., 2012), periodo comprendido entre los estadios isotópicos marinos 8 y 3. No obstante estudios recientes de industria lítica llevados a cabo en Kathu Pan (Northern Cape), retrasan los inicios del MSA en Sudáfrica a cerca de 500 ka (Porat et al., 2010; Wilkins y Chazan, 2012; Wilkins et al., 2012).

Aunque tradicionalmente se ha relacionado el MSA con los humanos anatómicamente modernos y con la aparición de un comportamiento humano moderno que ha quedado evidenciado en el registro arqueológico, las evidencias fósiles y genéticas muestran que los humanos anatómicamente modernos evolucionaron en África entre ~200 y ~160 ka (Day, 1969; Ambrose, 1998; Bräuer y Singer, 1996; Clark et al., 2003; White et al., 2003; McDougall et al., 2005; Stoneking y Soodyall, 2006; Fagundes et al., 2007; Gonder et al., 2007; Campbell y Tishkoff, 2008; Henn et al., 2011; Brown et al., 2012).

Son pocos los restos fósiles datados de este periodo hallados en Sudáfrica, e incluyen un cráneo incompleto, dos mandíbulas, parte de un esqueleto infantil y restos postcraneales en Border Cave (KwaZulu-Natal) (de Villiers, 1973; Rightmire, 1976, 1984; Bräuer, 1984a,b); restos mandibulares, restos craneales y postcraneales, varios dientes y un cúbito del antebrazo en Klasies River Mouth (Eastern Cape) (Singer y Wymer, 1982; Rightmire y Deacon, 1991); y por último, restos dentarios, un fragmento mandibular y dos falanges de la mano en Die Kelders Cave 1 (Western Cape) (Grine et al., 1991; Grine, 2000). La mayoría de los restos humanos han sido hallados de manera aislada, sin evidencias de haberse llevado a cabo enterramientos intencionados. Tan sólo el esqueleto infantil recuperado en Border Cave podría representar una excepción, al haberse hallado la mayor parte del esqueleto junto a una concha perforada del género *Conus* (Beaumont, 1980). A pesar de los pocos restos fósiles pertenecientes a humanos anatómicamente modernos encontrados hasta el momento en Sudáfrica, existen cerca de una cincuentena de yacimientos arqueológicos que datan de finales del Pleistoceno Medio, en los cuales se documenta una cultura material con claras evidencias de un

comportamiento humano moderno (p.ej., Henshilwood y Marean, 2003; d'Errico y Stringer, 2011; Wadley, 2015).

Existe una gran controversia en torno al concepto de comportamiento humano moderno en relación a su definición, así como dónde y cuándo apareció. En este trabajo seguimos la definición propuesta por Henshilwood y Marean (2003) los cuales definen el concepto de moderno como *aquel comportamiento que ha sido inferido por patrones construidos socialmente a través de un pensamiento simbólico, actos y comunicación tanto oral como gestual que permite el intercambio de cultura material y de información, así como una continuidad en la cultura a través de distintas generaciones*. Además, los autores añaden a esta conceptualización un aspecto del planteamiento desarrollado por Wadley (2001), quien considera que *la clave para la definición de comportamiento humano moderno no sólo se encuentra en la capacidad de generar un pensamiento simbólico sino en cómo usar ese pensamiento para la organización del comportamiento*.

Siguiendo esta definición, las primeras evidencias de lo que se ha considerado como un comportamiento humano moderno provienen del registro arqueológico sudafricano e incluyen la explotación de recursos marinos (Marean et al., 2007; Henshilwood et al., 2001a), tratamiento térmico de la materia prima lítica para su talla (Brown et al., 2009; Mourre et al., 2010; Schmidt et al., 2013), el uso de cuentas de conchas marinas (Henshilwood et al., 2004; d'Errico et al., 2005), herramientas en hueso (Henshilwood et al., 2001b; d'Errico y Henshilwood, 2007; Backwell et al., 2008), grabado de objetos como son nódulos de ocre, restos faunísticos y huevos de avestruz (Henshilwood et al., 2001a, 2002, 2009, 2011; Henshilwood y d'Errico, 2011; d'Errico et al., 2001, 2012; Watts, 2009; 2010; Texier et al., 2010), el uso de pigmentos (Barham, 2002; Marean et al., 2007; Watts, 2002, 2010), evidencias que muestran una planificación a largo plazo (Brown et al., 2009; Wadley et al., 2009; Wadley, 2010), tecnología microlaminar que prueba la elaboración de proyectiles (Pargeter, 2007; Lombard y Pargeter, 2008; Lombard y Phillipson, 2010; Brown et al., 2012) e incrustación de láminas en proyectiles de caza (Lombard y Phillipson, 2010; Wilkins y Chazan, 2012; Wilkins et al., 2012), recolección de conchas marinas por su belleza (Jerardino y Marean, 2010), construcción de espacios de vivienda (Henshilwood y Dubreuil, 2011; Wadley et al., 2011) y un comportamiento moderno en la caza detectado en los patrones de

mortalidad, las especies cazadas y la abundancia de restos animales encontrados en los yacimientos (Marean y Assefa, 1999; Faith, 2008; Dusseldorp, 2010).

II. 2. Cambios climáticos y ambientales durante el Pleistoceno Medio y Superior en Sudáfrica

Los cambios climáticos y ambientales han jugado un papel de gran importancia en las características biológicas y físicas, así como en la distribución geográfica del género *Homo* y de los primeros humanos modernos. Las fluctuaciones entre periodos glaciar/interglaciar, cambios ambientales rápidos y muy locales, y la variación de las líneas de costa, entre muchos otros factores, debieron influenciar los modos de vida de las poblaciones humanas y han sido utilizados como base para interpretar la relación entre los cambios climáticos y la evolución humana (p. ej., Potts, 1998; Ziegler et al., 2013; Compton, 2011).

El estudio de los cambios climáticos a lo largo del Pleistoceno tiene una tradición más antigua y se ha estudiado con mayor profundidad en el Hemisferio Norte. En Sudáfrica es todavía un tema de debate cómo los medioambientes respondieron a los cambios climáticos acontecidos en el Hemisferio Norte a lo largo del Pleistoceno, cuáles fueron las fuerzas generadoras y de qué manera influenciaron en la evolución del comportamiento humano moderno (Chase y Meadows, 2007; Bar-Matthews et al., 2010; Chase, 2010; Marean et al., 2014).

Los cambios en la temperatura acontecidos durante las fluctuaciones entre periodos glaciares e interglaciares en latitudes altas fueron de entre 8 y 16ºC (North Greenland Ice Core Project Members 2004) mientras que el registro del casquete glaciar de la Antártica sugiere cambios menos dramáticos de la temperatura en latitudes bajas, oscilando tan sólo de 1 a 3ºC (EPICA Community Members 2006). Estudios recientes han mostrado que durante el Pleistoceno, la variación latitudinal de la Zona de Convergencia Intertropical actuó como el principal factor de cambio climático (p. ej., Johnson et al., 2002; Schefuß et al., 2011). Durante fases frías en el Hemisferio Norte, el medioambiente en el Trópico de Cáncer (Trópico del Hemisferio Norte) experimentó una gran aridificación y enfriamiento mientras que en el Hemisferio Sur, en el Trópico de Capricornio (Trópico del Hemisferio Sur), se habría producido una humidificación del medioambiente.

Durante el estadio isotópico marino 6, estudios genéticos apuntan que los humanos que habitaban el sur de África sufrieron un proceso de aislamiento (o cuello de botella)

que aceleró el proceso de evolución de los humanos modernos (Harpending et al., 1993; Rogers y Jorde, 1995; Harpending y Rogers, 2000; Marth et al., 2003). Y es en este momento cuando el registro arqueológico sudafricano empieza a mostrar un cambio en la cultura material que evidencia una evolución hacia un comportamiento humano moderno (p.ej., Henshilwood y Marean, 2003; Marean, 2010; d'Errico y Stringer, 2011; Wadley, 2015). Así, Marean (2008, 2010) hipotetizó que mientras las condiciones climáticas en la mayor parte del continente africano debieron caracterizarse por una gran aridez, con la expansión de tierras áridas y desiertos, la costa sur de Sudáfrica (al igual que otras regiones como el Magreb, Etiopía o el África central– Marean, 2008; Basell, 2008) debió mantener unas condiciones climáticas más moderadas que el resto de África, constituyendo así una zona de refugio para las primeras poblaciones de humanos modernos y Pinnacle Point sería, pues, un ejemplo de ello.

La relación entre clima y comportamiento humano queda también evidenciada con el paso del estadio isotópico marino 5 al 4, cuando se observa un cambio en la distribución de la proporción de plantas (principalmente gramíneas – Poaceae) de tipo C_3 y C_4, con un aumento de las últimas y que se ha relacionado con la intensificación de las lluvias estivales y su expansión hacia el oeste de la costa sudafricana. Los cambios climáticos acontecidos se han considerado como el desencadenante de los cambios tecno-culturales observados en el registro arqueológico sudafricano perteneciente a este periodo (p. ej., McBrearty y Brooks, 2000; Henshilwood y Marean, 2003), con la aparición de las industrias Still Bay y Howiesons Poort que datan entre hace ~71 y ~59 ka y que en Pinnacle Point se observa de manera inequívoca (Jacobs, 2010; Marean et al., 2010; Brown et al., 2012).

A pesar de que la GCFR es una región pequeña en comparación a otros biomas presentes en Sudáfrica, ésta presenta una gran variedad de tipos de vegetación, cada cual con características bióticas distintas (Campbell et al., 1981). Marean et al. (2014) proponen que este hecho podría haber tenido implicaciones que favorecieron las estrategias de explotación de los recursos naturales por parte de aquellas poblaciones de humanos modernos que habitaron el sur de Sudáfrica, debido a que en un rango de distancia corto, podrían haber dispuesto de una gran variedad de recursos marinos, faunísticos y vegetales, así como una gran heterogeneidad geográfica (Cowling, 1990). La costa sur de Sudáfrica presenta, además, un ecosistema marino muy rico (Menge y Branch, 2001; De Vynck et al., 2015) que habría supuesto una parte importante de la

dieta de estas poblaciones. A su vez, Marean et al. (2014) proponen que durante ciertos momentos glaciares cuando el nivel del mar se encontrase en cotas muy bajas, la línea de costa estaría más alejada de los acantilados de Pinnacle Point, dejando expuesta la denominada "Palaeo–Agulhas Plain" (Cawthra et al., 2016), la cual podría haber ofrecido recursos naturales adicionales. Esta plataforma quedó expuesta durante la mayor parte de la ocupación humana en la costa sur y habría constituido un canal de paso para la migración de ungulados (Marean, 2010; Copeland et al., 2016).

En este contexto de cambio climático y evolución humana, la GCFR y nuestra zona de estudio en particular, debió de desempeñar un papel de gran importancia en las actividades cotidianas y de explotación de recursos naturales de estas poblaciones. Cambios en el clima podrían haber afectado la forma de distribución de los recursos vegetales y estos cambios deberían verse representados en el registro arqueológico, siendo esto objeto principal del presente trabajo de investigación.

II. 3. Sociedades cazadoras-recolectoras y la explotación de recursos vegetales

La visión tradicional que desde las disciplinas de la antropología y la arqueología se ha tenido sobre las prácticas de subsistencia de poblaciones cazadoras-recolectoras se basa en el dominio de la caza y la importancia del consumo de carne en la dieta, quedando la explotación y consumo de los recursos vegetales en un segundo plano. En la década de los sesenta esta concepción empezó a cambiar con el trabajo de Richard Lee y DeVore acerca de las poblaciones Khoi-San del sur de África, que publicó en 1968 en el libro irónicamente titulado "Man the Hunter" (Lee y DeVore, 1968) y posteriormente en "The !Kung San: Men, Women, and Work in a Foraging Society" (Lee, 1979). Destacan así mismo otros trabajos también publicados a finales de la década de los sesenta, principios de los setenta, en los que se documenta que cerca del 60-80% de la dieta de poblaciones cazadoras-recolectores de África se basa en recursos vegetales (Woodburn, 1968; Tanaka, 1978). La importancia de la mujer y de la explotación de los recursos vegetales en sociedades cazadoras-recolectoras se ve consolidada desde la corriente de reivindicación feminista que volvió a emerger a principios de la década de los setenta y que en antropología se ve plasmada en la publicación de Linton (1971), titulada "Woman the Gatherer". En la actualidad no cabe duda de que las plantas han constituido y constituyen uno de los principales recursos alimenticios para las sociedades cazadoras-recolectoras.

En el sur de África, diversas culturas actuales todavía llevan a cabo una explotación importante de los recursos vegetales para usos cotidianos entre los que destacan la construcción de cabañas y elementos de refugio, fuel para fuegos, contenedores de alimentos y herramientas varias (arcos, flechas, lanzas), esterillas para dormir, medicinas, cosméticos, etc. (van Wyk y Gericke, 2000). A pesar de ello, la literatura referente a la explotación de recursos vegetales por comunidades de cazadores-recolectores en Sudáfrica es escasa debido, por un lado, a las pocas investigaciones que se han llevado a cabo en este sentido, y por otro, por la baja documentación que se recogió antes de que estas comunidades fueran absorbidas por culturas ganaderas (KhoiKhoi) o por la llegada de colonos europeos a principios del siglo XVIII (Fox y Norwood Young, 1982; Parsons, 1993; van Wyk y Gericke, 2000).

El uso de las plantas con fines medicinales continúa siendo de gran importancia en diversas culturas del sur de África como los Khoi-San[1] (Von Koenen, 2001; van Wyk 2002). Destacan la elaboración de medicinas, tónicos, sustancias alucinógenas usadas en rituales o para mejorar los estados de la mente y el ánimo, curar problemas tópicos como heridas, quemaduras, cuidado buco-dental, la elaboración de perfumes, jabones y cosméticos, etc. La importancia de las plantas reside también en constituir la base para la elaboración de útiles cómo arcos y flechas, cuerdas y redes para la pesca, cestos, canastas, tejidos para las vestimentas, esterillas para dormir o crear áreas de descanso, así como para la construcción de muros y techos de cabañas (Tanaka, 1978; van Wyk y Gericke, 2000), y para la elaboración de veneno aplicado en arcos y flechas y utilizados en la caza (Neuwinger, 1996; d'Errico et al., 2012; Villa et al., 2012; Charrié-Duhaut et al., 2013).

El uso de plantas como combustible para producir fuegos también ha sido de gran importancia a lo largo de la historia de la humanidad, sobre todo si hablamos en términos de volumen (van Wyk y Gericke, 2000). El fuego se considera uno de los avances tecnológicos de mayor importancia en la evolución humana por sus implicaciones en la evolución física, social y cognitiva del genero *Homo* y sus ancestros (Heizer, 1963; Cooke, 1964; Oakley, 1970; Gregg y Grybush, 1976; Perlés, 1977; Stahl et al., 1984; Wrangham et al., 1999). Además restos de hogares o estructuras de combustión constituyen una de las principales evidencias físicas que pueden hallarse en yacimientos arqueológicos de la Edad de Piedra.

A pesar de ello, y como apuntábamos anteriormente, los estudios etnográficos llevados a cabo en las últimas décadas del siglo XX, recogen datos que apuntan a la importancia de las plantas en la dieta de sociedades cazadoras-recolectoras actuales como son los !Kung[2], Hadza, Aka Pygmy en África (Lee, 1969; Woodburn, 1968; Tanaka, 1976; Hladik et al., 1993), aborígenes australianos (Gould, 1980; O'Dea, 1991) y sociedades cazadoras-recolectoras de Papua Nueva Guinea (Dwyer y Minnegal, 1990). Por ejeplo, entre poblaciones !Kung, la ingesta de plantas supone cerca del 67% de la energía consumida de manera diaria (Lee, 1969).

[1] Khoi-San es una palabra que se refiere de manera colectiva y simplista a diversas culturas descendientes de las poblaciones cazadoras-recolectoras San y de las poblaciones ganaderas Khoikhoi o Khoekhoe (Hotentotes).
[2] Poblaciones San que viven en el desierto del Kalahari de Namibia y Botsuana.

Los Khoi-San, descendientes de la única comunidad cazadora-recolectora del sur de África, los San (Bushman), actualmente tan sólo habitan en ciertas zonas del desierto del Kalahari. La pérdida de su independencia y del control de sus tierras debido a la influencia europea tras su llegada a la región del Cabo y otras zonas del sur de África a finales del siglo XV, conllevó al progresivo abandono de las prácticas de recolección y caza. Aunque pocos estudios etnobotánicos se han llevado a cabo sobre poblaciones San (Liengme, 1983; van Wyk, 2002) diversos trabajos (Story, 1958, 1964; Milton, 2000) han recogido la importancia de los recursos vegetales como base de la dieta de poblaciones cazadoras-recolectoras, la cual se compone en un 67% de plantas y tan sólo en un 33% de carne. En la región del Kalahari, dónde el agua es escasa, siendo disponible tan sólo durante los meses de lluvia, plantas con órganos de reserva (USO– Underground Storage Organs, del inglés), como son los bulbos, tubérculos, rizomas y cormos, y que comúnmente son referidos cómo geófitos (Cowling et al., 1996; Rebelo et al., 2006; Bergh et al., 2014), constituyen el recurso de agua más importante durante los restantes nueve meses de sequía (Story, 1958, 1964). Según Marean (2010), este tipo de plantas que abundan tanto en Sudáfrica (Procheş et al., 2006) cómo en la costa sur de Sudáfrica (De Vynck et al., 2016), nuestra zona de estudio, habrían constituido un recurso de gran importancia durante la evolución de los primeros humanos modernos (Marean, 2010).

Los estudios de restos botánicos en yacimientos arqueológicos han permitido obtener información de gran valor para estudiar los patrones en las estrategias de explotación de los recursos vegetales y el comportamiento humano en el pasado, en relación a la dieta, el uso del fuego, etc. Evidencias de geófitos se han hallado en diversos yacimientos arqueológicos datados del periodo Holoceno. Entre ellos destacan Melkhoutboom (Deacon, 1976), Scott's Cave (Wells, 1965) y Sehonghon (Carter et al. 1988), donde se han hallado restos de *Watsonia* y *Moraea* (Iridaceae) y *Hypoxis* (Hypoxidaceae). Deacon (1976, 1983, 1984) propuso que la presencia de geófitos en yacimientos arqueológicos es indicativa de que los recolectores que habitaban la región florística del Cabo durante el Holoceno eran conscientes de la gran producción de este tipo de plantas en la zona, así como del mayor crecimiento de éstos después de eventos de fuego. Aunque no existen evidencias de geófitos en yacimientos que datan del MSA, varios investigadores han argumentado que también deberían haber constituido un componente importante en la dieta de poblaciones de cazadores-recolectores durante el MSA

(Deacon, 1976, 1989, 1993, 1995; Parkington, 1972, 1980, 1981; Marean et al., 2008, 2010).

En la sección quinta de este capítulo nos centramos en el estudio de los fitolitos como herramienta para el estudio del uso de las plantas en el pasado, el cual constituye el principal objeto de investigación de esta tesis.

II. 4. Clima y vegetación actual de Sudáfrica

La vegetación de Sudáfrica es entendida sobre la base del concepto de bioma. Un bioma es la entidad más elevada en la jerarquía de las unidades de vegetación. Los biomas se caracterizan por la relación existente entre las formas de vida (plantas y animales) y los patrones climáticos y medioambientales (régimen de lluvias y temperatura). Debido a que la vegetación es el factor dominante en todos los ecosistemas terrestres, la delimitación de los biomas se ha basado históricamente en relación a las características de la vegetación. En el sur de África, el concepto de bioma fue desarrollado y aplicado por primera vez por Rutherford y Westfall (1986, 1994) y definido como *amplia unidad ecológica que está representada por grandes áreas naturales, incluyendo tanto plantas como animales*. Rutherford y Westfall (1986, 1994) y posteriormente Rutherford (1997) reconocieron siete biomas vegetales: Desert, Forest, Fynbos, Grasslands, Savanna, Nama-Karoo y Succulent Karoo.

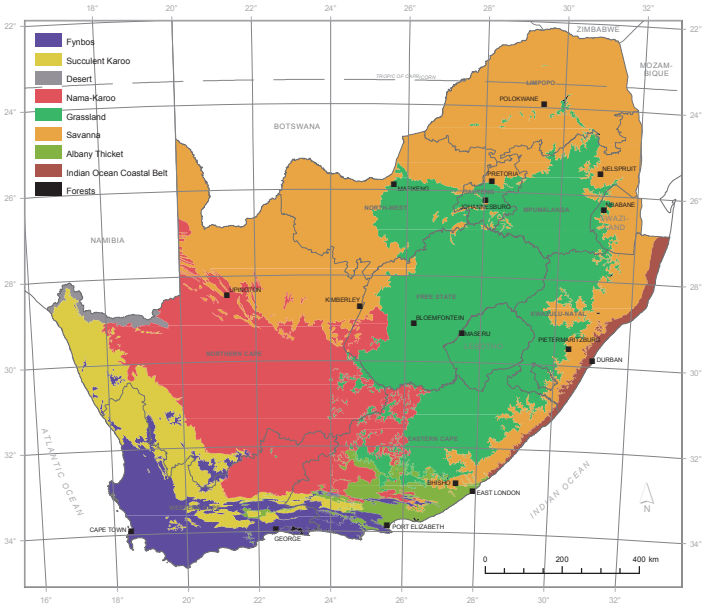

Figura 3. Biomas vegetales de Sudáfrica (mapa extraído de Mucina y Rutherford, 2006).

La definición y los aspectos considerados para la clasificación de los biomas en el sur de África fueron reconsiderados posteriormente por Mucina y Rutherford (2006), quienes consideran que los biomas deben ser distinguidos con base en criterios

florísticos y no faunísticos y que no deben existir delimitaciones espaciales. Por consiguiente, y siguiendo la descripción propuesta por dichos autores, un bioma se define como *amplia unidad ecológico-espacial que representa zonas de vida comprendidas dentro de amplias áreas naturales, y que son definidas con base en la estructura de la vegetación, el clima y factores de disturbio de amplia escala*. Con base en esta nueva definición de bioma, Mucina y Rutherford (2006) reconocen dos biomas adicionales a los planteados con anterioridad por Rutherford y Westfall (1986, 1994), y que son Albany Thicket e Indian Ocean Coastal Belt (Fig. 3). Ambos biomas formaban parte anteriormente del bioma de Savanna.

Los biomas son divididos a su vez en unidades espaciales terrestres conocidas como bioregiones, las cuales representan unidades intermedias entre biomas y unidades de vegetación. Rutherford et al. (2006) definen bioregión como *una unidad espacial que presenta aspectos bióticos y físicos similares, centrados principalmente en la diversidad vegetal*. En cualquier caso, en el presente trabajo no utilizamos las bioregiones como aspecto delimitador de nuestro estudio. Por el contrario, utilizamos principalmente el concepto de unidad vegetal o tipo de vegetación, que siguiendo la descripción planteada por Mucina y Rutherford (2006) se sitúa en el nivel más bajo de la jerarquía y se define como el *conjunto de comunidad vegetal que ocupa ecológica e históricamente hábitats complejos homogéneos a escala de paisaje*.

El clima de Sudáfrica está influenciado por diversas corrientes oceánicas y atmosféricas al encontrarse situado en la intersección de regiones de clima tropical, intertropical y temperado, así como entre los océanos Índico, Atlántico y Antártico. Las variaciones estacionales en la distribución regional de las lluvias ocurre como respuesta a los movimientos de la Zona de Convergencia Inter-Tropical (ITCZ). Las precipitaciones en la región norte de Sudáfrica tienen lugar principalmente durante la estación estival, "lluvias de verano" (SRZ, siglas del término inglés de "summer rainfall zone"), con el 66% de la precipitación media anual teniendo lugar en los meses de verano, entre Octubre y Marzo (Tyson y Preston-Whyte, 2000). La región oeste de Sudáfrica está influenciada por "fuertes lluvias de invierno" (S-WRZ, siglas del término inglés de "strong winter rainfall zone") y "lluvias de invierno" (WRZ, siglas del término inglés de "winter rainfall zone"), con el 66% de la precipitación media anual ocurriendo durante la estación invernal, entre los meses de Abril y Septiembre (Tyson y Preston-Whyte, 2000). Mientras que la costa sur, nuestra área de estudio, recibe la mayor parte

de las lluvias de los sistemas circumpolares de poniente, desencadenantes de la estación de invierno, y se ve afectada por eventos postfrontales, los cuales son una advección que cruza el cálido Océano Índico siendo la causa de la humedad en el aire y responsables de que las lluvias tengan lugar a lo largo del año (Deacon et al., 1992; Tyson y Preston-Whyte, 2000; Engelbrecht et al., 2014). Es por ello que esta región se conoce como la región de "lluvias a lo largo del año" (YRZ, siglas del término inglés de "all year rainfall zone") (Chase y Meadows, 2007). En la YRZ, el clima es moderado, con temperaturas medias anuales de 18ºC, un promedio de 6ºC de temperaturas mínimas y la media de temperaturas máximas que nunca supera los 30ºC. La estacionalidad de las lluvias es la principal responsable de la vegetación, y en particular de la distribución de plantas gramíneas (Poaceae) con distintos metabolismos fotosintéticos. Esto resulta en el dominio de plantas y gramíneas de tipo C_3 en la S-WRZ y la WRZ, un dominio de gramíneas de tipo C_4 en la SRZ y una presencia mixta de plantas y gramíneas de tipo C_3 y gramíneas de tipo C_4 en nuestra área de estudio, la YRZ.

II. 4.1. Greater Cape Floristic Region

En este trabajo de tesis seguimos el término y descripción propuesto por Born et al. (2007) de GCFR que constituye una región fitogeográfica que ocupa las regiones de Cape Floristic, Hantam-Tanqua-Roggeveld y Namaqualand (Fig. 2). La GCFR incluye los biomas Fynbos y Succulent Karoo descritos por Mucina y Rutherford (2006) y en la cual se localiza nuestra área de estudio.

Datos específicos sobre la geología y la vegetación de la GCFR se describen a continuación:

II. 4.1.1. Geología

Los depósitos subyacentes a la región que ocupa la GCFR son de origen Palaeozoico, los cuales conforman la roca madre de los sedimentos plegados del Cape Supergroup. Éstos son las areniscas del grupo Table Mountain, los cuales están asociados con

montañas y acantilados rocosos del Cape Folded Belt, y las cuarcitas con lutitas del grupo Bokkeveld, asociadas a los cabos costeros (Thwaites y Cowling, 1988).

Nuestra área de estudio se localiza en la llanura costera del sur de Sudáfrica, la cual presenta calizas Pliocenas de la formación Bredasdorp (Fig. 2). Cerca de los márgenes costeros, esta formación está cubierta por arenas alcalinas Plio-Pleistocénicas de origen marino. En las zonas situadas más al interior, nos encontramos parches de arenas de origen eólico acídicas y lixiviadas de mayor antigüedad (Rebelo et al., 1991). Los suelos derivados de esquistos y areniscas son moderadamente fértiles, mientras que los suelos asociados a arenas lixiviadas son infértiles. También, los suelos formados por arenas calcáreas asociadas a areniscas y dunas costeras son relativamente infértiles debido a la alta alcalinidad y los subsiguientes niveles bajos de fósforo (Thwaites y Cowling, 1988).

II. 4.1.2. Vegetación y Flora

La GCFR constituye la flora extratropical más diversa en términos de riqueza y endemismo (Colville et al., 2014). Presenta 11.423 especies vasculares y 1.119 géneros de los cuales, el 79% de las especies y el 22,2% de los géneros son endémicos de la región. La gran diversidad y endemismo de la vegetación (principalmente fynbos) en la zona oeste de la GCFR, en comparación con la zona este, debe tener su origen en los movimientos sucesivos de las lluvias de verano que se desplazan de este a oeste, lo que habría resultado en la extinción de taxones presentes en las regiones más al este de la GCFR (Cowling et al., 1999). Un elemento definitorio de la flora de la GCFR es su riqueza en geófitos, los cuales constituyen el 20% del total de la flora, y que pertenecen en su mayoría al grupo de las monocotiledóneas (Procheş et al., 2005, 2006).

Cinco biomas definidos en base florística y estructural ocurren en la GCFR: Fynbos, Renosterveld, Thicket, Forest y Succulent Karroo (Bergh et al., 2014). A continuación hacemos un repaso a los aspectos que caracterizan cada uno de éstos, principalmente en relación a los suelos, la vegetación y la flora. Ya que el bioma Succulent Karoo no ocurre en nuestra área de estudio, no haremos referencia a él.

El bioma Fynbos

El bioma Fynbos ocupa la mayor parte de la Cape Fold Belt, así como las tierras bajas adyacentes entre el sistema Cape Fold Felt y el Océano Atlántico en el oeste y sur, y entre el sistema Cape Fold Felt y el Océano Índico en el sur, en un área que cubre 71.337 km^2. La elevación máxima sobre el nivel del mar es de 2.325 m en el Klein Swartberg. El bioma Fynbos limita con el bioma Succulent Karoo en el norte y noroeste, con el bioma Albany Thicket en el este, y con el Afromontane Forest en el bosque de Knysna.

La arenisca (sandstone) es la roca más común y está principalmente asociada a la Cape Fold Belt. Los suelos que derivan de esta son pobres, arenosos y acídicos, con baja cantidad de nutrientes y de niveles de fósforo (Cowling, 1983). El 81% de los diferentes tipos de vegetación que ocurren en el bioma Fynbos se dan en este tipo de suelos. De todas formas, y aunque ocupe una parte pequeña del bioma, la presencia de roca madre de piedra caliza es de gran importancia, ya que está asociada con un tipo de vegetación, el limestone fynbos (limestone, caliza en castellano), que difiere en gran medida de otros tipos de vegetación por la dominancia de las familias Asteraceae, Restionaceae y Proteaceae, mientras que las plantas gramíneas están prácticamente ausentes.

La vegetación fynbos se caracteriza por ser perenne, arbustiva y proclive al fuego. Está determinada por el dominio de la familia Restionaceae, plantas comúnmente conocidas como restios. Se trata de una familia austral perenne con apariencia similar a las plantas graminoides de las familias Poaceae y Cyperaceae. Aunque presentes en África, Sudamérica, Australia, Nueva Zelanda y el sur del este Asiático, la mayoría de restios se encuentran en la Cape Floristic Region, siendo el elemento definidor de la vegetación fynbos. Entre el componente ericáceo destacan los arbustos de hojas finas de las familias Ericaceae, Rutaceae, Asteraceae, Bruniaceae, Polygalaceae, Thymelaceae, Rhamnaceae, Fabaceae y Rosaceae, constituyendo el grueso mayor de la flora. El elemento proteáceo (Proteaeceae) está representado por los arbustos de hoja ancha principalmente de los géneros *Protea*, *Leucadendron*, *Leucospermum* y *Mimetes*. La vegetación fynbos se caracteriza también por la elevada presencia de geófitos de la clase de las monocotiledóneas. Aunque los geófitos también ocurren en otros tipos de vegetación como por ejemplo en el bioma Renosterveld, la vegetación fynbos presenta la mayor variedad y endemicidad (Procheş et al., 2005, 2006; Manning y Goldblatt, 2012). La familia dominante de geófitos es la Iridaceae, mientras que otras familias

también relevantes son Orchidaceae, Hyacinthaceae y Amaryllidaceae. Las plantas gramíneas de la familia Poaceae no destacan en la vegetación fynbos y cuando están presentes pertenecen en su mayoría al tipo fotosintético C_3, principalmente de las subfamilias Danthonioideae y Ehrhartoideae. De todas formas, en la costa sur, nuestra área de estudio, y la zona este de la GCFR, se observa una presencia mixta de gramíneas de tipo C_3 y C_4.

Dentro del bioma Fynbos, y de nuestra área de estudio, destacan los siguientes tipos de vegetación: limestone fynbos, sand fynbos, grassy fynbos y mountain fynbos. Aunque existen diferencias florísticas entre los diversos tipos de vegetación, la principal diferencia reside en el tipo de suelos (profundidad, acidez y granulometría) en el que se desarrollan. El componente florístico es similar con excepción de la vegetación grassy fynbos, la cual, a diferencia de los otros tipos de vegetación, se caracteriza por presentar un componente importante de gramíneas (Poaceae).

El bioma Renosterveld

La vegetación renosterveld está presente mayoritariamente en western y southern Cape (Taylor, 1978, 1980). También ocurre en los valles interiores de Kamiesberg y en la región Vanrhynsdorp en Namaqualand y en largas áreas de Hantam-Roggeveld (Moll et al., 1984).

La roca madre asociada a este tipo de vegetación es el esquisto (shale), que es el segundo tipo de roca más común en la GCFR. Lo encontramos principalmente en zonas bajas y en valles intermontanos. Los suelos derivados de ésta son finos, poco acídicos, poco profundos, apedales y relativamente fértiles. A diferencia del bioma Fynbos, la vegetación del bioma Renosterveld nunca está asociada a cuarcitas y areniscas.

La flora se caracteriza por tener un importante componente arbustivo, de hojas finas y perennes, y graminoide, que en este caso está formado por la familia Poaceae, aunque las restios están también presentes. La importancia de esta familia es uno de los aspectos que diferencia a este bioma del bioma Fynbos. De entre esta familia destacan los géneros *Tribolium*, *Schismus*, *Sporobulus*, *Ehrharta*, *Cymbopogon* y *Eragrostis* (Bergh et al., 2014). El componente arbustivo está dominado por los géneros *Elytropappus*, *Eriocephalus*, *Helichrysum*, *Oedera*, *Pteronia* y *Relhania* pertenecientes a la familia Asteraceae. Otras familias importantes son Boraginaceae, Fabaceae,

Malvaceae, Thymelaceae, Apiaceae, Rosaceae y Rubiaceae (Goldblatt y Manning, 2002). Al igual que ocurre con la vegetación fynbos, la vegetación renosterveld también se caracteriza por la gran cantidad y diversidad en plantas geófitas (Procheş et al., 2005, 2006; Manning y Goldblatt, 2012).

El bioma Thicket

El reconocimiento del bioma Thicket como entidad vegetal única fue durante mucho tiempo obviado por la errónea concepción que se tenía respecto a las similitudes florísticas que presentaba con otros biomas como Savanna, Forest y el Karoo (Vlok et al., 2003; Cowling et al., 2005). Cowling et al. (2005) demostraron que la evolución de la vegetación thicket se remontaba a la época del Eoceno, formándose a partir de elementos procedentes de formaciones que prevalecieron durante el Cretácico Superior y el Paleógeno Inferior.

A pesar de que es una entidad geográficamente discontinua (Low y Rebelo, 1996; Vlok et al., 2003), el bioma Thicket ocurre principalmente en el sureste y la costa sur de Sudáfrica, al este del Little Karoo y en la mayoría de los valles fluviales a lo largo de la costa del Great Escarpment (Vlok et al., 2003). El clima va de semiárido a subhúmedo (250–800mm yr–1) y de subtropical a cálido-temperado (Acocks, 1953; Low y Rebelo, 1996). Una característica distintiva de este bioma es el régimen de lluvias bimodales, con picos en primavera y en otoño, aunque pueden ocurrir copiosas lluvias a lo largo de todo el año (Vlok et al., 2003).

Este bioma está asociado a suelos profundos ricos en nutrientes, aunque también se puede encontrar en otro tipo de sustratos ya que una vez las plantas características de este bioma se establecen, son capaces de enriquecer los suelos. Los suelos son de origen marino y presentan un pH entre neutral y alcalino. Ocurren en largas áreas de las costas del oeste y del sur, constituyendo el sustrato donde la mayor parte de la vegetación strandveld está presente (Franceshini y Compton, 2006). De todas formas la alcalinidad de los suelos es baja en la costa sur debido a una mayor presencia de lluvias (Watkeys, 1999). Lutitas y tillitas están también asociadas al bioma Thicket en zonas interiores del Cape Fold Belt.

La vegetación thicket se caracteriza por tener una capa arbórea (0,5–5m) y arbustiva muy densa y frondosa, generalmente perenne, esclerófila, muy espinosa y con

abundante flora suculenta. El sotobosque está compuesto por geófitos tolerantes a la sombra, plantas herbáceas, y gramíneas (Poaceae) tanto de tipo C_3 como C_4. A diferencia de lo que ocurre en la mayoría de los biomas en Sudáfrica, la acción del fuego es prácticamente nula (Vlok et al., 2003; Bergh et al., 2014). Géneros diagnósticos son *Brachylaena* (Asteraceae), *Diospyros* y *Euclea* (Ebenaceae), *Grewia* (Malvaceae), *Mimusops* y *Sideroxylon* (Sapotaceae), *Clausea* (Rutaceae), *Cassuonia* (Araliaceae), *Olea* (Oleaceae) y *Searsia* (Anacardiaceae) (Cowling et al., 2005; Vlok y Villiers, 2007). La familia arbustiva Celastraceae tiene una gran importancia y destacan los siguientes géneros: *Cassine*, *Gymnosporia*, *Lauridia*, *Maytenus*, *Mystroxylon*, *Pterocelastrus*, *Putterlickia* y *Robsonodendron*. Algunas de las familias de plantas suculentas de mayor importancia son: Aizoaceae, Asphodelaceae (el aloe), Crassulaceae, Euphorbiaceae y Apocynaceae.

Dentro del bioma Thicket y de nuestra área de estudio destacan los siguientes tipos de vegetación: subtropical thicket, coastal thicket, strandveld y dune cordon.

El subtropical thicket está formado por una vegetación arbustiva cerrada y densa dominada por arbustos y árboles pequeños de hoja perenne y un gran número de plantas suculentas, mientras que el componente herbáceo es escaso. La coastal thicket presenta una vegetación similar al anterior pero se localiza en zonas cercanas a la costa. Strandveld se caracteriza por presentar elementos característicos de la vegetación subtropical thicket y de la vegetación fynbos. También se localiza en zonas cercanas a la costa. Por último, dune cordon comprende una flora que es una variación de la vegetación subtropical ticket y está asociada al sistema de dunas que ocurre a lo largo de la costa.

El bioma Forest

Los bosques indígenas en Sudáfrica ocurren de manera dispersa a lo largo de Western, Eastern, Northern y Southern Cape, desde el Soutpansberg en el norte y Maputaland en el este, hasta la Cape Peninsula en el oeste. Aunque es en Southern Cape donde tienen una mayor presencia. En la GCFR ocurren dos tipos de bosques, el southern afromontane forest y el southern coastal forest mientras que en nuestra área de estudio tan sólo está presente el último (Bergh et al., 2014).

El southern coastal forest se distribuye en el Western Cape a lo largo de la costa entre Alexandria y el cañón Van Stadens River, y en las dunas costeras de Eastern Cape. A pesar de su nombre, no sólo ocurre en la costa, sino también en dunas, en profundos valles fluviales, en zonas protegidas del fuego y zonas bajas de profundos barrancos. El southern coastal forest puede ocurrir en tres tipos de suelos: i) suelos arenosos bien drenados procedentes de dunas costeras asentadas sobre rocas sedimentarias del Algoa Group, ii) suelos margosos del Bokkeveld Group, y iii) suelos arenosos profundos y ricos en nutrientes (Bergh et al., 2014; Mucina y Geldenhuys, 2006). La vegetación es densa y se caracteriza por ser un bosque de dosel bajo. En zonas de dunas dominan las especies *Celtis africana*, *Sideroxylon inerme*, *Mimusops caffra* y *Dovyalis rotundifolia*, mientras que las llanuras costeras están principalmente dominadas por *Celtis africana* (Bergh et al., 2014; Mucina y Geldenhuys, 2006). Las regiones más al este presentan desde un punto de vista florístico y estructural, capas arbóreas de dosel bajo y con un componente arbustivo y herbáceo bien desarrollado (Bergh et al., 2014; Mucina y Geldenhuys, 2006).

II. 5. El estudio de fitolitos

La identificación de restos vegetales preservados en yacimientos arqueológicos se lleva a cabo generalmente a través del estudio de macro- y microrestos vegetales. Entre los macrorrestos destacan los estudios de carbones, semillas y restos de plantas fósiles, y entre los microrrestos, los estudios de polen, almidones, palinomorfos no polínicos y fitolitos. En este trabajo utilizamos los fitolitos como herramienta de estudio para la identificación y análisis de las estrategias de recolección, explotación y uso de los recursos vegetales llevados a cabo por poblaciones de cazadores-recolectores, así como la reconstrucción de la vegetación y el clima, en la costa sur de Sudáfrica durante el Pleistoceno Medio y el Pleistoceno Superior.

II. 5.1. Producción

Los fitolitos son micrrorestos minerales que reproducen los tejidos intra- y extracelulares de ciertas plantas. La producción de los fitolitos empieza después de que el sílice soluble (ácido monosilícico– H_4SiO_4), presente en suelos, es absorbido por las raíces de las plantas y conducido hasta las partes aéreas de éstas, rellenando los muros celulares, los interiores de las células y los espacios intracelulares, adoptando la forma de la estructura celular al precipitar el sílice en forma de ópalo ($SiO_2 \cdot nH_2O$) (Piperno, 1988, 2006).

El grado de deposición de los fitolitos en las plantas vivas está influenciado por diversos factores entre los que destacan: i) las condiciones climáticas y ambientales en que la planta ha crecido, por ejemplo, plantas que crecen en ambientes húmedos o en regiones con una elevada presencia de agua normalmente producen un número más elevado de fitolitos y una mayor silicificación (p.ej., Rosen y Weiner, 1994), ii) elevados niveles de evapotranspiración pueden también ser causa de una mayor deposición de sílice en las células de las plantas (Jones y Handreck, 1965; Sangster y Parry, 1969; Bremond et al., 2005a), iii) propiedades fisicoquímicas de los suelos, iv) la cantidad de sílice presente en los suelos (p.ej., Jones y Handreck, 1965); v) la edad de la planta, y vi) el grupo taxonómico al que pertenecen. A pesar de que los fitolitos pueden encontrarse en un gran número de plantas y en diferentes estructuras y órganos de estas, ciertas familias como Poaceae, Cyperaceae y Arecaceae producen un gran número de

fitolitos (p.ej., Piperno, 1988, 2006; Bamford et al., 2006; Albert et al., 2009). Otros grupos sin embargo no producen fitolitos o lo hacen en pequeñas concentraciones como son las plantas gimnospermas y la madera de plantas eudicotiledóneas (p.ej. Metcalfe, 1960, 1971; Metcalfe y Chalk, 1979; Albert y Weiner, 2001; Tsartsidou et al., 2007; Mercader et al., 2009; Collura y Neumann, en prensa). Para un mayor detalle de diversos estudios llevados a cabo en plantas procedentes de distintas regiones del mundo ver Piperno (2006) y las referencias en ellos citadas.

II. 5.2. Clasificación

La descripción, identificación y clasificación de los fitolitos se lleva a cabo con base en sus características morfológicas que dependen de tres factores principalmente: el taxón específico al que pertenecen (familia, género y especie), la parte de la planta y el tipo de estructura celular en el que se han formado. Para una correcta clasificación, los fitolitos primeramente deben ser descritos por su origen taxonómico y/o anatómico. En caso de no ser posible se debe realizar una descripción geométrica de los mismos, teniendo en cuenta forma, tamaño, textura y ornamentación.

Una de las principales características a tener en cuenta durante la clasificación de fitolitos es que diferentes morfotipos pueden ser producidos en un mismo tipo de planta o parte de ella (multiplicidad), del mismo modo, un mismo morfotipo puede ser producido en diferentes tipos de plantas (redundancia) (p.ej., Rovner, 1971; Mulholland, 1989; Fredlund y Tieszen, 1994). Es por ello que la elaboración de colecciones de referencia de plantas modernas es de gran importancia en el estudio de fitolitos y en los últimos años son un gran número los estudios llevados a cabo a este respecto (p.ej., Twiss, 1987, 1992; Brown, 1984; Fredlund y Tieszen, 1994; Kondo et al., 1994; Mulholand, 1989; Piperno y Pearsall, 1998; Zucol, 1998; Albert y Weiner, 2001; Iriarte, 2003; Strömberg, 2003; Gallego y Distel, 2004; Blinnikov, 2005; Bamford et al., 2006; Fahmy, 2008; Barboni y Bremond, 2009; Albert et al., 2009; Cordova, 2013; Novello et al., 2012; Neumann et al., en prensa). Cabe destacar los estudios morfométricos de fitolitos, los cuales se han centrado principalmente en el estudio de plantas gramíneas y que han demostrado ser de gran eficacia para su identificación taxonómica (a nivel de género y especie), en especial en aquellos morfotipos a priori similares entre si. Desde

los primeros estudios morfométricos de fitolitos llevados a cabo por Ball et al. (1993, 1996, 1999), Pearsall et al. (1995) y Zhao et al. (1998), son cada vez mayores los trabajos publicados a este respecto y que han demostrado, aunque con ciertas limitaciones, ser de gran eficacia para la identificación taxonómica de fitolitos de gramíneas (Poaceae) (p.ej., Ball et al., 1996, 1999, 2016; Pearsall et al., 1995; Zhao et al., 1998; Berlin et al., 2003; Iriarte, 2003; Portillo et al., 2006; Lu et al., 2009; Zhang et al., 2011; Petö et al., 2013; Out et al., 2014). Aunque en los últimos años los estudios morfométricos han empezado a centrarse también en otros tipos de plantas. Cabe destacar los trabajos llevados a cabo por Albert et al. (2009) de esferoides equinados de palmáceas (Arecaceae), Benvenuto et al., (2015) de esferoides y otros morfotipos equinados de las familias Bromeliaceae, Strelitziaceae, Orchidaceae, Marantaceae, Cannaceae, y Zingiberaceae de Argentina, o el estudio de morfotipos vulcaniformes de banana (Musaceae) llevados a cabo por Ball et al. (2006) y Vrydaghs et al. (2009).

II. 5.3. Preservación

La preservación de los fitolitos procedentes tanto del registro moderno (suelos modernos) como fósil (paleosuelos y sedimentos arqueológicos) puede depender de dos factores principalmente: por un lado, del tipo de fitolito, y por otro, de diversos procesos pre y postdeposicionales que pueden haber afectado la preservación de estos microrrestos.

Diversas morfologías como por ejemplo pelos (hair cells) o fitolitos procedentes de tejidos epidérmicos de plantas eudicotiledóneas (epidermal ground mass) son menos estables que aquellos que proceden de frutos y semillas de estas mismas plantas (Cabanes y Shahack-Gross, 2015).

En contextos arqueológicos tanto abiertos como cerrados (cuevas y/o abrigos rocosos) la preservación de los fitolitos puede verse afectada por diversos procesos postdeposicionales (procesos químicos y físicos) que tuvieron lugar en el momento de su deposición.

Estando formados principalmente por sílice, los fitolitos son relativamente solubles bajo condiciones alcalinas y pueden ser disueltos completamente con pH superiores a 9

(Piperno, 1988, 2006; Karkanas, 2010). Por ejemplo, en contextos de estructuras de combustión, la calcita en contacto con agua puede elevar el pH de los suelos a niveles superiores a 8.5 (Karkanas et al., 2000; Fraysse et al., 2006) acelerando la disolución de los fitolitos. Cabanes et al. (2011) demostraron que los fitolitos quemados son aparentemente menos estables que los no quemados y esto es un aspecto a tener en cuenta en el momento de interpretar conjuntos de fitolitos en contextos arqueológicos de sedimentos procedentes de estructuras de combustión. Los mismos autores además observaron que las decoraciones de los márgenes de los fitolitos son también más vulnerables pudiendo desaparecer con rapidez debido al efecto del fuego y la alcalinidad de los sedimentos.

La preservación de los fitolitos en suelos y sedimentos también puede verse afectada por su transporte a través del viento o agua, siendo como resultado su fragmentación o rotura, astillado y/o abrasión (Osterrieth et al., 2009; Madella y Lancelotti, 2012).

La translocación o percolación de los fitolitos a través de los sedimentos por bioturbación también puede afectar la integridad de su conjunto, habiéndose observado por ejemplo en algunos perfiles naturales de suelos (Piperno y Becker, 1996; Alexandre et al., 1997; Hart y Humphreys, 2003; Runge, 1999; Humphreys et al., 2003; Farmer, 2005). La velocidad y el alcance del transporte puede variar dependiendo de las propiedades físicas de los suelos, así como del tamaño de los fitolitos (Fishkis et al., 2009, 2010). Asimismo, en suelos de grano grueso las posibilidades de percolación aumentan, sobre todo en fitolitos de dimensiones similares o inferiores a 5µm (Fishkis et al., 2009, 2010).

La actividad humana también puede ser responsable del estado de preservación de los fitolitos, por ejemplo a través del pisado continuo de suelos (*trampling*), el cual se ha observado así mismo en suelos modernos en Tanzania (Albert et al., 2015) por el efecto del fuego a altas temperaturas (Cabanes et al., 2011; Wu et al., 2012), la rotura de los fitolitos durante su procesado (p.ej., el molido de cereales) (Portillo, 2006; Portillo et al., 2013), etc.

II. 5.4. Aplicaciones

Los estudios de fitolitos, aplicados a la arqueología y la paleoecología, constituyen una herramienta de gran eficacia para detectar y caracterizar la explotación de los recursos vegetales, el uso de las plantas y la dieta de poblaciones humanas del pasado, así como la reconstrucción del paleoambiente, paleoclima y paleovegetación, aplicándose a una gran variedad de épocas y regiones geográficas.

Las estrategias de explotación de los recursos vegetales llevadas a cabo por poblaciones del pasado depende principalmente del tipo de economía. Por ello, el tipo de plantas que pueden quedar representadas en el registro variará dependiendo del tipo de sociedad y cultura estudiada.

La versatilidad de los fitolitos hace que su estudio se haya aplicado en contextos arqueológicos de diversos períodos cronológicos: el estudio de poblaciones de cazadores-recolectores de la Edad de Piedra (o Paleolítico en Europa) (p. ej., Albert et al., 1999, 2000; Madella et al., 2002; Cabanes et al., 2007, 2010; Tsartsidou et al., 2015; Esteban et al., en prensa-b; Rodriguez-Cintas y Cabanes, en prensa), el estudio de los inicios de la agricultura y la emergencia de sociedades productoras neolíticas (p. ej., Piperno, 1988; Piperno et al., 2000; Piperno y Flannery, 2001; Madella, 2003; Piperno y Stothert, 2003; Li et al., 2007; Lu et al., 2009; Portillo et al., 2010; Power et al., 2014; Madella et al., 2014; García-Granero et al., en prensa), así como sociedades productoras desde el Neolítico hasta períodos recientes como la época moderna e incluso en contextos urbanos (p. ej., Piperno, 1988; Bozarth, 1993; Hart et al., 2003; Berlin et al., 2003; Albert et al., 2008; Portillo et al., 2009; Cabanes et al., 2012; Devos et al., en prensa). Debido a la gran cantidad de aplicaciones y estudios llevados a cabo en las últimas dos décadas, en este apartado tan sólo profundizaremos en la aplicación del estudio de fitolitos en contextos de la Edad de Piedra, centrándonos principalmente de Sudáfrica, al ser éste objeto principal del presente trabajo de tesis.

II. 5.4.1. El estudio de fitolitos en contextos arqueológicos de la Edad de Piedra

A través del estudio de fitolitos en contextos arqueológicos de la Edad de Piedra se pueden estudiar las diversas estrategias de recolección llevadas a cabo por poblaciones cazadoras-recolectoras y su relación con una gran variedad de actividades de la vida cotidiana, como el uso de las plantas en relación al fuego, la dieta, la preparación de

lechos (*bedding*). El estudio de fitolitos también es una herramienta adecuada para la caracterización de suelos de ocupación, la organización espacial de los yacimientos y sus periodos de ocupación, etc.

Las estructuras de combustión son el resto arqueológico más recurrente en yacimientos de la Edad de Piedra, independientemente de la región geográfica a estudiar. Los análisis de fitolitos se han aplicado al estudio de estructuras de combustión para detectar el tipo de combustible utilizado en la elaboración y mantenimiento de los fuegos (p. ej., Albert et al., 1999, 2000, 2003; Karkanas et al., 2002; Rosen, 2003; Schgiel et al., 2004; Cabanes et al., 2007; Albert, 2010; Albert y Marean, 2012; Esteban et al., en prensa-b; Rodríguez-Cintas y Cabanes, en prensa). El estudio de fitolitos en contextos de estructuras de combustión complementa otras disciplinas arqueobotánicas como la antracología (estudio de carbones) o la carpología (estudio de semillas) permitiendo la identificación de elementos no leñosos y de diversas partes de plantas como hojas de árboles y arbustos que podrían haber sido utilizados como combustible, como parte funcional de los hogares o simplemente en la identificación de tipos o partes de plantas que fueron desechados en los hogares después de su uso.

A través del estudio de fitolitos también se puede inferir el uso de camas y zonas de reposo (*bedding*). Aunque en contextos de la Edad de Piedra existen pocos ejemplos de ello, el más antiguo se localiza en Sudáfrica, en el yacimiento de Sibudu Cave (KwaZulu-Natal) en niveles que datan de hace 77ka (Wadley et al., 2011). Otros ejemplos de prácticas de bedding han sido identificados en el yacimiento sudafricano de Strathalan B Cave, perteneciente al final del MSA (Opperman, 1996), así como en el yacimiento del Paleolítico Medio de Esquilleu Cave, en el norte de España (Cabanes et al., 2010).

Evidencias de consumo de plantas a través del registro arqueológico con base en el estudio de fitolitos en contextos de cazadores-recolectores es escaso. Algunos ejemplos a destacar son los trabajos llevados a cabo por Madella et al. (2002) y Rosen (2003) en contextos Neandertales en los yacimientos del Paleolítico Medio de Amud Cave (Israel) y Tor Faraj (Jordania), respectivamente. Ambos interpretaron la excesiva presencia de panículas de gramíneas (Poaceae) como evidencia de una recolección intencionada de los granos de éstas con fines alimenticios.

El único ejemplo en que el estudio de fitolitos en contextos de la Edad de Piedra que evidenció un uso diferencial del espacio de suelos habitacionales, lo encontramos en el yacimiento del Paleolítico Medio de Tor Faraj en Jordania (Rosen, 2003; Henry et al., 2004).

II. 5.4.2. Los fitolitos como herramienta de reconstrucción paleoambiental

Estudios de fitolitos aplicados a la paleoecología para la reconstrucción del medioambiente, el clima y la vegetación del pasado se pueden aplicar desde diversas vertientes, como por ejemplo los sondeos sedimentológicos de lagos y estanques, terrestres y marinos (p. ej., Twiss, 1987; Piperno y Becker, 1996; Blinnikov et al., 2002; Novello et al., 2012; Fisher et al., 2013; Aleman et al., 2013, 2014), así como a través del registro arqueológico y paleoantropológico. Aunque cabe mencionar que la interpretación del conjunto de fitolitos procedente de yacimientos arqueológicos, tal como discutiremos en la sección VI. 4.1., debe realizarse con cautela, principalmente cuando el conjunto de fitolitos estudiado ha sido interpretado como de origen antrópico, implicando pues que hubo una selección intencionada de las plantas por parte de los habitantes del sitio.

Existen numerosos ejemplos de estudios centrados en la reconstrucción del medioambiente y el clima del pasado en diversas zonas geográficas. En África son numerosos los trabajos de reconstrucción paleoambiental llevados a cabo, muchos de ellos con base en el estudio de depósitos paleoantropológicos (p.ej., Barboni et al., 1999; Mercader et al., 2000; Albert et al., 2006, 2009; Albert y Bamford, 2012; Bamford et al., 2006, 2008; Neumann et al., 2009; Barboni et al., 2010; Ashley et al., 2010a,b; Albert y Bamford, 2012; Barboni, 2014; Backwell et al., 2014) así como de sondeos sedimentológicos lacustres (p.ej., McLean y Scott, 1999; Novello et al., 2012, 2015).

El estudio de los isótopos estables de carbono presente en los núcleos de los fitolitos de gramíneas también constituye una de las aplicaciones llevadas a cabo para el estudio de la historia evolutiva de esta familia, así como para el estudio de su relación con el clima y el medioambiente en el pasado (Kelly et al., 1991a,b; McInerney et al., 2011).

II. 5.5. Estudios actualísticos

Como en otras disciplinas paleobotánicas y arqueobotánicas, los estudios de fitolitos en contextos paleoambientales y arqueológicos se basan en estudios actualísticos (estudios modernos) usados como elemento análogo para la reconstrucción de la paleovegetación y el paleoclima así como los tipos de plantas y las partes de las mismas que fueron recolectados y usados por sociedades del pasado. Por ello desde hace varias décadas la comunidad científica se ha esforzado en la elaboración de colecciones de referencia para el estudio de fitolitos tanto de plantas como de suelos modernos procedentes de diversos tipos de vegetación actuales.

La composición vegetal y florística de diversos tipos de vegetación, y en concreto de praderas y bosques, y mosaicos de ambos tipos de vegetación, está estrechamente relacionada con diversos condicionantes climáticos, como son los regímenes de lluvias y la temperatura. Esta relación se ve claramente reflejada en la distribución de plantas gramíneas en relación a la subfamilia a la que pertenecen así como a su ruta metabólica fotosintética, que puede ser de tipo C_3, C_4 y CAM (crassulacean acid metabolism). Las gramíneas producen las que se conocen como células cortas (de aquí en adelante GSSC– Grass Silica Short Cell), y de las cuales forma y taxonomía coinciden en gran medida. Twiss et al. (1969) fueron los primeros en reconocer la diferente producción morfológica de las GSSC en relación al modo fotosintético así como a la subfamilia. Aunque investigaciones posteriores han demostrado que el patrón propuesto por Twiss et al. (1969) no siempre se cumple, en la mayoría de los casos sí que se confirma la tendencia general hacia la clasificación propuesta por dichos autores (p. ej., Twiss, 1987, 1992; Brown, 1984; Fredlund y Tieszen, 1994; Kondo et al., 1994; Mulholand, 1989; Piperno y Pearsall, 1998; Zucol, 1998; Iriarte, 2003; Strömberg, 2003; Gallego y Distel, 2004; Blinnikov, 2005; Bamford et al., 2006; Fahmy, 2008; Barboni y Bremond, 2009; Rossouw, 2009; Cordova y Scott, 2010; Cordova, 2013; Novello et al., 2012; Neumann et al., en prensa).

Los estudios de fitolitos también se han centrado en plantas arbustivas (gimnospermas, eudicotiledóneas y palmáceas) por su importancia para la reconstrucción de vegetación de carácter arbóreo como son bosques, bosques galerías, formaciones selváticas, etc., así como para la identificación de aquellas plantas que fueron utilizadas por las poblaciones del pasado (p. ej., Kerns et al., 2001; Albert y

Weiner, 2001; Delhon et al., 2003; Bremond et al., 2004; Bamford et al., 2006; Albert et al., 2009; Iriarte y Paz, 2009; Mercader et al., 2009, 2011; Collura y Neumann, en prensa).

Por último, el estudio combinado de fitolitos de plantas y suelos modernos, permite testar el potencial del conjunto de fitolitos para la reconstrucción de la vegetación actual y constituir así la base (el puente análogo) para la interpretación del registro fósil en clave paleoambiental (p. ej. Twiss et al., 1969; Runge, 1999; Barboni et al., 1999, 2007; Delhon et al., 2003; Gallego et al., 2004; Bremond et al., 2004, 2005a, 2005b; Carnelli et al., 2004; Albert et al., 2006, 2015; Iriarte y Paz, 2009; Novello et al., 2012; Watling y Iriarte, 2013). Y este método de análisis actualístico es el que seguimos en esta tesis.

II. 6. El complejo arqueológico de Pinnacle Point

Nuestra área de estudio se localiza en el complejo arqueológico de Pinnacle Point y sus inmediaciones. Se conoce con el nombre de Pinnacle Point el área que rodea un pequeño promontorio en una zona de acantilados cuarcíticos situados en la costa sur del océano Pacífico, aproximadamente a 10 km al oeste de Mossel Bay (Fig. 1).

Pinnacle Point presenta un gran número de cuevas y abrigos rocosos con restos arqueológicos, paleontológicos y de interés geológico que hace de ésta un área de gran interés paleoantropológico. Dataciones llevadas a cabo a través de uranio-plomo (U-Pb, por sus siglas en inglés) y de luminiscencia ópticamente estimulada por transformación térmica (TT-OSL, por sus siglas en inglés) en depósitos sedimentarios marinos y eólicos procedentes de tres localidades cercanas a Pinnacle Point (Jacobs et al., 2011), así como de espeleotemas y granos de cuarzo provenientes de depósitos eólicos, dunas fósiles y sedimentos antropogénicos en dos cuevas situadas en Pinnacle Point (PP13G y PPOH) (Pickering et al., 2013) sitúan la formación de las cuevas en cerca de 1.1 millones de años (ma).

Los trabajos arqueológicos en Pinnacle Point se han centrado en diversas cuevas y abrigos rocosos (Fig. 1), entre las que destacan dos localidades, la cueva PP13B y el abrigo rocoso PP5-6 (Fig. 4). Los trabajos de campo en PP13B se empezaron en el año 2000 y se extendieron hasta el 2006, año en que empezaron los trabajos de campo en PP5-6. En el año 2010 se publicó una edición especial en la revista *Journal of Human Evolution* (núm. 59, ediciones 3-4) donde se publicaron la mayor parte de los trabajos llevados a cabo en la cueva PP13B. El estudio de fitolitos de esta cueva fue publicado en la revista *Geoarchaeology* (Albert y Marean, 2012).

Nuestro estudio se centra en el yacimiento PP5-6, el cual es uno de varios abrigos rocosos que abarca del Pleistoceno Medio final hasta mediados del Pleistoceno Superior (Bar-Matthews et al., 2010; Brown et al., 2009, 2012; Marean, 2010; Marean et al., 2004; Matthews et al., 2011). El yacimiento se ha divido en dos partes principales, PP5-6 Norte y PP5-6 Sur, áreas que probablemente estuvieron conectadas en el pasado, pero que ahora están separadas por una zona de erosión y por el colapso de parte del acantilado.

El depósito principal en PP5-6 Norte se conoce como Long Section y es donde la mayor parte de los trabajos arqueológicos se han llevado a cabo. Se trata de un depósito de sedimentos de unos 30 m de potencia que fueron acumulados contra la pared del abrigo y parcialmente bajo el refugio de la cubierta del abrigo. Abarca un periodo cronológico que va de hace ~100 a 50 ka (Marean et al., 2014). Los depósitos antropogénicos en PP5-6 son de una gran riqueza. Destaca la presencia de restos líticos, faunísticos, ocre, cáscaras de huevo de avestruz, restos de malacofauna y un gran número de estructuras de combustión bien preservados (Brown et al., 2009, 2012; Karkanas et al., 2015). Restos vegetales como carbones o polen, por el contrario, no se preservan.

Figura 4. Foto panorámica de los yacimientos arqueológicos PP13B y PP5-6.

La metodología de excavación se encuentra descrita en Bernatchez y Marean (2011), Dibble et al. (2007), Marean et al. (2010) y Oestmo y Marean (2014). La secuencia de la cueva PP5-6, la cual es objeto de nuestro estudio, ha sido dividida en doce agregados estratigráficos (StratAggs[3]) (Brown et al., 2009, 2012; Karkanas et al., 2015). La parte más antigua de la secuencia se caracteriza por la presencia de brecha, aunque el resto del depósito que se ha preservado está formado por arena de transporte eólico, la cual muestra alteraciones en la parte más reciente de la secuencia. La presencia de roof spall (cuarcitas procedentes del desprendimiento de la pared rocosa, término que utilizaremos

[3] Unidades sedimentarias que reflejan los mayores cambios en procesos sedimentarios geogénicos y antropogénicos. En la literatura científica en lengua castellana se conocen también como niveles o unidades arqueológicas.

a lo largo de este trabajo) es constante a lo largo de toda la secuencia, aunque la concentración y las características de este material cambian de acuerdo con los StratAggs. Se han registrado actividades humanas en forma de cenizas, acumulación de concheros y un gran número de restos de cultura material. La intensidad en la ocupación humana varía igualmente a lo largo de la secuencia (Brown et al., 2009, 2012; Karkanas et al., 2015).

Los principales StratAggs en PP5-6, la mayoría objeto de nuestro estudio, se describen a continuación por sucesión cronológica de más antiguo a más moderno (Fig. 5):

Yellow Brown Sand (YBS, ~90 ka). Este estrato constituye la base de la secuencia de PP5-6. Sin presentar ocupación humana, esta constituido por una gruesa capa de duna eólica y que ha sido identificada como la misma duna que selló las cuevas PP13B y Crevice Cave, ambas en el complejo arqueológico de Pinnacle Point (Bar-Matthews et al., 2010).

Yellow Brown Sand and Roofspall (YBSR, ~ 90 ka). Este estrato presenta las primeras evidencias de ocupación humana del yacimiento. Se caracteriza por presentar un sedimento de color amarillento-marronáceo claro y de fracción gruesa, con una gran presencia de roofspall. Abundan los restos de malacofauna, principalmente en las estructuras de combustión, las cuales tienden a ser de efímera y de pequeñas dimensiones.

Light Brown Sand and Roofspall (LBSR, ~ 90-74 ka). Al igual que en YBSR, roofspall domina el componente sedimentario en todas las capas de este estrato. Las capas de intensa ocupación humana se ven intercaladas con capas de baja o no-ocupación. Las capas con ocupación humana intensa se caracterizan por la abundancia de restos de malacofauna, así como de fauna e industria lítica. Algunas de estas ocupaciones podrían ser clasificadas como concheros.

Aeolian Light Brown Sand (ALBS, ~ 74-72 ka). ALBS se caracteriza por la presencia de capas de arena eólica que se ven alternadas con capas antropogénicas ricas en restos de malacofauna. El contacto entre LBSR y ALBS representa la transición del estadio isotópico 5 a 4, y muestra un cambio de sedimento dominado por roofspall en LBSR a sedimentos de arena eólicos en ALBS. Este cambio en el sedimento ha sido

interpretado como reflejo de la cercanía de la costa a Pinnacle Point durante el momento de ocupación de ALBS (Karkanas et al., 2015).

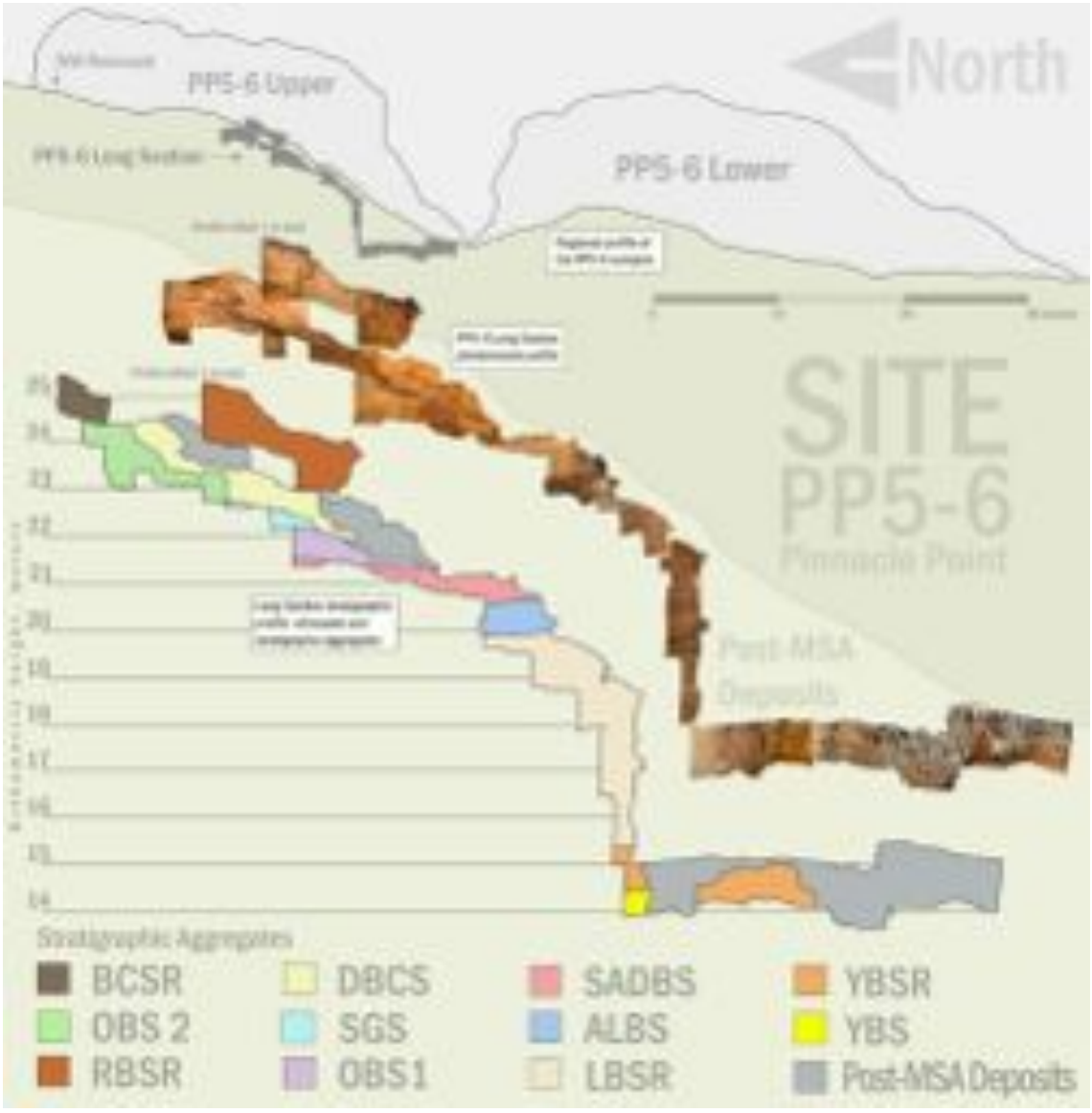

Figura 5. Agregados estratigráficos de PP5-6 de los cuales proceden nuestras muestras de estudio.

Shelly Ashy Brown Sand (SADBS, ~ 72-71 ka). SADBS consiste en un paquete sedimentario con un importante componente de cenizas y cantidades moderadas de roofspall. Se observa una alta intensidad en la ocupación humana caracterizada por la presencia de un gran número de estructuras de combustión y procesos de pisoteo

(*trampling*) que evidencia al carácter reiterado e intensivo de las ocupaciones. En este estrato se observa un cambio en la cultura material (industria lítica) con la aparición de la tecnología microlítica y un mayor uso de silcreta (*silcrete*), la cual se exponía al fuego para facilitar su talla (Brown et al., 2009).

Orange Brown Sand 1 (OBS1, ~ 71-65 ka). OBS1 se trata de un paquete sedimentario de arena eólica de color marrón anaranjado y en general con niveles bajos de roofspall. Se han identificado capas con cultura material y presencia de restos de malacofauna y estructuras de combustión que se alternan con niveles geogénicos de desocupación humana.

Shelly Grey Sand (SGS, ~ 65-63 ka). SGS se caracteriza por presentar un sedimento de origen eólico interestratificado con capas de color marrón oscuro rojizo y un elevado componente en cenizas y restos de malacofauna, y capas de arena eólica de color marrón claro anaranjado con baja densidad de restos de cultura material.

Orange Brown Sand (OBS, ~ 63-60 ka). Este estrato está compuesto principalmente por arenas de origen eólico y presenta varias capas de densa ocupación humana.

Black Ashy Sand (BAS, ~ 60-59 ka). BAS se caracteriza por presentar un sedimento con alto componente en cenizas, de color marrón oscuro y sedimentos negros producto de la gran concentración de estructuras de combustión, que junto con la elevada concentración de restos de cultura material evidencia una intensa ocupación humana.

Black and Brown Coarse Sand and Roofspall (BBCSR, anteriormente BCSR en Karkanas et al., 2015, ~ 60-55 ka). Este estrato se caracteriza por presentar un sedimento de fracción gruesa y una elevada presencia de roofspall. Presenta capas con intensa ocupación humana que se ven alternadas con capas de menor ocupación.

Reddish Brown Sand and Roofspall (RBSR, anteriormente MBSR en Brown et al., 2009, ~ 55-50 ka). Paquete sedimentario caracterizado por un componente eólico de color marrón rojizo y que presenta concentraciones medias de roofspall. Gran parte del sedimento de este StratAgg se ha visto pedogénicamente alterado.

III. Objectives

III. 1. General objectives

This thesis aims to detect patterns in plant exploitation strategies by first modern humans inhabiting Pinnacle Point on the south coast of South Africa during the MSA using phytoliths and mineralogical analyses through infrared spectroscopy.

A second main aim is to understand the response of GCFR environments to glacial-interglacial cycles and rainfall shifts and its implications with the evolution of first modern humans that inhabited the south coast of South Africa during the Late Pleistocene [marine isotope stages (MIS) 5 to MIS3].

III. 2. Specific objectives

1. Build a phytolith reference collection of modern plants from the GCFR that are susceptible of having been used by past populations inhabiting the south coast of South Africa during the MSA. The main goal is to detect phytolith morphotypes characteristic of certain plants and plant parts that can be used as proxies for plant identification in the archaeological deposits at PP5-6.

2. Implement the modern plant phytolith reference collection with phytolith assemblages from modern soils in order to: i) identify phytolith assemblages representative of different vegetation types from extant habitats and to assess the potential preservation biases in natural environments and ii) identify plant uses and reconstruct past environments and climate changes at Pinnacle Point and other south coast sites on the south coast of South Africa.

3. Understand the taphonomic processes that might have affected phytolith preservation and thus their representation in the phytolith record. This accounts for both modern surface soil and archaeological phytolith assemblages.

4. Using the data from the modern plants and soils reference collections together with the mineralogical analysis of the archaeological sediments this thesis aims to characterize the origin (natural or anthropogenic) of phytoliths in the archaeological record. Once anthropogenic phytoliths have been characterized, the study of the archaeological phytolith assemblage from PP5-6 will focus on plant exploitation

strategies. In order to study plant exploitation strategies three main aspects of the phytolith record will be studied:

i. Detect fire fuel used by first modern humans inhabiting Pinnacle Point as well as characterize combustion feature properties through the different StratAggs at PP5-6.

ii. Detect the uses that first modern humans made of plants at PP5-6 in regards to plant consumption (e.g. geophytes) or other practices such as bedding practices, and collecting strategies.

iii. Mode of occupation of the cave in relation to plant exploitation.

5. Relate the strategies of exploitation of vegetal resources detected through the different occupation periods with the reconstruction of the vegetation and the climate of the Pinnacle Point area from MIS5 to 3.

IV. Materials and Methods

IV. 1. Materials

IV. 1.1. Modern plants

Fifty-six plant species were collected over three field seasons, June 2009, November 2010 and June 2012 from three GCFR biomes (Fynbos, Renosterveld, Thicket and Forest) in the south coast of South Africa (Fig. 6). Plants were collected from the natural settings due to the fact that the production of phytoliths and degree of silicification in plants relates, in addition to the plant taxonomic affiliation, to several physical factors such as the climate and environment of plant growth, the physicochemical properties of soils and the silica content in soils (Piperno, 2006 and references therein). Plants were separated whenever possible into their different anatomical components.

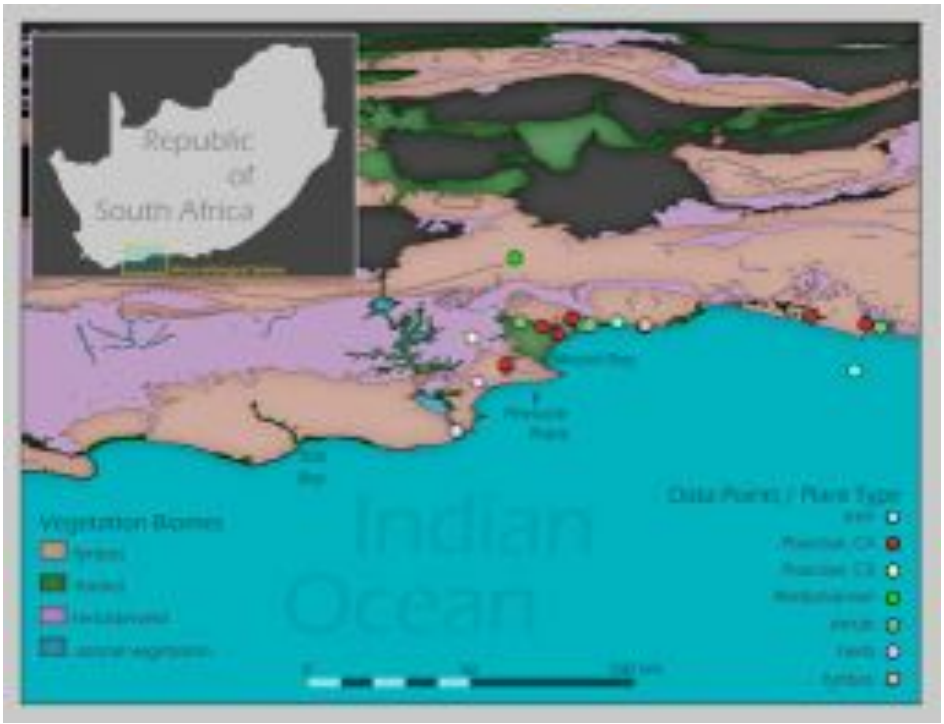

Figure 6. Map showing the location of the modern plant specimens by vegetation types and the major GCFR biomes after Mucina and Rutherford (2006) (map by Erich Fisher).

A total of ninety-seven plant anatomical parts (leaves/bracts, wood, bulb, bulb scale leaf, whole plant) were analyzed from four plant groups: eudicot trees and shrubs, geophytes, restios and grasses.

Twenty-four species of eudicot plants comprising twenty-two genera and fourteen families were analyzed. The anatomical origin of the phytoliths of eudicot species was studied by manually dividing the leaves and the wood. Four herbaceous species, which are *Helichrysum pandurifolium*, *Metalasia muricata*, *Rhoicissus digitata* and *Stoebe plumosa*, were analyzed by processing the whole above-ground part of the plant.

Thirteen species of geophytes comprising eleven genera and five families were analyzed. All the species are monocotyledonous (hereafter monocots) with the exception of *Pelargonium triste*, which belongs to eudicotyledonous plants (hereafter eudicots). The leaves, the bulb scale leaves and the bulbs (plant root) were analyzed separately whenever possible.

Among graminoids, four species comprising three genera were analyzed from the Restionaceae family. Fifteen species comprising thirteen genera and six subfamilies were analyzed from the Poaceae family. In both cases the complete above-ground organs (leaves, steams and the inflorescence– for grasses, and bracts, culms and the inflorescence– for restios) were processed together.

IV. 1.2. Modern surface soil samples

A total of seventy-two modern soil samples (Fig. 7) were collected during June (2006 and 2009), November (2010) and from August to October (2011) from twelve vegetation types corresponding to 4 GCFR biomes, namely limestone fynbos, sand fynbos, mountain fynbos, grassy fynbos (Fynbos biome); renosterveld (Renosterveld biome); strandveld, dune cordon, subtropical thicket, coastal thicket (Thicket biome); coastal forest (Forest Biome) and riparian and wetlands (both azonal) (Fig. 8 and 9).

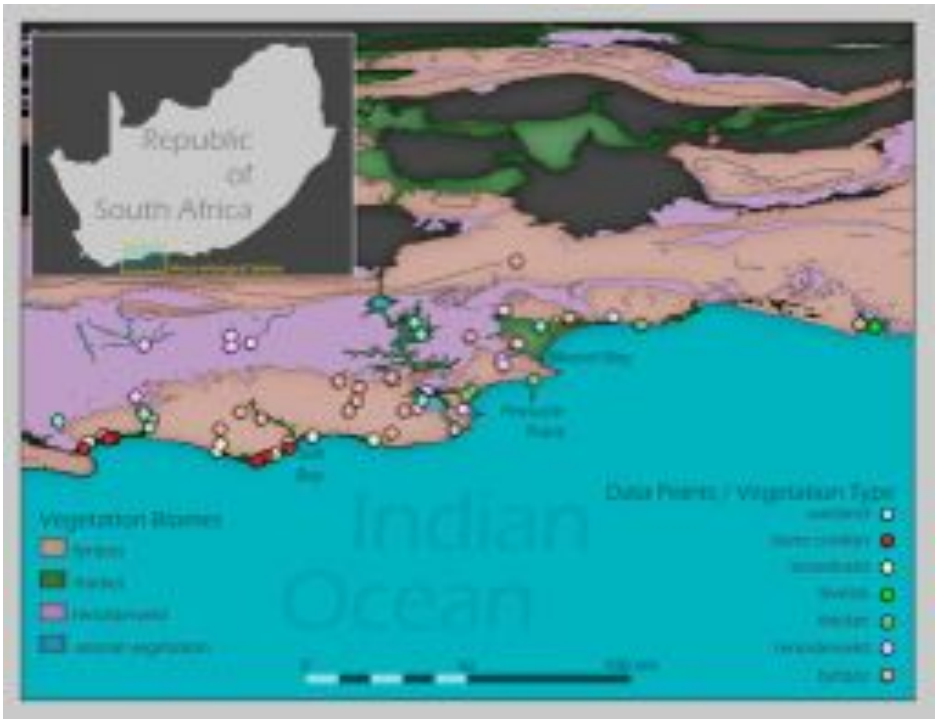

Figure 7. Map showing the location of the modern surface soil samples by vegetation types and the major GCFR biomes after Mucina and Rutherfore (2006) (map retrieved from Esteban et al., in press-a).

Soils were collected beneath intact (not impacted by human-managed activities) soils at 5-10 cm depth in the different vegetation types in proportion to their relative extents in the study area. The study area has not experienced any tectonic activity or significant climate shifts over the past few thousand years (Marean et al., 2014), thus the phytolith assemblages in the topsoil should be representative of the modern vegetation. Since renosterveld in the Southern Cape has been extensively transformed for agriculture, most samples were collected from slopes too steep for cultivation (Kemper et al., 2000). Several related aspects that might have influenced the configuration of phytolith assemblages and their concentration and preservation in modern soils have also been taken into account, including: vegetation type, dominant plant species, soil texture and soil pH.

Figure 8. Photographs of the different vegetation types studied. a-b) limestone fynbos; c-d) sand fynbos; e) grassy fynbos; f) renosterveld.

IV. 1.3. Archaeological samples

A total of one hundred eighty-three samples were collected from the Long Section at PP5-6 belonging mainly to combustion features and other general anthropogenic layers. Of these, twenty-three control samples were collected from different geogenic layers in order to establish whether the plant phytolith remains found in anthropogenic layers represent anthropogenic input. Figure 10 shows the StratAggs of PP5-6 site from where samples were collected.

Figure 9. Photographs of the different vegetation types studied. a) subtropical thicket; b) coastal thicket; c) strandveld; d) dune cordon; e) riparian; f) wetland; g) coastal forest.

Samples from combustion features were collected from different layers, which are from top to bottom the white, black and red layers (Fig. 11). Samples from above and outside the visible hearths were also collected whenever possible. The red layer is

understood as the sample from below hearths (Albert et al., 2000; Mallol et al., 2013). This was mainly possible in YBSR and LBSR StratAggs where practically intact combustion features are preserved as the result of high and relatively constant rate of geogenic input, particularly roofspall, together with low rates of anthropogenic activity (most probably trampling) that prevented their destruction (Karkanas et al., 2015).

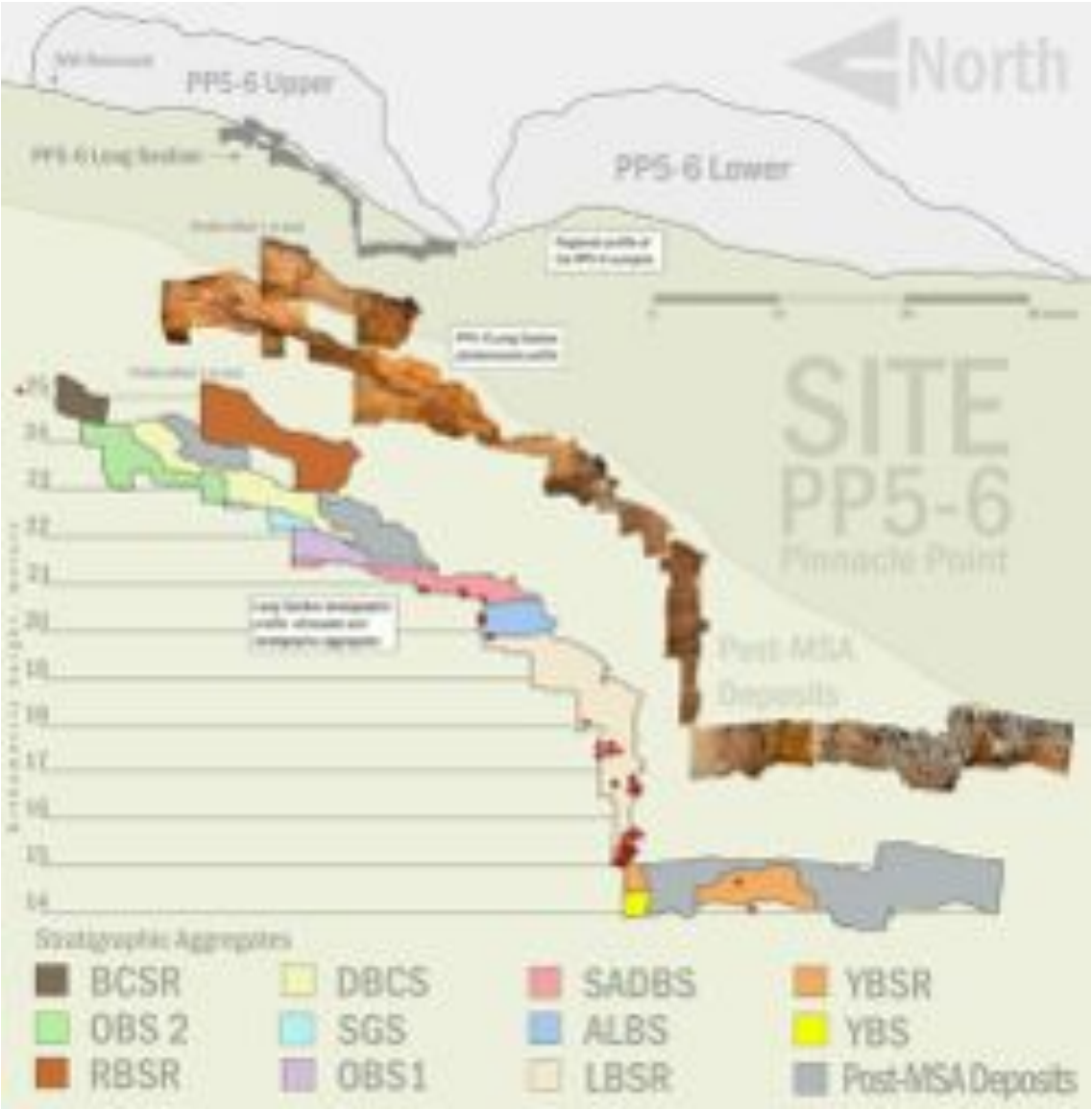

Figure 10. Long Section stratigraphic silhouette showing the stratigraphic aggregates and phytolith sample location (bottom) after Karkanas et al. (2015) (figure by Erich Fisher).

Conversely in SADBS complete single combustion features were not easily discernible since this StratAgg consists of a thick sequence of overlapping trampled combustion microfacies with a few isolated lenses of intact combustion features identified mostly microscopically (Karkanas et al., 2015).

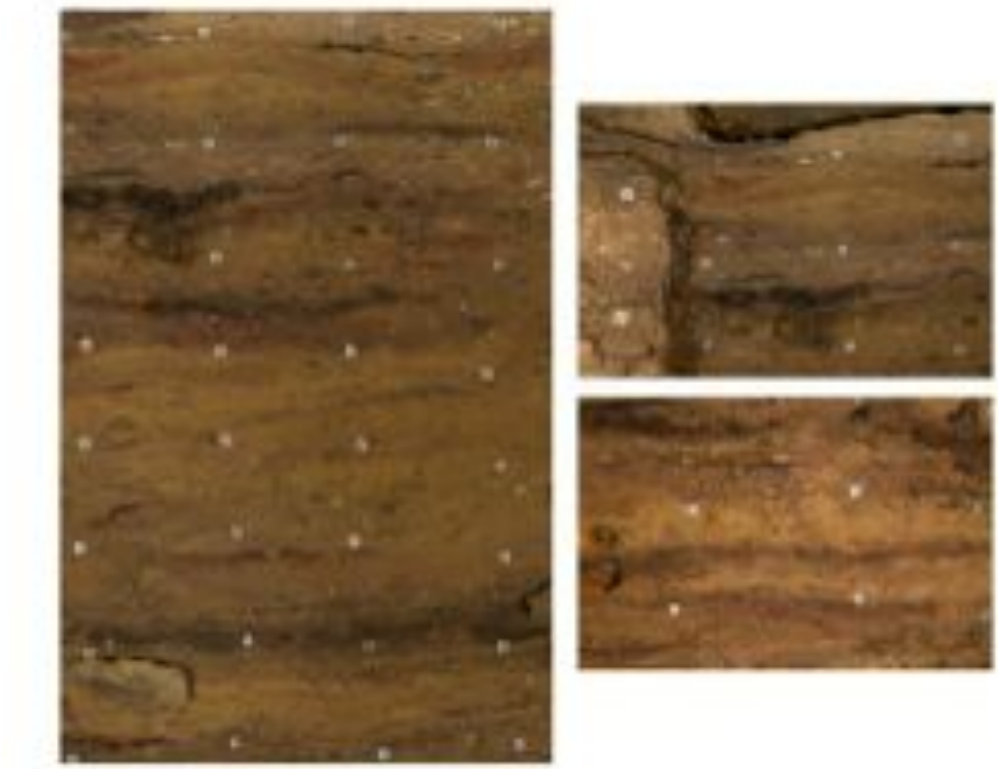

Figure 11. General photographs of the cliff face of the LBSR unit showing distinct combustion features.

IV. 2. Methods

IV. 2.1. Phytolith extraction

IV. 2.1.1. Phytolith extraction from modern plants

Phytolith extraction from plants was carried out at the Laboratory of History and Archaeology of the University of Barcelona. The procedure is a modification of the methods described in Albert and Weiner (2001) and Parr et al. (2001). Washed and air dried aliquots were weighed and burned in a muffle furnace at 500 ºC for 2.5 hours. The wood of eudicot trees and shrubs were burned for 4 hours. The ash was treated with hydrochloric acid (1 N HCl) for 30 min at 500ºC, to leave only the siliceous minerals where phytoliths are found. The inorganic acid insoluble fraction (AIF)[4] was centrifuged, re-suspended in deionized water, and centrifuged again. The supernatant was discarded and the washing was repeated three times. The pellet was transferred to a Petri dish and about 10 ml of 30% hydrogen peroxide (H_2O_2) was added. The sample was evaporated on a hot plate at 70°C. More hydrogen peroxide was added as needed until all bubbling ceased. The remaining residue was carefully removed from the Petri dish, weighed, and transferred into an Eppendorf tube for storage. Microscope slides were prepared using around 1 mg of the final fraction with Entellan mounting media (Merck). Quantification and morphological identification of phytoliths took place at 400x magnification using an optical microscope (Olympus BX41). The quantification of phytolith production in plants follow the calculation developed by Albert et al. (1999).

The wood material was processed together with the bark and contrariwise to Albert and Weiner (2001) no previous sonication was conducted in order to assess the percentage of phytolith contamination from other plants. Assessing phytolith contamination from other plants when studying the use of fuel wood in combustion features from archaeological sites is of major importance for the possible bias in the interpretation of the data. And that is why this procedure was only carried out on the wood and not in other plant parts. Here we consider that a phytolith morphotype is the

[4] The AIF is the fraction remaining after the more acid soluble minerals have been removed and it is mainly composed of siliceous aggregates and silica phytoliths (Albert et al., 1999).

result of contamination when they are known to be produced exclusively by grasses (Poaceae) and these are the GSSCs (Piperno, 1988, 2006).

IV. 2.1.2. Phytolith extraction from modern soils and archaeological sediments

The phytolith extraction from modern soils and archaeological sediments was carried out at the Laboratory of History and Archaeology of the University of Barcelona and followed Katz et al. (2010). An initial sediment weight of between 30 and 50 mg was required. Carbonate minerals were dissolved adding 50 µl of 6 N HCl. After the bubbling ceased, 450 µl of 2.4 g/ml sodium polytungstate solution $Na_6(H_2W_{12}O_{40}).H_2O$] was added. The tube was vortexed, sonicated and centrifuged for 5 min at 5000 rpm (MiniSpin plus, Eppendorf). The supernatant was subsequently removed to a new 0.5 ml centrifuge tube and vortexed. For examination under the optical microscope, an aliquot of 50 µl of the supernatant was placed on a microscope slide and covered with a 24 mm 24 mm cover-slip. Quantification of the total phytoliths was based on 20 fields at 200 magnification whereas morphological identification of phytoliths took place at 400 magnification using the same optical microscope referenced above. A minimum of 200 phytoliths were counted for the morphological analysis and when this was not possible only those samples with a minimum number of 50 phytoliths were analyzed in order to obtain as much information as possible (Albert and Weiner, 2001).

IV. 2.2. Phytolith morphological identification and classification

Phytolith identification and characterization was conducted on the basis of the anatomical and taxonomical origin and when this was not possible of the morphological features, which consist mainly of the three dimensional structure of the morphotypes what is the top, the side and the base, were used (following Mullholland and Rapp, 1992). Table 1 lists the phytolith morphotypes identified in plant specimens and modern surface soils from the GCFR and archaeological sediments from PP5-6. The classification of the phytolith morphotypes from graminoids was also checked on previous studies from modern grasses and restios from South Africa (Rossouw, 2009;

Cordova and Scott, 2010; Cordova, 2013). For the classification of eudicot plants previous studies conducted in other geographical areas were also consulted (Albert and Weiner, 2001; Bamford et al., 2006; Tsartsidou et al., 2007; Mercader et al., 2009; Collura and Neumann, in press; Albert et al., 2016- available in www.phytcore.org). Additionally, standard literature (Mulholland and Rapp, 1992; Piperno, 1988, 2006; Twiss et al., 1969 and references therein) was also accessed when necessary.

Morphological identification of phytoliths from modern surface soils and archaeological sediments was based on the modern plant reference collection built in this thesis and on the previous works cited. The terminology for describing phytolith morphotypes was based on the anatomical and/or taxonomic origin of the phytoliths. When this was not possible, geometrical traits were followed. The International Code for Phytolith Nomenclature (ICPN) was followed for naming and describing the phytoliths (Madella et al., 2005).

Sample data including microphotographs, samples information, counting and morphological classification from the material studied in this thesis work (plants, soils and archaeological sediments) will be available in www.phytcore.org.

IV. 2.3. Phytolith indices

Phytolith indices have been used widely for paleoecological reconstructions as indicators of aridity [Iph (%) index] (Diester-Haass et al., 1973; Alexandre et al., 1997; Novello et al., 2012); climate conditions based on the C_3-C_4 grass distribution [Ic index] (Twiss, 1992; Barboni et al., 2007; Bremond et al., 2008); tree cover density [D/Pº index] (Alexandre et al., 1997-D/P index; Barboni et al., 1999; Bremond et al., 2005b, 2008); evapotranspiration and water stress [Fs index] (Delhon, 2005; Bremond et al., 2005a; Strömberg et al., 2007); and aquatic and xerofitic grass dominance [Iaq and Ixe indices] (Novello et al., 2012, 2015).

Here, we used the D/Pº index (Bremond et al., 2008) to identify shrubby vegetation/tree cover density, which is defined as follows:

$$\frac{psilate\ spheroids + rugulate\ spheroids}{\sum Grass\ Silica\ Short\ Cells\ (Rondels,\ Lobates,\ Saddles, and\ Oblongs)}$$

The Ic (Twiss, 1992; Barboni et al., 2007; Bremond et al., 2008) and Iph (Diester-Haass et al., 1973; Alexandre et al., 1997; Novello et al., 2012) indices were also used in order to further characterize grass distribution among vegetation types. We modified the formula by eliminating the percentage in order to be compared with the other indices used, so they are defined as follows:

$$\text{Ic} = \frac{GSSC\ Rondels\ (rondels, towers, trapezoids\ and\ oblongs)}{\sum GSSCs}$$

$$\text{Iph} = \frac{GSSC\ Saddles}{\sum GSSCs\ Saddles\ and\ Lobates\ (bilobates,\ polylobates\ and\ crosses)}$$

The Fs index (after Strömberg et al., 2007) was used in order to detect wet conditions or high evapotraspiration rates of grasses, and it is defined as follows:

$$\frac{Bulliform\ cells}{\sum GSSCs}$$

Furthermore, we use a new phytolith index that is specific to the identification of fynbos vegetation, which is termed the Fy index (Esteban et al., in press-a). Since fynbos is shrub-dominated vegetation with a high Restionaceae and a low grass component (Bergh et al., 2014), we defined the Fy index as the ratio of restio phytoliths and spheroids psilate and rugulate phytoliths to the sum of GSSCs, which is defined as follows:

$$\frac{restio + psilate\ spheroids + rugulate\ spheroids\ phytoliths}{\sum GSSCs\ (Rondels,\ Lobates,\ Saddles\ and\ Oblongs)}$$

IV. 2.4. Statistical analysis

IV. 2.4.1. Modern plants

Shaphiro-Wilk test was used to test if phytoliths were normally distributed among all plant species. Since data was normally distributed, one-way ANOVA and a post hoc Tukey Honest Significant Differences (HSD) tests was performed to detect statistically significant differences in phytolith morphotypes among plant types and plant parts

(eudicot wood, eudicot leaves, whole eudicots, leaves of geophytes, bulb scale leaves of geophytes, edible part of the bulb of geophytes, restios, C_3 and C_4 grasses). These tests account for the variation in total numbers of phytolith morphotypes counted for each plant type and plant part. All phytolith morphotypes were considered in the analyses including those that are known to come from contamination. The null hypothesis in each test assumes that there are no significant differences in the distribution of phytolith morphotypes between plant types and plant parts. All statistical procedures were performed with the JMP-SAS12.1.0 software.

Table 1. List of phytolith morphotypes observed in plant specimens and modern surface soils from the GCFR and archaeological sediments from PP5-6. L= length, W= width, T=tall.

Morphotypes	**Description**	**References**
Bulliform	Outgrowths of the cell wall, sometimes forming part of the ground tissue of the leaf	Kondo et al., 1994; Albert, 2000; ICPN working group-Madella et al., 2005
Blocky Polyhedral	Compacted or elongated, faceted, relatively plate-like bodies with polyhedral outline	Bozarth, 1993; Strömberg, 2003; Mercader et al,
Cone-shape	Widest at the base and tapering to the apex	ICPN working group-Madella et al., 2005
Cystolith	Large phytoliths with verrucate, echinate or tuberculate surface decorations. They have a characteristic stalk where the phytoliths were attached to the cell wall	Bozarth, 1992
Ellipsoid	A body with at least one set of parallel cross-sections resembling ellipses and the rest resembling circles.	Albert, 2000
Ellipsoid echinate	Ellipsoid with echinate ornamentation	
Elongate without decoration margin	Elongate bodies with circular or parallelepipedal (four-sided) shape in cross section and without ornamentation in the margins; L>2W and W>T	Runge, 1999; Kondo et al., 1994; Albert, 2000; ICPN working group-Madella et al., 2005; Piperno, 1988
Elongate blocky	Elongate; L>W and T>1/2W	Barboni et al., 1999; Albert 2000
Elongate blocky echinate	Elongate blocky with echinate ornamentation in the margins	

Parallelepiped blocky striate	Parallelepiped blocky showing striate decoration	
Elongate bulbous	Elongate with bulbous outlines	
Elongate curved	Elongate with curved outlines	
Elongate facetate	Elongate with facetate surface ornamentation	
Elongate striate	Elongate with striate texture	
Elongate tuberculate	Elongate with tuberculate ornamentation in the margins	
Elongate verrucate	Elongate with verrucate texture	
Elongate with decorated margins	Elongate bodies with circular or parallelepipedal (four-sided) shape in cross section having ornamentation in the margins; L>2W and W>T	Runge, 1999; Kondo et al., 1994; Albert, 2000; ICPN working group-Madella et al., 2005; Piperno, 1988
Elongate dendritic	Elongates with dendrifrom ornamentation in the margins	
Elongate echinate	Elongates with echinate ornamentation in the margins	
Elongate echinate one side	Elongates with echinate ornamentation only in one of the margins	
Elongate sinuate	Elongates with sinuate ornamentation in the margins	
Elongate polylobate	Elongate with polylobate ornamentation in the margins	
Epidermal ground-mass	Silicification of the groundmass of the epidermal tissue. No outlines discernible	Metcalfe and Chalk, 1957; Stromber, 2003; ICPN working group-Madella et al., 2005
Epidermal ground mass elongate	Epidermal ground mass, cells showing elongate outlines	
Epidermal ground mass polyhedral	Epidermal ground mass, cells showing polyhedral outlines	
Epidermal ground mass sinuate	Epidermal ground mass, cells showing sinuate outlines	
Epidermal ground mass rings	Epidermal ground mass, cells showing ring shape	
Epidermal ground mass dots	Epidermal ground mass with dot ornamentation	
Hair cell (trichomes)	Epidermal appendage hair cells (trichomes)	Albert, 2000
Hair cell (prickles)	Silicified bodies from both epidermal and subepidermal tissue and typically are more massive than trichomes.	ICPN working group-Madella et al., 2005
Hair cell aciculate	Epidermal appendage hair cells (trichomes), needle-shaped	ICPN working group-Madella et al., 2005
Hair cell armed	Epidermal appendage hair cells (trichomes), with appendices	ICPN working group-Madella et al., 2005
Hair cell with protuberances	Epidermal appendage hair cells (trichomes), with protuberances	ICPN working group-Madella et al., 2005
Hair cell curved	Epidermal appendage hair cells (trichomes), curved shape	ICPN working group-Madella et al., 2005

Hair cell unciform	Epidermal appendage hair cells (trichomes), hook-shaped	ICPN working group-Madella et al., 2005
Hair base	Epidermal appendage hair base	ICPN working group-Madella et al., 2005
Hair base sinuates shape	Epidermal appendage hair base with sinuates outlines	
Hat-shape	Conical shapes with round base and apex	Ollendorf, 1992; Runge, 1999; Albert et al., 2006; Piperno, 2006
Indeterminate	Indescribable phytolith elements, broken or that cannot be identified as geometrical or cannot be described in any other way	Albert, 2000
Irregular	Phytoliths showing irregular, non-geometrical shapes	Albert, 2000
Irregular echinate	Irregulars with echinate ornamentation	
Irregular facetate	Irregulars with facetate surface ornamentation	
Irregular verrucate	Irregulars with verrucate surface ornamentation	
Irregular with protuberance	Irregulars with protuberances surface ornamentation	
Papillae	Epidermal appendage from grasses that have a wide, spheroid or angular base and a small short tip. The tip can have a rounded or pointed top	Ollendorf, 1992; ICPN working group-Madella et al., 2005
Parallelepiped thin	Four-sided geometrical figure in which every side is parallel to the side opposite; L<2W and T<l/2 T	Albert, 2000
Parenchyma strand	Poor silicified parenchymatous tissue	
Polyhedral	Isolated cell showing polyhedral outlines that probably belongs to an epidermal ground mass	Geis, 1973; Bozarth, 1992
Platelet	Irregular forms, thin, with variable surface. Probably from epidermal ground mass tissues	Albert, 2000
Sclereid	Silicified sclereid cell showing elongate irregular shapes sometimes branchy-shaped	Kondo and Pearson, 1981; Piperno, 1988; Kondo et al., 1994; Runge, 1999
GSSC lobate		Mulholland, 1989; Fredlund and Tieszen, 1994; ICPN working group-Madella et al., 2005Piperno, 2006; Fahmy, 2008; Novello et al., 2012; Rossouw, 2009; Cordova and Scott, 2010
bilobate tabular flattened-concave	GSSC bilobate tabular with flattened-round lobes and short sank	

	lobes		
	bilobate tabular flattened lobes	GSSC bilobate tabular with flattened lobes and short sank	
	bilobate tabular rounded lobes, short shank	GSSC bilobate tabular with rounded lobes and short shank	
	bilobate tabular rounded lobes, long shank	GSSC bilobate tabular with rounded lobes and long shank	
	bilobate trapeziform notched lobes	GSSC bilobate trapeziform with notched lobes and short sank	
	bilobate tabular angulate lobes	GSSC bilobate tabular with angulate lobes and short sank	
	bilobate tabular angulate asymmetrical lobes	GSSC bilobate tabular with angulate asymmetrical lobes and short sanks	
	bilobate tabular segmented angulate/planar lobes	GSSC bilobate tabular with one lobe showing an angulate shape and the other lobe showing a planar shape	
	bilobate trapezoid	GSSC bilobate trapezoid similar to the so-called Stipa-type bilobate	
	bilobate trapezoid wavy top	GSSC bilobate trapeziform with wavy top decoration	
	cross trapeziform	GSSC trapeziform with four lobes	
	cross tabular	GSSC tabular four lobes	
	trilobate	GSSC three lobes	
	polylobate	GSSC more than three lobes	
GSSC rondel			Mulholland, 1989; Fredlund and Tieszen, 1994; Piperno and Pearsall, 1998; ICPN working group-Madella et al., 2005; Piperno, 2006; Novello et al., 2012; Rossouw, 2009; Cordova and Scott, 2010
	rondel cilyndric	GSSC rondel cilyndric	
	rondel conical	GSSC rondel conical	
	rondel conical wavy top	GSSC rondel conical with wavy top	
	rondel keeled	GSSC rondel keeled	
	long tower	GSSC long tower	
	long tower wavy top	GSSC long tower with wavy top	
	trapeziform	Cubic/parallelepipedal/four-sides bodies	
GSSC oblong			Mulholland, 1989; Fredlund and Tieszen, 1994; Rossouw, 2009; Cordova and Scott, 2010;

		ICPN working group-Madella et al., 2005;
oblong tabular	GSSC oblong tabular	
oblong trapeziform sinuate	GSSC oblong trapeziform sinuates	
rounded tabular	GSSC round tabular	
GSSC saddle		Piperno and Pearsall, 1998; ICPN working group-Madella et al., 2005; Piperno, 2006
saddle	GSSC saddle	
collapsed saddle	GSSC saddle with collapsed sides	
Spheroid echinate	Spherical bodies showing echinate ornamentation	Piperno, 1988, 2006; Barboni et al., 1999, 2007; Runge, 1999; Mercader et al., 2000; Strömberg, 2004; Albert et al., 2006, 2009
Spheroid psilate	Spherical bodies showing psilate texture	Albert, 2000
Semi spheroid	Semi-spherical bodies	-
Small spheroid	Small spherical bodies	-
Large spheroid	Large spherical bodies	-
Large spheroid facetate	Large spherical bodies showing facetate ornamentation	-
Large spheroid granulate and verrucate	Large spherical bodies, sometimes irregular or with protuberances, showing granulate and verrucate surfaces. Produced by Restionaceae	Cordova and Scott, 2010; Esteban et al., in press-a
Spheroid spiraling decorations	Spherical bodies showing spiraling decorations, sometimes showing a double ring on the edges. Produce by Restionaceae	Cordova and Scott, 2010; Esteban et al., in press-a
Spheroid rugulate	Spherical bodies showing rugulate texture	Albert, 2000, ICPN working group–Madella et al., 2005
Stomata	Silicified stomal pores, sometimes surrounded by neighboring or guard cells	Rovner, 1971
Tracheid (vascular tissue)	Elongates/cylindric shapes with sulcate ornamentation	Kondo et al., 1994; Piperno, 2006

IV. 2.4.2. Modern surface soil samples

The statistical analysis conducted for the phytolith dataset from modern surface soil samples was performed through one-way ANOVA and a post hoc Tukey (HSD) tests in order to identify those morphotypes that are statistically representative of specific vegetation types or biomes. These tests account for the variation in total numbers of

phytolith morphotypes counted for each vegetation type and biome. The null hypothesis in each test assumes that there is no significant difference in the distribution of phytolith morphotypes between the different vegetation types and biomes from the GCFR. The non-parametric Kruskal Wallis test was also used to identify significant differences in the mean values of phytolith indices between vegetation types since data were non-normally distributed (Shapiro-Wilk test for normality). All statistical procedures were performed with the JMP- SAS12.1.0 software. Samples from mountain fynbos, fynbos/renosterveld, dune cordon, coastal forest and wetlands were excluded from the statistical analysis due to the absence of replicated samples from the same vegetation type or because phytoliths were absent or identified in few concentrations as occurred for dune cordon vegetation. Only samples from riparian vegetation represent Azonal vegetation.

IV. 2.4.3. Archaeological sediments

We use the same statistical approach for the archaeological sediment samples as for modern surface soil samples (Section IV. 2.4.2.). Statistical analysis one-way ANOVA and a post hoc Tukey (HSD) tests were performed on the dataset in order to identify specificities in the distribution of phytolith indices between samples from different StratAggs from PP5-6. The null hypothesis in each test assumes that there are no significant differences in the distribution of phytoliths among StratAggs at the site. Statistical procedures were performed with the JMP-SAS12.1.0 software. The only sample interpreted from BBCSR of PP5-6 site was excluded from the statistical analysis due to the absence of replicated samples from this StratAgg.

IV. 2.5. Plant anatomy

Thamnochortus insignis (Restionaceae) was selected for anatomical analysis. The culm and the bracts were investigated. Material was sectioned with a freezing and rotary microtome (Ernst Leitz GMBH, Wetzlar, Germany and Jung AG Heidelberg, Germany); the thickness of the sections between 30-60 µm. After that some sections were stained with a mixture of alcian blue and safranin other kept unstained. Sections were mounted in Euparal and studied under a light microscope (Olympus CX41RF).

Digital images were taken with an Olympus Stream Essentials 1.8 Imaging System. All the analyses were undertaken at the Department of Botany of the University of Johannesburg.

The sections were also analyzed by scanning electron microscopy (SEM) (Quanta 200 SEM) at the Microscopy and Microanalysis Unit of the University of the Witwatersrand. Energy-dispersive X-ray analysis (EDXA) was performed by using the INCA 200 system in order to detect the chemical composition of the particles identified as phytoliths.

IV. 2.6. Mineralogical analysis

Fourier Transform Infrared Spectroscopy (FTIR) was used to identify the bulk mineral components of the archaeological sediments. Infrared spectra were obtained using KBr pellets at 4 cm-^{1} resolution with a Nicolet iS5 spectrometer. In order to assess the origin of the calcite, we have applied the infrared grinding curve method developed by Regev et al. (2010) based on the measurement of the ratio of v_2/v_4 heights (1420 cm^{-1} and 713 cm^{-1}, respectively) normalized to a v_3 height (874 cm^{-1}). Clays exposed to high temperatures were identified using specific absorptions in the clay spectrum (Berna et al., 2007).

V. Results

V. 1. Modern plants

Phytolith results obtained from the study of modern plants, including the total number of phytoliths counted, and the relative phytolith concentration in grams per plant material (hereafter – /g plant) is listed in Table 2. Phytolith concentration accounts for any phytolith identified indistinctively of the plant type they are known to be produced by. Grasses were the highest phytolith producers among the different plants and plant parts analyzed, while the wood/bark of eudicot plants together with the leaves were the lowest. Geophytes presented high phytolith concentration and mainly from the bulb scale leaves. Nevertheless, most of the phytoliths identified were GSSCs, which are known to be produced by grasses.

A total of eighty phytolith morphotypes were identified in the whole data set. Phytolith frequencies of each morphotype identified in plant species is available in the Appendix (Table A1). Grasses and restios produced characteristic phytolith morphotypes that did not occur in other plant groups and that are diagnostic of the Poaceae and Restionaceae families. But many other phytolith morphotypes occurred in more than one plant group. We used statistical analysis in order to see finer distinctions among phytolith morphological distribution between plant parts and plant types.

Phytolith contamination in plants was evaluated on the basis of the identification of phytolith morphotypes known to be characteristic from other plants such is the case of GSSCs, which belong to and characterize the Poaceae family or restio phytoliths (see Section V. 1.2.2.).

One-way ANOVA and a post hoc Tukey's HSD tests showed statistical significant differences in twenty-five out of the eighty phytolith morphotypes identified between the nine plant types analyzed and a population of ninety [C_3 grasses (Pooideae, n= 2; Ehrhartoideae, n= 1; Danthonioideae, n= 3; Aristidoideae, n= 1); C_4 grasses (Panicoideae, n= 6; Chloridoideae, n= 2); Restionaceae, n= 4; leaves of geophytes, n= 13; the bulb scale leaves of geophytes, n= 9; edible part of the bulb of geophytes, n= 9; the wood/bark of eudicot plants, n= 18; the leaves of eudicots, n= 18, and whole shrubs, n= 4]. Despite we are aware that this is a small reference sampling, because there are not previous studies of the nature of the present study from the GCFR, we consider that these results establish a key starting point for future research. The *p-values* after ANOVA and the results of the post hoc Tukey's test for the eighty phytolith morphotypes are given in Table 3.

V. 1.1. Eudicotyledonous plants

V. 1.1.1. Wood/bark

Phytolith concentration– Phytolith concentration in the wood/bark of trees and shrubs was very low, ranging from 100 to 13,000 phytoliths/g original plant material, with the highest concentration in *Acacia karoo* and *Celtis africana*. Only *Grewia occidentalis* did not present phytoliths (Table 2).

Contamination from other plants– Phytolith morphotypes known to be produced by grasses (GSSC) and restios, such as large spheroids with granulate and verrucate surfaces and spheroids showing spiraling surface ornamentation, were identified in relatively high frequencies in the wood/bark samples (see Section V. 1.2.2.). Because *Pterocelastrus tricuspidatus* did not show any characteristic phytolith morphotype from wood/bark and only two phytoliths were detected, it was not considered when calculating the range of contamination in wood/bark. Thus, phytolith contamination in wood/bark varies from 0 to 44.4% of the total of the phytolith assemblage identified (mean: 16.3%) (Fig. 12).

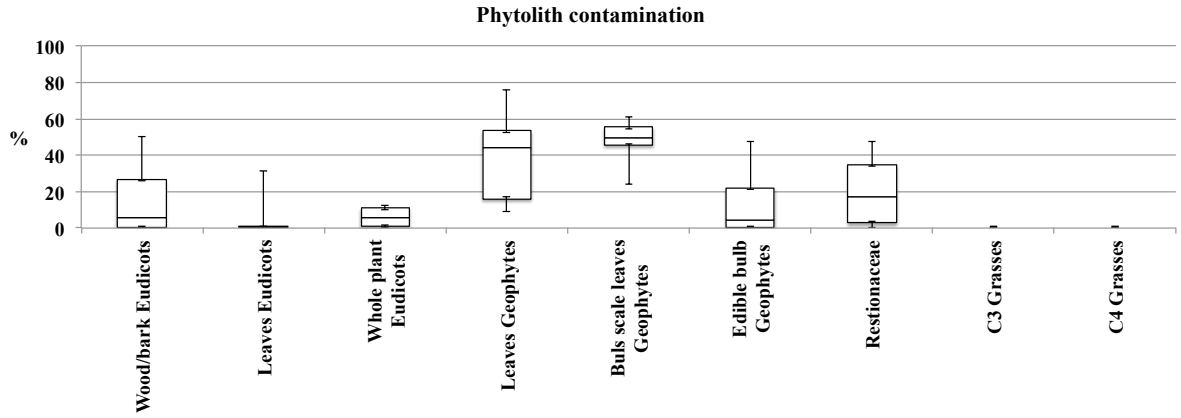

Figure 12. Box plot showing the phytolith contamination from other plants in the nine plant types analyzed (wood/bark, leaves and whole plant of eudicots, leaves, bulb scale leaves and edible part of the bulb of geophytes, restios and C_3 and C_4 grasses). The mean values (mid-line), standard error ± (box) and standard deviation (whiskers) are given for the eight plant types and plant parts.

Table 2. Plant species and plant parts analyzed, taxonomic affiliation, photosynthetic pathway of Poaceae, plant significance, vegetation type where plants were collected and the coordinates of the sampling area, as well as the total of phytoliths counted, and the relative phytolith concentration in grams per plant material.

Plant species	Plant type	Family/Subfamily/Photosynthetic pathway	Potential plant information	Vegetation type provenance	Sampling area (coordinates)		Plant part	# Phytoliths counted	Phyt / gram of plant
Acacia karoo	Tree or shrub	Fabaceae	Tree good for fire	Riparian	34º10.751'	022º57.653'	Leaves	117	1,158
							Wood	69	5,759
Cassine peragua	Tree	Celastraceae	Typical of the coastal areas	Coastal Thicket	34º02.799'	022º18.670'	Leaves	546	11,613
							Wood	49	138
Celtis africana	Tree or shrub	Celtidaceae	Big tree, wood for fire and maybe spears, climate indicator	Coastal Forest	34º03.693'	023º01.834'	Leaves	340	276,317
							Wood	111	12,996
Elytropappus rhinocerotis	Shrub	Asteraceae	Medicinal uses. Vegetation indicator	Renosterveld	34º02.863'	022º02.741'	Leaves	539	4,125
							Wood	28	1,530
Eriocephalus africanus	Shrub	Asteraceae	Medicinal uses.	Subtropical Thicket	34º03.543'	022º23.043'	Leaves	4759	8,931
							Wood	8	1,137
Euclea racemosa	Tree or shrub	Ebenaceae	Typical of the coastal areas	Coastal Thicket	34º03.375'	022º13.347'	Leaves	0	0
							Wood	21	1,744
Grewia occidentalis	Tree or shrub	Tiliaceae	Good for fire and maybe spears, quite flexible	Coastal Thicket	34º04.257'	022º09.863'	Leaves	79	150,773

							Wood	0	0
Leucospermum praecox	Shrub	Proteaeceae	Fire test	Sand Fynbos	34º20.679'	021º52.121'	Leaves	0	0
							Wood	58	134
Morella cordifolia	Shrub	Myricaceae	Vegetation indicator	Dune Cordon	34º03.373'	022º14.190'	Leaves	1137	2,493
							Wood	4	374
Olea europaea* subsp. *africana	Tree or shrub	Oleaceae	Good for fire and spear	Coastal Thicket	34º04.257'	022º09.863'	Leaves	778	367
							Wood	10	538
Passerina vulgaris	Shrub	Thymelaeaceae	Bark for tying things, flexible bark and strong	Renosterveld	34º02.863'	022º02.741'	Leaves	204	5,316
							Wood	2	334
Protea lanceolata	Shrub	Proteaceae	Vegetation indicator	Sand Fynbos	34º02.858'	022º02.747'	Leaves	426	298
							Wood	16	165
Protea repens	Tree or shrub	Proteaceae	Fire test and vegetation indicator	Sand Fynbos	34º20.679'	021º52.121'	Leaves	11	555
							Wood	1	100
Pterocelastrus tricuspidatus	Tree or shrub	Celastraceae	Good for fire and spears	Coastal Thicket	34º04.257'	022º09.863'	Leaves	504	151,713
							Wood	2	168
Searsia crenata	Tree or shrub	Anacardiaceae	Good for fire and small branches, good to start fires	Coastal Thicket	34º04.257'	022º09.863'	Leaves	942	5,321
							Wood	9	562

Searsia pterota	Tree or shrub	Anacardiaceae	Bush good for fires, edible berries	Coastal Thicket	34º04.773'	022º09.226'	Leaves	430	27,485
							Wood	7	224
Sideroxylon inerme	Tree or shrub	Sapotaceae	Good for fire, hard Wood. Bark for medicinal purposes	Coastal Thicket	34º04.257'	022º09.863'	Leaves	1199	4,710
							Wood	595	3,383
Vepris undulata	Tree or shrub	Rutaceae	Big tree, wood for fire and maybe spears, climate indicator	Coastal Forest	34º03.693'	023º01.834'	Leaves	968	49,576
							Wood	1	98
Tarchonanthus camphoratus	Tree or shrub	Asteraceae	Narcotic-medicinal uses	Thicket	34º04.773'	022º09.226'	Leaves	142	64,561
					34º04.773'	022º09.226'	Wood	43	544
Leucadendron galpinii	Shrub	Proteaceae	Fire test	Sand Fynbos	34º20.679'	021º52.121'	Leaves	0	0
Helichrysum pandurifolium	Herb	Asteraceae	Medicinal uses. Perfume and repellent	Renosterveld - Thicket transition	34º12.632'	021º55.742	Whole plant	146	4,129
Metalasia muricata	Shrub	Asteraceae	Good to start fires	Strandveld	34º03.315'	022º23.206'	Whole plant	1099	106,683
Rhoicissus digitata	Climber	Vitaceae	Edible tubers raw or roasted	Coastal Thicket	34º03.313'	022º23.207'	Whole plant	555	24,218
Stoebe plumosa	Shrub	Asteraceae	Good to start fires	Grassy fynbos	34º03.693'	023º01.834'	Whole plant	272	23,250
Babiana fourcadei	Herb, geophyte	Iridaceae	Edible	Renosterveld	34º09.816'	022º00.456'	Leaves	166	60,500
							Cover bulb	256	252,200
							Bulb	11	50
Trachyandra sp	Geophyte	Asphodelaceae	Edible	Renosterveld	34º09.816'	022º00.456'	Leaves	334	70,000

Tritonia crocata	Herb, geophyte	Iridaceae	Edible	Renosterveld	34º09.823'	022º00.481'	Leaves	228	13,400
							Cover bulb	289	40,900
							Bulb	6	300
Pelargonium triste	Geophyte	Geraniaceae	Edible	Renosterveld	34º09.854'	022º00.518'	Leaves	352	617,200
							Bulb	106	86,000
Watsonia laccata	Herb, geophyte	Iridaceae	Edible	Renosterveld	34º09.865'	022º00.447'	Leaves	268	15,200
							Cover bulb	279	154,700
							Bulb	12	50
Moraea unguiculata	Herb, geophyte	Iridaceae	Edible	Renosterveld	34º09.889'	022º00.415'	Leaves	309	22,700
							Cover bulb	346	126,250
							Bulb	0	0
Moraea sp	Herb, geophyte	Iridaceae	Edible	Renosterveld	34º09.957'	022º00.411	Leaves	416	117,300
							Cover bulb	28	25,200
							Bulb	25	100
Freesia alba	Herb, geophyte	Iridaceae	Edible	Sand Fynbos	34º20.679'	021º52.121'	Leaves	22	1,750
							Cover bulb	0	0
							Bulb	24	100
Gladiolus rogersii	Herb, geophyte	Iridaceae	Edible	Sand Fynbos	34º20.679'	021º52.121'	Leaves	47	2,600
							Cover bulb	0	0

							Bulb	0	0
Cyanella hyacinthoides	Geophyte	Tecophilaea-ceae	Edible	Sand Fynbos	34º09.816'	022º00.456'	Leaves	151	20,050
							Cover bulb	67	93,900
							Bulb	13	100
Albuca maxima	Geophyte	Hyacinthaceae	Edible	Renosterveld	34º04.773'	022º09.226'	Leaves	30	10,300
							Cover bulb and bulb	151	46,300
Tritoniopsis antholyza	Herb, geophyte	Iridaceae	Edible	Renosterveld-Fynbos transition	34º02.218'	022º11.269	Leaves	243	12,300
							Cover bulb	199	32,000
							Bulb	39	10
Watsonia fourcadei	Herb, geophyte	Iridaceae	Edible	Renosterveld	34º02.233'	022º11.357'	Leaves	28	5,600
							Cover bulb	28	7,800
							Bulb	0	0
Elegia juncea	Graminoid	Restionaceae	Sleeping mats, huts, roofs, fences	Mountain Fynbos	33º52.383'	022º01.880'	Whole plant	242	219,600
Restio triticeus	Graminoid	Restionaceae	Sleeping mats, huts, roofs, fences	Renosterveld	34º09.729'	022º00.449'	Whole plant	251	3,250
Thamnochortus insignis	Graminoid	Restionaceae	Sleeping mats, huts, roofs, fences	Sand Fynbos	34º09.865'	022º00.447'	Whole plant	309	4,100
Thamnochortus rigidus	Graminoid	Restionaceae	Sleeping mats, huts, roofs, fences	Mountain Fynbos	33º52.383'	022º01.880'	Whole plant	88	9,900
Ehrharta bulbosa	Grass	Poaceae – Ehrhartoideae – C_3	Edible tubers	Renosterveld	34º04.702'	022º08.902'	Whole plant	526	3,998,300
Eragrostis curvula	Grass	Poaceae – Chloridoideae – C_4	Famine food	Open grassy fynbos	34º05.362'	021º54.794'	Whole plant	1,154	4,062,800

Eragrostis capensis	Grass	Poaceae – Chloridoideae – C_4	-	Renosterveld	34º09.825'	022º00.477'	Whole plant	1,720	13,537,500
Tribolium uniolae	Grass	Poaceae – Danthonioideae – C_3	-	Renosterveld	34º09.729'	022º00.449'	Whole plant	1,307	15,191,000
Festuca scabra	Grass	Poaceae – Pooideae – C_3	-	Renostervedl-Fynbos transition	34º02.235'	022º11.331'	Whole plant	873	5,550,800
Pentachistis pallida	Grass	Poaceae – Danthonioideae – C_3	-	Grassy Fynbos	34º03.198'	022º59.413'	Whole plant	1,262	2,177,700
Pentachistis colorata	Grass	Poaceae – Danthonioideae – C_3	-	Open grassy fynbos	34º05.362'	021º54.794'	Whole plant	955	8,745,150
Stipa dregeana	Grass	Poaceae – Pooideae – C_3	-	Coastal forest	34º01.600'	022º50.082'	Whole plant	2,214	2,941,700
Setaria sphacelata	Grass	Poaceae – Panicoideae – C_4	Famine food	Grassy Fynbos	34º03.198'	022º59.413'	Whole plant	1,154	3,745,750
Tristachya leucothrix	Grass	Poaceae – Panicoideae – C_4	-	Grassy Fynbos	34º03.198'	022º59.413'	Whole plant	1,435	3,701,000
Stenotaphrum secundatum	Grass	Poaceae – Panicoideae – C_4	Famine food	Wetland	34º03.648'	022º06.472'	Whole plant	8,76	4,535,600
Heteropogon contortus	Grass	Poaceae – Panicoideae – C_4	Common in transition areas	Renostervedl-Fynbos transition	34º02.235'	022º11.331'	Whole plant	1,643	7,409,400
Panicum deustum	Grass	Poaceae – Panicoideae – C_4	Edible grains	Coastal thicket	34º04.773'	022º09.226'	Whole plant	1,668	7,390,800
Themeda triandra	Grass	Poaceae – Panicoideae – C_4	-	Renosterveld	34º09.729'	022º00.449'	Whole plant	9,32	11,799,500
Stipagrostis zeyheri	Grass	Poaceae – Aristidoideae – C_3	Shelter and huts	Grassy Fynbos	34º01.949'	022º50.391'	Whole plant	1,527	6,948,700

Classification, description and distribution of common morphotypes– A total of twenty-five phytolith morphotypes were identified in the wood and bark, from which ten seemed to be the result of contamination (eight to grasses, one to the leaves of eudicot plants and one to restios) (Table A1).

Spheroid phytoliths with psilate and rugulate textures were the most recurrent phytolith morphotypes identified (Fig. 13 and Fig. 14). Nonetheless, this presence was uneven among species being for example the only morphotype present in *Protea repens*, very abundant in *Cassine peragua*, and absent in *Celtis africana*, *Pterocelastrus tricuspidatus*, *Vepris undulata*, *Olea europaea* sub. *africana* and *Passerina vulgaris* (Table A1).

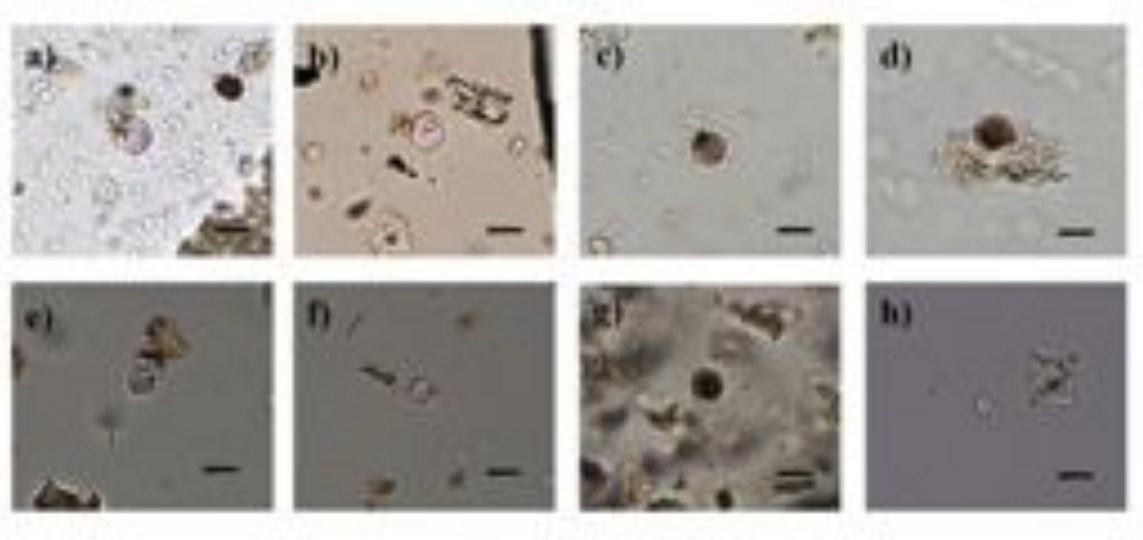

Figure 13. Microphotographs of spheroid psilate phytoliths identified in eudicotyledoneous plants. Pictures taken at 400x. a) Wood/bark of *Protea lanceolata*, b) wood/bark of *Leucospermum praecox*, c) wood/bark of *Elytropappus rhinocerotis*, d) wood/bark of *Protea repens*, e-f) *Stoebe plumosa*, g) leaves of *Acacia karoo*, h) leaves of *Pterocelastrus tricuspidatus*. Scale bar represents 10 mm.

Ellipsoids and elongate morphologies with no surface ornamentation were also identified (Fig. 14). Ellipsoids were present in high frequencies in *Vepris undulata*, *Sideroxylon inerme*, *Morella cordifollia*, *Euclea racemosa* and *Searsia pterota* (Table A1). Spheroids with psilate textures and ellipsoids were detected through ANOVA and the post hoc Tukey's test as

statistically significant different in the wood/bark respectively to other plants (Table 3). Irregular and indeterminate morphologies (these are the *non-identified* phytoliths of Zurro et al., 2016) were also identified for most of the species but in moderate frequencies (Fig. 14), with the exception of *Passerina vulgaris* (50%) and *Acacia karoo* (23%) (Table A1). Parallelepipeds blocky and thin were identified but in very low numbers (Fig. 14).

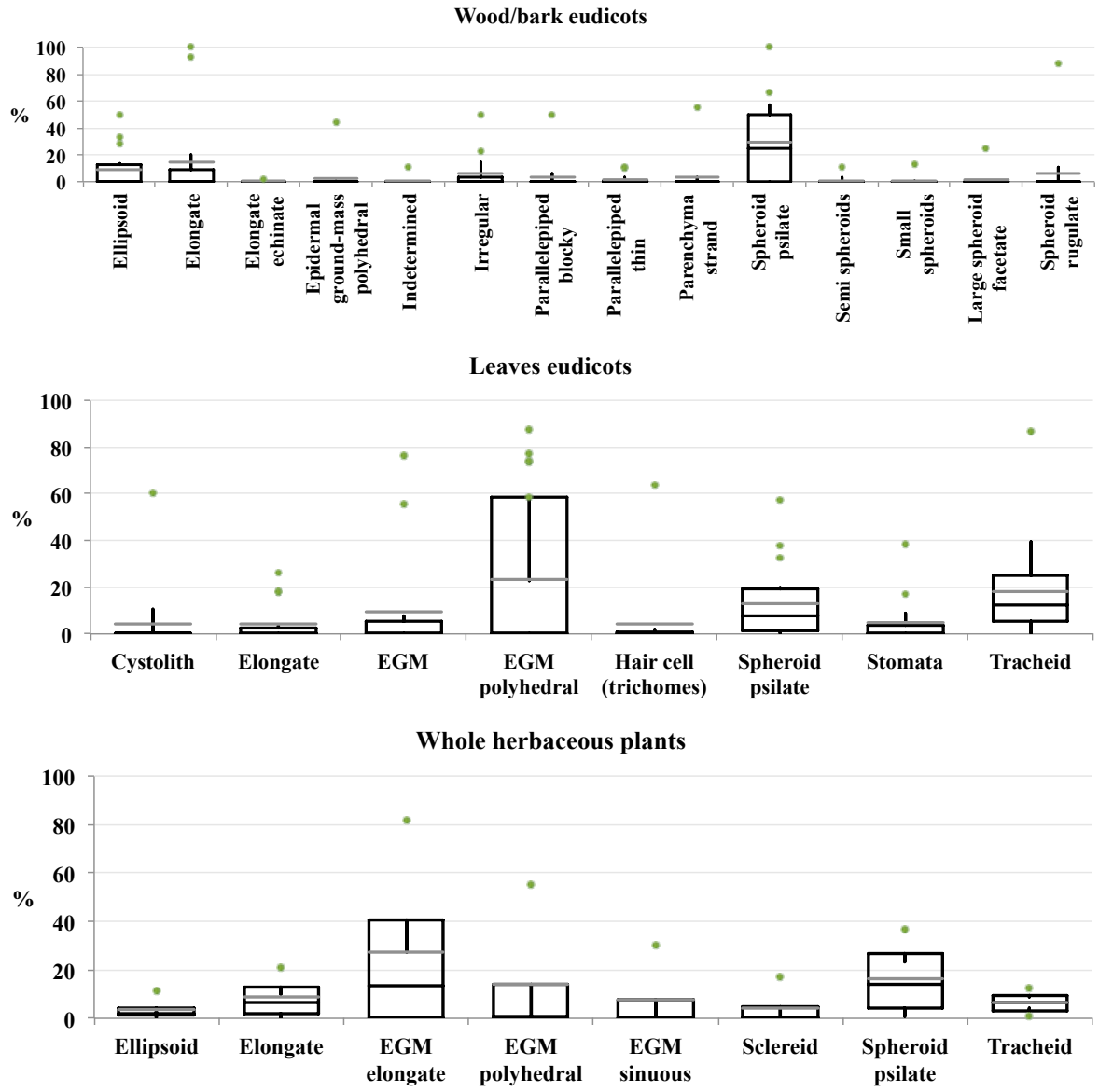

Figure 14. BoxPlot showing those phytolith morphotypes that more abounded in the twenty-four species of eudicotyledoneous plants (wood/bark, leaves and whole plant). The sample mean (grey line), standard error ± (box), standard deviation (whiskers) and outliers (green dots) are given. EGM = epidermal ground mass phytolith morphotypes.

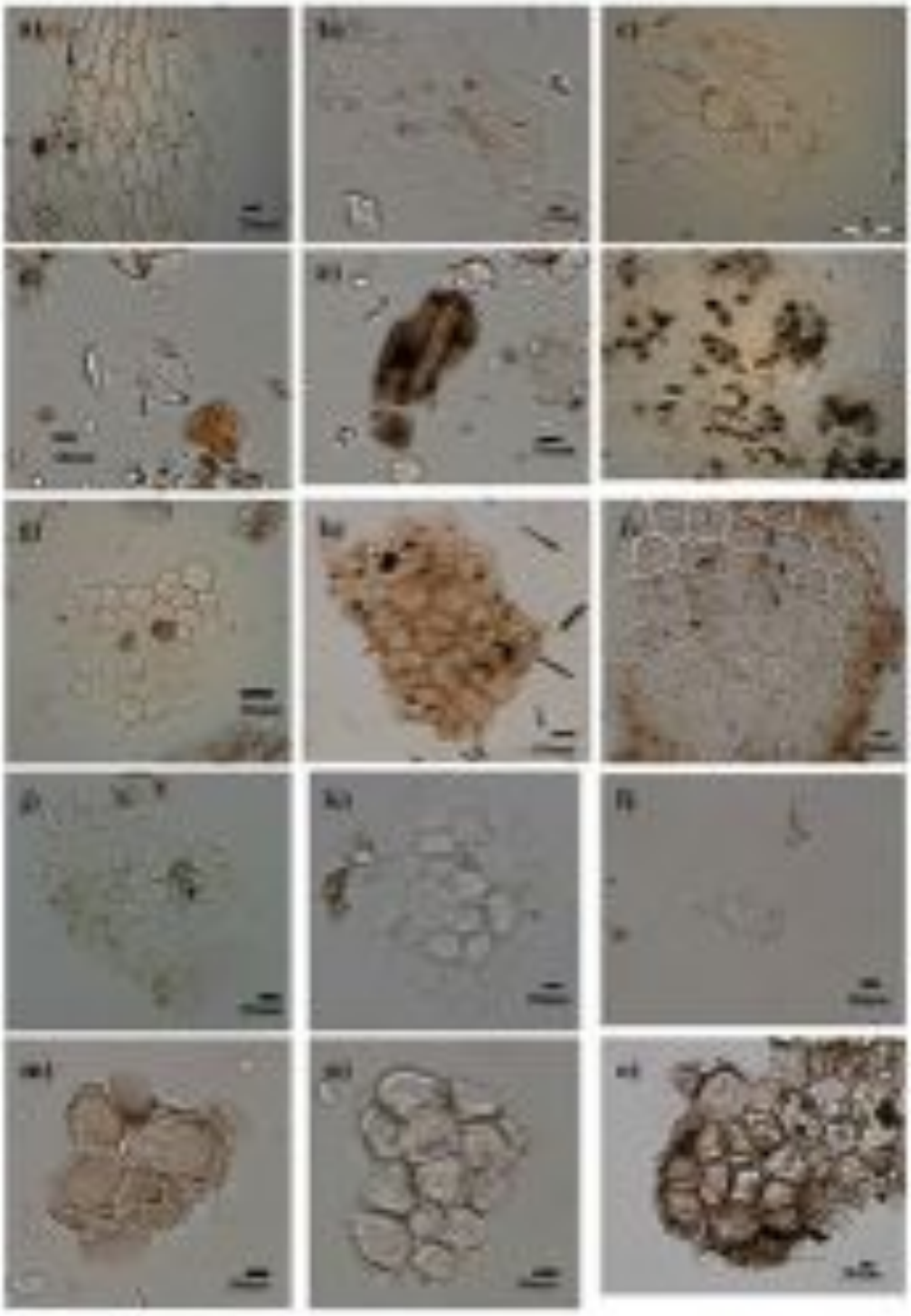

Figure 15. Microphotographs of epidermal ground mass phytoliths (EGM) identified in eudicotyledoneous plants. Pictures taken at 400x. a-c) EGM elongate from *Metalasia muricata*, d-e) EGM elongate from *Stoebe plumosa*, f-g) EGM polyhedral from the leaves of *Vepris undulata*, h-i) EGM polyhedral from the leaves of *Tarchonanthus camphoratus*, j-k) EGM polyhedral from the leaves of *Grewia occidentalis*, l-m) EGM sinuate from the leaves of *Rhoicissus digitata*, n-o) EGM polyhedral from the leaves of *Pterocelastrus tricuspidatus*. Scale bar represents 10mm.

V. 1.1.2. Leaves

Phytolith concentration– The leaves of eudicot trees and shrubs generally presented low phytolith concentration, with no phytoliths identified in *Euclea racemosa*, *Leucospermum praecox* and *Leucadendron galpinii*, and the highest phytolith concentration occurring in the leaves of *Celtis africana* (280,000 phytoliths/g original plant material) (Table 2).

Phytolith contamination from other plants– Phytolith morphotypes characteristic of grasses, and restios but the latters in a lesser extent, were identified in the different specimens. The frequencies of phytolith contamination from other plants went up to 60% (mean= 7%), the latter observed in the leaves of *Cassine peragua* (Fig. 12).

Classification, description and distribution of common morphotypes– A total of forty-six phytolith morphotypes were identified, of which seven came from grasses and one from restios (Table A1). Tracheids (vascular elements) and epidermal ground mass were the most common morphotypes, and this was statistically confirmed (Table 3). Tracheids were identified in most of the plants with the exception of *Acacia karoo*, *Searsia crenata* and *Celtis africana* (Fig. 14 and Table A1). In contrast, it was the only morphotype identified in the leaves of *Elytropappus rhinocerotis*, and in *Morella cardifolia* it made up to 84% (Table A1).

Epidermal ground mass phytoliths were variable in size and shape. Four different shapes were observed, which are polyhedral, elongate, sinuate and rings, with the polyhedral being the most abundant (Fig. 15). Moreover, *Protea lanceolata* and *Helichrysum pandurifolium* showed epidermal ground mass with granulate ornamentation (dots). Ellipsoid and spheroid morphologies, which are usually related to wood/bark, were also detected in most of the species analyzed making up more than 30% of the total in the leaves of *Searsia crenata, Searsia pterota, Eriocephalus africanus* and *Olea europaea* subsp. *africana* (Fig. 14 and Table A1). Hair cells (trichomes) were present in the majority of the species and were the dominant morphotype in *Celtis africana*, making up 71% of the total (Table A1). The leaves of *Sideroxylon inerme* (11%), *Acacia karoo* (10%), *Eriocephalus africanus* (7%) and *Grewia occidentalis* (6%) followed in abundances (Table A1). In contrast, hair cells were absent in *Vepris undulata*, *Searsia crenata*, *Grewia occidentalis*, *Tarchonanthus camphoratus*, *Protea repens* and *Eriocephalus africanus* (Fig. 14). ANOVA also showed that eudicot leaves are characterized and differed from the other plant parts by the high frequencies of hair base cell

(Table 3). Sclereid cells were rarely identified (Fig. 14). Cystoliths were only found in the leaves of *Celtis africana* by 9% (Fig. 14 and Table A1). Elongate morphologies and parallelepipeds thin and blocky were also noticed but in small numbers (Table A1).

V. 1.1.3. Whole herbaceous plants

Phytolith concentration– When the whole plant was analyzed without previous separation (including leaves and stems), phytolith concentration was also very low, ranging from 4,000 to 30,000 phytoliths/g original plant material. Phytolith concentration was, thus, similar to that reported from both the wood/bark and the leaves of other eudicot plants (Table 2).

Phytolith contamination from other plants– Unlike the wood/bark and the leaves of trees and shrubs, the four whole plants analyzed presented low phytolith contamination from other plants, with 0% in *Metalasia muricata* and only 11% in *Helichrysum pandurifolium*, (Fig. 12) and these were exclusively GSSCs.

Classification, description and distribution of diagnostic morphotypes– A total of thirty-two phytolith morphotypes were identified in the samples, of which ten belonged to grasses and one to restios from contamination. The phytolith assemblage was similar to the one observed in the leaves and the wood/bark. Spheroid and ellipsoid morphologies were the dominant morphotype in most of the species with the exception of *Metalasia muricata* and *Rhoicissus digitata* (Fig. 14 and Table A1). Elongate morphologies were the second most abundant morphotype. The only exception was *Helicrhysum pandurifolium* where these were absent (Fig. 14). Epidermal ground mass morphologies were also identified in high numbers (Fig. 14). Epidermal ground mass morphologies without discernible outlines accounted for 54% in *Helicrhysum pandurifolium*, and elongate outlines dominated in *Rhoicissus digitata*. Tracheids followed in abundances by 27.4% in *Helicrhysum pandurifolium* and 12.5% in *Rhoicissus digitata*. Sclereid cells were only detected in *Stoebe plumosa*, accounting for the 17% (Fig. 14 and Table A1). Finally, stomata and parenchyma strand were also identified but in low numbers (Fig. 14 and Table A1). The statistical analysis showed that the whole herbaceous plants were characterized by the high presence of epidermal ground mass with elongate and sinuate outlines, parallelepipeds blocky striate and sclereid cells (Table 3).

V. 1.2. Monocotyledonous plants

V. 1.2.1. Geophytes

The leaves, the bulb scale leaves and the edible part of the bulbs of geophytes were analyzed separately whenever possible (Table 2). *Pelargonium triste* (Geraniaceae) was the only eudicot geophyte, so it was analyzed in this study with the monocot geophytes for an easier understanding of the results.

Phytolith concentration– Phytoliths in the bulb scale leaves had the highest phytolith concentration ranging from 25,000 to 250,000 phytoliths/g original plant material. Only the bulb scale leaves of *Freesia alba* and *Gladiolus rogersii* did not contain phytoliths (Table 2). The leaves produced in general very low phytolith concentration with the exception of *Moraea* sp. and *Pelargonium triste* (120,000 and 620,000 phytoliths/g plant, respectively). Finally, phytoliths were rarely identified in the edible part of the bulbs of all the species analyzed (Table 2).

Phytolith contamination from other plants– All the different parts analyzed from the geophytes showed high number of phytoliths that are known to be part of other plants such as grasses and restios (Fig. 12). The presence of grass phytoliths, mainly of GSSCs, account for between 24.1% and 61.1% (mean of 47.5%) of the phytolith assemblage identified in the bulb scale leaves, between 72.4% and 4.5% (mean of 36%) in the leaves and between 47.5% and 0% (mean of 12.7%) in the edible part of the bulbs.

Classification, description and distribution of common phytolith morphotypes– A total of fifty-three phytolith morphotypes were identified in the different species and different plant parts analyzed, of which seventeen corresponded to contamination mainly from grasses (Table A1).

Table 3. ANOVA results of the eighty phytolith morphotypes identified as statistically significant different among plant types and plant parts (*p*-values in bold). The **X** indicates those plant types or plant parts characterized through the post hoc Tukey's test by the high presence of that specific phytolith morphotype.

	***p*-values**	**C_4 Poaceae**	**C_3 Poaceae**	**Restionaceae**	**Leaves of Geophytes**	**Bulb scale leaves of Geophytes**	**Bulb of geophytes**	**Leaves Eudicots**	**Wood/bark Eudicots**	**Whole Eudicots**
Bulliform	0.7082									
Blocky Polyhedral	**0.0069**						**X**			
Cone-shape	0.4579									
Cystolith	0.6958									
Ellipsoid	**0.0119**								**X**	
Ellipsoid echinate	0.6805									
Elongate	**0.0222**				**X**					
Elongate blocky	**0.0004**				**X**	**X**				
Elongate blocky echinate	0.3567									
Elongate blocky striate	**0.0002**									**X**
Elongate bulbous	**0.0002**			**X**						
Elongate curved	0.6805									
Elongate facetate	**0.0151**			**X**						
Elongate striate	0.6794									
Elongate tuberculate	0.2359									
Elongate verrucate	0.2555									
Elongate dendritic	0.3567									

Elongate echinate	0.1070							
Elongate sinuate	**<0.0001**	**X**	**X**					
Elongate polylobate	0.7657							
EGM	0.1861							
EGM elongate	**<0.0001**							**X**
EGM polyhedral	**0.0036**						**X**	
EGM sinuous	**0.0035**							**X**
EGM rings	0.8487							
EGM dots	0.4728							
Hair cell (trichomes)	0.6281							
Hair cell (prickle)	0.1727				**X**			
Hair cell aciculate	0.8864							
Hair cell armed	0.7576							
Hair cell with protuberances	0.8487							
Hair cell curved	0.8487							
Hair cell unciform	0.1034							
Hair base	**0.0255**						**X**	
Hair base sinuous shape	0.8487							
Indeterminate	0.5521							
Irregular	**0.0053**					**X**		
Irregular echinate	0.0672							

Irregular facetate	0.6753			
Papillae	**<0.0001**		**X**	
Parallelepiped thin	0.2504			
Parenchyma strand	0.8428			
Platelet	0.3756			
Sclereid	**0.0016**			**X**
GSSC bilobate tabular flattened-round lobes	**0.0006**	**X**		
GSSC bilobate tabular flattened lobes	**0.0007**	**X**		
GSSC bilobate tabular rounded lobes, short shank	**0.0212**		**X**	
GSSC bilobate tabular rounded lobes, long shank	0.1778			
GSSC bilobate trapeziform notched lobes	**0.0070**	**X**		
GSSC bilobate tabular angulated lobes	**<0.0001**		**X**	
GSSC bilobate tabular angulated asymmetrical lobes	0.1582			
GSSC bilobate tabular segmented angulated/planar lobes	0.1582			
GSSC bilobate trapeziform	**0.0051**	**X**		
GSSC bilobate trapeziform wavy top	0.2555			
GSSC cross trapeziform	**0.0218**		**X**	

GSSC cross tabular	0.1062				
GSSC trilobate	**0.0017**	**X**			
GSSC polylobate	0.2555				
GSSC rondel cilyndric	0.3728				
GSSC rondel conical	**<0.0001**			**X**	
GSSC rondel conical wavy top	0.2413				
GSSC rondel keeled	0.1466				
GSSC long tower	0.1844				
GSSC long tower wavy top	0.1582				
GSSC trapeziform	**<0.0001**			**X**	
GSSC oblong tabular	0.1729				
GSSC oblong trapeziform sinuate	0.3903				
GSSC rounded tabular	0.4239				
GSSC saddle	0.3163				
GSSC collapsed saddle	0.6963				
Spheroid psilate	**0.0050**				**X**
Semi spheroids	0.2981				
Small spheroids	0.4585				
Large spheroid	0.4049				
Large spheroid facetate	0.8743				
Large spheroid granulate and verrucate	**0.0004**		**X**		

Spheroid spiraling decorations	**<0.0001**	**X**	
Spheroid rugulate	0.6846		
Stomata	0.1021		
Tracheid	**<0.0001**		**X**

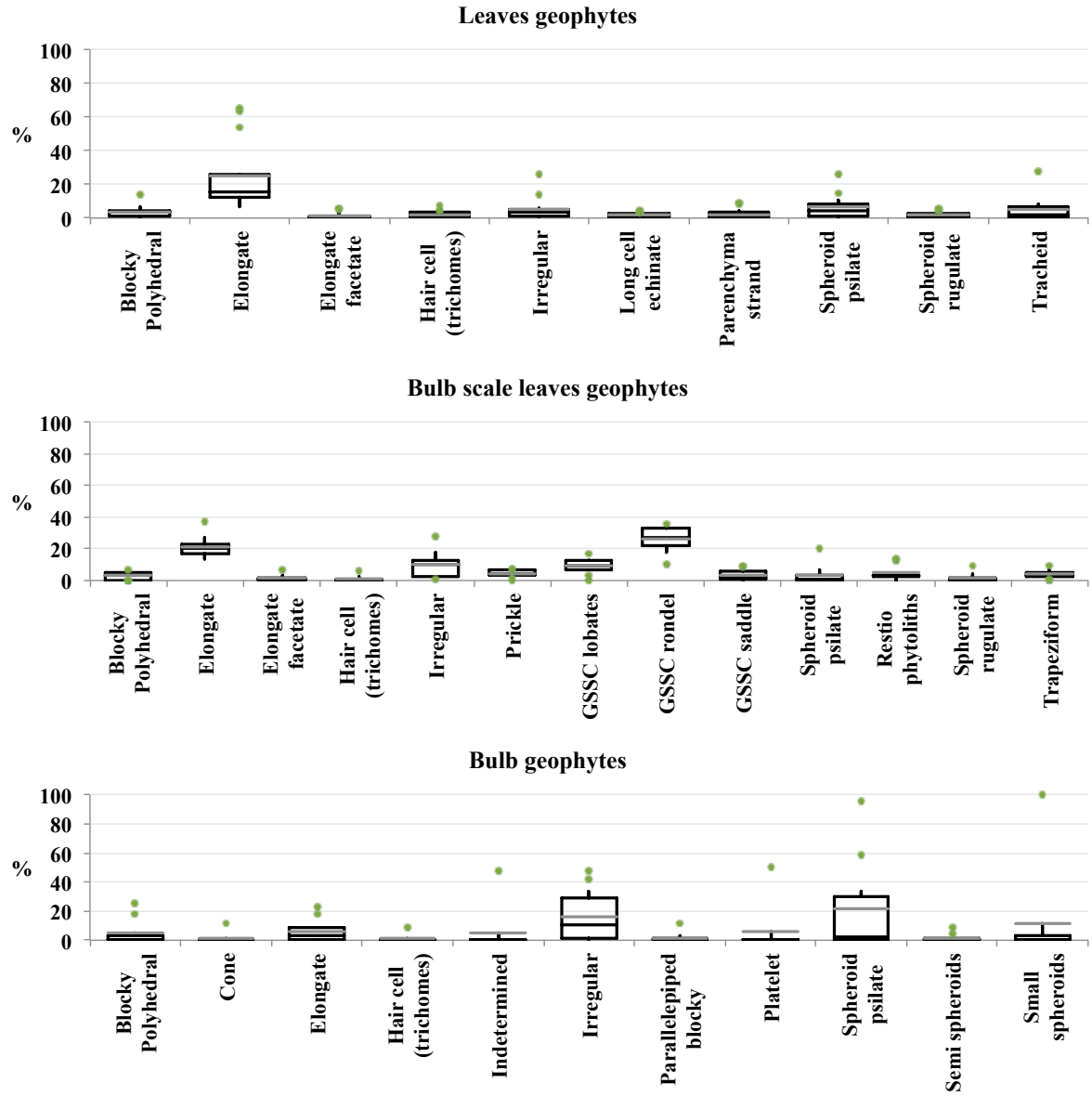

Figure 16. Box-plots showing those phytolith morphotypes that more abounded in the thirteen species of geophyte in the leaves, the bulb scale leaves and the edible part of the bulb (bulb). The sample mean (grey line), standard error ± (box), standard deviation (whiskers) and outliers (green dots) are given for each phytolith morphotype.

Despite geophytes had the highest diversity of phytolith morphotypes of all the plant types, the phytolith assemblage did not show any diagnostic morphotype. However, we observed that elongate morphologies without decorated margins were the most common morphotype, and this was especially true in the leaves, mostly in the two species from the genus *Moraea* (Fig. 16 and Table A1), and this was detected through ANOVA and the post hoc Tukey's test (Table 3). The leaves were also characterized by the dominance of spheroids

with psilate and rugulate texture and tracheids followed by blockys polyhedral and parenchyma strand (Fig. 16). Elongates, spheroids psilate and rugulate and irregular morphologies were the dominant morphotypes identified in the bulb scale leaves and the edible parts of bulbs (Fig. 16). ANOVA and the post hoc Tukey's test showed that the bulb scale leaves of geophytes were characterized and differed from the rest of the plant types by the high numbers of elongate blocky morphologies, hair cells (prickles) and GSSCs conical and trapeziform (Table 3). Finally, the bulbs of geophytes were characterized and differed from the rest of the plant types by the high numbers of blocky polyhedral and irregular morphologies (Table 3).

V. 1.2.2. Restionaceae

Phytolith concentration– Restios produced very few phytoliths/g original plant material, with *Elegia juncea* being the only species showing a relatively high phytolith concentration (220,000 phytoliths /g original plant material) (Table 2).

Phytolith contamination from other plants– The four species analyzed showed high phytolith contamination from grasses and mainly GSSCs (mean: 17.2%, range: 2.8-35.3%) (Fig. 12).

Classification, description and distribution of common phytolith morphotypes– A total of twenty-eight phytolith morphotypes were identified, of which eight belonged to grasses. Two morphotypes were dominant. These are large spheroids, sometimes showing protuberances, with granulate or verrucate decoration (~25 mm) (Fig. 17a-c) and spheroids showing spiraling ornamentation, sometimes showing a double ring on the edges (10-15 mm) (Fig. 17d-f). These morphotypes resemble those described by Cordova and Scott (2010) and Cordova (2013) as being representative of Restionaceae plants and named "papillated and non-papillated rondels". In this work we have chosen not to follow Cordova's (Cordova and Scott, 2010; Cordova, 2013) distinction between papillated and non-papillated rondels since they have, in fact, spheroidal shapes that can be recognized when rotating phytoliths under the microscope.

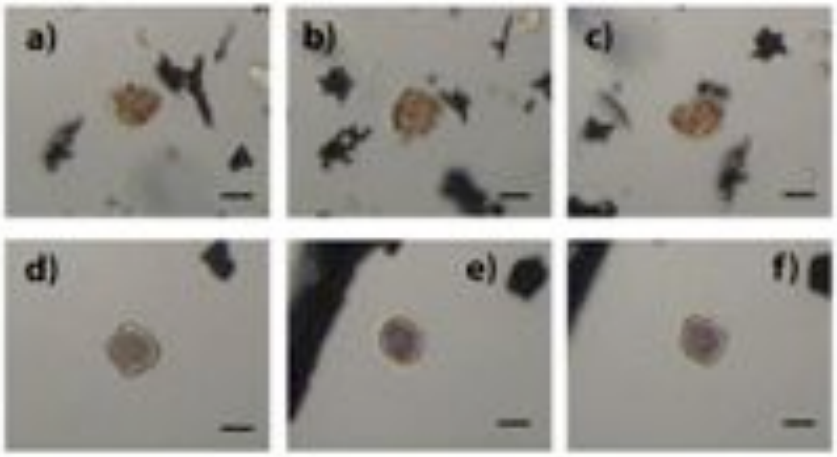

Figure 17. Microphotographs of two restio phytoliths identified in Restionaceae modern plants. Phytoliths are shown from three different points of view by its rotation on the slide. Pictures taken at 400x. a-c) spheroid showing protuberances, with granulate/verrucate ornamentation (*Thamnochortus insignis*); d-f) spheroids showing spiraling decoration with a double ring on the edges (*Elegia juncea*). Scale bar represents 10 mm.

Other morphotypes also present in restios were elongates with and without decorated margins and reniforms, the latters in very few numbers (Fig. 18). Hair cells trichomes were also identified in high numbers (Fig. 18). Spheroids with psilate and rugulate textures were also abundant (Fig. 18), and showed similar shapes, textures and sizes as those identified in the wood/bark of the trees and shrubs. In order to circumvent any confusion between psilate or rugulate spheroid phytoliths from Restionaceae and those from eudicot wood/bark, spheroids were isolated when grouping phytolith morphotypes among plant parts and plant types for the analysis of modern soil and archaeological samples. The characteristic large granulate and verrucate spheroids, and the spheroids showing spiraling decoration from Restionaceae are both referred to herein as restio phytoliths.

Because little is known about the origin of phytoliths in Restionaceae plants, sections of the culms (stems) and bracts of *Thamnochortus insignis* were analyzed in order to identify formation and distribution of the phytoliths. This species was chosen because it had the highest content of the characteristic restio phytoliths. Large silica bodies showing in most cases protuberances with verrucate or granulate ornamentation were found in the sheath

parenchyma cells of the culms (Fig 19a-d). In order to validate this finding, we analyzed the culm sections through SEM. Conversely, silica bodies were not identified in the bracts analyzed of this species.

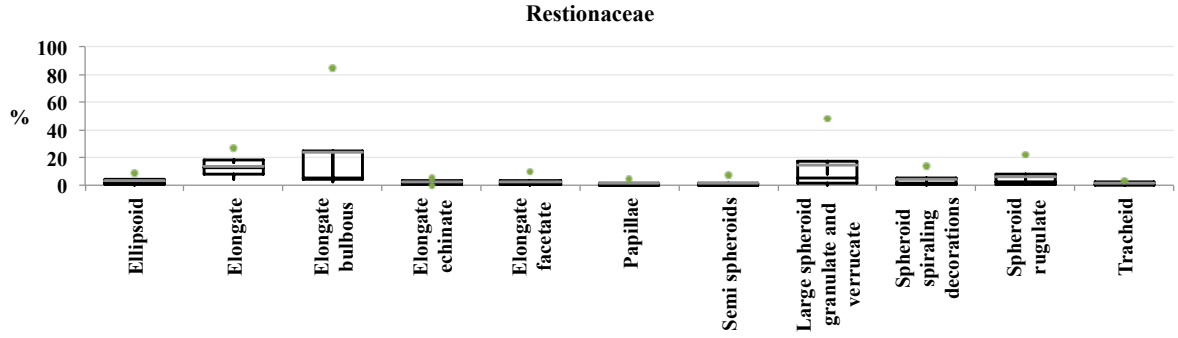

Figure 18. Box-plots showing those phytolith morphotypes that more abounded in the four Restionaceae specimens. The sample mean (grey line), standard error ± (box), standard deviation (whiskers) and outliers (green dots) are given for each phytolith morphotype.

The spheroids, showing protuberances, with verrucate and granulate ornamentation present in the parenchyma sheath cells of the culms were identified (Fig. 19e-h) and the EDXA analysis conducted on these particles showed that the silica concentration was above the 60%. We also identified through SEM a spheroid shape that could belong to the so-called spheroids with spiraling ornamentation or to the spheroids psilates, but it was detected outside cells so we cannot assure the provenience of this phytolith. These analyses confirmed that these morphotypes belong to and characterize this plant family. Furthermore, ANOVA and the post hoc Tukey's test showed that in a mixed phytolith assemblage, Restionaceae phytoliths are characterized and differed from the rest of plant types by the two characteristic restio phytoliths (Table 3).

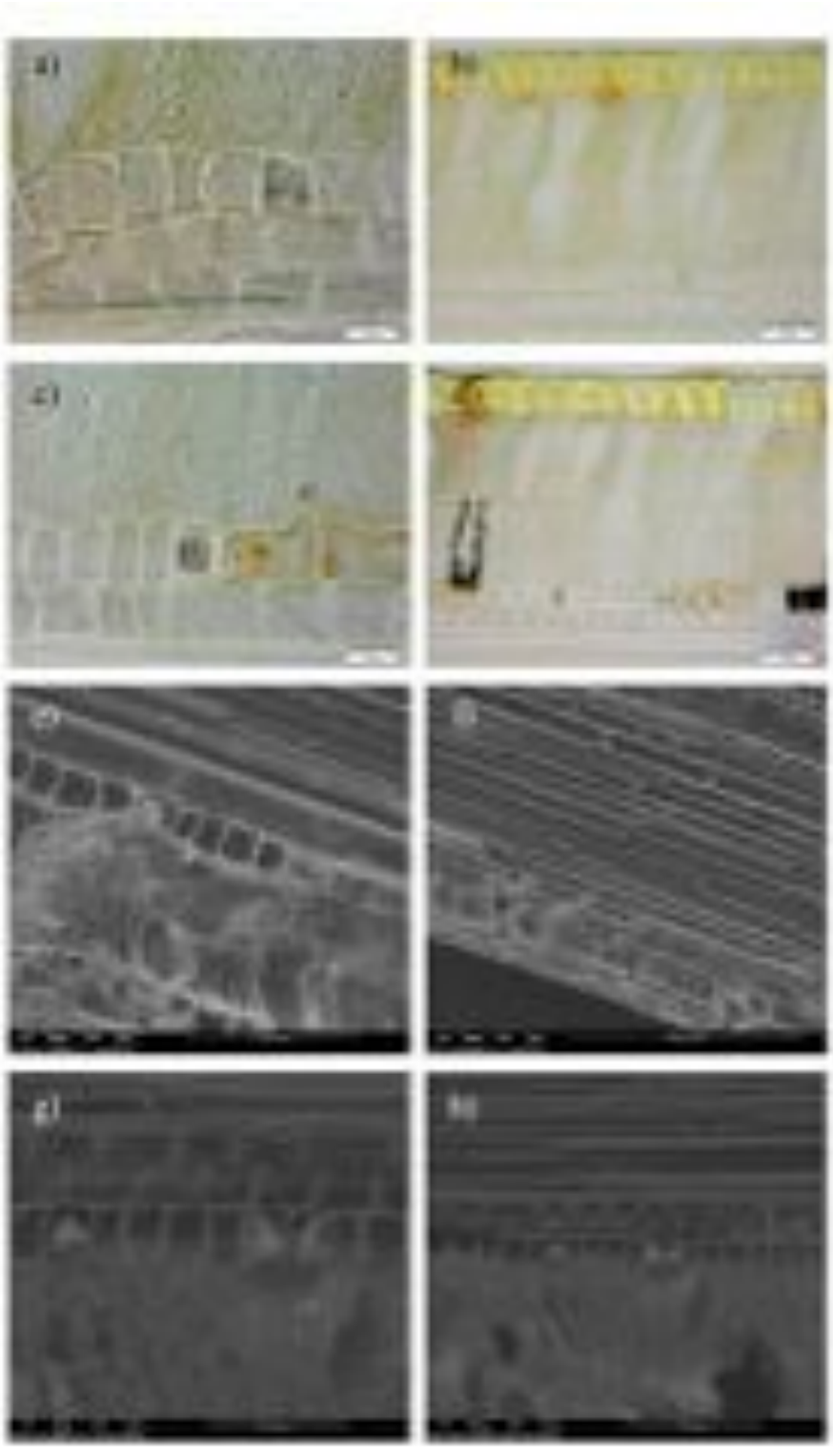

Figure 19. Thin section (a-d) and SEM (e-h) images of the culms of *Thamnochortus insignis.*

V. 1.2.3. Poaceae

Phytolith concentration– Grasses were the greatest phytolith producers among all the plants analyzed, ranging from 2 to 15 million phytoliths/g original plant material. *Tribolium uniolae*, *Eragrostis capensis* and *Themeda triandra* produced the highest concentrations (15, 13 and 12 million phytoliths/g original plant material, respectively) (Table 2).

Phytolith contamination from other plants– No apparent contamination of phytoliths known to be characteristic of other plants was noted in grasses.

Classification, description and distribution of common phytolith morphotypes– A total of forty-five phytolith morphotypes were identified in grasses of which twenty-six corresponded to GSSCs. The grasses studied were grouped by their photosynthetic pathway, C_3 and C_4 (Grass Phylogeny Working Group II, 2012). C_3 taxa is composed of four subfamilies (Ehrhartoideae, Pooideae, Aristidoideae and Danthonioideae), C_4 taxa is composed of two subfamilies (Panicoideae and Chloridoideae). Information of subfamily and photosynthetic pathway of each grass species is given in Table 2. The twenty-six GSSCs identified were classified on the basis of the three dimensional structure of the morphotypes what is the top, the side and the base (following Mullholland and Rapp, 1992). Four classes were stablished: rondels, lobates, saddles and oblongs. We classified these clases further into twelve types and these are rondels, trapezoids and towers (rondel class), bilobates, crosses, trilobates and polylobates (lobate class), saddles and collapsed saddles (saddle class) and tabular, trapeziform and rounded (oblong class). Despite some redundancy and multiplicity (Rovner, 1971; Mulholland, 1989; Fredlund and Tieszen, 1994) were observed in the distribution of GSSCs among grass subfamilies and photosynthetic pathway (C_3 and C_4), it was detected that in general C_4 grasses, from the Panicoideae subfamily, were characterized by the presence of bilobates. And C_3 grasses by rondels and trapezoids, and *Festuca scabra* from the Pooideae subfamily by the presence of long oblongs (for further discussion see Section VI. 1.). And these results also supported previous studies (Rossouw 2009; Cordova and Scott, 2010; Cordova, 2013).

V. 1.2.3.1. C_3 grasses

Elongate morphologies, with sinuate decorated margins, and elongate morphologies without decorated margins were most common (Fig. 20). The formers were mainly detected in *Stipagrostis zeyheri* (Aristidoideae) (63.3%) (Fig. 21, A-a) and *Stipa dregeana* (Pooideae) (41%) (Table A1). Elongates with echinate decorated margins followed in abundance (Fig. 20 and Fig. 21, A-b). Other morphotypes, such as epidermal appendages (hairs– trichomes and prickles, and papillae), stomata cells and bulliform cells, were also well represented (Fig. 20 and Fig. 21, A-c). *Ehrharta bulbosa* (Ehrhartoideae) was the only species showing a relatively high presence of bulliforms, and *Festuca scabra* (Pooideae) of papillae cells (Table A1 and Fig. 21, A-d).

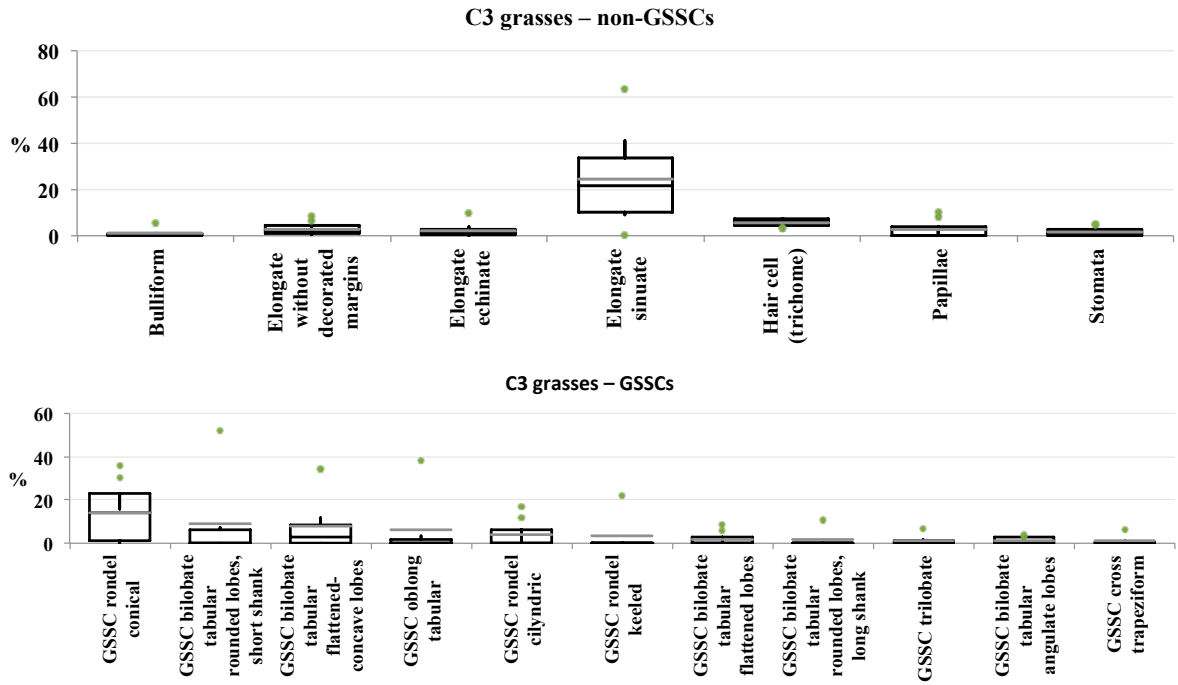

Figure 20. Box-plots showing those phytolith morphotypes that more abounded in the seven C_3 species of Poaceae plants. The sample mean (grey line), standard error ± (box), standard deviation (whiskers) and outliers (green dots) are given for each phytolith morphotype.

GSSCs from the rondel class were the most common morphotypes identified in C_3 grasses, followed in abundances by those from the lobate and oblong classes. Among the twenty-one GSSCs morphotypes identified, rondels conical, bilobates tabular with rounded lobes and

short shank, bilobates tabular with flattened-round lobes and oblongs tabular were most common (Fig. 20).

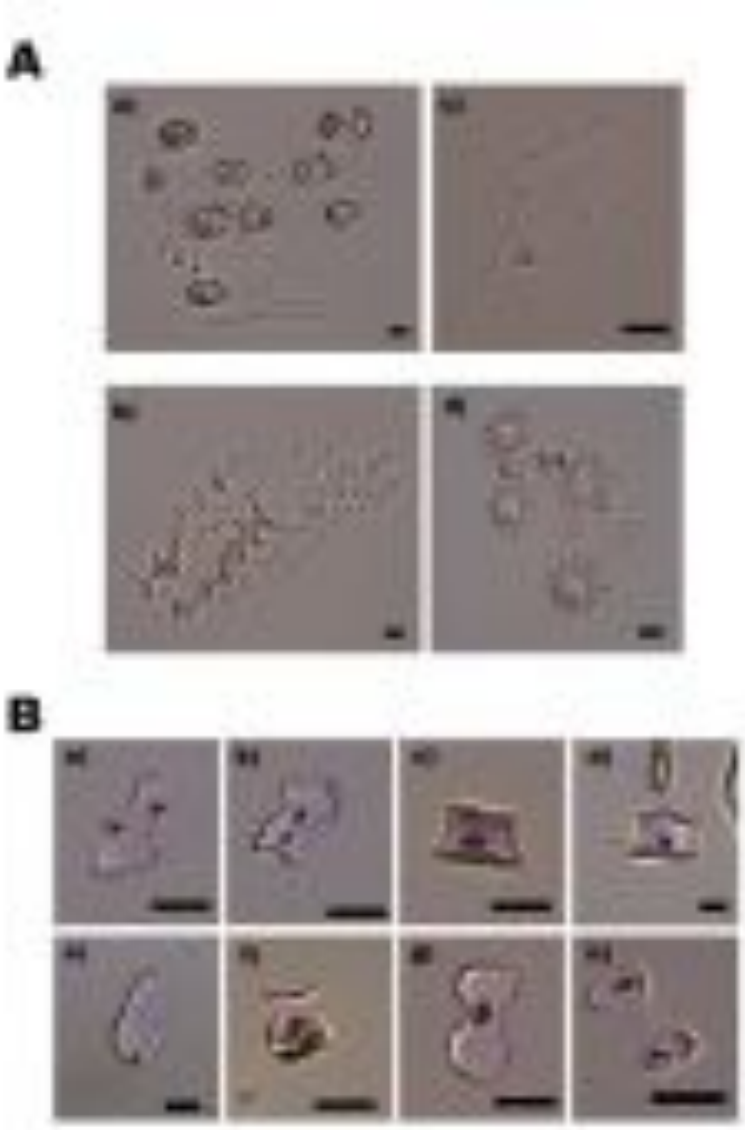

Figure 21. Micrographs of common non-GSSCs (A) and GSSCs (B) morphotypes observed in C_3 grasses. Pictures taken at 400x. See Table 1 for detailed descriptions of the phytolith morphotypes. A: a) elongate morphologies with sinuate decorated margins (together with GSSC rondel cylindric) from *Stipagrostis zeyheri* (Aristidoideae); b) elongate morphologies with echinate decorated margins from *Ehrharta bulbosa* (Ehrhartoideae); c) hair cell traichomes from *Ehrharta bulbosa* (Ehrhartoideae); d) papillae from *Festuca scabra* (Pooideae). B: a-c) GSSC bilobate tabular with angulate lobes from *Pentachistis colorata* (Danthonioideae); d) GSSC rondel conical from *Stipa dregeana* (Pooideae); e) GSSC rondel conical with wavy top from *Stipagrostis zeyheri* (Aristidoideae); f) GSSC rondel keeled from *Tribolium uniolae* (Danthonioideae); g) GSSC bilobates with flattened-rounded lobes from *Pentachistis colorata* (Danthonioideae). Scale bar represents 10 mm.

We reported here a new bilobate morphotype noted mainly in *Pentachistis colorata* but also in *Ehrharta bulbosa* and *Stipa dregeana* and which is the bilobates with angulate lobes (angulate lobes, angulate asymmetrical lobes and segmented angulate/planar lobes) (Table A1 and Fig. 21, B-a and b). *Stipa dregeana* from the Pooideae subfamily was mainly characterized by the presence of rondel conical (Fig. 21, B-c) and bilobate tabular with flattened-round lobes. *Festuca scabra* was characterized and differed from the other two by the presence of tabular oblong and tabular oblong with sinuate margins (Fig. 21, B-d), while they were absent in *Stipa dregeana* and both belong to the Pooideae subfamily (Table A1). *Stipagrostis zeyheri* was characterized by a high presence of elongate morphologies with sinuate margins (63%) and few GSSCs, among which stands the absence of bilobates, while rondel conical and conical with wavy top (Table A1 and Fig. 21, B-e) dominated.

Finally, tabular oblong were also identified in *Ehrharta bulbosa* (Ehrhartoideae) but in very low numbers (Table A1). *Tribolium uniolae* (Danthonioideae) presented high frequencies of rondels conical and keeled (Fig. 21, B-f). The genera *Pentachistis* (Danthonioideae) was characterized by the presence of bilobates with flattened-rounded lobes (*Pentachistis colorata*) (Fig. 21, B-g) and round lobes with short shanks (*Pentachistis pallida*) (Fig. 21, B-h).

ANOVA and the post hoc Tukey's test showed that C_3 grasses are characterized and differed from the rest of the plant types by the high number of elongates with sinuate decorated margins, papillae, bilobates tabular with angulate lobes and bilobates tabular with rounded lobes and short shanks. Surprisingly trilobates and crosses, which are usually related to C_4 grasses (e.g., Piperno and Pearsall, 1998), were detected as statistically significant characteristic of C_3 grasses (Table 3).

V. 1.2.3.2. C_4 grasses

Elongate morphologies with sinuate decorated margins were identified in C_4 grasses in high frequencies (Fig. 22, A-a and b and Fig. 23). Other morphotypes such as hair cell (trichomes), elongate with echinate decorated margins and elongates without decorated margins and others showing verrucate and tuberculate ornamentation and stomata were also common. Bulliform cells were also identified but in lesser extent, with the exception of

Stenotaphrum secundatum where bulliform cells were identified in high frequencies (10%) (Table A1 and Fig. 22, A-c).

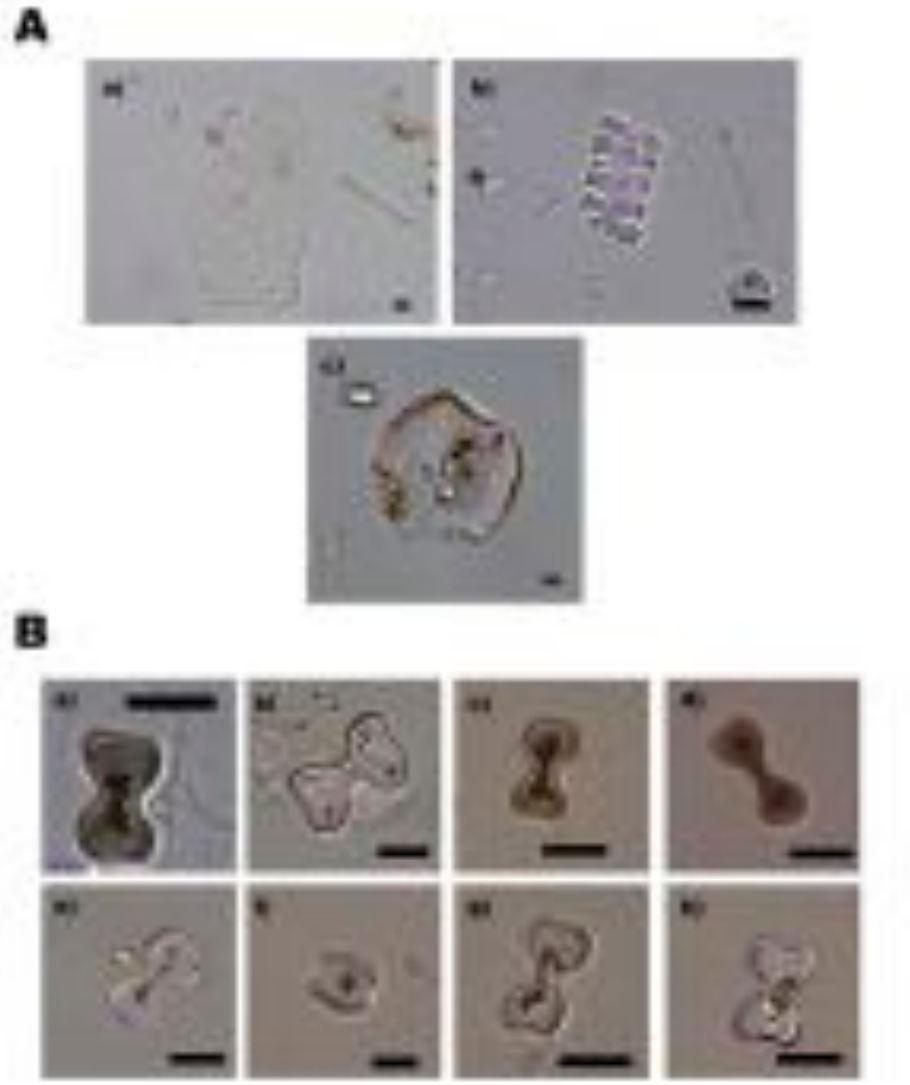

Figure 22. Micrographs of common non-GSSCs (A) and GSSCs (B) morphotypes observed in C_4 grasses. Pictures taken at 400x. See Table 1 for detailed descriptions of the phytolith morphologies. A: a-b) elongate morphologies with sinuate decorated margins from *Setaria sphacelata* and *Tristachya leucothrix* (Panicoideae); c) Bulliform cell from *Stenotaphrum secundatum* (Panicoideae). B: a-b) GSSC bilobate tabular flattened lobes from *Panicum deustum* and *Heteropogon contortus* (Panicoideae); c-d) GSSC flattened-rounded lobes from *Stenotaphrum secundatum* (Panicoideae); e) GSSC tabular round lobes from *Setaria sphacelata* (Panicoideae); f) GSSC saddle from *Eragrostis curvula* (Chloridoideae); g-h) GSSC bilobate trapeziform with notched lobes from Panicum deustum and *Heteropogon contortus* (Panicoideae). Scale bar represents 10 mm.

GSSCs morphotypes from the lobate and saddle classes were most common in C_4 grasses. Among the seventeen GSSCs morphotypes identified, bilobates tabular with flattened (Fig. 22, B-a and b), flattened-round (Fig. 22, B-c and d) and round lobes (Fig. 22, B-e) were the most recurrent morphotypes (Table A1 and Fig. 23), while they were absent in *Stipagrostis zeyheri* (Aristidoideae) and in *Eragrostis curvula* and *Eragrostis capensis* (Chloridoideae). GSSC saddles (Table A1 and Fig. 22, B-f) were only detected in Chloridoideae grasses and characterize this subfamily.

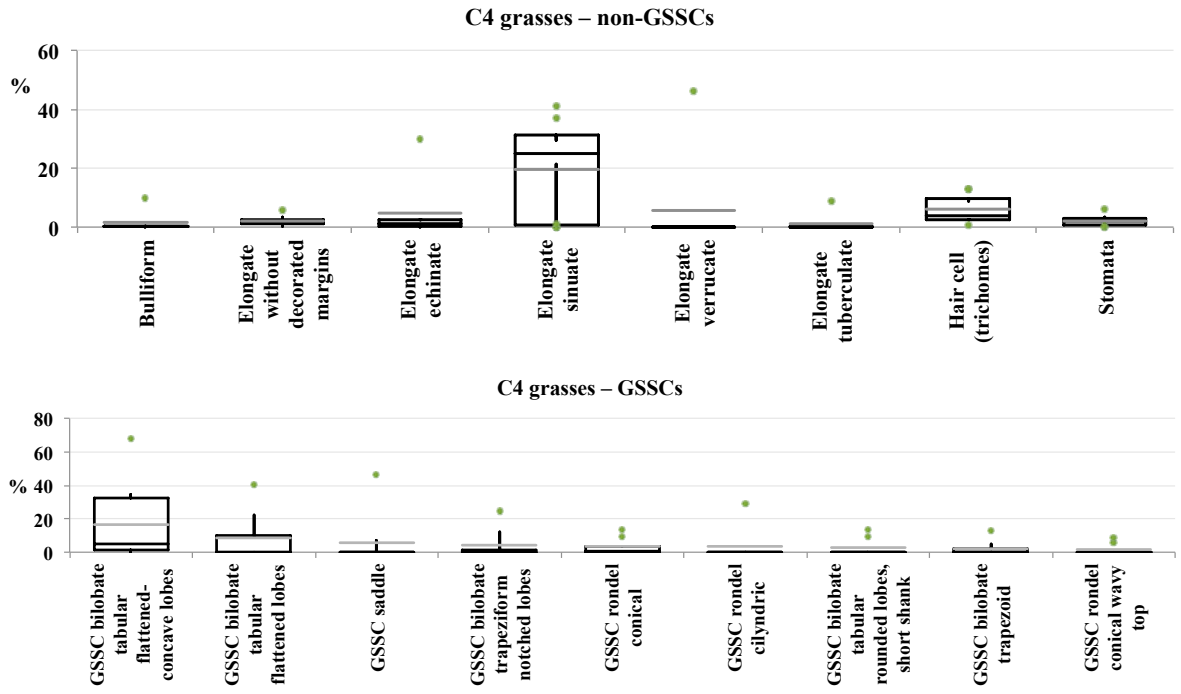

Figure 23. Box-plots showing those phytolith morphotypes that more abounded in the eight C_4 grass species of Poaceae plants. The sample mean (grey line), standard error ± (box), standard deviation (whiskers) and outliers (green dots) are given for each phytolith morphotype.

Despite saddles were exclusively identified in the Chloridoideae subfamily, *E*ragrostis *pallida* produced rondels in much higher frequencies than saddles (Table A1). Rondels were not abundant in Panicoideae grasses (Table A1 and Fig. 23). Tabular oblong morphologies were absent in C_4 grasses (Table A1).

ANOVA and the post hoc Tukey's test showed that C_4 grasses are characterized and differed from the rest of plant types and plant parts by the high presence of elongates with sinuate decorated margins, bilobates tabular with flattened-round and flattened lobes and bilobates trapeziform and trapeziform with notched lobes (Table A1 and Fig. 22, B-g and h) (Table 3).

V. 2. Modern surface soil samples

Phytoliths were identified in different concentrations in all of the samples. Renosterveld, riparian, and grassy fynbos vegetation provided the highest amount of phytoliths per gram of sediment (phyt /g sed) (Table 4). In contrast, the samples that were collected from limestone fynbos, dune cordon, coastal thicket and strandveld vegetation had the lowest amount of phytoliths. Weathered morphotypes –non-recognizable phytoliths with signs of chemical dissolution and or mechanical damaged– (and these are the *unidentifiable* phytoliths of Zurro et al., 2016). Those morphotypes withs signs of chemical dissolution showed irregular shapes and pitted surfaces were identified in low numbers in all the samples and almost never above 20%, with the exception of samples from coastal thicket (Table 4). No phytoliths with mechanical signs were detected. Together with phytoliths, diatoms and sponge spicules were also recovered from most of the samples, albeit in varying amounts. Samples from riparian, subtropical and coastal thicket vegetation contained the highest number of diatoms.

Table 4 lists the results of the modern soil samples, which includes description of the samples, vegetation type, geographical coordinates, the dominant taxa, the type of soils and the pH of soils as well as the estimated phytolith concentration in sediments, the total number of phytoliths identified, the percentage of weathered morphotypes and the D/P^o, Fy, Iph and Ic indices values. Table 5 lists the phytolith morphotypes identified and their plant attribution (plant types and plant parts). These morphotypes were later related to the vegetation type, the dominant plants, and the type of soil. All of the samples showed an acidic to a moderate alkaline pH. FTIR results further indicated that clay and quartz are the main mineral components in all the samples but these minerals occurred in different proportions depending on the type of soils.

Grass phytoliths were common to all vegetation types analyzed. Samples from limestone fynbos showed a low grass phytolith component (Table 5). Among grasses, GSSCs were the most representative morphotypes, together with the presence of prickles, bulliforms fan-shaped as well as elongates with decorated margins (mainly echinates) (Fig. 24a-c, respectively). Following the system used in our plant reference collection, GSSCs have been classified in four categories: rondels (rondels, trapezoids and towers), lobates (bilobates, crosses, trilobates and polylobates), saddles and oblongs (Section V. 1.2.3.3.). Rondels were the most common GSSCs recognized in the samples (Fig. 24d-f), while lobates (Fig. 24g and h) and saddles (Fig. 24i) were also represented, albeit in lower numbers. The distribution of

grasses in the phytolith record was traced using a ternary diagram highlighting composition differences among vegetation types and GSSCs (Fig. 25). In this figure, the category rondels include also the oblong morphotypes. And these morphotypes were the dominant in samples from most of the vegetation types while samples from riparian vegetation present higher proportion of saddles (Fig. 25).

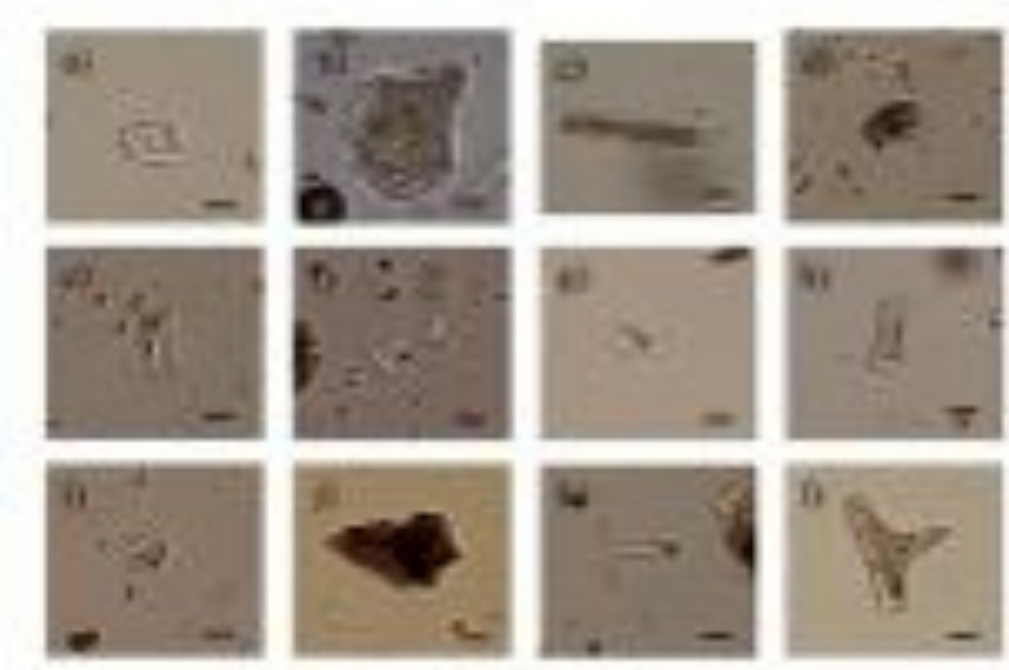

Figure 24. Microphotographs of phytoliths identified in samples analyzed. Pictures taken at 400x. a) prickle (RV10-04), b) bulliform cell (GF10-10), c) elongate with echinate margin (RV11-58), d-f) rondel GSSCs (SF11-42, SF11-43 and RV11-15), g-h) bilobates GSSCs (GF10-14, CF10-13), i) saddle GSSCs (CT06-05), j) epidermal ground mass polyhedral (STV11- 01), k) eudicot hair cell (SF11-37), l) sclerenchyma (RP11-59). Scale bar represents 10 mm (retrieved from Esteban et al., in press-a).

Among phytoliths from eudicot plants identified in modern soils, the most representative ones were parallelepiped blockys, epidermal ground mass polyhedral (Fig. 24j), hair cells (Fig. 24k) and sclerenchyma (Fig. 24l). Psilate and rugulate spheroids were also identified in high frequencies mainly in samples from limestone fynbos vegetation.

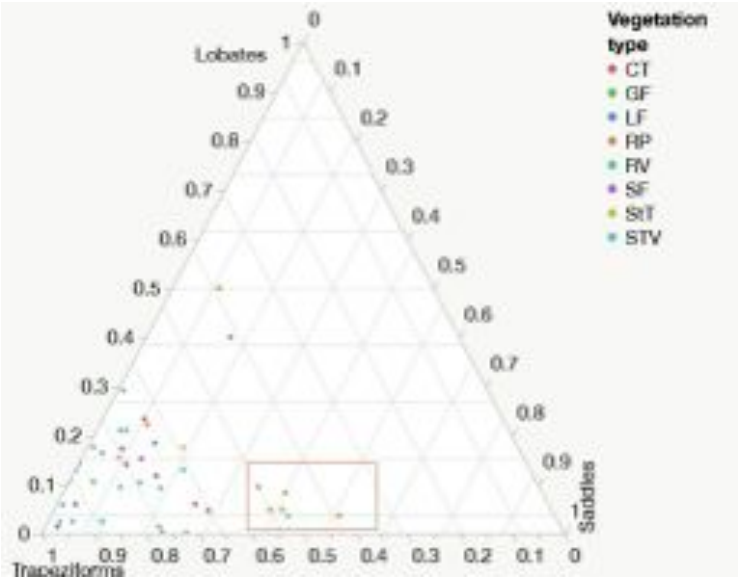

Figure 26. Ternary plot showing the grass silica short cells, grouped by the three fundamental categories: rondels, lobates and saddles, distribution among vegetation types. Rondel category includes also the oblong morphotypes. Legend: CT, coastal thicket; GF, grassy fynbos; LF, limestone fynbos; RP, riparian; RV, renosterveld; SF, sand fynbos; StT, subtropical thicket; STV, strandveld (retrieved from Esteban et al., in press-a).

Other morphotypes commonly identified included the large spheroids, sometimes showing protuberances, with granulate or verrucate decoration (~25 mm) (Fig. 26a-c) and spheroids showing spiraling decoration, sometimes showing a double ring on the edges (10-15 mm) (Fig. 26d-f). They were mainly found in fynbos, strandveld, and dune cordon vegetation (both thicket-fynbos mosaics), and marginally in renosterveld vegetation. The comparison with the modern phytoliths morphotypes from the modern plant reference collection (*Elegia juncea*, *T. insignis*, *T. rigidus* and *Restio triticeus*) and the plant anatomy study confirmed that these morphotypes correspond to Restionaceae plants (Fig. 18a-f) (Section V. 1.2.2.).

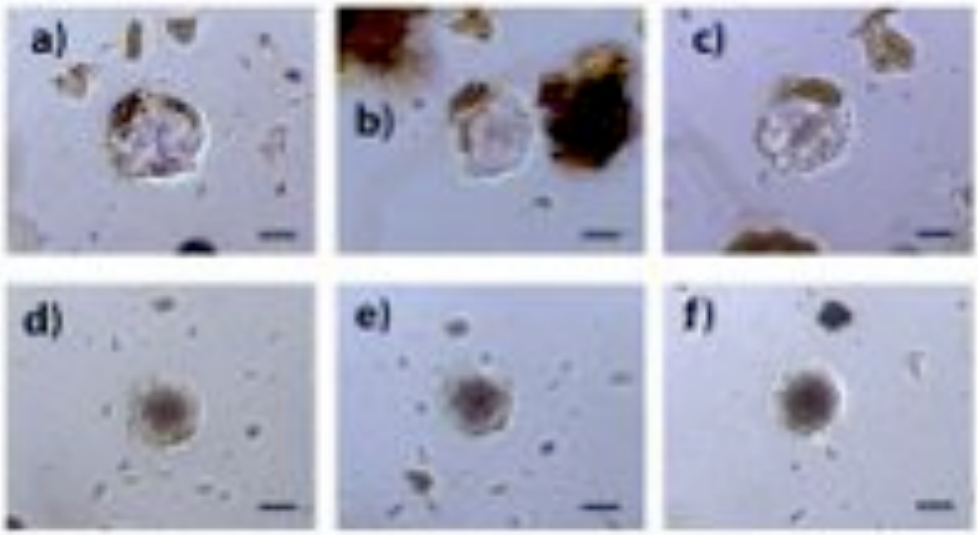

Figure 26. Microphotographs of two restio phytoliths identified in modern soils. Phytoliths are shown from three different points of view by its rotation on the slide. Pictures taken at 400x. a-c) large spheroid showing protuberances, with granulate decoration (LF11-68); d-f) spheroids showing spiraling decoration (LF11- 85). Scale bar represents 10 mm (retrieved from Esteban et al., in press-a).

V. 2.1. Phytolith indices

Four phytolith indices were used to identify and characterize vegetation types through phytolith assemblages in modern surface soils of extant habitats from the south coast of South Africa. As we pointed out above, in the modern plant reference collection, spheroids with psilate and rugulate surface phytoliths were identified in the wood of trees and shrubs and in Restionaceae plants making it impossible to characterize the provenance of these morphotypes from one plant type to another. Considering that fynbos is a shrub-dominated vegetation and Restionaceae are the diagnostic family of the Fynbos biome, we have therefore assumed that the identification of spheroids psilate and rugulate, whether they are produced by woody eudicots or Restionaceae, are representative of fynbos vegetation. Thus the Fy index provides a signal for the presence of vegetation characteristic of the Fynbos biome. Furthermore, we assume that in samples from vegetation types devoid of Restionaceae plants, and also having no restio phytoliths, spheroid morphotypes might be representative of woody eudicots.

The Kruskal-Wallis test showed a statistically significant difference between the D/Pº and Fy index values by vegetation type (x^2<24.92, p<0.0008 and x^2<24.84, p<0.008, D/Pº and Fy indices respectively) with the highest mean ranks for limestone fynbos (46.33 for both indices) and the lowest mean ranks for grassy fynbos (8.5 and 19.5, D/Pº and Fy indices respectively) and riparian vegetation (12.86 and 11.07, D/Pº and Fy indices respectively) (Fig. 27a and b). Iph values also detected statistically significant differences between vegetation types (x^2<16.84, p<0.0184) with the highest mean rank of 39.93 for riparian, 33.75 for coastal thicket and 32.5 for subtropical thicket (Fig. 27c). There were no significant differences in the Ic index between vegetation types (x^2<12.81, p<0.0769). Nonetheless, samples from renosterveld had the largest numbers of GSSC rondels, while riparian and coastal thicket the lowest (Fig. 27d).

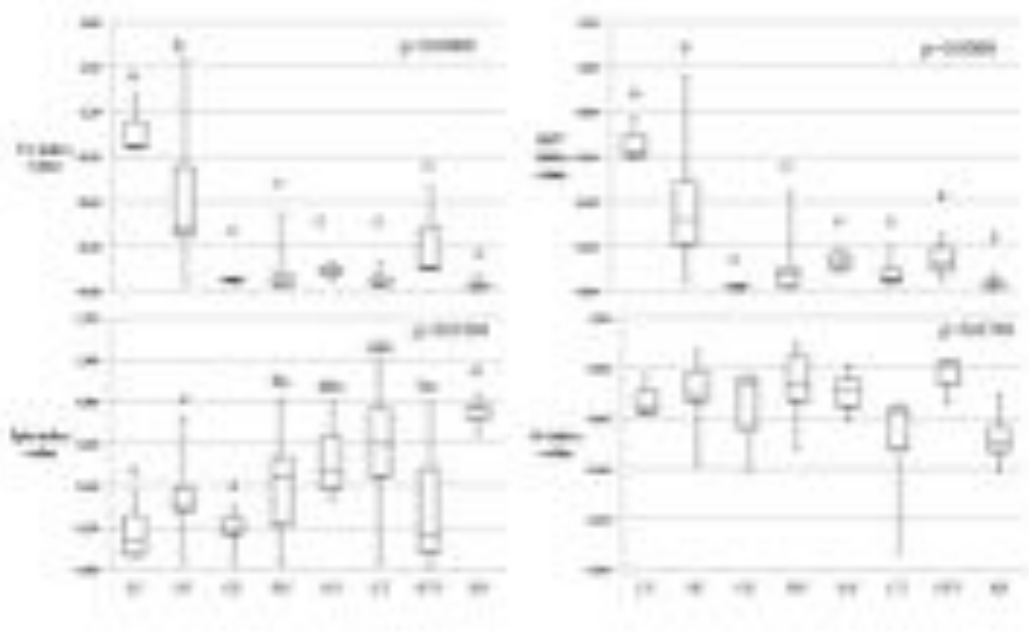

Figure 27. Box-plots showing the phytolith indices values among vegetation types. a) D/P^{O} index [Σ (psilate and rugulate spheroids)/∑ grass silica short cells] and the standard deviation among the different vegetation types; b) Fy index [Σ (psilate and rugulate spheroids and restio phytoliths)/grass silica short cells] and the standard deviation among the different vegetation types; c) Iph index [GSSC saddles/ Σ (GSSC saddles and lobates)]; d) Ic index [GSSC rondels and oblongs/ Σ (GSSC rondels, lobates and saddles)]. The mean values (mid- line), standard error ± (box) and standard deviation (whiskers) are given for the four indices. Legend: LF, limestone fynbos; SF, sand fynbos; GF, grassy fynbos; RV, renosterveld; StT, subtropical thicket; CT, coastal thicket; STV, strandveld; RP, riparian. Different letters indicate means that are significantly different based on a Kruskal-Wallis test (retrieved from Esteban et al., in press-a).

Table 4. Description of samples, provenance and main phytolith results: soil type and soil pH, estimated number of phytoliths per gram of sediment, total number of phytoliths identified, percentage of weathered morphotypes and D/Pº (Bremond et al., 2005b) and Fy indices. WM = weathered morphotypes. (retrieved from Esteban et al., in press-a).

Sample number	Vegetation type	Dominant taxa	Soil type	Soil pH	# Phytoliths identified	Estimated # of phytoliths g/sed	% WM	D/Pº index	Fy index
Fynbos biome									
LF11-19	Limestone fynbos	Restionaceae; Asteraceae; *Carpobrotus acinaciformus*	Sand	7.6	22	7,700	15		
LF11-23	Limestone fynbos	*Themeda triandra*; *Olea europea* subs. *Africana*; Restionaceae	Sand	7.3	97	60,400	0	0.77	0.97
LF11-25	Limestone fynbos	Restionaceae; *Protea repens*; *P. obtusifolium*; *Leucadendron platyspermum*	Sand	7.2	30	74,500	4		
LF11-26	Limestone fynbos	Restionaceae; *Erica* sp; Asteraceae	Sand	7.5	21	61,500	0		
LF11-68	Limestone fynbos	*Leucadendron coniferum*; Restionaceae	Sand	7	62	164,000	5.6	0.62	1.31
LF11-74	Limestone fynbos	*Leucadendron coniferum*; Restionaceae	Sand	7.6	49	69,100	8.9		
LF11-85	Limestone fynbos	Restionaceae	Sand	7.3	68	70,900	5.2	0.59	0.95
SF10-05	Sand fynbos	*Freesia* sp.	Sand	5.8	83	99,500	3.5	0.37	0.43
SF10-06	Sand fynbos	Restionaceae	Sand	5.9	74	689,300	7.5	0.21	0.38
SF11-37	Sand fynbos	*Leucadendron salignum*; *Leucospermum praecox*; Restionaceae	Sand	5.3	89	311,400	2.5	0.65	0.83
SF11-42	Sand fynbos	Poaceae; *Aloe ferox*; *Osyris compressa*	Sand	3.5	211	2,913,400	1.4	0.04	0.05
SF11-43	Sand fynbos	*Elytropappus rhinocerotis*; *Erica*; Poaceae; *Schotia afra*	Loam	4.4	210	1,285,800	0.5	0.04	0.08
SF11-45	Sand fynbos	*Leucadendron salignum*; *Protea repens*; *Leucospermum praecox*; *Erica* sp.	Sand	4.8	163	1,051,100	3.9	0.48	1.27
SF11-47	Sand fynbos	*Leucospermum praecox*; *Erica* spp; *Leucadendron* spp.	Sand	5.8	109	288,900	1	0.96	1.56

SF11-62	Sand fynbos	Restionaceae; *Leucospermum muirii*; *Brunia*	Sand	4.2	109	225,500	7.8	0.32	0.50
SF11-82	Sand fynbos	*Thamnochortus insignis*; *Leucadendron galpinii*; *Leucospermum praecox*	Sand	5.3	93	154,300	5.7	0.25	0.40
GF10-10	Grassy fynbos	*Themeda triandra*; *Eragostris capensis*; *E. curvula*	Sand	5.5	182	2,326,000	7.6	0.03	0.05
GF10-11	Grassy fynbos	*Pentaschistis colorata*	Sand	5.9	175	2,341,000	6.4	0.03	0.08
GF10-14	Grassy fynbos	Poaceae	Sand	5.9	153	1,317,400	4.4	0.00	0.08
MF12-01	Mountain fynbos	Restionaceae; Cyperaceae	Sand	5	127	898,200	0	0.16	0.23
F/R10-07	Fynbos/Renosterveld	*Tritoniopsis* spp. Restionaceae	Sand	5.5	115	1,893,000	2.8	0.31	0.34
Renosterveld biome									
RV09-01	Renosterveld	*Themeda tiandra*; *Brachiaria serrate*; *Eragrostis* sp.	Loam	5.4	155	2,411,200	27.7	0.08	0.09
RV09-02	Renosterveld	Restionaceae*;* Poaceae	Loam	5.2	172	1,977,400	11.4	0.08	0.10
RV09-03	Renosterveld	*Elytropappus rhinocerotis; Searsia lucida*	Loam	5	130	3,404,200	11.8	0.00	0.00
RV09-07	Renosterveld	*Elytrotrappus rhinocerotis*	Sandy	5.4	104	2,036,000	19.7	0.05	0.05
RV09-08	Renosterveld	*Eragrostis curvula*; *Elytrotrappus rhinocerotis*	Sandy	5.8	193	2,253,400	19.4	0.04	0.04
RV10-01	Renosterveld	*Romulea flava*	Loam	6.2	201	3,001,700	4	0.03	0.05
RV10-02	Renosterveld	*Moraea* sp.	Loam	5.9	179	2,503,900	2.4	0.02	0.04
RV10-03	Renosterveld	*Hypoxis villosa*	Loam	5.8	196	2,743,500	9.6	0.14	0.15
RV10-04	Renosterveld	*Ehrharta bulbosa*	Loam	5.6	171	2,992,500	4.8	0.15	0.17
RV10-09	Renosterveld	*Elytropappus rhinocerotis*	Sand	5.8	177	1,382,300	5.8	0.11	0.11
RV11-04	Renosterveld	*Eriocephalus africanus*; *Elytopappus rhinocerotis*; *Ruschia* sp.	Sand	5	230	1,480,000	0.4	0.07	0.08
RV11-11	Renosterveld	*Elytropappus rhinocerotis*; *Eriocephalus africanus*; *Themeda triandra*	Loam	5.3	220	4,850,600	2.4	0.12	0.17

RV11-15	Renosterveld	*Elytropappus rhinocerotis*; Restionaceae; Asteraceae	Loam	6.8	64	126,700	0.	0.44	0.52
RV11-22	Renosterveld	*Elytropappus rhinocerotis*; *Searsia graveolens*; Poaceae	Loam	4.9	186	2,550,600	0.5	0.03	0.04
RV11-32	Renosterveld	*Elytropappus rhinocerotis*; *Aloe ferox*; *Ehrharta villosa*; *Themeda triandra*	Sand	4.8	200	2,258,700	1.6	0.01	0.01
RV11-58	Renosterveld	*Roepera morgsana*; *Euphorbia mauritanica*; *Aloe ferox*	Loam	6.3	187	621,000	3.3	0.08	0.11
RV11-67	Renosterveld	*Searsia glauca*; *Aloe ferox*; *Euphorbia mauritanica*	Loam	5.2	186	1,201,300	3.3	0.00	0.02
Thicket biome									
StT09-04	Subtropical thicket	*Sideroxylon inerme*	Sandy/loam	6.1	94	446,000	13.8	0.14	0.14
StT09-05	Subtropical thicket	*Eriocephalus africanus*	Sand	7	79	264,600	16.8	0.19	0.19
StT09-06	Subtropical thicket	*Searsia pterota*	Sand	5.3	127	1,188,300	15.9	0.08	0.08
CT06-01	Coastal thicket	Dense shrubby vegetation	Sand	8	61	153,400	39	0.06	0.06
CT06-02	Coastal thicket	Dense shrubby vegetation	Sand	8	68	225,900	26.9	0.20	0.20
CT06-03	Coastal thicket	Dense shrubby vegetation	Sand	7.9	39	78,000	46.6		
CT06-04	Coastal thicket	Dense shrubby vegetation	Sand	7.5	12	23,400	29.4		
CT06-05	Coastal thicket	Open grassy area of *Eragrostis curvula*	Sand	8	71	75,900	5.3	0.02	0.02
CT06-06	Coastal thicket	*Acacia karroo*	Sand	6.6	54	100,300	35.7	0.06	0.06
CT06-07	Coastal thicket	Dense shrubby vegetation	Loam	8.3	20	922,200	56.5		
CT10-12	Coastal thicket	*Eragrostis rehmannii*; *Asparagus* sp.; *Chasmanthe aethiopica*; *Rhoicissus* sp.	Loam	6	45	28,300	4.3		
STV11-01	Strandveld	*Stoebe cinorera*; *Erharta villosa*. Restionaceae	Sand	5.3	103	185,200	4.8	0.25	0.69
STV11-16	Strandveld	Poaceae; Restionaceae; *Sideroxylon inerme*	Sand	5.9	122	512,800	4.5	0.05	0.16
STV11-20	Strandveld	*Agathosma* sp.; Asteraceae	Sand	7.6	24	20,200	14.3		

STV11-21	Strandveld	Asteraceae; Poaceae	Sand	7.4	60	83,200	5	0.13	0.13
STV11-51	Strandveld	Restionaceae; *Olea europaea* subsp. *Africana*; *Metalasia* sp.; *Agathosma* sp.	Sand	7.5	48	75,000	8.3		
STV11-54	Strandveld	*Metalasia* sp.; *Searsia graviolens*; *Chrysanthemoides monilifera; Thamnochortus insignis*	Sand	7.9	11	7,500	10		
STV11-55	Strandveld	*Sideroxylon inerme*; *Chasmanthe aethiopica*; *Searsia glauca*; *Thamnochortus insignis*	Sand	7.6	11	7,500	22.2		
DC11-18	Dune cordon	Restionaceae; *Chrysanthemoides monilifera*; *Sideroxylon inerme*	Sand	5.6	65	83,200	3.2	0.27	0.30
DC11-38	Dune cordon	*Roepera morgsana*; *Carpobrotus accinaciformus; Euphorbia mauritanica*	Sand	6.7	36	7,300	8.8		
DC11-39	Dune cordon	*Osteospernum moniliferum*; *Carpobrotus edulis*; *Roepera morgsana*	Sand	7.4	19	27,300	5.3		
DC11-71	Dune cordon	*Searsia glauca*; *Phylica ericoides*; Asteraceae	Sand	7.9	9	21,900	11.1		
DC11-72	Dune cordon	*Sideroxylon inerme*	Sand	7.3	21	37,200	0		
DC11-73	Dune cordon	*Roepera morgsana*; Asteraceae; *Carpobrotus edulis*	Sand	7.8	27	28,000	0		
DC11-75	Dune cordon	*Pterocarpus tricuspidatus*; *Phylica ericoides*	Sand	7.8	13	38,400	0		
Forest biome									
CF10-13	Coastal Forest	*Celtis* sp.; *Vepris* sp.	Loam	6	108	345,500	2.7	0.03	0.03
Azonal									
RP11-13	Riparian	*Acacia karroo*; Poaceae; Asteraceae	Sand	5.5	166	2,444,900	0.6	0.02	0.02
RP11-14	Riparian	*Acacia karroo*; Poaceae; Asteraceae	Sand	6.2	203	1,238,100	3	0.01	0.01
RP11-48	Riparian	*Euphorbia mauritanica; Roepera morgsana*	Sand	7.3	55	97,300	3.8	0.07	0.11

RP11-49	Riparian	*Acacia karroo*; Poaceae	Loam	6.9	220	4,301,700	2.7	0.04	0.04
RP11-59	Riparian	*Acacia karroo*; Poaceae	Sand	7.3	156	851,700	1.9	0.04	0.05
RP11-79	Riparian	*Acacia karroo*; *Albuca maxima*; Poaceae; *Aloe ferox*	Sand	4.7	193	1,166,000	3.1	0.04	0.05
RP11-80	Riparian	*Acacia karroo*; *Albuca maxima*	Sand	5.4	64	342,200	0	0.00	0.00
W10-08	Wetland	*Cyperus textilis*; *Stenotaphrum secundatum*; *Arundo* sp.	Loam	6	183	1,586,600	7.6	0.12	0.12

V. 2.2. Fynbos biome

V. 2.2.1. Limestone fynbos

The dominant vegetation of the sampled areas consisted mainly of restios, Asteraceae shrubs and other eudicot small trees and shrubs. Grasses were either absent or barely present (Table 4). The few grasses noted corresponded to either *Ehrharta* or *Themeda*.

Phytoliths from limestone fynbos vegetation were identified in low concentrations ranging from 7,000 to 160,000 phytoliths g/sed (Table 4). This low phytolith concentration might be related to the restio and Asteraceae dominance, which produce low amounts of phytoliths, combined with the low presence of grasses (Table 2). Interestingly, the only sample (LF11-23) where *Themeda triandra* (C_4 Panicoideae) was part of the dominant vegetation also showed low phytolith concentration.

Out of the seven samples analyzed from this vegetation type, three showed enough phytoliths for a reliable morphological interpretation (LF11-23, LF11-68 and LF11-85). Although grasses were not common in this vegetation type, grass phytoliths were well represented in the phytolith record. Rondel phytoliths were most common among GSSCs (mean: 51.3%) whereas lobates were also frequent (mean: 38.7%). Interestingly, we observed that despite *Themeda triandra* was the dominant grass species from sample LF11-23 area, which produces GSSC bilobates (tabular flattened-round lobes) in high numbers (Section V. 1.2.3. Table A1), it had the lowest counts of GSSC lobates. Consistent with the vegetation, restio phytoliths were identified in high frequencies in all the samples (Table 5). Hat-shape phytoliths from the Cyperaceae family were identified in samples LF11-68 although sedges were not identified in the field. Eudicot phytoliths, mainly from wood and bark, were identified in high quantities in all the samples analyzed, where spheroid psilates were the most representative morphotype (Table 5).

V. 2.2.2. Sand fynbos

The vegetation present during sampling varied greatly in the different sampled areas. However, eudicots such as *Leucadendron salignum*, *Leucospermum praecox* and *Leucospermum muirii*, *Protea repens* and some *Erica* spp. were highly represented. Restios

were also well represented and grasses dominated in some of the areas (Table 4).

Out of the nine samples analyzed from sand fynbos, those from grass-dominated areas exhibited the highest phytolith concentration (SF11-42 and SF11-43). The samples having the lowest phytolith concentration corresponded to areas where eudicot plants dominated (SF10-05, SF10-06, SF11-37, SF11-47, SF11-62, SF11-82) (Table 4). The exception was sample SF11-45, which showed a high phytolith concentration and little grass-cover.

Overall, grass phytoliths dominated sand fynbos samples and GSSC rondels were the most representative morphotypes, accounting for 57% (mean) of the different GSSCs (Table 5 and Fig. 25). Restio phytoliths were also identified in high frequencies. Interestingly, samples SF11-45 and SF11-47, which were collected from areas where restios did not dominate, showed the highest concentration of these morphotypes (Tables 4 and 5). Cyperaceae hat-shape phytoliths were also identified in some sand fynbos samples, and these morphotypes were also observed in samples from limestone fynbos vegetation, even though they were not dominant in the vegetation (SF10-05, SF11-37, SF11-47 and SF11-62). Spheroids were identified in all the samples in high numbers with the exception of samples SF11-42 and SF11-43.

V. 2.2.3. Grassy fynbos

Grassy fynbos vegetation was composed of grasses such as *Themeda triandra* (C_4 Panicoideae), *Eragrostis capensis* and *Eragrostis curvula* (C_4 Chloridoideae) and *Pentachistis colorata* (C_3 Danthonioideae) (Table 4). Phytolith results showed a high phytolith concentration with a dominance of grass characteristic phytoliths (mainly GSSCs and bulliform cells) (Table 5). Samples SF11-42 and 43 presented the highest grass content among all the samples. Among GSSCs, rondels are represented in high frequencies in the two samples (GF10-10 and GF10-11), where *Pentachistis colorata*, *Themeda triandra* and *Eragrostis curvula* and *Eragrostis capensis* were dominant (Fig. 25). Even though chloridoids dominated in sample GF10-10, GSSC saddles were identified in low frequencies. Conversely, sample GF10-14, which was collected from a hilltop in the Brenton Lake area, contained high frequencies of GSSC lobates and saddles. Restios and eudicot phytoliths (leaves and wood and bark) were also identified although in very low frequencies (Table 5). These results are consistent with the low presence of these plants in this vegetation type.

Table 5. List of morphotypes identified, their plant type and plant part attribution and the percentage average of their presence in the vegetation types (modified after Esteban et al., in press-a).

			Fynbos biome				Fynbos/Renosterveld transition	Renosterveld biome	Thicket biome				Forest biome	Azonal vegetation	
Total ∑ Plant type	**Phytolith morphotypes**	**Plant attribution**	**Limestone Fynbos**	**Sand Fynbos**	**Grassy Fynbos**	**Mountain Fynbos**	**Fynbos/renoster-veld**	**Renoster-veld**	**Subtropical Thicket**	**Coastal Thicket**	**Strand -veld**	**Dune Cordon**	**Coastal Forest**	**Ripa-rian**	**Wet-land**
	Bulliform	Grass leaves	1.7	3.6	7.0	4.7	13.9	4.5	1.6	1.5	7.3	6.7	1.9	4.8	6.0
	Papillae	Grass leaves	0.0	0.0	0.0	0.0	0.0	0.2	3.9	1.4	0.0	0.0	0.0	0.0	0.0
	Trichome	Grass leaves	6.0	4.8	6.7	3.9	7.0	5.7	8.5	2.4	4.6	3.3	0.0	4.2	7.1
	Elongate with decorated margins	Grass inflorescenc	2.9	2.5	2.0	1.6	0.0	2.7	1.1	0.8	2.8	3.3	0.0	2.8	3.3
	GSSC Rondels	Grasses	20.9	26.0	24.6	33.1	10.4	37.5	22.5	24.5	30.1	31.7	21.3	28.3	26.2
	GSSC Lobates	Grasses	8.5	8.0	12.7	5.5	5.2	8.2	7.3	7.3	5.9	1.7	49.1	8.7	9.8
	GSSC Saddles	Grasses	2.2	3.8	3.4	1.6	12.2	6.3	6.3	26.4	5.0	13.3	10.2	22.4	2.7
	GSSC Oblongs	Grasses	1.7	4.2	5.2	10.2	2.6	5.0	7.1	3.0	4.9	3.3	3.7	4.5	7.1
TOTAL GRASSES			**43.9**	**52.7**	**61.7**	**60.6**	**51.3**	**70.0**	**58.2**	**67.3**	**60.6**	**63.3**	**86.1**	**75.8**	**62.3**
	Restio morphotype	Restionaceae	13.0	7.1	2.2	3.9	0.9	0.9	0.0	0.0	6.6	1.7	0.0	0.4	0.0
TOTAL RESTIOS			**13.0**	**7.1**	**2.2**	**3.9**	**0.9**	**0.9**	**0.0**	**0.0**	**6.6**	**1.7**	0.0	0.4	0.0
	Hat-shaped	Cyperaceae	0.7	1.3	0.0	0.0	0.0	0.0	0.0	0.0	0.0	0.0	0.0	0.2	0.0
TOTAL SEDGES			**0.7**	**1.3**	**0.0**	**0.0**	**0.0**	**0.0**	**0.0**	**0.0**	**0.0**	**0.0**	**0.0**	**0.2**	**0.0**
	Sclereid	Eudicot leaves	0.4	0.3	0.0	0.0	0.0	0.4	0.3	0.0	0.6	0.0	0.0	0.5	0.5
	Ellipsoid	Eudicot wood/bark	1.0	0.6	0.8	2.4	0.0	0.1	1.5	0.0	0.0	0.0	0.0	0.1	0.0

	Hair cell Eudicot	Eudicot leaves	0.0	1.0	1.4	0.8	0.0	0.5	0.4	0.0	0.3	0.0	0.0	0.6	0.0
	Hair Base Eudicot	Eudicot leaves	0.0	0.0	0.0	0.0	0.0	0.0	0.4	0.0	0.0	0.0	0.0	0.0	0.0
	Stomata	Eudicot leaves	0.0	0.1	0.0	0.0	0.0	0.0	0.0	0.0	0.0	0.0	0.0	0.2	0.0
	Parallelepiped blocky	Eudicot wood/bark	3.6	2.2	2.2	0.8	2.6	1.6	0.7	0.4	1.2	0.0	0.0	0.2	4.4
	Vascular elements	Eudicot leaves	0.4	0.1	0.0	0.0	0.0	0.0	0.0	0.0	0.0	0.0	0.0	0.4	0.0
	Fibers	Eudicots	0.0	0.0	0.0	0.0	0.0	0.0	0.0	0.0	0.0	0.0	0.0	0.1	0.0
	Epidermal ground-mass polyhedral	Eudicot leaves	0.0	0.8	0.2	0.0	0.0	0.2	0.0	0.0	2.0	1.7	0.9	0.6	0.0
	Fruit phyotliths	Eudicot fruits	0.0	0.0	0.0	0.0	0.0	0.0	0.0	0.0	0.0	0.0	0.0	0.1	0.0
TOTAL EUDICOTS			**27.4**	**16.7**	**5.4**	**11.8**	**12.2**	**7.3**	**8.8**	**4.7**	**10.2**	**15.0**	**3.7**	**4.5**	**10.4**
	Elongates without decoration margin	Non-diagnostic	9.2	17.4	26.6	21.3	23.5	16.5	18.1	8.5	16.6	11.7	7.5	13.7	23.47
	Parallelepiped thin	Non-diagnostic	2.7	1.7	0.6	1.6	6.1	1.2	3.1	2.4	2.9	3.3	0.0	2.1	1.6
TOTAL ELONGA-TES			**11.9**	**19.0**	**27.2**	**22.8**	**29.6**	**17.6**	**21.3**	**11.0**	**19.5**	**15.0**	**7.4**	**15.8**	**25.1**
	Spheroid	?	22.0	11.6	0.9	7.9	9.6	4.4	5.5	4.3	6.0	13.3	2.8	1.9	5.5
	Spheroid echinate	?	0.0	0.0	0.0	0.0	0.0	0.0	0.0	1.1	0.6	0.0	0.0	0.0	0.5
	Irregular/Indetermina-te	Non-diagnostic	3.3	3.2	3.5	0.8	6.1	4.0	11.7	16.0	2.5	5.0	2.8	3.3	1.6

V. 2.2.4. Mountain fynbos

Only one sample was collected from mountain fynbos vegetation (MF12-01). The sample was collected from an area where restios and sedges dominated the plant cover, but there were some associated shrubs (Table 4). Phytoliths were identified in relatively high concentration and were dominated by rondel GSSCs (Table 5; Fig. 25). Characteristic restio phytoliths were not recorded in high numbers, despite these plants dominated the vegetation. Spheroid phytoliths were also identified in relatively high concentrations, which might belong in part to restios (Table 5).

V. 2.3. Renosterveld biome

V. 2.3.1. Renosterveld

Renosterveld vegetation on the Cape south coast (south of Langeberg and Riviersonderend Mountains) is considered to be a distinct vegetation type on account of the high abundance of largely C_4 grasses and 50-70% plant cover (Mucina and Rutherford, 2006). The species composition of renosterveld differs significantly from any fynbos vegetation types due to the lack of Proteaceae and Ericaceae species. The vegetation in the 17 samples analyzed from renosterveld was composed of shrubs such as *Elytropappus rhinocerotis* (commonly known as renosterbos), other Asteraceae shrubs and various family grasses (C_4 Panicoideae and Chloridoideae, and C_3 Ehrhartoideae and Danthonioideae) (Table 4).

Quantitatively most of the samples from renosterveld showed the highest phytolith concentration in comparison to other vegetation types, ranging from 4.8 to 1.2 million phytoliths /g sed. The only exceptions were samples RV11-15 and RV11-58, with much lower numbers (Table 4). As with other vegetation types, samples containing the highest phytolith concentration were collected from areas where grasses were dominant.

All the samples showed similar phytolith assemblages with grasses dominating and restios and eudicot plants represented in lesser amounts (Table 5). GSSC rondels were the most abundant morphotypes identified among grasses. The exceptions were samples RV09-01, RV11-15 and RV11-58, which contained a higher presence of GSSC saddles and lobates, by approximately 30%. Sample RV09-01 was collected from an area where C_4 grasses

dominated, such as *Themeda triandra* and *Brachiaria serrata* (C_4-Panicoideae) and *Eragrostis curvula* and *E. capensis* (C_4-Chloridoideae) along with *Cymbopogon marginatus* (C_4-Andropogonae). The latter subfamily has not been studied in our modern plant reference collection. Restio phytoliths were also identified but in low frequencies (Table 5). In spite of restios being recognized in most of the sampled areas, they did not represent a dominant component. Among eudicots, spheroid phytoliths were present in slightly higher frequencies with the exception of samples RV09-03 and RV11-67, even though the vegetation in these later samples was similar to the previous ones. Nonetheless, we need to bear in mind that because grass phytoliths were identified in high numbers both restio and woody plants, which are low phytolith producers, might appear underrepresented in the phytolith record.

V. 2.4. Transition fynbos/renosterveld

One sample was collected from this area where the vegetation showed characteristic elements from both fynbos and renosterveld vegetation, with high presence of grasses, restios, and shrubs (F/ RV10-07). This sample was collected from below *Tritoniopsis* sp. and Restionaceae. The phytolith concentration was similar to both grassy fynbos and renosterveld samples (Table 4). Grasses dominated the phytolith assemblage although restios and eudicot phytoliths were also well represented. GSSC saddles dominated among other GSSCs by 50% of the total assemblage (Table 5). No further characterization of transition vegetation could be inferred through the phytolith assemblage.

V. 2.5. Thicket biome

V. 2.5.1. Subtropical thicket

Subtropical thicket vegetation was dominated by eudicot plants characterized mainly by *Sideroxylon inerme*, *Eriocephalus africanus* and *Searsia pterota*. Of the three samples analyzed from this vegetation type, only sample StT09-06 contained a high phytolith concentration (1.2 million phytoliths /g sed) (Table 4). The phytolith assemblage from this sample showed low morphological variety with a dominance of grasses even though wood/bark phytoliths were also well represented. Among the grasses, GSSCs rondels were

the dominant morphotypes and lobates and saddles were identified in much lower frequencies (Table 5).

V. 2.5.2. Coastal thicket

Six samples were collected from the densely vegetated cliff area around Pinnacle Point where *Euclea racemosa*, *Euphorbia* spp., *Sideroxylon inerme*, *Grewia occidentalis*, *Lycium* sp., *Zygophyllum morgsana* and *Cassine peragua* dominated. Grasses were also present in some of the areas, and *Eragrostis* spp. dominated in sample CT06-05 (Table 4). These results showed an overall low phytolith concentration, with the exception of sample CT06-07 (900,000 phytoliths /g sed), which was collected from a loamy soil. Out of the eight samples collected, only four (CT06-01, CT06-02, CT06-05 and CT06-06) contained enough phytoliths for a reliable interpretation of the data. Furthermore, despite the diversity of eudicot plants in coastal thicket vegetation, samples showed low morphological variety with characteristic grass phytoliths being the most abundant. Among these grasses, GSSC saddles dominated along with lobate morphotypes (Table 5). For example, in sample CT06-05, where *Eragrostis* spp. was the dominant plant component, GSSC saddles represented the 92%. Spheroid echinates were identified in samples CT06-02 and CT06-05, although in low frequencies. Spheroids and characteristic eudicot leaf phytolith morphotypes were identified in low numbers in spite of the denser woody vegetation occurring in the area (Table 5).

V. 2.5.3. Strandveld

The dominant vegetation in the sampled areas was composed of grasses (mainly C_3 Ehrhartoideae), restios, asteraceous plants and other trees or shrubs such as *Stoebe cinorera*, *Sideroxylon inerme*, *Agathosma* spp., *Searsia* spp. and *Metalasia* sp. (Table 4).

Out of the seven samples analyzed, only three (STV11-1, STV11-16 and STV11-21) contained enough phytoliths for reliable interpretation. As with other vegetation types, the highest phytolith concentration corresponded to areas where grasses were dominant (Table 4). The phytolith assemblage is most characteristic of fynbos vegetation, whereas grass phytoliths dominated in all the samples. Among GSSCs, rondels were dominant and

associated with lobates and saddles in most of the samples (Table 5). This is consistent with Ehrhartoideae being the most representative grass family in the area. Restio phytoliths and spheroids were present in high frequencies in sample STV11-1.

V. 2.5.4. Dune cordon

The vegetation present in dune cordon areas was characterized by asteraceous plants and other shrubby vegetation with few grassy elements (only *Ehrharta villosa* was identified). Dune cordon samples also had the lowest phytolith concentration and did not exceed 100,000 phytoliths /g sed (Table 4). Only sample DC11-18 did contain enough phytoliths for a reliable interpretation of the data. Furthermore, grass phytoliths dominated these samples even though grasses were rarely observed in the understorey vegetation (Tables 4 and 5). Among grasses, GSSC rondels were the dominant morphotypes while saddles were also well-represented. Restio phytoliths were noted although in low numbers. Spheroids were also identified in relatively high frequencies in all the samples (Table 5).

V. 2.6. Forest biome

V. 2.6.1. Coastal forest

Coastal forest area was densely vegetated and dominated by eudicot trees such as *Celtis* sp. and *Vepris* sp., as well as other eudicot herbs and shrubs. The understorey was composed of grasses, although they were not part of the dominant vegetation. The quantitative results showed relatively high phytolith concentration (345,000 phytolith /g sed) (Table 4). In relation to morphology, grasses dominated the phytolith assemblage making up 86%. Contrary to other samples, GSSC lobates dominated here, by 50% of the total phytolith morphotypes identified. Few phytoliths characteristics of eudicot leaves as well as few parallelepiped blocky morphotypes from the wood and bark of eudicot plants were identified (Table 5).

V. 2.7. Azonal vegetation

V. 2.7.1. Riparian

The winter-deciduous *Acacia karroo* and other eudicot trees or tall shrubs, as well as several asteraceous plants, dominated in most of the sampled areas. Grasses were present as part of the dominant vegetation for most of the areas in association to other herbaceous plants (Table 4).

Together with grassy fynbos and renosterveld, samples from riparian vegetation contained the highest phytolith concentration, ranging from 4.3 million to 97,000 phytoliths /g sed. Samples with the highest phytolith concentration corresponded to areas dominated by grasses (Table 4). Morphologically, grass phytoliths were the major component with a minor presence of phytoliths from other plants (Table 5). GSSC saddles were the most representative morphotypes. Although restios were not present, diagnostic restio phytoliths were identified in samples RP11-48, RP11-59 and RP11-79. Cyperaceae hat-shape characteristic phytoliths were only identified in sample RP11-79, and in very small abundance (~1%). Eudicot phytoliths, both from wood/bark and leaves, were noted in low frequencies in all the samples (Table 5).

V. 2.7.2. Wetlands

The wetlands in the study area are seasonally inundated sites that are adjacent to rivers and floodplains. Water levels may vary throughout the year, but the sites are inundated for at least several weeks per annum. The only sample analyzed was collected from the riverside of the Little Brak River where Cyperaceae and Arundo grasses dominated. Some eudicot trees and shrubs were also present. Phytoliths were identified in high numbers (1,590,000 phytolith g/ sed) (Table 4). The phytolith assemblage was dominated by grass and wood/bark phytoliths. Despite C_4 Panicoideae grasses dominated the vegetation, GSSC lobates were identified in low frequencies (Table 5). Characteristic Cyperaceae hat-shape phytoliths were absent from the phytolith assemblage.

V. 2.8. Statistical analysis

The results from the ANOVA test showed statistically significant differences in nine out of the twenty-two phytolith morphotypes between vegetation types and in eight out of the twenty-two phytolith morphotypes between biomes ($p<0.05$) (Tables A2 and A3, respectively). Subsequently, we ran those significant phytolith morphotypes through a post hoc Tukey's HSD test, which is represented in Fig. 28 (phytolith morphotypes in regards to vegetation types) and Fig. 29 (phytolith morphotypes in regards to vegetation biomes). These results indicated that the null hypothesis can be rejected, which stated that no significant difference can be found between the phytolith morphological distribution from each of the vegetation types or biomes on the south coast of South Africa.

The ANOVA analysis also showed that parallelepiped blocky (ANOVA, $p<0.0378$), spheroids (psilate and rugulate) (ANOVA, $p<0.0001$) and restio phytoliths (ANOVA, $p<0.0001$) are the defining phytolith morphotypes of limestone fynbos vegetation (Table A2 and Fig. 28). No other vegetation type showed this pattern (Fig. 28). These results are in agreement with those observed through the D/Pº and Fy indices (Fig. 27a and b). The post hoc Tukey's HSD test confirmed a clear separation among limestone fynbos vegetation and the rest of the vegetation types (Fig. 28). Contrariwise, the statistical analysis conducted did not show any defining phytolith morphotype in samples from sand and grassy fynbos (Table A2 and Fig. 28). Nevertheless grassy fynbos vegetation is characterized by the low presence of woody and restio elements (Fig. 28).

Renosterveld vegetation is characterized mainly by a very low presence of GSSC saddles (ANOVA, $p<0.0024$), spheroids (psilate and rugulate) (ANOVA, $p<0.0001$) and restio phytoliths (ANOVA, $p<0.0001$) (Table A2 and Fig. 28). The post hoc Tukey's HSD test showed that Renosterveld differed the most from the Thicket biome by the low presence of ellipsoids, GSSC saddles and irregular and indeterminate morphotypes, and from the Fynbos biomes by the low presence of limestone and sand fynbos vegetation types by the presence of spheroids and restio phytoliths (Fig. 28).

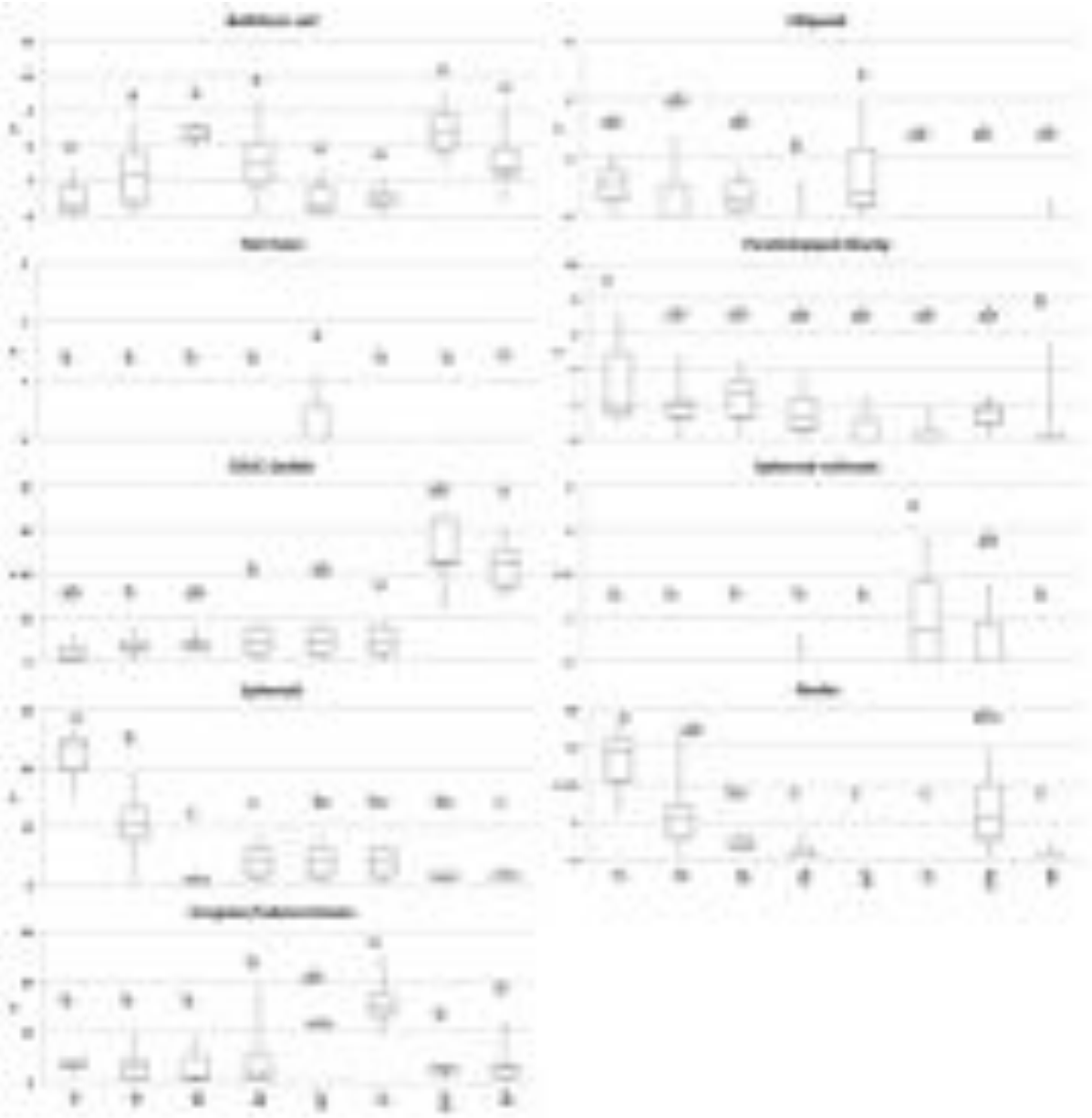

Figure 28. Box-plots of the nine phytolith morphotypes pointed out by ANOVA and a post hoc Tukey Honest Significant Differences (HSD) as statistically significant different among vegetation types. The mean values (mid-line), standard error ± (box) and standard deviation (whiskers) are given for the nine phytolith morphotypes. Legend: CT, coastal thicket; GF, grassy fynbos; LF, limestone fynbos; RP, riparian; RV, renosterveld; SF, sand fynbos; StT, subtropical thicket; STV, strandveld. Different letters indicate means that are significantly different based on the post hoc Tukey (HSD) test (retrieved from Esteban et al., in press-a).

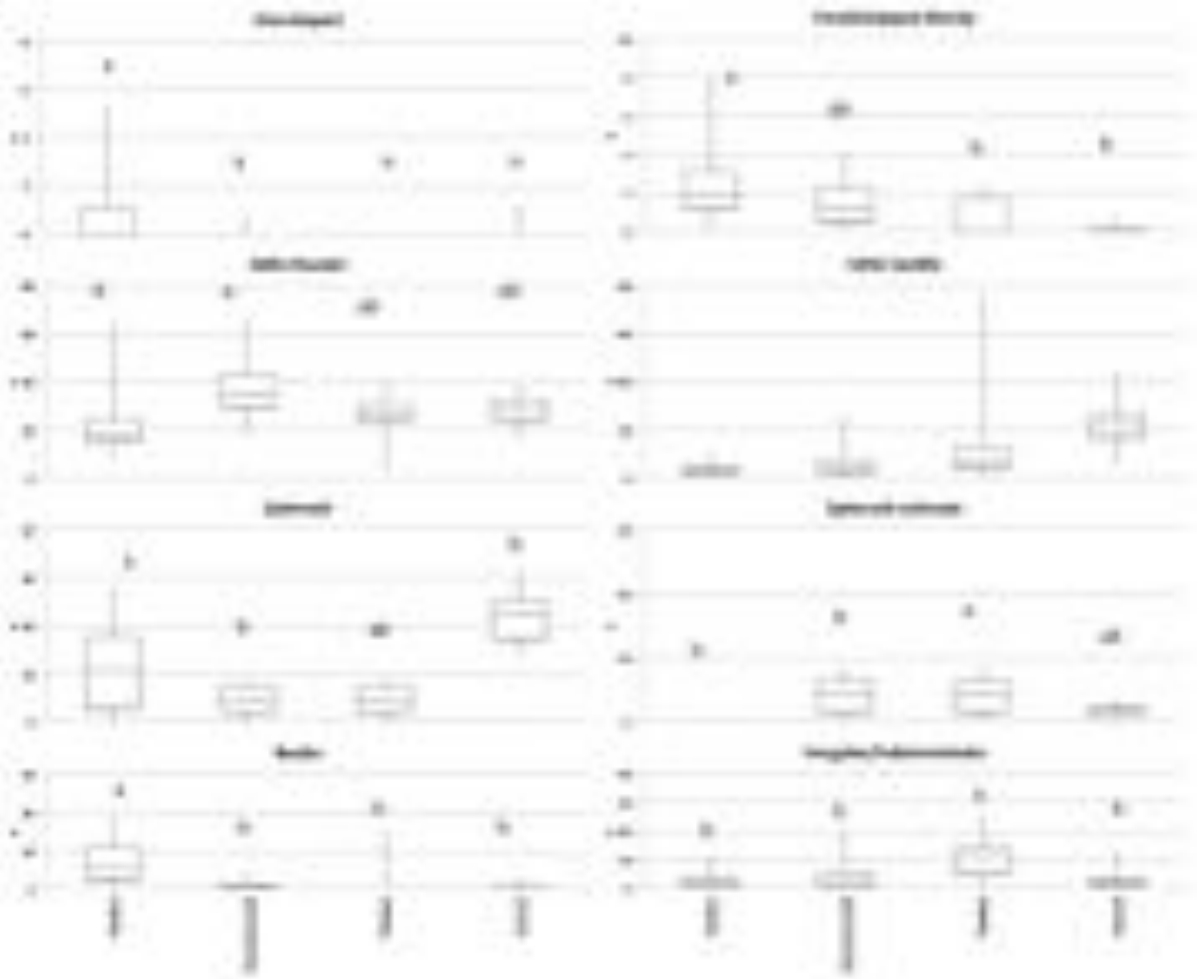

Figure 29. Box-plots of the eight phytolith morphotypes pointed out by ANOVA and a post hoc Tukey Honest Significant Differences (HSD) as statistically significant different among vegetation biomes. The mean values (mid-line), standard error ± (box) and standard deviation (whiskers) are given for the eight phytolith morphotypes. Different letters indicate means that are significantly different based on the post hoc Tukey (HSD) test (retrieved from Esteban et al., in press-a).

ANOVA and post hoc Tukey's HSD test results identified hair base phytoliths (ANOVA, $p<0.0195$) and ellipsoids (ANOVA, $p<0.026$) as the diagnostic morphotypes for subtropical thicket vegetation (Fig. 28). Coastal thicket vegetation is correlated with an abundance of GSSC saddles (ANOVA, $p<0.0024$), irregular and indeterminate morphotypes (ANOVA, $p<0.0001$), and spheroid echinates (Table A2 and Fig. 28). The statistical analysis did not show any defining phytolith distribution in samples from strandveld vegetation (Table A2 and Fig. 28). Finally, ANOVA and post hoc Turkey's HSD method demonstrated a clear

separation of riparian vegetation among the other vegetation types by the abundance of GSSC saddles (ANOVA, $p<0.0024$) (Table A2 and Fig. 28).

When analyzing the phytolith assemblage on a broader scale (vegetation biomes) it was observed that ANOVA and post hoc Tukey's HSD test clearly differentiate the Fynbos biome from other local biomes. Like the results of the limestone fynbos vegetation, the Fynbos biome itself can be defined based on parallelepiped blockys (ANOVA, $p<0.005$), spheroids psilate and rugulate (ANOVA, $p<0.0021$), and restio phytoliths (ANOVA, $p<0.0001$) (Table A3 and Fig. 29). ANOVA showed that Renosterveld biome is mainly characterized by the abundance of GSSC rondels (ANOVA, $p<0.0128$) and a low presence of GSSC saddles (Fig. 29). The post hoc Tukey's HSD test showed that the highest differences in the presence of GSSC rondels are observed between Renosterveld and Fynbos biome (Fig. 29). Thicket biome is mainly characterized by the abundance of irregular and indeterminate morphotypes (ANOVA, $p<0.0015$) as well as the abundance of spheroid echinate phytoliths (ANOVA, $p<0.0103$). The post hoc Tukey's HSD test showed that Thicket vegetation can be clearly differentiate among biomes by the abundance in the presence of irregular phytoliths (ANOVA, $p<0.0015$) (Fig. 29). Finally, ANOVA showed that riparian vegetation is correlated with the abundance of GSSC saddles (ANOVA, $p<0.0027$). The post hoc Tukey's HSD test showed that riparian vegetation differs mainly from Fynbos and Renosterveld biomes by GSSC saddle concentration and placed closely to the Thicket biome (Table A3 and Fig. 29).

V. 3. Archaeological sediment samples from Pinnacle Point 5-6

Table 6 lists only the sixty-three samples with a minimum number of recognizable phytolith morphotypes (50), together with their stratigraphic location and description, and the main phytolith and mineralogical results including total number of phytoliths morphologically identified, relative number of phytoliths per gram of sediment (/g sed), percentage of weathered morphotypes and delicate morphologies, diatoms and sponge spicules, FTIR results and the D/P^o, Fy, Ic, Iph and Fs indices. The description of samples with insufficient number of identifiable phytoliths is given in the Appendices (Table A4). Sixty-two phytolith morphotypes were identified, which were later grouped by plant types and plant parts into thirteen general categories (grasses, restios, sedges, leaves, wood/bark and fruits of eudicotiledonous plants, spheroids, spheroids echinate, stomata, epidermal appendages, elongates with and without decorated margins and irregular and indeterminate morphologies). The phytolith morphotypes identified, taxonomic association and its frequencies in samples from the different StratAggs given sample type information are listed in Table A5.

V. 3.1. Mineralogy

FTIR analyses showed that the main mineral components of the samples were clay, quartz, calcite, dahllite and aragonite in different proportions (Table 6 and Table A4). The main differences in the mineralogical composition were related to the stratigraphic location of the samples as well as to the sample types from combustion features (hearth facies). In the lower StratAggs YBSR and LBSR, clay, quartz and calcite were the main minerals, whereas dahllite and aragonite were barely present. Mineralogical composition with respect to different sample types (hearth facies) from these StratAggs is given in detail in Section V. 3.4. In ALBS StratAgg, quartz and clay predominated and calcite was mostly present in the white layers. Traces of dahllite and aragonite were also identified in some samples but in small proportions. Samples from SADBS StratAgg differed from the rest of StratAggs by showing the highest calcite concentration in all the samples. Dahllite was also detected in all the samples (Table A4). Moreover, samples from SADBS showed also the highest concentration of aragonite in samples. The origin of aragonite in archaeological sites usually derives from land snails, clams or marine mollusks (Weiner, 2010), such as mussels.

Aragonite can also be formed from aqueous solution at high-temperatures (Lippmann, 1973). In order to assess the origin of the aragonite, fragments of seashells recovered from those sediment samples where aragonite was detected were also analyzed through FTIR. The majority of the seashells analyzed preserved aragonite, what attests for the marine mollusk origin of the aragonite detected in the sediment samples. Finally, in the uppermost StratAggs (OBS2, SGS, OBS1, BBCSR, RBSR), quartz and clay dominated the mineral component and calcite was absent. Only four samples from BBCSR (418152, 418153, 418154, 418155) showed calcite as the main mineral component, with clay being exposed at high temperatures and the presence of dahllite.

V. 3.2. Phytolith concentration

Phytoliths were detected in samples along the PP5-6 sequence but in different concentrations (Table 6 and Table A4). As it was pointed out in Section IV 2.1.2., a minimum of 200 phytoliths were counted for the morphological analysis and when this was not possible only those samples with a minimum number of 50 phytoliths were considered for morphological interpretation in order to obtain as much information as possible (Albert and Weiner, 2001). However, the error margin in the interpretation of the phytolith representation when using a minimum of 50 phytoliths is very high (40%; Albert and Weiner, 2001).

The twenty-three control samples collected from geogenic/sand dune layers had few or no phytoliths independently of their provenance along the sequence, and none of them reached the minimum number of phytoliths necessary to conduct a reliable interpretation of the data (Table A4). All the samples containing enough phytolith concentration for a reliable morphological interpretation of the data belonged to combustion features. It was observed a decrease in the phytolith concentration from the lowermost StratAggs (YBSR, LBSR, ALBS and SADBS), with LBSR and YBSR showing the highest concentration, to the uppermost StratAggs (OBS2 and OBS1, SGS, DBCS, BBCSR, RBSR), which were sterile with the only exception of sample 418155 from BBCSR (Table 6 and Table A4). Despite this sterility in the upper-most layers, the PP5-6 phytolith sequence crosses the inter-glacial to glacial transition of MIS5 to MIS4 where there are interesting changes in stone tools and site occupation.

Table 6. List of the sixty-three samples with sufficient number of recognizable phytoliths to be interpreted, together with their stratigraphic location and description, and the main phytolith and mineralogical results, total number of phytoliths morphologically identified, relative number of phytoliths per gram of sediment (/g sed), percentage of weathered morphotypes, delicate morphologies (according to Cabanes and Shahack-Gross, 2015) diatoms and sponge spicules, FTIR results and the D/Pº, Fy, Ic, Iph and Fs indices. WM = weathered morphotypes. Clay (b=burned), (nb=not burned), (b?= probably burnt).

Sample Number	Stratigraphic Aggregate	Sample Type	# Phyt counted	Phyt g/sed	% WM	% Delicate morphologies	% Diatoms	% Sponge spicule	FTIR	D/Pº index	Fy index	Ic index	Iph index	Fs index
418155	BBCSR	White layer	112	135,100	46.43	55	0	0	Ca, Cl (b), Qz, Dah	0.00	0.00	0.00	0.00	0.00
162466	SADBS	White layer	214	300,000	30.37	2.01	0	0	Ca, Qz, Cl (b), Dah	0.00	0.02	0.92	0.29	0.06
162467	SADBS	Black layer	93	69,000	24.73	2.86	0	0	Ca, Qz, Cl (b), few Dah	0.02	0.16	0.87	0.25	0.06
46682	SADBS	Black layer	75	67,000	37.33	2.13	0	0	Ca, Qz, Cl (nb), some Dah	0.13	0.67	1.00	0.00	0.00
356487	SADBS	White layer	59	75,100	72.88	0.00	0	0	Ca, Qz, Cl (b?), few Dah	0.33	0.50	1.00	0.00	0.00
356491	SADBS	Grey color	86	78,900	27.91	0.00	0	0	Cal, Qz, Cl (b), some Dah	0.00	0.44	0.81	0.33	0.06
357374	ALBS	Grey color	60	58,200	21.67	1.00	0	2.08	Ca, Qz, Cl (nb)	0.38	0.05	0.75	0.33	0.11
357383	ALBS	Grey color	202	284,100	28.71	0.00	3.36	34.25	Ar transforming to Ca, Qz, Cl (nb)	0.03	0.10	0.90	0.44	0.03
357380	ALBS	Grey color	202	230,300	21.78	12.77	0	2.47	Ca, Qz, Cl (nb)	0.06	0.27	1.00	0.00	0.00
162483	ALBS	Red layer	153	123,700	34.64	9.49	1.96	6.54	Ca, Qz, Cl (nb)	0.13	0.04	0.84	0.09	0.00
162481	ALBS	Black layer	216	314,600	18.98	2.78	0	9.33	Ca, Qz, Cl (nb)	0.03	0.08	0.85	0.31	0.04
162494	LBSR	Outside Hearth	73	87,600	28.77	0.00	0	3.7	Qz, Cl (nb), few Ca, few Ar, some	0.06	0.08	0.98	0.00	0.01
162493	LBSR	Red layer	112	107,000	25.00	1.54	0	8.7	Qz, Cl (nb), Ca, few Ar	0.08	0.28	0.93	0.00	0.07
162492	LBSR	Black layer	165	239,600	47.27	12.28	1.14	7.45	Ar transforming into Ca, Qz, Cl	0.21	0.04	1.00	0.00	0.00

356476	LBSR	Black layer	112	117,400	10.71	0.00	0	5.66	Ca, Cl (nb), Qz, Dah	0.04	0.35	0.93	0.00	0.02
162558	LBSR	Black layer	126	108,800	36.51	0.00	0	3.61	Cl (nb), Qz, Ca, few Dah?	0.16	0.33	0.94	0.00	0.06
162557	LBSR	Red layer	149	320,100	33.56	3.41	0	1	Ca, Qz, Cl (nb), few Dah	0.22	0.05	0.88	0.20	0.04
162549	LBSR	Red layer	161	416,000	71.43	0.67	0	8	Cl (nb), Qz, Ca	0.05	0.34	0.89	0.25	0.04
162550	LBSR	Black layer	183	355,500	30.05	21.13	0	3.76	Ca, Cl (nb), Qz	0.34	0.08	0.92	0.00	0.00
162548	LBSR	Above Hearth	50	122,600	32.00	0.00	0	0	Qz, Cl (nb), Ca	0.08	0.04	0.95	0.38	0.05
356475	LBSR	White layer	278	1,117,500	76.98	1.79	0	0	Qz, Cl (nb), few Ca	0.01	0.03	0.97	0.00	0.00
356474	LBSR	Black layer	245	392,700	24.90	1.28	1.6	2.13	Cl (nb), Qz, Ca, few Dah	0.03	0.04	0.85	0.14	0.00
357368	LBSR	Black layer	199	833,200	18.22	1.48	0	1,97	Ca, Cl (nb), Qz, Dah	0.02	0.02	0.95	0.10	0.09
357369	LBSR	Black layer	214	404,900	8.88	1.02	0	1.02	Ca, Cl (nb), Qz, Dah	0.00	0.01	0.99	0.00	0.01
357370	LBSR	Black layer	225	855,350	6.22	0.59	0	0.94	Ca, few Cl (nb), few Qz, Dah	0.01	0.03	0.89	0.50	0.00
356470	LBSR	White layer	97	161,100	22.68	0.48	0	2.60	Ca, Qz, Cl (nb), few Dah	0.02	0.02	0.88	0.47	0.01
356471	LBSR	Black layer	220	354,000	20.91	0.56	0	0	Ca, Cl (nb), Qz, Dah	0.02	0.04	0.98	0.00	0.01
357363	LBSR	White layer	206	3,780,500	58.25	0.00	0	2.27	Ca, Cl (nb), Qz, Dah	0.04	0.09	0.97	0.00	0.00
357362	LBSR	Black layer	170	887,900	20.59	20.83	1.46	2.88	Cl (nb), Qz, Ca, Dah	0.06	0.17	0.83	0.00	0.00
357364	LBSR	Black layer	132	310,800	13.64	1.23	0.00	7.32	Ca, Cl (nb), Qz, Dah	0.17	0.21	0.93	0.25	0.10
357365	LBSR	Black layer	64	362,700	23.44	0.51	2	7.55	Qz, Cl (nb), some Ca, few Dah	0.21	0.08	0.96	0.00	0.03

357366	LBSR	Black layer	138	185,600	11.59	0.00	0.00	1.61	Ca, Qz, Cl (nb), Dah	0.08	0.28	0.99	0.00	0.01
356454	LBSR	Black layer	185	558,700	19.46	3.51	3.87	0	Cl (nb), Qz	0.28	0.51	0.91	0.00	0.00
356453	LBSR	Black layer	314	866,200	6.69	18.37	3.93	1.35	Cl (nb), Qz	0.51	0.13	0.88	0.00	0.00
356455	LBSR	Black layer	227	372,500	5.73	1.64	0	0.47	Cl (nb), Qz, some Ca, Dah	0.13	0.17	0.90	0.17	0.02
162778	LBSR	Black layer	219	1,237,700	67.58	2.72	1.39	2.74	Qz, Cl (nb), few Ca	0.17	0.22	0.75	0.39	0.19
356464	LBSR	Black layer	179	364,500	22.91	0.00	0	0	Ca, Cl (nb), Qz, few Dah	0.13	0.03	0.89	0.50	0.11
356469	LBSR	Black layer	136	220,400	17.65	1	0	0	Qz, Cl (nb), few Ca, some Dah	0.03	0.13	0.66	0.15	0.05
356462	LBSR	Black layer	119	135,400	5.88	2.9	0	2.61	Cl (nb), Qz, some Dah	0.05	0.15	0.90	0.14	0.06
356456	LBSR	Black layer	90	225,100	13.33	0.00	0	3.7	Cl (nb), Qz, few Dah	0.10	0.21	0.88	0.50	0.06
162781	LBSR	Black layer	379	1,185,500	11.08	1.33	0.59	0.59	Cl (nb), Qz, Ca, some Dah	0.10	0.08	1.00	0.00	0.00
356457	LBSR	Black layer	212	771,000	7.55	2.3	0	3.92	Cl (nb), Qz few Ca, Dah	0.04	0.07	0.96	0.00	0.01
356458	LBSR	Black layer	180	539,800	5.56	1.48	0.58	3.41	Cl (nb), Qz, few Ca, Dah	0.02	0.38	0.82	0.50	0.29
356459	LBSR	Black layer	230	491,300	10.00	9.3	0.48	6.33	Ca, Cl (nb), Qz, Dah	0.24	0.14	0.86	0.60	0.08
162782	LBSR	Black layer	244	255,300	29.92	5.88	0	2.84	Ca, few Cl (nb) and Qz, Dah	0.03	0.27	0.73	0.33	0.00
356463	LBSR	White layer	77	155,100	68.83	10.87	0	0	Ca, few Qz and Cl (b), Dah	0.18	0.27	0.82	0.00	0.45
356460	LBSR	Black layer	187	216,600	4.28	3.13	0	4.79	Ca, Cl (nb), Qz, few Dah	0.18	0.47	0.90	0.33	0.20
356461	LBSR	Black layer	128	174,200	19.53	3.03	0	11.97	Ca, Cl (nb), Qz, some Dah	0.23	0.45	0.82	0.00	0.00

162717	LBSR	Red layer	100	75,100	35.00	6.25	0	7.14	Ca, Cl (nb), Qz, some Dah	0.37	0.42	0.68	0.00	0.47
162728	LBSR	Black layer	260	212,500	28.85	17.24	0	2.63	Ca, Qz, Cl (nb), Dah	0.32	0.10	0.88	0.60	0.10
162749	LBSR	White layer	142	141,900	27.46	1.19	0	9.65	Ar transfoming into Ca, Qz, Cl	0.08	0.32	0.82	0.00	0.11
162750	LBSR	Black layer	91	117,100	42.86	1.92	0	7.14	Ar, Qz, Cl (nb), some Ca, some	0.07	0.22	0.89	1.00	1.11
162783	YBSR	Red layer	110	115,700	4.55	1.14	0	1.87	Qz, Cl (nb)	0.22	1.31	0.81	0.00	0.06
356479	YBSR	White layer	126	935,700	15.87	0.00	0	0.93	Ca, Qz, Cl (nb), few Dah	0.75	0.85	0.73	0.11	0.00
388612	YBSR	White layer	62	1,165,700	30.51	0.00	0	0	Qz, Ca, Cl (nb)	0.64	0.12	0.94	0.00	0.04
388613	YBSR	Red layer	135	289,400	64.44	3.96	0	0	Qz, Cl (nb), Ca	0.04	0.10	0.85	0.22	0.02
388614	YBSR	Grey color	122	350,900	31.15	6.00	0	0	Ca, Qz, Cl (b), Dah	0.05	0.39	0.83	0.00	0.00
388615	YBSR	Black layer	228	482,500	76.75	5.66	0	3.64	Qz, Ca, Cl (nb)	0.17	0.00	0.84	0.20	0.13
388588	YBSR	Black layer	109	210,600	57.80	6.25	0	8	Ca, Cl (nb), Qz	0.00	0.69	1.00	0.00	0.15
356478	YBSR	Black layer	111	106,000	20.72	59.76	0	3.30	Qz, Cl (nb), few calcite	0.54	0.29	1.00	0.00	0.29
162710	YBSR	Black layer	97	117,700	21.65	8.94	0	0	Qz, Cl (nb)	0.29	0.08	0.99	0.00	0.01
356414	YBSR	Black layer	105	143,400	9.01	13.04	0.98	5.61	Ar transforming into Ca, Qz, Cl	0.04	0.44	0.81	0.33	0.19
356417	YBSR	Red layer	111	133,900	22.58	0.00	0	2.04	Qz, Cl (nb), Ca	0.13	0.18	0.89	0.17	0.02

V. 3.3. Phytolith stability

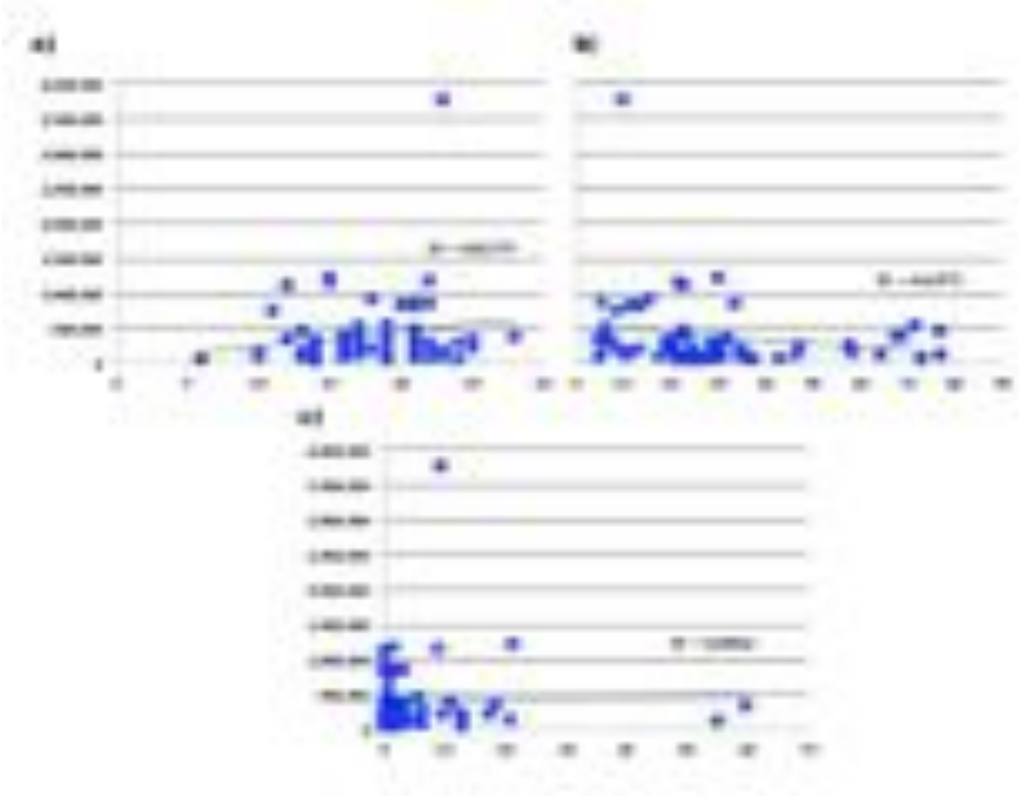

Figure 30. Scatterplot and trendline of the phytolith concentration per gram of sediment against a) number of phytolith morphotypes; b) percentage of weathered morphotypes; c) percentage of delicate morphologies.

Weathered morphotypes were identified in all the samples in moderate frequencies with some exceptions as described below (Table 6). Moreover, delicate morphologies, which are the first ones that disappear under certain post-depositional processes (Cabanes et al., 2011; Cabanes and Shahack-Gross, 2015), such as hair cells, tracheids, stomata, papillae, epidermal ground mass and parenchyma strands, were also preserved in most of the samples (Table A5). Samples with high frequencies of weathered morphotypes also had delicate morphologies being identified in very high frequencies in samples 418155 (55%) from BBCSR, and 162778 (22.5%) and 356463 (20.8%) from LBSR. The exceptions were samples 356487, 356475 and 162750 from LBSR, which showed high frequencies of weathered morphotypes and an absence of delicate morphologies. Samples from ALBS showed in general low frequencies of weathered morphotypes and only one sample (356487) from

SADBS showed high frequencies of them (72.88 %) and this came from a white layer. In this sample it was observed that the only phytoliths identified corresponded to non-delicate morphologies such as elongates, parallelepiped blockys, irregular morphologies, restios and grass silica short cell (GSSC) rondels which are resistant morphotypes (Cabanes and Shahack-Gross, 2015). This is suggestive that partial dissolution processes affected the phytolith assemblage of this sample.

To determine the degree of preservation of the phytolith assemblage at PP5-6 we used three correlation measurements between the phytolith concentration (per g/ sed) and i) the total number of morphotypes identified (Lancelotti, 2010; Madella and Lancelotti, 2012) (Fig. 30a), ii) the percentage of weathered morphotypes identified (Fig. 30b) and iii) the percentage of delicate morphologies (Fig. 30c). We observed that the correlation coefficient R^2 was low for the three measurements and this indicates that taphonomy might have not affected the representativeness of the phytolith assemblage in high extents.

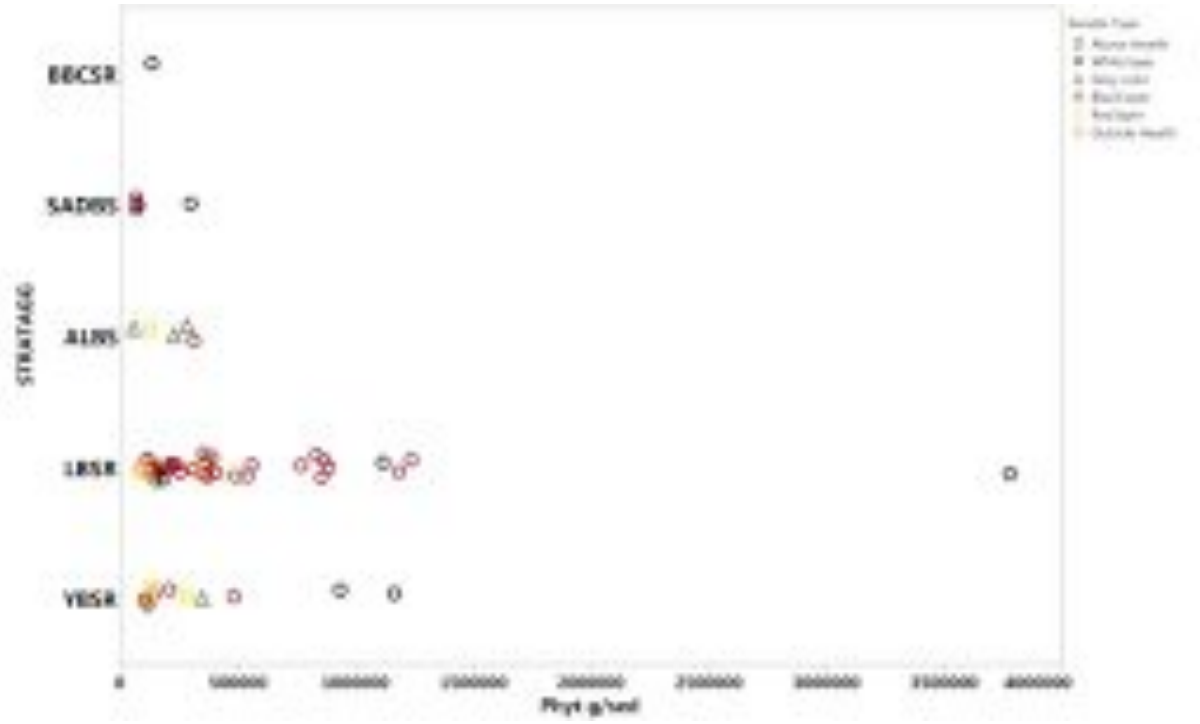

Figure 31. Distribution of the phytolith concentration per gram of sediment among sample types from the different StratAggs studied.

V. 3.4. Combustion features: lateral and vertical variation

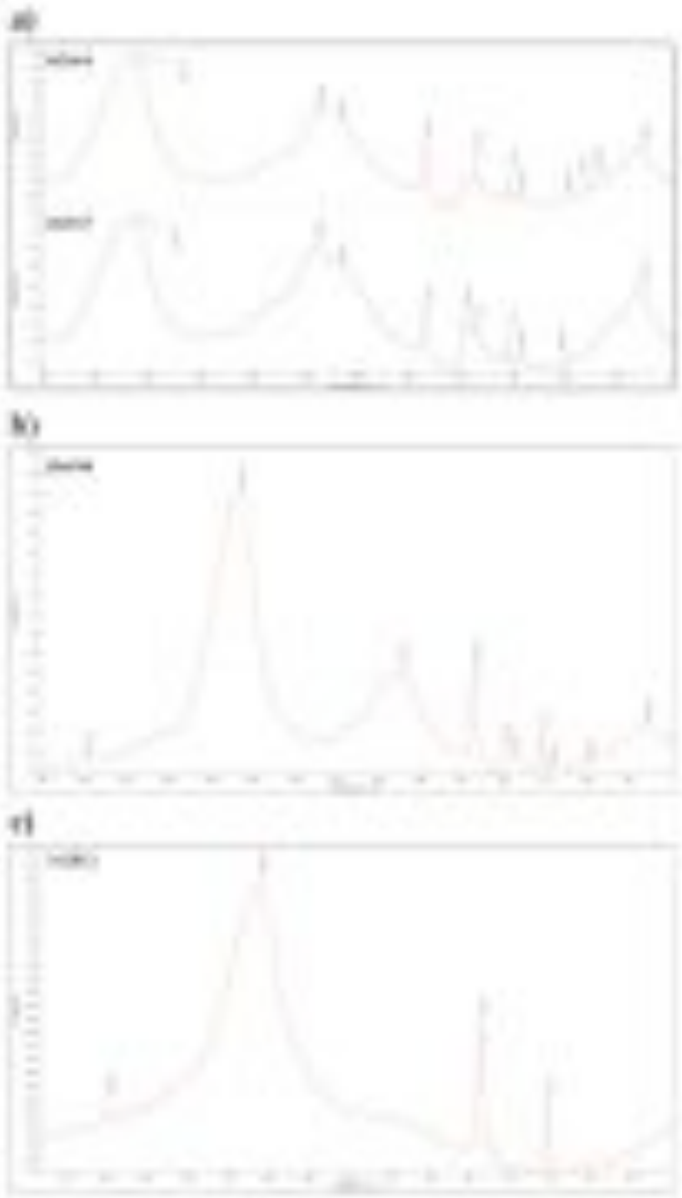

Figure 32. Representative FTIR spectra of sediment samples from different StratAggs and sample types (hearth facies). a) white layer (162466) showing clay absorption peak at 1038 cm^{-1} characteristic of burned clay; b) white layer showing clay absorption peak at 1047 cm^{-1} characteristic of clay exposed to high temperatures; c) white layer showing three calcite absorption peaks at 1420, 874 and 712 cm^{-1}.

In this section we analyzed the phytolith assemblage and major mineral components in samples from combustion features taking into account the hearth facies. Samples belonging

to the same combustion feature had a similar pattern in phytolith concentration independently of the hearth facies (white, black and red layer). Figure 31 shows the phytolith concentration distribution among samples in relation to the different StratAggs giving sample type information. When phytoliths were preserved, we observed that black layers contained the highest phytolith concentration, followed by white layers (Fig. 31 and Table 6) and these differed the most from the red layers. Samples from above and outside hearths showed the lowest phytolith concentration. Calcite and clay were the dominant mineral components in the white and black layers in YBSR and LBSR StratAggs, while the red layers as well as samples from above hearths contained little or no calcite, being mostly quartz and clay.

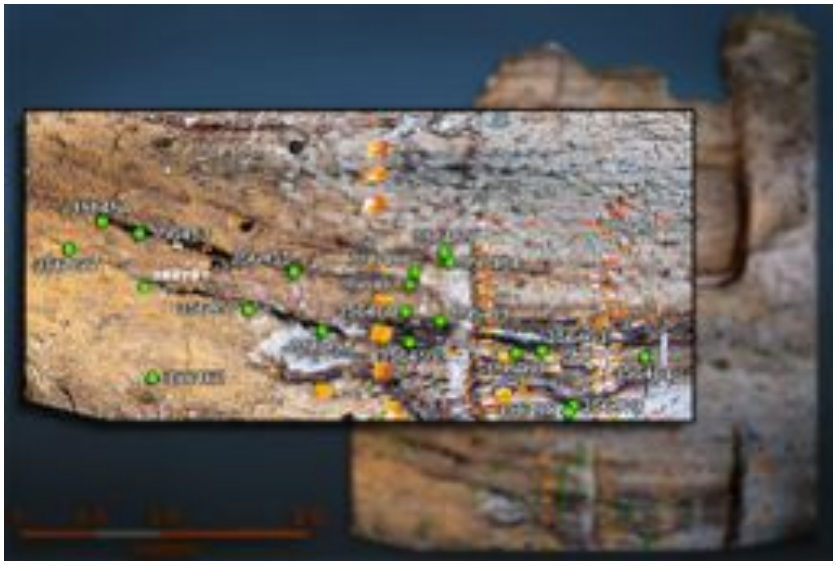

Figure 33. Photograph of the LBSR profile showing the sample location in two hearth layers (hearth 1: 356454, 356453, 356455; hearth 2: 356456, 162781, 356457, 356458) (figure by Erich Fisher).

Traces of burned clay were found in most of the samples from white layers (Fig. 32a), some of them at high temperatures (Fig. 32b) (following Berna et al., 2007) and this agrees with the calcite being of anthropogenic origin (wood ash) (following Regev et al., 2010). For example, sample 162812 from a white layer from LBSR did only contained calcite and this was from anthropogenic origin (Fig. 32c). Conversely, calcite was also an important mineral component in four out of the nine samples analyzed from outside hearths whereas phytoliths

were found in low concentrations (Table A4). Some samples from the red layer contained calcite as the main mineral component and this might be explained by the reworking of the sediments with the top facies (black and white layers). It was noteworthy the absence of calcite as the main mineral component in two black layers from LBSR (hearth 1: 356454, 356453, 356455; hearth 2: 356456, 162781, 356457, 356458) (Table 6 and Fig. 33).

Morphologically, phytoliths from white layers differed from the black and the red layers by showing the highest frequencies of irregular morphotypes (Fig. 34) and the lowest frequencies of grass phytoliths (Table A5). Black layers had high frequencies of restio phytoliths in comparison with other hearth facies. Irregulars (non-diagnostic morphologies) have been traditionally associated to the wood and bark of trees and shrubs (Albert and Weiner, 2001; Tsartsidou et al., 2007). Collura and Neumann (in press) noticed the presence of these irregular morphologies mainly in the bark. Our plant reference collection showed a relatively high presence of irregular phytoliths in the wood/bark of trees and shrubs although they were also abundant in other plant types, such as in the bulb scale leaves and the edible part of the bulbs of geophytes (Section V. 1.2.1.). Because they were mainly observed in samples from white layers, which also contained the highest concentration of wood ash calcite, it is plausible that the majority of them came from the wood of trees and shrubs.

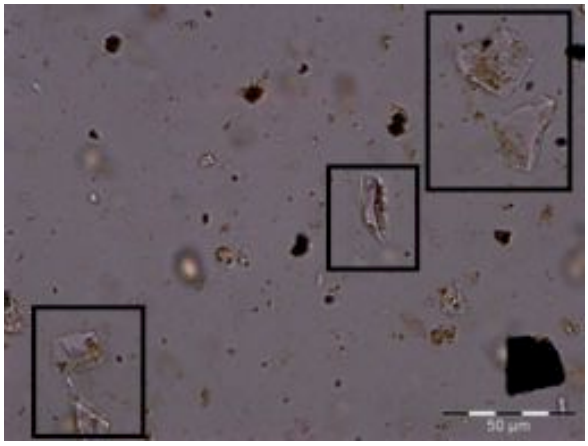

Figure 34. Microphotograph from a white layer from LBSR showing high presence of irregular morphologies (sample 356475). Picture taken at 400.

V. 3.5. The stratigraphic and temporal variation in phytolith morphological distribution along the Long Section of PP5-6

Here we describe the phytolith morphological distribution of samples considering its stratigraphic location along the PP5-6 sequence. Figure 35 shows box-plots presenting the phytolith distribution grouped by plant types in each StratAgg. Furthermore, five phytolith indices were used to identify differences in the plant distribution from the different StratAggs of PP5-6 in order to detect vegetation and climate shifts (Fig. 36 and Table 6). Phytolith indices were not possible to be calculated for the only sample (418155) interpreted from BBCSR StratAgg because of the absence of GSSCs and restio phytoliths. It is also of importance to underline that index values among samples from the different StratAggs are highly variable (Table 6).

The phytolith assemblage from the different StratAggs of PP5-6 was dominated by grass phytoliths and elongate morphologies without decorated margins indistinctively of the sample type (Fig. 35 and Table 6). Among grasses, GSSCs were identified in very high frequencies and mainly from the rondel type (Fig. 37). Together with GSSCs, bulliform cells were also noted although the latters in low frequencies (Table A5). Elongate morphologies with decorated margins (mainly sinuate) were also identified in all the StratAggs of PP5-6 in similar numbers (Fig. 35 and Table A5). Restio phytoliths were identified in all the StratAggs in relatively low numbers. Among eudicot phytoliths, leaves were the most common part found and was represented by epidermal ground mass and by tracheids on a minor extent. Epidermal ground mass phytoliths outlines showed different shapes such as polyhedral, polyhedral elongate, elongate, jigsaw puzzle, sinuate and octagonal, and among them polyhedral shapes were the most abundant (Fig. 38). Phytoliths from the wood/bark of eudicot plants (composed of parallelepiped blockys and ellipsoids) were also noted. Spheroids psilate and rugulate were also identified in relatively high numbers in all the StratAggs (Fig. 35). Despite spheroid morphologies (non–decorated) being typically associated to the wood/bark of eudicot and other non-flowering plants (Gymnosperms) (e.g., Klein and Geiss, 1978; Bozarth, 1993; Albert and Weiner, 2001; Collura and Neumann, in press), they were grouped separately as they also constitute an important component in Restionaceae plants as well as detected in other plant types (Section V. 1. and VI. 1.). Finally, the occurrence of irregular and indeterminate morphologies, probably from woody plants, was moderately high in most of the StratAggs but mainly in SADBS (Fig. 35). Specific

features of the phytolith assemblage distribution and phytolith indices among StratAggs from PP5-6 are given in detail below:

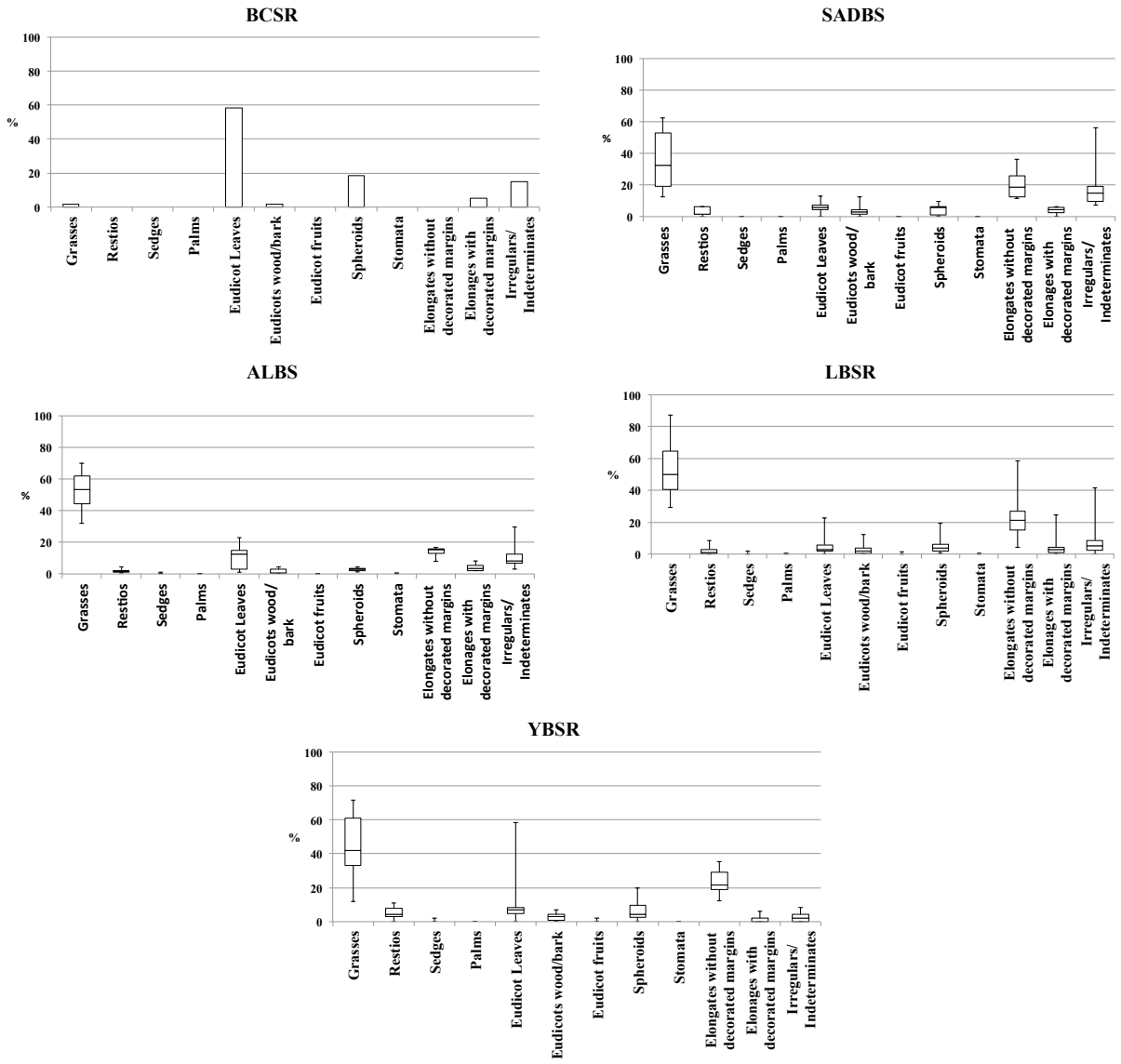

Figure 35. Box-plots showing the plant types and plant parts distribution for the different StratAggs at PP5-6. The mean values (mid- line), standard error ± (box) and standard deviation (whiskers) are given for each of the plant groups with the exception of those from BBCSR StratAgg since only one sample was considered for morphological interpretation.

At the oldest moments of occupation of PP5-6, at YBSR StratAgg (~85-90 ka), samples were characterized and differed from other StratAggs by having the highest frequencies of restio phytoliths (mean: 4.6%) (Fig. 39a-b). Despite GSSC rondels dominated in all the StratAggs at PP5-6, the highest frequencies of lobates were found in samples from YBSR (Fig. 37). Based on the modern plant reference collection from grasses (Section V. 1.2.3.) and

on two reference collections from South African graminoids (Rossouw, 2009; Cordova and Scott, 2010; Cordova, 2013), the bilobates identified can be associated to the C_4 Panicoideae subfamily (Fig. 39c-d). Sample 388614 contained the highest frequencies of epidermal ground mass from eudicot leaves among all the samples from the different StratAggs of PP5-6 (Table A5). Finally, irregulars and indeterminate morphologies showed the lowest frequencies (Fig. 35). Samples from this StratAgg showed the highest D/Pº mean value (0.26) among StratAgss (Fig. 36). Despite the mean value of the Fy index in samples from YBSR was lower than in samples from SADBS, it is worth to mention that the highest values were detected in samples from this StratAgg (356478, 356479 and 388613) (Fig. 36 and Table 6). Regarding grass phytolith indices (Ic, Iph and Fs), samples from YBSR showed the lowest Iph mean values (0.09) (Fig. 36 and Table 6).

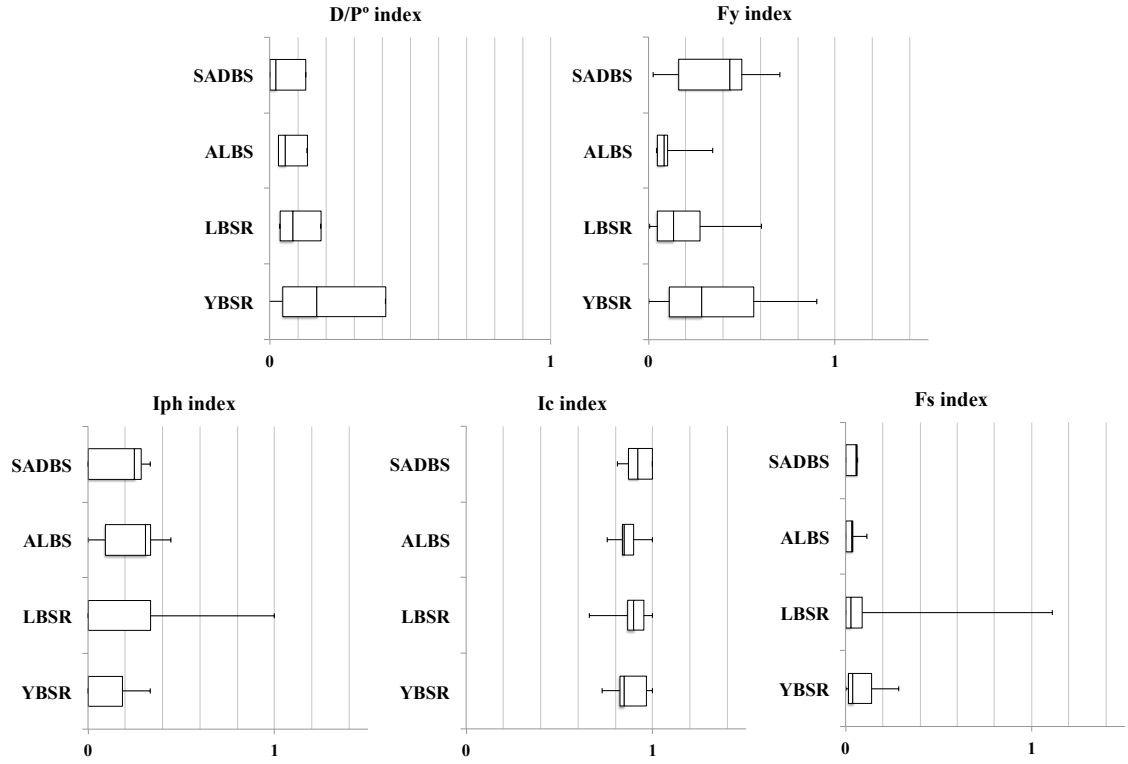

Figure 36. Box-plots showing the phytolith indices values among StratAggs of PP5-6. D/P^o index [(psilate and rugulate spheroids)/ ∑GSSCs]; Fy index [(psilate and rugulate spheroids and restio phytoliths)/∑GSSCs]; Iph index [GSSC saddles/ (∑GSSC saddles and lobates)]; Ic index [GSSC rondels and oblongs/ (∑GSSC rondels, lobates and saddles)] and Fs index [Bulliform cells/∑GSSCs. The mean values (mid- line), standard error ± (box) and standard deviation (whiskers) are given for the five indices.

During the occupation of LBSR StratAgg (~74-85ka), grasses dominated the phytolith assemblage (Fig. 35), and among GSSCs, rondels (Fig. 39e-f) and oblongs dominated (Fig. 37). A worth mentioning feature observed in LBSR was the identification of spheroid echinate phytoliths (Fig. 39g) in samples 162782, 356455 and 356459, although in very low numbers. This was not observed in other StratAggs at PP5-6. It is worth mentioning that irregular morphologies with protuberances from eudicot fruits were detected in four samples from this StratAgg (357366, 356474, 356464 and 162558) (Fig. 39h). Regarding phytolith indices, LBSR was characterized by high Ic mean values and despite mean Iph and Fs values were low some of the samples presented the highest values among samples from different StratAggs (Table 6).

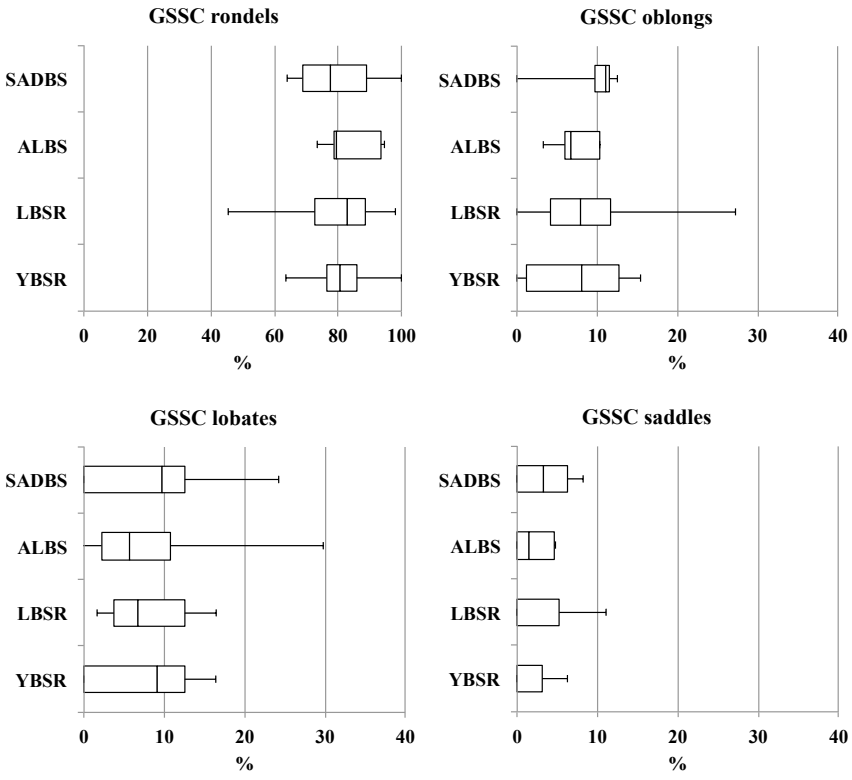

Figure 37. Box-plots showing the GSSC distribution among StratAggs of PP5-6. The mean values (mid- line), standard error ± (box) and standard deviation (whiskers) are given for the four GSSC categories.

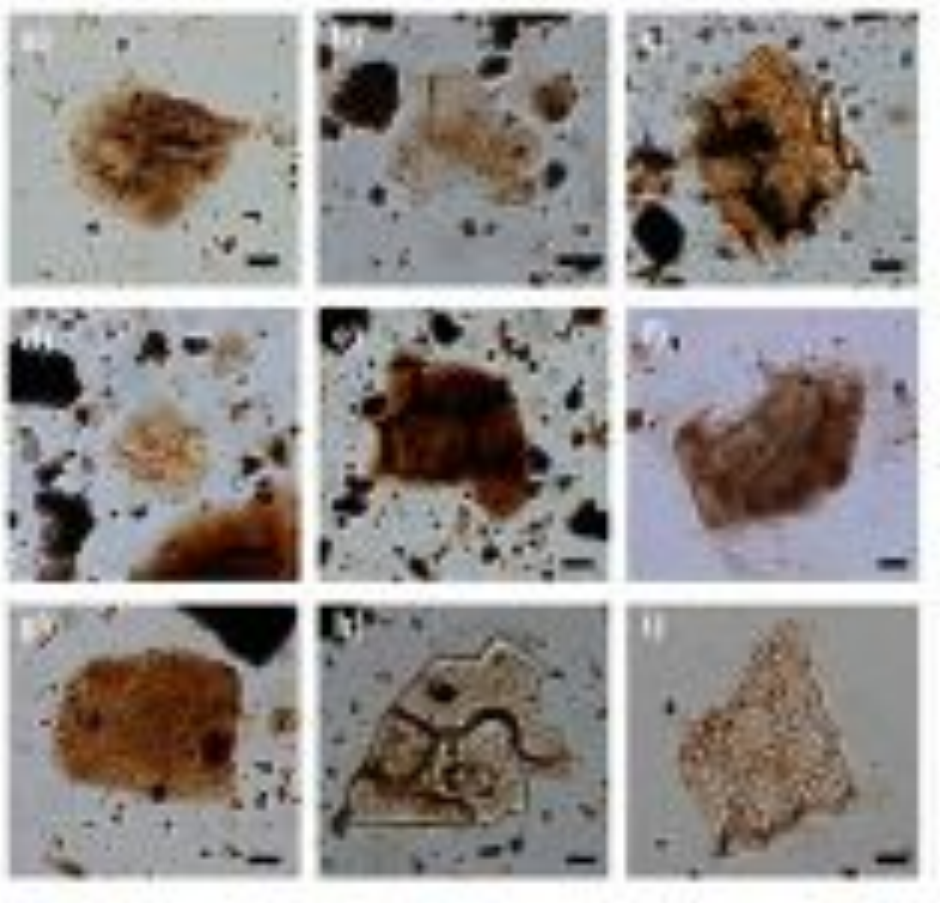

Figure 38. Microphotographs of epidermal ground mass (EGM) from samples from different StratAggs of PP5-6. Pictures taken at 400x. a) EGM indeterminate outlines from ALBS (357374); b) EGM indeterminate outlines from LBSR (357366); c) EGM polyhedral outlines from LBSR (357368); d) EGM indeterminate outlines from LBSR (357368); e) EGM polyhedral outlines from LBSR (356474); f) EGM polyhedral outlines from LBSR (162782); g) EGM sinuate outlines from LBSR (357365); h) EGM sinuate outlines from LBSR (162778); i) EGM sinuate outlines from LBSR (162549). Scale bar represents 10 mm.

During the transition from MIS5 to MIS4, throughout the occupation of ALBS StratAgg (~72-74ka) grasses dominated the phytolith assemblage in concentrations similar to those observed in YBSR (mean: 51%) (Fig. 35). Although the C_3 GSSC rondels dominated, C_4 grass subfamilies were here better represented, showing high frequencies of saddles and lobates (Fig. 37). Samples from ALBS were characterized by the high frequencies of grass phytoliths (mean: 51%). Grasses from the C_4 type (lobates and saddles) were also abundant (Fig. 39i-j). Elongate morphologies without decorated margins, although common, showed

here the lowest occurrence of all the StratAggs, with the exception of the sample from BBCSR. Finally, restio phytoliths, elongates with decorated margins, spheroids and wood/bark phytoliths were scarcely present (Fig. 35). ALBS presented the lowest Fy mean values (0.11) and the highest Iph mean values (0.23) among StratAggs (Fig. 36).

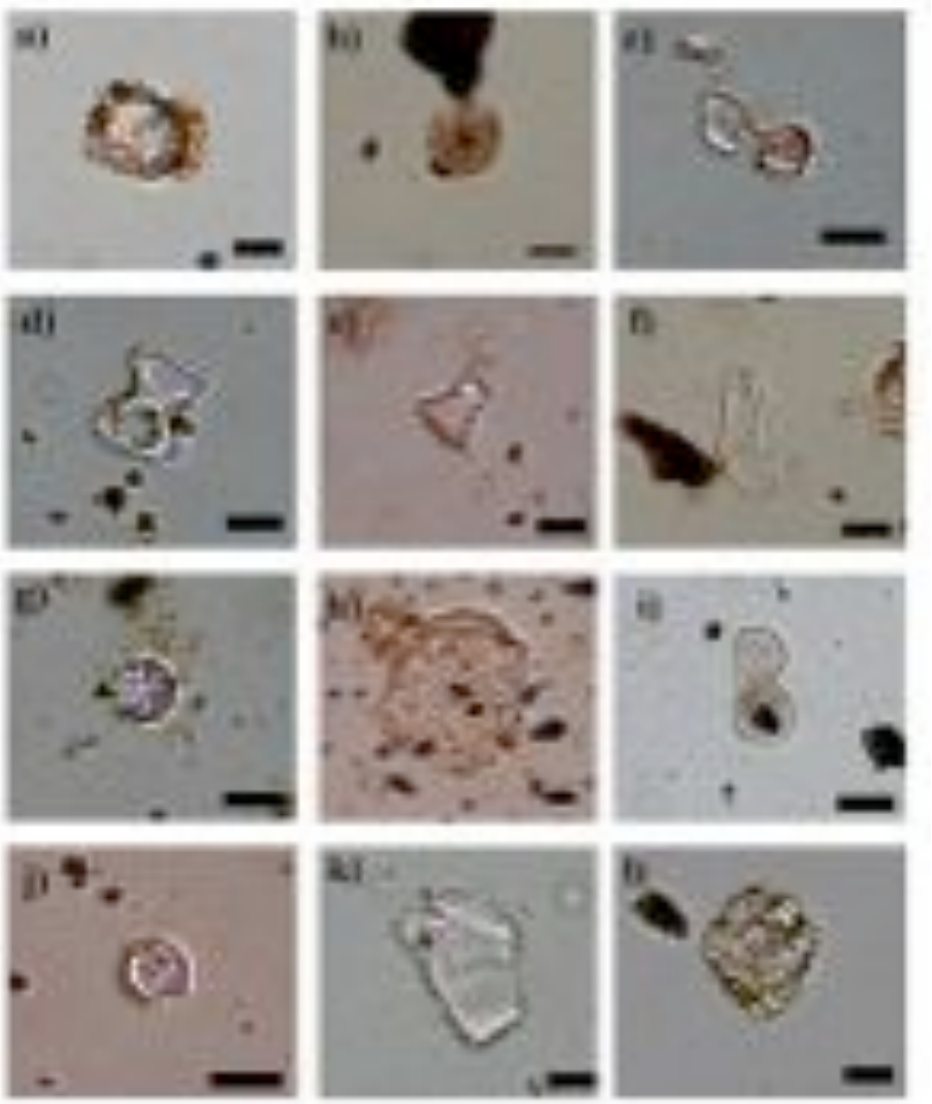

Figure 39. Microphotographs of common phytolith morphotypes identified in samples from different StratAggs of PP5-6. Pictures taken at 400x. a-b) restio phytoliths from samples 356417 and 388588 from YBSR; c-d) GSSC bilobates from samples 356414 and 388615 from YBSR; e) GSSC rondel from sample 356457 from LBSR; f) GSSC oblong tabular from sample 356455 from LBSR; g) spheroid echinate from sample 162782 from LBSR; h) irregular morphology with protuberances from an eudicot fruit from sample 357366 from LBSR; i) GSSC bilobate from sample 162483 from ALBS; j) GSSC saddle from sample 162483 from ALBS from SADBS; k) irregular psilate morphology from sample 162467; l) restio phytolith from sample 46682 from SADBS. Scale bar represents 10 mm.

During the occupation of SADBS at the beginning of MIS4 (~70-72ka), irregular and indeterminate morphologies (Fig. 39k) dominated SADBS assemblages and this constitutes the defining feature of this StratAggs. Grasses were also well represented, with GSSC lobates being identified in high frequencies (Fig. 37). It should be noted that restio phytoliths (Fig. 39l) showed the highest frequencies in samples from this StratAgg together with samples from YBSR (Fig. 35). And this is observed in the Fy index values in SADBS samples that showed the highest mean value (0.36) among StratAggs. Samples from SADBS showed the lowest D/Pº mean values (0.10) among StratAgss despite some samples presented the highest values (Fig. 36 and Table 6).

Lastly, the trend observed in the phytolith assemblage of the only sample from BBCSR (~60-55 ka) containing enough phytoliths for a reliable morphological interpretation (418155) differed greatly from other StratAggs. It contained high frequencies of eudicot leaf phytoliths, spheroids and elongates with decorated margins dominated whereas grasses, restios and elongate morphologies without decoration margins were absent (Fig. 35 and Table A5).

VI. Discussion

VI. 1. Plant Phytolith Reference Collection from the Greater Cape Floristic Region: a selection of plants susceptible to have been exploited by past hunter-gatherers on the south coast of South Africa

This study offers an overview of the phytolith morphological and quantitative production of a selection of South African plants from the GCFR potentially susceptible to have been exploited by past hunter-gatherers inhabiting the south coast. Its importance relies in the fact that this constitutes the first modern plant reference collection of eudicot plants and geophytes from the GCFR. Additionally, this will be the first modern plant reference collection that analyzes different plant types and plant parts in South Africa. Following previous homologous studies from other study areas (Albert and Weiner, 2001; Bamford et al., 2006; Tsartsidou et al., 2007), this reference collection contains different plant types and plant parts that have been collected from the same area and that have been analyzed using the same approach. These allow for comparison of the phytolith production in different plant types from a quantitative and qualitative approach and so making realistic assumptions regarding the usefulness of phytoliths for the study of fossil assemblages.

Although this plant reference collection is small (fifty-six species and ninety-six plant parts) compared to the high species diversity occurring in the GCFR, it is a solid starting point for understanding the phytolith concentration and morphological production of different plants from the GCFR.

The importance of the Restionaceae family when studying phytoliths in fossil records lies in the fact that they are a useful tool for the identification of fynbos vegetation (Esteban et al., in press) and winter rainfall (Cordova, 2013). The possibility for identifying restios in fossil records is also of importance since it constitutes a plant widely used in South Africa by many different cultures for building, thatching and for making sleeping mats (van Wyk and Gericke, 2000). Furthermore, their identification in the fossil record is of great importance to improve our knowledge on plant uses and for South African palaeoclimate research. In this study it has been demonstrated that the two phytolith morphotypes detected in restio plants are produced, at least, in the parenchyma sheath of the culms of *Thamnochortus insignis*, confirming that they belong to and characterize the South African Restionaceae family. Silica bodies (phytoliths) were observed in previous studies on the anatomy of Australian and African

Restionaceae species. Silica bodies were reported in the sclerenchyma sheaths of the mature culms, in the sclerenchyma sheath of the rhizomes of *Rhodocoma* (Linder and Vlok, 1991) and sclerenchymatous inner and outer bundle sheath of the leaves of several species from this family (Linder and Caddick, 2001). However, phytoliths were not detected in the leaves of *Thamnochortus insignis*.

Geophytes have been hypothesized as an important source of nutrition for past hunter-gatherers inhabiting the south coast of South Africa (Marean et al., 2014). Geophyte remains, such as *Watsonia* and *Moraea* (Iridaceae) and *Hypoxis* (Hypoxidaceae), have been also identified in the archaeological record from several South African Later Stone Age (LSA) sites (Deacon, 1976, 1983, 1984; Wells, 1965; Carter et al. 1988). However, there is no evidence to date of geophyte consumption in MSA archaeological sites.

The phytolith morphologies detected in all the geophytes here analyzed lacked of specialized and reliable diagnostic characteristics that could be used for taxonomic classification. Several morphotypes have been identified through ANOVA as characteristic of the leaves and the bulb scale leaves of geophytes, including blocky polyhedrals, elongate polyhedrals, prickles and irregular morphologies but these were also well represented in other plant types. Elongate morphologies were identified through ANOVA as characteristic of the leaves of geophytes. These were the most common phytolith morphotypes identified in the two species of the genus *Moraea*. However, the lack of diagnostic phytolith morphotypes in geophytes might make difficult their identification in the fossil record.

This study showed that Poaceae plants from the area can be distinguished among other plant types and plant parts on the basis of the phytolith assemblage, what is generally acknowledged in the literature (Piperno, 1988, 2006, and references therein). Similarly, grass phytoliths appeared to differ among grass photosynthetic pathway (C_3 and C_4) (Table 3). Although we are aware that this study presents a limited number of species belonging to different genera and subfamilies, mostly if comparing to previous studies on South African grasses (Rossouw, 2009; Cordova and Scott, 2010; Cordova, 2013), four main outcomes were noticed:

1) Grasses appeared as the highest phytolith producers among all the different plant types analyzed in this study as it has been reported elsewhere (e.g., Wilding and Drees,

1971; Kondo, 1977; Albert and Weiner, 2001; Strömberg, 2003; Tsartsidou et al., 2007).

2) GSSCs have been widely used as climatic indicators due to their characteristic morphologies that generally relate to different Poaceae subfamilies. Our results showed that some multiplicity and redundancy (Rovner, 1983; Piperno, 1988) exists in regards to the distribution of GSSCs among the photosynthetic pathway of the grasses and among subfamilies, and this has been reported previously for South African grasses (Rossouw, 2009; Cordova and Scott, 2010; Cordova, 2013) and elsewhere (e.g., Twiss et al., 1969; Twiss, 1992; Fahmy, 2008; Barboni and Bremond, 2009; Radomski and Neumann, 2011; Novello et al., 2012; Neumann et al., in press). We observed that the grasses here studied are characterized by the presence of both GSSC rondels and bilobates indistinctively of the photosynthesis pathway they belong to. Despite rondels were identified in C_4 grasses as well as bilobates in C_3 grasses, it is observed a general trend in which bilobates (with flattened, rounded and flattened-round lobes) were more abundant in C_4 grasses, and rondels (rondel conical, long tower and trapeziforms) in C_3 grasses (Table A1 and Table 3). Nevertheless, this was not clearly detected through the statistical analysis and this stresses the importance to further extend the reference collection on grasses in order to obtain more reliable statistical results. The exception was the two *Eragrostis* species from the Chloridoideae subfamily, which presented an absence of bilobates, while saddles and rondels were well represented. Previous studies conducted on South African grasses also observed that despite some rondels and trapeziforms dominated in both C_3 and C_4 grasses, the latters, and mostly from the Panicoideae subfamily, are characterized by the presence of bilobates (Rossouw, 2009; Cordova and Scott, 2010; Cordova, 2013). We observed that the bilobates that most characterized C3 grasses, and particularly those from the Ehrhartoideae and Danthonioideae subfamilies, have angulate and segmented angulate/planar lobes and this was statistically detected through ANOVA (Table 3). These bilobates were not identified in C4 grasses. Rossouw (2009) and Cordova's work (Cordova and Scott, 2010; Group 4 in Cordova, 2013) found that the oblong morphotype is characteristic of the Pooideae subfamily. Of the two species belonging to two different genera from the Pooideae subfamily analyzed in this study, only *Festuca scabra* showed the highest frequencies of this morphotype.

3) This study stresses the importance of the relationship between high production of bulliform cells and high water availability. *Stenotaphrum secundatum* (Panicoideae), which was the only grass species collected from a wetland (in Geelbeksvlei) (Table 2), was the only one that produced high numbers of bulliform cells (Table A1). Sangster and Parry (1969) demonstrated that an excess supply of water availability to plants is directly linked to a higher silicification of bulliform cells. Bremond et al. (2005a) proposed that the water stress and transpiration suffered by the grass cover lead to higher rates of bulliform silicification. Furthermore, the authors proposed that this could also occur in local wet areas in dry zones. Other studies also associated a higher silicification of phytoliths (Rosen and Weiner, 1994) and bulliform cells (Strömberg et al., 2007; Fisher et al., 2013) with water availability and wet habitats. Although these results are limited and further studies focused on the GCFR must be conducted to corroborate this observation, based on the previous studies mentioned and the evidence here reported, the association of high bulliform production and water availability might be used as a reliable tool for paleoenvironmental reconstruction in the GCFR.

Table 7. Phytolith concentration per gram of original plant material of grass phytoliths (bulliform cells and GSSCs) by average in the wood/bark and the leaves of eudicot plants, in geophytes (leaves, bulb scale leaves and bulbs), restios and in grasses.

	Grass phytoliths /g plant in grasses	Grass phytoliths /g plant in wood/bark specimens	Grass phytoliths /g plant in eudicot leaves	Grass phytoliths /g plant in restios	Grass phytoliths /g plant in leaves of geophytes	Grass phytoliths /g plant in bulb scale leaves of geophytes	Grass phytoliths /g plant in bulb of geophytes
Average	2,824,512	135	236	3,300	30,000	33,000	1,000
Max	7,189,137	1,364	1,763	8,166	468,255	154,222	40,888
Min	1,154,365	0	0	13	154	0	0

4) We observed grass phytolith contamination in the wood/bark of eudicot plants in similar proportions as Albert (2000) and Tsartsidou et al. (2007), even though we did not conduct previous sonication unlike Albert and Tsartsidou. The grass phytolith

contamination in the wood/bark and the leaves of eudicot plants (that varied from 0 to 44.4% with a mean of 16.3% and from 0 to 60% with a mean of 7%, respectively) as well as in geophytes (with a mean of 36% in the leaves 47.5 in the bulb scale leaves and 12.7% in the edible part of the bulb) may also contribute to the input of phytoliths in archaeological deposits and mostly in combustion features. These support previous studies, which suggested that grass phytoliths in archaeological deposits might also be partially a result of contamination from other plants (Albert and Weiner, 2001; Albert et al., 2000; Bamford et al., 2006; Tsartsidou et al., 2007). Table 7 shows the relative phytolith concentration of grass phytoliths (only considering bulliform cells and GSSCs) in the wood/bark and the leaves of eudicot plants, in geophytes (leaves, bulb scale leaves and bulbs), restios and in grasses. The grass phytolith concentration per gram of plant material in the wood/bark as well as in the other plant types was very low when compared to grasses (Table 7). Thus, we hypothesize that in a scenario in which past-humans only used wood to make fire, even though in high amounts, we might expect to find a phytolith assemblage characterized by a low phytolith concentration, with a mix of eudicots as well as grass phytolith morphologies. And the other way round, a phytolith assemblage characterized by high phytolith concentration in association to high presence of grass phytoliths may not necessarily be only associated to wood or other plant contamination but most probable due to the intentional use of grasses in the past. Therefore, the grass presence in archaeological deposits due to contamination, in terms of phytolith concentration, might be minimal and this consideration has important implications when interpreting the origin provenance of grass phytoliths in the archaeological record (Table 7).

Regarding eudicot plants, this study reported three main outcomes that must be considered when studying fossil phytolith assemblages in the archaeological record:

1) Both the wood/bark and the leaves of eudicot plants are low phytolith producers and therefore they will be underrepresented in the fossil record. This is especially true when comparing with grasses and this has been previously reported elsewhere (e.g. Wilding and Drees, 1971; Kondo, 1977; Albert and Weiner, 2001; Tsartsidou et al., 2007; Mercader et al., 2009). So the contribution of eudicot plants to the phytolith assemblage in archaeological sediments at the south coast of South Africa might be small. Moreover, when studying archaeological deposits where wood was the main

plant source we might expect to find a very low phytolith concentration and this have been also previously reported (e.g., Albert, 2000).

2) Spheroids and parallelepiped blockys were the most recurrent morphotypes identified in the species analyzed. Nonetheless, these morphotypes have also been detected in many different plant families along Africa and other continents (e.g. Piperno, 1988, 2006; Runge, 1996; Kondo et al., 1994; Albert and Weiner, 2001; Strömberg, 2003; Bamford et al., 2006; Tsartsidou et al., 2007; Mercader et al., 2009; Collura and Neumann, in press). In this study spheroids were also identified in high frequencies in the leaves of eudicot plants, restios and geophytes. And despite spheroids psilate and ellipsoids were detected statistically characteristic of this plant type, these results stress the fact that the probability of detecting wood in mixed assemblages through the study of phytoliths in the GCFR is limited.

3) The leaves of eudicot plants from the GCFR were characterized by the high presence of epidermal ground mass phytoliths (mainly with polyhedral shapes) and tracheids, and this was statistically confirmed. And this has been documented in other phytogeographical regions (e.g. Kondo and Pearson, 1981; Piperno 1985, 1989; Bozarth, 1992; Albert and Weiner, 2001; Strömberg, 2003; Bamford et al., 2006; Tsartsidou et al., 2007).

VI. 2. Modern soil phytolith assemblages used as proxies for Paleoscape reconstruction on the south coast of South Africa

VI. 2.1. Phytolith deposition and preservation in modern soils

Pre- and post-depositional processes may affect phytolith deposition and preservation in soils (Piperno, 1988, 2006). Pre-depositional processes are the factors that may influence the plant accumulation in soils and their subsequent release of phytoliths after organic material decay. External factors like the degree of vegetation cover, the differential phytolith production in different plants, and the life cycles of specific plants have all been shown to influence the pre-deposition of phytoliths in modern soils (Piperno, 1988, 2006 and references therein). Other external factors may relate to wildlife and consumption of certain plant parts such as fruits or seeds, which when consumed will not contribute to the soil component (Bamford et al., 2006). Aeolian or fire impact may also influence phytolith deposition in soils (see below).

South African grasses, for example, are high phytolith producers while other plants such as trees, shrubs, restios and most geophytes from the Iridaceae family are low phytolith producers. Furthermore, phytoliths from the wood/bark of trees are often less well represented because, in addition to be lower phytolith producers, these parts of the plants live longer and their tissues are not often deposited in the soils. In contrast, grasses and other herbaceous plants often contribute with a higher phytolith input in soils because these plants have shorter life cycles. In areas with a dense understory it is therefore more likely to find phytoliths from graminoids and herbs rather than from the trees themselves. This has been also detected in modern surface soils from Tanzania (Eastern Africa) (Albert et al., 2015).

The analysis of the sediment samples from the study area showed a similar phytolith pattern. The samples that were collected from shrubby vegetation, such as limestone fynbos, dune cordon and strandveld, or samples that were collected from thicket (mainly coastal thicket) did not contain high phytolith concentration. Conversely, samples from dense grassy vegetation, such as renosterveld and riparian vegetation, contained the highest phytolith concentration. The differences in these cases are less likely to be the product of actual vegetation changes rather than the dominance of grassy phytoliths at the expense of plants that produce much fewer phytoliths. The

implication is that when grasses are present then it makes accurate vegetation identification more difficult.

After their deposition, preservation of phytoliths in modern soils is associated with the silicon cycle in which phytoliths are recycled by plant roots immediately upon their deposition in the soil A horizon (Alexandre et al., 1997; Derry et al., 2005). Soils with slow development and under constant biomass activity might have low preservation of the phytolith assemblage. Soils in the Southern Cape are from slightly fertile to infertile (Thwaites and Cowling, 1988), with a slow development and under a low biomass activity. Consequently, we can assume that the rate of deposition of phytoliths in fynbos vegetation (where perennial plants dominate) might be lower than that of other vegetation types with a large representation of annual plants such as grasses, which are also high phytolith producers as it has been shown from our plant reference collection (Section V.1.). Thus, the differences between the deposition rate and the rate of recycling of phytoliths in the fynbos vegetation might account for their low concentration in soils. Moreover, phytolith dissolution cannot be considered as cause for their low concentration in samples since all of the samples showed an acidic to a moderate alkaline pH.

Another possibility that might explain the low phytolith concentration in samples from some of the vegetation types here studied such as limestone and sand fynbos, strandveld or dune cordon is the downward translocation of phytoliths. Low phytolith concentration in very coarse soils or in very active bioturbation soils has also been shown to be the result of phytolith translocation (e.g. Fiskish et al., 2010). These authors showed size dependence on phytolith percolation by water, with phytoliths with a size diameter of 5 mm being the most susceptible to move downward. In this study, if phytolith translocation had occurred in samples with low number of phytoliths (limestone fynbos, coastal thicket, strandveld vegetation types) then we would not expect to see small-sized morphotypes, such as GSSC rondels and saddles or spheroids psilates and rugulates, what is not the case. Nonetheless, this should be further tested by analyzing the bottom of soil profiles.

The presence of restio phytoliths in some riparian plots where Restionaceae plants were not present might be related to the alluvial character of these soils, and thus, restio phytoliths might represent the runoff soil from up stream. Another likely explanation of

its presence can be explained due to their transport in ash clouds after fire events in fynbos vegetation as it has been observed in other, although not-homologous, environments (Osterrieth et al., 2009; Aleman et al., 2014). Thus, either water flow or aeolian transport or both could account for the small quantities of restio phytoliths in some riparian plots despite the lack of restio plants.

VI. 2.2. Recognition of GCFR vegetation through modern phytolith assemblages

Fynbos constitutes one of the most characteristic vegetation types of the GCFR and thus the identification of key plants like restios and shrubby vegetation in fossil phytolith assemblages is critical to undertake accurate paleovegetation reconstructions. The results showed that limestone fynbos can be characterized through the analyses of phytoliths from modern soils as well as by the identification of certain characteristic phytolith morphotypes (Fig. 28), such as restio phytoliths and spheroids. The modern plant reference collection, however, has shown that both restios and the wood of eudicot plants produce very few phytoliths per gram of plant material. Whereas the identification of these morphotypes in samples, may be related to their good preservation conditions, previous studies have shown that the stability of phytolith morphotypes do differ from each other with spheroids showing the highest stability (Cabanes and Shahack-Gross, 2015). Despite no dissolution experiments have been conducted on restio phytoliths to date, their heavily silicified bodies suggests that they might be relatively stable in soils and sediments.

Fire regime is another important factor in fynbos ecology, but its role in phytolith deposition in soils has been rarely discussed. Fire regime is responsible for the decay of shrubby and herbaceous plants and the subsequent regeneration of shrubs and herbaceous plants. Because modern soil phytolith assemblages represent an amalgamation of the vegetation mosaic over a period of years to several decades, the effects of fire may favor a higher phytolith deposition rate in soils, thereby increasing the representation of fynbos elements (shrubs and restios) in the phytolith record. Therefore, an increased presence of spheroids and restio phytoliths in fynbos soils despite low phytolith production of eudicots and Restionaceae might, in fact, be related to the effects of a persistent fire regime. Burned phytoliths were not detected in our

samples, whereas this is something to take into account for futures studies.

Grass phytoliths were identified in all of the samples from fynbos vegetation even though mature fynbos (i.e. unburnt for ca. 10-20 yr) is characterized by a restio understorey with few grasses. Grasses are most abundant immediately following burning episodes (Linder and Ellis, 1990). Moreover, grasses produce large amounts of phytoliths per gram of sediment (e.g., Wilding and Drees, 1971; Kondo, 1977; Albert and Weiner, 2001; Strömberg, 2003; Bamford et al., 2006; Tsartsidou et al., 2007; section V.1.2.3.). Thus, the effect of fire might be also responsible of leaving grass phytoliths as component of the soils. However, we observed that in any case the relative phytolith concentration in fynbos vegetation (with the exception of grassy fynbos) exceeds that of other vegetation types where grasses abound in the landscape.

In addition to the characterization of limestone vegetation, this study also showed how D/Pº and Fy (high values) indices can be used for the identification of vegetation types with a high grass component, like grassy fynbos, renosterveld, and riparian vegetation (low values) (Fig. 27a and b). This observation is especially important because it provides insights into the true character of the paleovegetation regardless of any overbearing plant components. Sand fynbos samples, for example, showed a mean Fy index value of 0.6 with a high standard deviation of 0.5. This high deviation among samples is caused by the presence of grasses in samples SF11-42 and SF11-43, which showed a very low Fy values (Fig. 27b). These results show that when grasses abound, their occurrence might mask the correct identification of vegetation types what might constitute a problem facing paleoenvironmental studies across South Africa.

Forest and Thicket biomes are characterized by dense vegetation and dominated by trees and shrubs that are often succulent. D/P (Alexandre et al., 1997; Barboni et al., 1999; Bremond et al., 2005b) and D/Pº (Bremond et al., 2008) indices have been used to estimate the density of woody elements in different habitats in West and East Africa, but they have not been applied to South African studies. In this study, we found that low D/Pº values (<0.20) are not representative of dense tree and shrub vegetation from the Thicket and the Forest Biomes rather than being from Renosterveld and Strandveld (Fig. 27a). These findings imply that the D/Pº index may not be a useful tool to identify thicket or forest vegetation through fossil phytolith assemblages when working on the south coast of South Africa.

ANOVA and post host Tukey's HSD test showed that the Thicket biome might be characterized by the abundance of irregular and other unknown phytolith morphotypes, probably produced by eudicot plants though those were not detected in the woody species analyzed in the modern plant reference collection (see Section V1.1. 1.), as well as by GSSC saddles as a secondary term (Table A3 and Fig. 29). In regards to vegetation types, the statistical analysis showed that epidermal hair base (from eudicot plants) and ellipsoid phytoliths are the defining features of subtropical thicket vegetation. Similarly, the statistical analysis showed that coastal thicket vegetation might be characterized through fossil phytolith assemblages by the presence of GSSC saddles, spheroid echinates and irregular phytoliths (Table A2 and Fig. 28). Nevertheless, because few phytoliths were identified in these samples, results must be taken with caution.

Spheroids echinate were identified in samples from coastal thicket and strandveld vegetation (Thicket biome) in very low percentage. Despite these morphotypes are known to be very common in the Arecaceae family (palms), they have been also detected in other plant families such as Bromeliaceae, Strelitziaceae, Orchidaceae, Marantaceae, Cannaceae, and Zingiberaceae (see Piperno, 2006; Benvenuto et al., 2015, and references therein). Only Strelitziaceae and Orchidaceae (some geophytes belong to the latter) occur along the south coast, and the former only in the Thicket biome from the GCFR and the Albany Thicket biome. To date no quantitative studies of phytolith per gram of plant material (following for example Albert et al., 1999) have been conducted on South African species from these plant families. Hence, taking into account that the Arecaceae family is known to produce high amounts of these morphotypes (e.g. Piperno, 1988; Albert et al., 2009), the low amount recovered in our samples suggest, either contamination by different factors, including human introduction of palms for horticulture in the area or that they belong to other plants, that in this case might belong to the Strelitziaceae and/or the Orchidaceae families.

As GSSCs have been linked to different subfamilies, their morphotypes can be used to differentiate between C_3 and C_4 grasses and thus offer information on paleoecological conditions. In this study, all the samples from the different vegetation types showed a mix of C_3 and C_4 GSSCs (Table 3). However, it was also observed that there is a higher presence of GSSC rondels in samples from renosterveld vegetation and this was statistically detected through ANOVA. These were observed to be dominant in C_3

grasses (and mostly in the Ehrhartoideae and Pooideae subfamilies) from our modern plant reference collection (Section V 1.2.3.). And this was statistically detected through ANOVA.

GSSC lobates (mainly bilobates) have also been recovered in most of the samples from the different vegetation types while dominating in the sample collected from coastal forest in Brenton lake area where C_4 grasses dominated (Table 4). GSSCs lobates are common in C_4 Panicoideae (Twiss et al., 1969), but have also been identified in the C_3 Ehrhartoideae and Danthonioideae grasses (Cordova and Scott, 2010). And this has been detected in the grass species analyzed from the modern plant reference collection (Section V 1.2.3.). Therefore, although the grass attribution of bilobates should be made with caution, the statistical analysis from the modern plant dataset showed that C_4 grasses (mainly from the Panicoideae subfamily) can be distinguish and differ from other plants and grasses by the high presence of GSSC bilobates (Section V1.2.3.). Finally, despite the results indicate a clear dominance of GSSC lobates in coastal forest vegetation, more samples from this vegetation are needed to corroborate the statistically significance of these results.

The C_4 Chloridoideae subfamily is a short tropical subfamily adapted to dry climates and/or low available soil moisture (xeric environments) (Vogel et al., 1978; Tieszen et al., 1979). GSSC saddles, characteristic of C_4 Chloridoideae, were identified in all the vegetation types but dominating in samples from riparian vegetation (ANOVA, $p<0.0024$) and coastal thicket (ANOVA, $p<0.0024$) (Fig. 28). These results correlate well with those from the Iph index, which showed a statistically significance correlation between high Iph index values and riparian vegetation (Fig. 27c). *Cynodon dactylon* would be a dominant grass in riparian (floodplain) habitats of the Gouritz valley and are generally very common between thicket clumps in coastal thicket areas. Thus the phytolith assemblage from riparian and coastal thicket vegetation seems to record the presence of this grass species. Furthermore, this species occurs on almost all soil types but especially in fertile (loamy) soils and it is common in disturbed areas like riparian environments. Consequently, these results demonstrate that the distribution of GSSC saddles in phytolith assemblages, as well as the Iph index, can be used for identifying riparian and coastal thicket habitats through the fossil phytolith record on the south coast of South Africa. Finally, distinguishing between both riparian and coastal thicket vegetation (Thicket Biome) might be assessed by the higher presence of irregular and

unknown phytoliths, probably from the eudicot group, detected in the latter, and this has important implications when analyzing fossil phytolith assemblages.

VI. 3. Phytoliths as an indicator of early modern human plant gathering strategies during the Middle Stone Age at Pinnacle Point (south coast, South Africa).

VI. 3.1. Phytolith provenience and preservation

In order to better interpret the phytolith record, and thus the plant presence in archaeological sites, there are two aspects that need to be taken into account. The first lies on whether phytoliths come from an anthropogenic origin, and this is even more significant in the case of rockshelters. The second regards to the phytolith preservation, whether it is due to post-depositional processes affecting phytolith preservation or to the type of plants used.

At PP5-6, the sole identification of phytoliths from anthropogenic layers (dominated by combustion features) compared to the rarity or absence of phytoliths in geogenic layers suggested that plants were intentionally introduced in the site by human action. The identification of anthropogenic calcite (wood ash) through FTIR, attests to the past presence of wood even in those samples with an absence or a low phytolith concentration. But this leads us to question whether this absence of phytoliths in some combustion features is due to post-depositional processes affecting phytolith preservation or to the type of plants used as fuel. Phytolith preservation and the role of partial dissolution on phytolith assemblages are critical for avoiding bias when interpreting the data. Cabanes and Shahack-Gross (2015) showed that partial dissolution is responsible for the decrease of absolute quantities of phytoliths, and an increase in the presence of weathered morphotypes and morphotypes showing rugulate textures. This is because the stability of various morphotypes differs even though mineral composition and solubility is the same. Nevertheless, we need to keep in mind that different plant types, plant parts and plants growing in diverse environments (where availability to silicon and/or water in soils might differ) produce phytoliths in different concentration (Piperno, 2006). For example, grasses in Eastern Africa produce three times more phytoliths than in the Levant (Albert and Weiner 2001; Bamford et al., 2006). Thus, even though partial dissolution might be responsible for the decrease of phytolith counts in sediments, a link between phytolith concentration and the state of phytolith preservation could be misleading. But this question remains open until further studies on this regard are conducted.

Under chemical instability of sediments, it should also be expected that the most delicate morphologies would be the first to disappear. Here we considered the association of the mineralogical composition of the sediments together with correlation measurements of the phytolith concentration against the total number of morphotypes identified, the percentage of weathered morphotypes and the frequencies of delicate morphologies in order to understand the state of preservation of phytoliths at PP5-6 (Fig 30). The correlation coefficient R^2 was low for the three measurements and this means that the phytolith assemblage can be considered representative of the original phytolith input.

Furthermore, we observed a co-occurrence of delicate morphologies and weathered morphotypes in most of the samples and this can be interpreted in two different ways. Firstly, this suggests that even though partial dissolution might have affected phytoliths, weathering processes did not affect completely the assemblage and thus the interpretation of the data here reported might still be reliable. A second possibility is that a double input of phytoliths occurred at two different deposition times. In other words, a first plant deposition in sediments occurred and this phytolith assemblage was weathered, and afterwards, a second deposition of phytoliths occurred and this was not weathered, and thus the result is a mixed assemblage in which weathered morphotypes and delicate morphologies co-occur.

Samples from ALBS and SADBS StratAggs contained very low phytolith concentration and in most of the samples we did not identify the minimum number of phytoliths (50) established by Albert and Weiner (2001) as necessary for a reliable morphological interpretation of the data. Aragonite was detected in most of the samples and this is one of the more unstable minerals of the calcium carbonate forms. Its preservation in these StratAggs attests for the chemical stability of those sediments. Then, if dissolution processes did not take place here, the most plausible reason that explains the low phytolith concentration in samples relates to the type of fuel used rather than preservation and this will be a focus of interpretation below. And this is even more significant in SADBS deposits where the micromorphological studies observed minimum chemical alteration of the sediments (Karkanas et al., 2015) and thus phytoliths should be relatively stable.

Moreover, because aragonite was found in sediments and related to the presence of

mollusks in the context of combustion features, there are two potential explanations as to why aragonite was preserved. The first explanation is the presence of low-intensity fires that did not surpass 400ºC, since this is the minimum temperature at which aragonite starts transforming into calcite (Yoshioka and Kitano, 1985). The second explanation accounts for a behavioral trait when, once consumed, seashells were thrown out after the fires were extinguished favoring the preservation of aragonite. But this remains an open question for future studies.

Finally, the absence of phytoliths in samples from the uppermost StratAggs (OBS2, OBS1, SGS, DBCS and RBSR) together with the lack of calcite in sediments might be indicative of some postdepositional processes affecting mineral stability in the uppermost levels of PP5-6. And this is related to the location of these layers near to and partially below and outside the drip line (Karkanas et al., 2015).

VI. 3.2. Plant selection for fire production at PP5-6

Hearth structures in the lowermost StratAggs deposits (mainly from YBSR and LBSR) are generally intact, single hearths showing relatively small disturbance and trampling except in their periphery (Karkanas et al., 2015). This is corroborated through phytoliths and FTIR since anthropogenic calcite (wood ash) was the main mineral component in only four out of the nine samples analyzed from outside hearths, and only one contained high phytolith concentration, which suggests slight dispersion of ashes and burned remains. However, some samples from below hearths showed high phytolith concentration and the presence of calcite that must be explained by the reworking of the black layer and the soil occupation surface beneath the fire, whereas some downward translocation of phytoliths from the black layer might also account for this.

The presence of a large variety of phytolith morphotypes is indicative of the high variety of plant types and plant parts used by the inhabitants of the cave. The presence of a large variety of phytolith morphotypes is indicative of the high variety of plant types and plant parts used by the inhabitants of the cave. The high variety of epidermal ground mass phytoliths from the leaves of trees and shrubs identified in hearth structures along the oldest occupation at PP5-6 (YBSR and LBSR StratAggs) suggests a wide-ranging selection of trees and shrubs foraged by inhabitants of the site. And this is

suggestive to us of the large variety of plant fuel used for the hearths during 90-74ka, the last phases of MIS5 at PP5-6.

Black layers from the LBSR StratAggs were characterized by a high phytolith concentration being grasses the dominant vegetal component; woody phytoliths were also detected but in much lesser amounts. Furthermore, the calcite concentration in most of the samples collected from black layer is minimal. We showed from our plant reference collection that the wood and leaves of eudicot plants contained grass phytoliths from contamination and thus these plant types might contribute to the grass phytolith input in archaeological deposits and mostly in hearth structures to some extent. However, the grass phytolith concentration per gram of plant material in other plant types but grasses was very low if compared to the latters (Table 7) and therefore, the grass presence in archaeological deposits due to contamination, in terms of phytolith concentration, might be minimal. Karkanas et al. (2015) also interpreted the internal microstratigraphy of hearth features as suggestive of the existence of several combustion events but for a relatively short period of time, and these are always associated with shellfish. On this basis, the scenario here observed is suggestive of a human behavior in the use of fire characterized by the presence of a grassy soil at the base of the hearth, probably to help start the fire, after which wood would be added. This explains why the black layers contained high phytolith concentration and the highest frequencies of grass phytoliths, and that wood/bark phytoliths and irregular morphologies were identified in much lesser frequencies (Table 6 and Table A5). And then, fire was fed with wood, explaining why wood ash and irregular morphologies dominate the white layers. In this scenario, bands inhabiting the rockshelter during these short-term occupation events may need to do fast fires and for that they might use mainly grasses with some wood from trees and/or shrubs in order to make quick and brief fires, perhaps for shellfish cooking. Ethnographical comparisons for these interpretations are unfortunately not possible, since there is very little to nothing in the literature on this regard.

VI. 3.3. Foraging practices and subsistence strategies at Pinnacle Point 5-6

We reported for the first time the identification of the family Restionaceae in an

archaeological context and this occurs during the occupation of YBSR StratAgg at PP5-6 (~90 ka). Their identification in anthropogenic layers indicates the gathering and intentional introduction into the site of these plants by MSA hunter-gatherers inhabiting the south coast of South Africa. Restio plants are a diagnostic family of the Fynbos biome. They were used traditionally in southern Africa, and still do, for building, thatching and for the construction of brooms and sleeping mats (van Wyk and Gericke, 2000 and references therein). After the arrival of European settlers to the Cape, restios were mainly used for building and thatching, being *Thamnochortus insignis* the most widely species used because of its long culms (Rourke, 1974; van Wyk and Gericke, 2000). Evidence for what was the use of restios by San people during the contact period with European settlements is not known. On the contrary, KhoiKhoi people, who were herders of both cattle and sheep, used mats made with different graminoids for housing and safekeeping the cattle, as they are easily dismantled and loaded onto cattle for transport when wandering in search of richer pasture areas and water sources (Beck, 2015). Such ethnographic evidence for the use of restios and other graminoids by past and current southern African inhabitants raises the question as to their use by first modern humans. Restio phytoliths were found in contexts of combustion features so their use might be related to fire purposes as for fire maintenance. Nonetheless, their presence in hearth contexts can also be related to some extent as the result of wood contamination (Section V.1.1.1.) although marginal (Section VI.1.). Restios have similar characteristics as sedges in terms of shape, thickness and resistance, as well as the uses of the plants, which overlap considerably (van Wyk and Gericke, 2000). Thus, it might be likely that people inhabiting the Cape during the Middle and Late Pleistocene used them for other purposes in addition to fire such as sleeping mats and these could have been placed close by the fires so they could have been burned at some point and mixed with the rest of the plant fuel and that could be why restio phytoliths have been identified in combustion features. At Sibudu Cave in KwaZulu-Natal, the presence of remains of burnt bedding was reported during the post-Howiesons Poort sequence (Goldberg et al., 2009; Wadley et al., 2011) and these were constructed mainly from sedges, other monocotyledons and topped with aromatic, insecticidal and larvicidal eudicot leaves (e.g. *Cryptocarya woodii*) (Wadley et al., 2011).

Changes in the vegetal but mainly in the mineralogical component along the occupation of PP5-6 were noteworthy between the lower StratAggs (YBSR, LBSR, and

ALBS dated from ~90 to ~72ka) and the SADBS (dating to ~72-71ka). The phytolith assemblage at SADBS differed from the rest of the StratAggs in the higher presence of irregular morphologies, which might come from wood (Albert, 2000; Albert and Weiner, 2001; Section V 1.1.1.). SADBS also differed from the rest of the StratAggs in the mineralogical composition of the sediments, with this StratAgg presenting the highest concentration of anthropogenic calcite (wood ash). An experimental study conducted by Albert and Cabanes (2009) on wood fuel showed that the percentage of ashes was much higher when fires were made with dry wood, while the percentage of charcoal fragments was much higher when fresh wood was used. And this is because dry wood produces a more complete combustion of the plant material (Albert and Cabanes, 2009). The results of our plant reference collection showed that phytolith production in wood is very low and thus wood may contribute little to the phytolith record in archaeological deposits. Thus, despite phytoliths were not identified in high frequencies in this StratAgg, the high concentration of anthropogenic calcite (wood ash), showing the highest concentrations among StratAggs, indicates the continuous and extensive presence of fire events and this is not seen at the oldest moments of occupation of the site (YBSR and LBSR). At Sibudu Cave, Wadley (2012) also related a higher presence of calcite in hearths with high amounts of wood fuel. Therefore, the higher presence of calcite in samples from this StratAgg might point towards a different form of exploitation of plant resources and a different way to make fires compared to other StratAggs at PP5-6. In this scenario, it is likely that during the time of occupation of SADBS at Pinnacle Point people were collecting high amounts of dry wood intentionally as it is easier to gather and transport. Furthermore, this change in the exploitation of plant resources for fire purposes is contemporaneous to the change observed in the lithic tools observed at SADBS when the inhabitants of the cave were heating silcrete tools in order to improve flaking properties (Brown et al., 2009). Thus, our results might point towards the use by past inhabitants of Pinnacle Point during MIS4 of dry wood in large amounts in order to improve combustion and to create the proper conditions for the continuous practice of heating silcrete.

The micromorphological study also showed that the occupation character of the site changed from low-intensity activities, suggesting relatively small groups and/or relatively short occupations in the lowermost StratAggs, to larger groups and/or longer occupations in the upper SADBS StratAgg (Karkanas et al., 2015). Associated with this

shift in the vegetal and mineralogical component, a major change in stone tool raw material from predominantly quartzite to silcrete was observed (Brown et al., 2009; Brown et al., 2012). As pointed out above, stone tools in SADBS were also made primarily on heat-treated silcrete (Brown et al., 2009; Brown et al., 2012). A change in human behavior was also observed in terms of marine resource exploitation since during the time span of inhabitance of SADBS (~72-71ka), despite the coastline was further away from Pinnacle Point (14 km in average) (Fisher et al., 2010), the cultural material recovered showed that people were still exploiting the coast and transporting shellfish back to PP5-6 (Karkanas et al., 2015). Micromorphology showed that SADBS deposits consisted of overlapping combustion features with some *in situ* fine hearth features but in general trampling and raked out hearth remains dominated, indicating intense combustion activities and also intense human occupation (Karkanas et al., 2015). This frequency of combustion features was also seen as indicative of frequent visits to the site, perhaps even on a seasonal base (Karkanas et al., 2015). Our results, indicating the continuous and extensive presence of fire events, may be also interpreted as the result of intense human occupation what is consistent with the micromorphological study. Thus the phytolith and mineralogical evidence along with the micromorphological evidence from PP5-6 showed that changes in the plants used by PP5-6 inhabitants are in association to changes in cultural material and intensity of human occupation of the site.

VI. 3.4. Comparison with PP13B

The differences in the vegetal component between PP13B (Albert and Marean, 2012) and PP5-6 sites is suggestive to us of important changes in the patterns of plant foraging strategies by past hunter-gatherers inhabiting the south coast of South Africa through the Middle and Late Pleistocene (Fig. 40). The modern plant reference collection from the study area here reported affords the opportunity to shed light on some puzzling results described by Albert and Marean (2012) at PP13B, as well as the comparison of the Pinnacle Point sites underscoring the differences between them in relation with their location, appearance, size and preservation conditions. PP13B is a true cave and very protected from the wind and rain. All the hearths are inside and within the drip line. The cave has a restricted floor space and therefore only one small human band of people

could be inside. At PP13B the front and back of the cave have different preservation conditions (Karkanas and Goldberd, 2010), with better phytolith preservation at the back (Albert and Marean, 2012). This may result in bias in the plant representation in the site because of the possible different plant uses in different site areas (Albert and Marean, 2012).

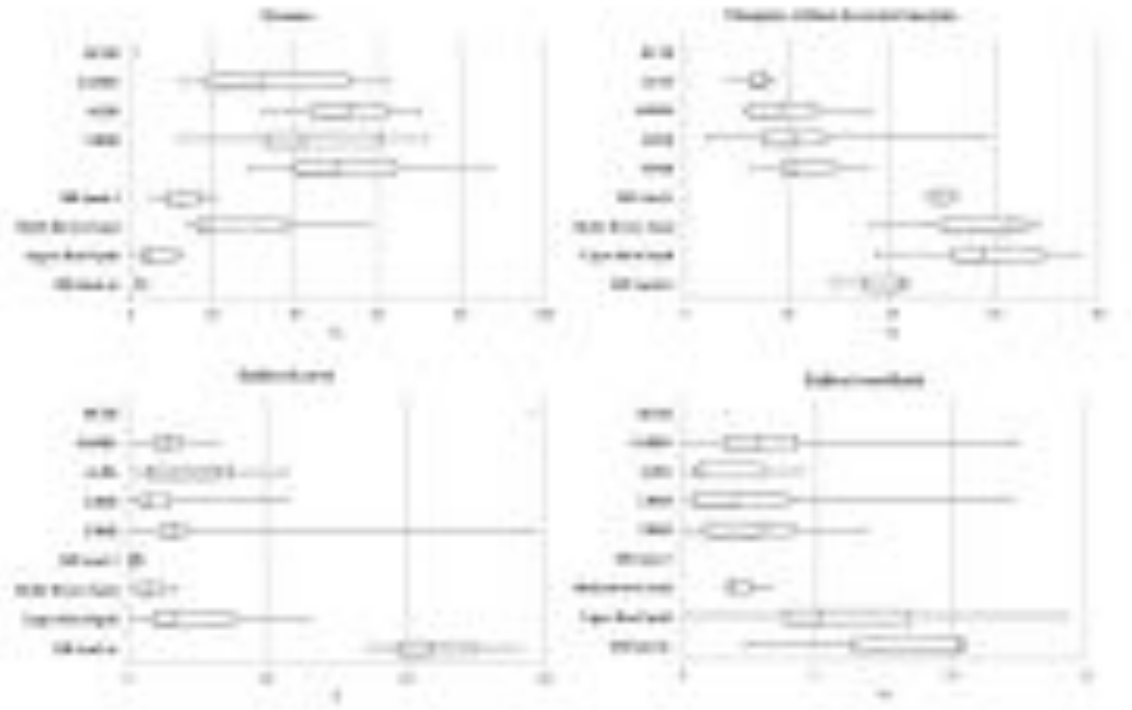

Figure 40. Box-Plots showing the distribution of grass, elongate without decoration margins, eudicot leaf and wood/bark phytoliths among the different StratAggs from PP13B (Albert and Marean, 2012) and PP5-6 sites. The mean values (mid- line), standard error ± (box) and standard deviation (whiskers) are given for the four plant types.

Conversely, PP5-6 is a rockshelter and during the occupation of the site it would have been relatively exposed. It presents a much wider open area available for occupation so more people could conceivably inhabit it. Such differences might also be influenced by the mode of occupation of the two sites, influencing the strategies on the patterns of exploitation of the vegetal resources. At PP13B the vegetal component identified from hearth remains were mainly eudicot plants. Noteworthy was the

identification of eudicot leaves in the oldest moments of occupation at the back of the cave (DB Sand 4c) (Albert and Marean, 2012). Keeping in mind that the wood of trees and shrubs from the central south coast of South Africa analyzed in this study produce very low number of phytoliths per gram of plant material (Section V1.1.1.), the high frequencies of wood/bark phytolith morphotypes is suggestive of the deliberate introduction of large quantities of wood in the cave and this is not observed at PP5-6. Albert and Marean (2012) interpreted the high abundance of eudicot leaf phytoliths during DB Sand 4c as the result of the production of fires with specific properties, including short-term activities or to a different use or activities such as cooking. Our reference collection has not been able to identify the taxonomic provenance of these eudicot phytoliths. Thus, their specific provenience besides to belong to eudicot plants remains unknown. Nevertheless, it is worth to mention that the epidermal ground mass morphotypes found at both sites presented a high variability in their shapes what might imply a different plant provenance. However, this is tentative and further studies towards the expansion of the plant reference collection are necessary.

The high presence of elongate morphologies without decoration margins in most of the StratAggs of PP13B was ascribed to monocot plants, and related to grasses, in those samples where characteristic grass phytoliths were identified (Albert and Marean, 2012). At PP5-6, although these morphologies were also identified in high frequencies, they are not as abundant as at PP13B (Fig. 40). This is true even though restios and grasses are an important component of the phytolith assemblage at PP5-6 and these plants are also high producers of elongate morphologies (Section V.1.2.2. and 1.2.3., respectively). These results stress the importance of these morphotypes during the occupation of PP13B and mostly during Upper Roof Spall and Shelly Brown Sand StratAggs, dating to ~120-95ka (Albert and Marean, 2012) (Fig. 40). Geophytes from the GCFR are mostly from the monocotyledonous class. Furthermore the now available plant phytolith reference collection here presented showed that geophytes, and mostly from the genera *Moraea* from the Iridaceae family, produce high numbers of elongate morphologies without decoration margins (Section V.1.2.1.). Despite the ethnobotany of the Khoi-San people is poorly recorded (Liengme, 1983; Van Wyk, 2002), it is known that geophytes were an important resource for food and water for San people (Bushman) from southern Africa (Story, 1958; 1964). Furthermore, geophyte remains have been found in a variety of Later Stone Age archaeological sites, and some

examples are Melkhoutboom (Deacon, 1976), Scott's Cave (Wells, 1965) and Sehonghon (Carter et al. 1988), where evidences of consumption of *Watsonia* and *Moraea* (Iridaceae) and leaf sheaths of *Hypoxis* (Hypoxidaceae) have been recorded. In the light of this, it is feasible that the higher presence of these morphologies at PP13B might be related to other plants aside from grasses such as geophytes, and particularly from the *Moraea* genus (Section V1.2.1.). Nonetheless the lack of diagnostic phytoliths in geophytes (Section V1.2.1.) and the absence of other plant remains such as pollen, charcoal or seeds for comparison at Pinnacle Point sites make difficult to validate this hypothesis.

With the exception of the samples from Shelly Brown Sand (dating to MIS 5c), one common trait among the samples from PP13B deposits was the general low abundance of grass phytoliths (Albert and Marean, 2012). Despite the bad preservation conditions of phytoliths in some of the areas of the cave, the low grass phytolith presence noted in those well preserved samples was interpreted as this family not being common in the local area (Albert and Marean, 2012). PP5-6 shows that at Pinnacle Point in later periods, grasses were present and people used them, and thus, until further studies are conducted in other archaeological sites for periods contemporaneous to PP13B, the results observed in both caves can be indicative of a change in vegetation cover towards a grassier environment. A second possibility is that changes in the strategies of plant exploitation by people inhabiting Pinnacle Point changed overtime. And this has been detected in the phytolith record from PP5-6 with the transition from LBSR/ALBS during MIS5 to SADBS during MIS4 and it is associated to changes in human behavior through an advance stone tool technology.

VI. 4. MIS5 to MIS3 environmental change on the south coast of South Africa as indicated by phytolith analysis at Pinnacle Point 5-6

VI. 4.1. The usefulness of archaeological phytolith assemblages for paleoenvironmental reconstruction

Phytoliths were deposited in the Pinnacle Point archaeological sites by the human action (Albert and Marean, 2012; Section VI 3.1.). This implies that the plants introduced into the site were the result of human selection. And this can be problematic when conducting paleoenvironmental interpretation of the data because of the human bias. The viability of using phytoliths from archaeological deposits in order to conduct paleoenvironmental reconstructions in our study area is made on the basis of the following proposals, as we discuss some of the results accordingly. Most of these considerations are based on the phytolith results from the modern phytolith reference collections of plants and soils presented in this thesis (Section V 1. and V 2., respectively).

1. The first regards to the bulliform cells as high presence of these phytolith morphotypes is indicative of water stress and high evapotranspiration rates suffered by plants growing under dry conditions or in local wet areas in dry zones (Sangster and Parry, 1969; Rosen and Weiner, 1994; Bremond et al., 2005a). We observed in our modern plant reference collection that the only species showing high frequencies of bulliform production was the one collected from a wetland area and this belongs to the Panicoideae subfamily (Section V. 1.2.3. and VI. 1.). In paleoanthropological contexts the concentration of bulliform cells (Fs index) resulted in a useful tool for detecting moisture fluctuations (e.g., Messager et al., 2010). Therefore, variations in the proportion of bulliform cells under chemical stability of the sediments may indicate changes in climate conditions from dry to moderate periods and vice versa, or indicative of the presence of wet environments such as wetlands or riverine zones in the vicinity areas of sites.

2. The second proposition is that high phytolith concentration in relation to a high presence of grasses in the whole phytolith assemblage might be interpreted in two

different but complementary ways. The first might be indicative of their introduction into the cave of the human's preference for their used for several purposes and this is also suggestive (second explanation) of their availability in the surrounding areas of the site.

3. The third proposition concerns the presence of C_3 and C_4 GSSCs and their distributions. We propose that hunter-gatherers collected grasses in the immediate vicinity of the sites roughly in relation to their availability and not in a highly biased manner. Thus the proportions of concentrations of C_3 and C_4 GSSCs in the Pinnacle Point archaeological deposits can be used to infer the grass photosynthetic pathway distribution along the center south coast of South Africa and thus is a proxy for the presence and absence of summer and winter rain. As it has been pointed out along the previous two sections of the discussion chapter, the grass specimens analyzed in this study showed that a general trend in the distribution of GSSCs occurred among grass photosynthetic pathway and among subfamilies to some extent in which bilobates are mainly produced by C_4 grasses and mostly from the Panicoideae subfamily, rondels by C_3 grasses and saddles are exclusively produced by Chloridoideae grasses although this subfamily also produce other GSSCs such as rondels.

4. The fourth relates to the presence of phytoliths characteristic of the Restionaceae family. Although restio phytoliths could have been intentionally foraged due to various economic, skill and craft uses, their identification in archaeological deposits also implies that fynbos vegetation was present around Pinnacle Point within the normal hunter-gatherer daily foraging radius of around 10-15 km (Kelly, 1995; Marlowe, 2005). And this has important implication for the reconstruction of past conditions in terms of geology, soil conditions, climate and environment.

5. The fifth concerns the presence of GSSC saddles and irregular and indeterminate phytolith morphologies, which reflects thicket vegetation (Section VI 2.2.). We observed that those StratAggs where there was a higher presence of irregular and indeterminate morphologies also contained higher frequencies of C_4 GSSCs compared to other StratAggs.

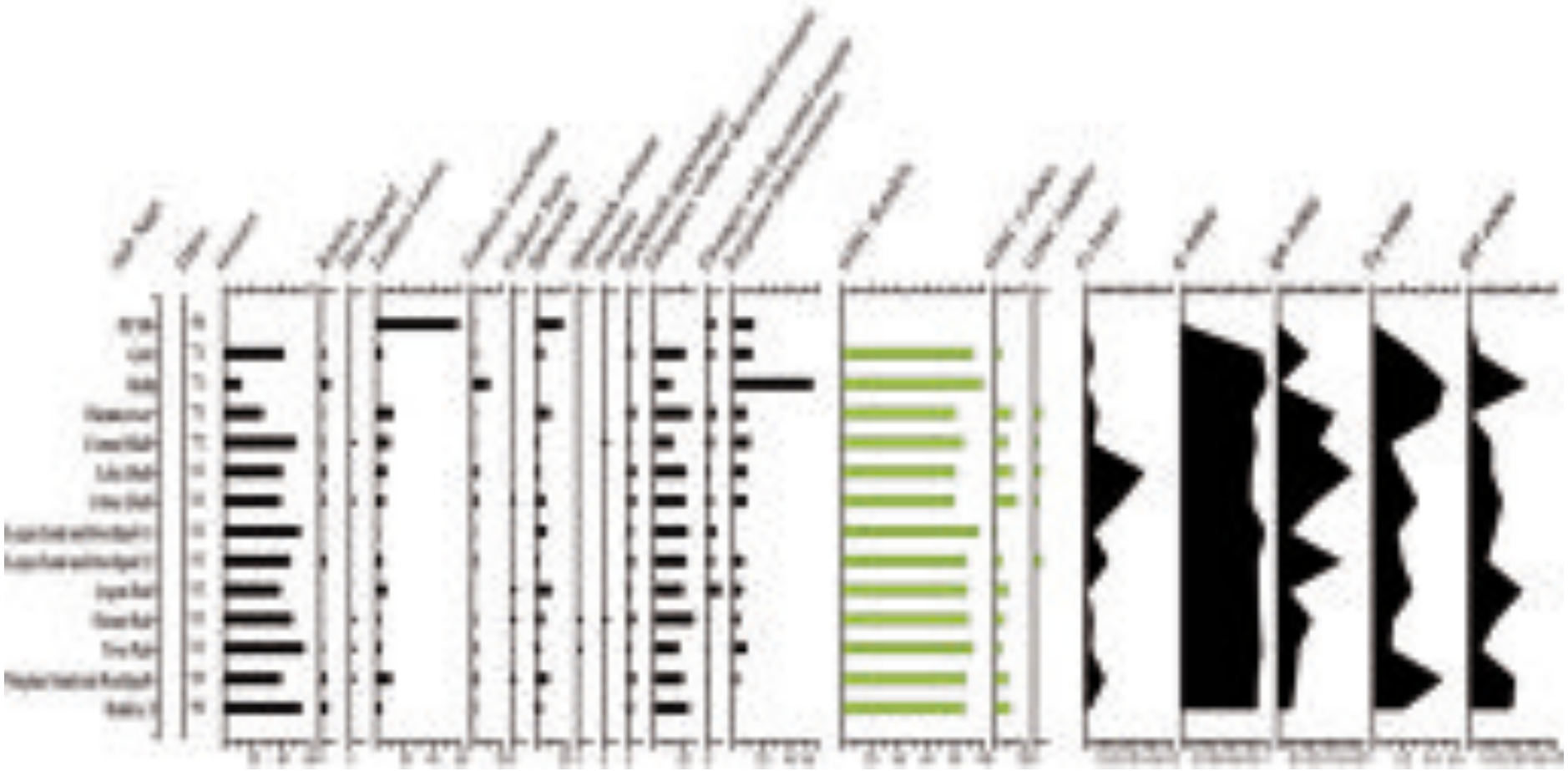

Figure 41. Phytolith diagram for the PP5-6 sequence showing the frequencies of the different plant type identified, the distribution of the GSSCs (rondels, lobates and saddles) expressed as the percentage of the total sum and the phytolith indices. GSSC Rondels account for both Rondel and Oblong categories. Values below 1% are represented by circles.

VI. 4.2. Paleoscape reconstruction at Pinnacle Point

The record of the phytolith assemblage compiled from Pinnacle Point sites has important implications for the reconstruction of the climate and vegetation of the central south coast of South Africa during the Middle and Late Pleistocene. Few phytolith studies have been conducted on the MSA record and previous to the work here presented, only the study of cave PP13B focused on the south coast (Albert and Marean, 2012). The phytolith record from PP13B (Albert and Marean, 2012) and PP5-6 sites enable us to add new data to the multi-proxy picture developed for the vegetation and the climate occurring in the surrounding areas of Pinnacle Point from MIS5 to MIS3 based on speleothem (Bar-Matthews et al., 2010; Braun et al., submitted), large mammals (Rector and Reed, 2010), micromammals (Matthews et al., 2009, 2011) and pollen (Quick et al., 2015) archives available from the south coast. One of the main outcomes observed is the important vegetation change observed in the sequence from Pinnacle Point sites, where grasses were little or absent in some of the occupation moments of PP13B, while they were abundant all along the occupation of PP5-6. At first glance, this may seem indicative that between ~160-90ka few grasses might have occurred in the immediate surroundings of Pinnacle Point. Conversely, after 90ka grasses were regularly abundant in the immediate surroundings of the cave.

The beginning of MIS5b comes with the end of the dune building phase at ~90 ka at Pinnacle Point when humans occupied a new site, the rockshelter PP5-6. It is with the occupation of this new site, in the oldest deposits (YBSR), at ~90ka, when Restionaceae appeared in the archaeological record and they occurred consistently along the occupation of the site (Fig. 35 and Fig. 41). Grasses are also well represented and this happens all through the sequence. A mix of C_3 –C_4 grasses occurred at this time although C_3 grasses dominated the assemblage with a high presence of GSSC oblongs, probably from the Pooideae subfamily (Section V 1.2.3.; Rossouw, 2009). And C_3 grasses became even more dominant during the occupation of LBSR StratAgg during MIS5a (Fig. 35 and Fig. 41), and this is concurrent with the speleothem signal that shows a return to stronger C_3 conditions (Bar-Matthews et al., 2010; Braun et al., submitted).

For the latter phases of MIS5 (~96-70 ka), Quick et al. (2015) observed an increase in the Ericaceae component and declined in *Podocarpus* pollen implying that, fynbos

elements and also colder conditions, with probably an increase in rainfall seasonality, might be better represented on the south coast. The occurrence of fynbos vegetation has also been detected through the phytolith record at PP5-6 during this period, although restio plants have been recorded all along the occupation of the site, with the only exception of the latest moments of occupation of the cave during MIS3. The co-occurrence of a high presence of grasses, mostly from the C_3 type, what has been also detected through the speleothem record (Bar-Matthews et al., 2010), along with the presence of restio plants, what is indicative of fynbos vegetation, may point towards the presence of some sort of fynbos-renosterveld mosaic vegetation where grasses are well represented and people were using them and these were mainly of the C_3 type while restios and woody plants were also present. Thus, based on the phytolith assemblage and the speleothem record, similar vegetation to that occurring today should have prevailed above (fynbos) and below the cliffs (thicket and strandveld) (Mucina et al., 2006).

It is during this period of time when we also noticed the presence, although in very low numbers, of spheroid echinate phytoliths (Fig. 35 and Fig. 41). As it has been pointed out before (Section VI.2.2.), these phytolith morphotypes are known to come from different plant families but only two occur in the GCFR and these are Strelitziaceae and Orchidaceae. Arecaceae plants produce high number of spheroid echinate phytoliths but this plant family does not occur in the GCFR but in eastern South Africa. These phytolith morphotypes have been statistically detected as a characteristic element of coastal thicket vegetation. The spheroid echinates at PP5/6 are identified in a period when the coastline would have been as close as it is today (Fisher et al., 2010) and it is plausible that some sort of thicket could be present in the surrounding areas of the site. Nevertheless and as it has been pointed out in the previous section, further work needs to be done on expanding the plant phytolith reference collection what might help identify the origin of these morphotypes in the GCFR.

MIS4 was a return to global glacial conditions. In Southern Africa, Chase (2010) proposed that this stage was relatively humid as a result of warm SW Indian Ocean SSTs (van Campo et al., 1990), an increased influence of westerly storm tracks (Stuut et al., 2002), and perhaps the increased interaction of tropical and temperate systems in the form of SSTs resulted in more humid conditions in southwestern Africa (Shi et al.,

2001; Stuut et al., 2002). The isotopic (18O and 13C) speleothem data from Pinnacle Point Crevice Cave indicated that during MIS5 when global conditions were warmer there was an increase in winter rainfall, and in C_3 plants while in the cooler MIS4 there was an increase in summer rain and C_4 grasses (Bar-Matthews et al., 2010). SST records from the southwest Indian Ocean showed that MIS4 was characterized by periods of relatively elevated SSTs combining with a more northerly position of the STF to enhance both summer rainfall and westerly derived rainfall and wet conditions (Caley et al., 2011). Following the change from MIS5 to MIS4 there is a shift in the archaeological record with the development of and an advanced bifacial stone tool technology, the Still Bay industry (for a review see Henshilwood, 2012; Mackay et al., 2014). The changes in technology between 74-60 ka are the most rapid seen in the entirety of the South African MSA (Marean et al., 2014). At PP5-6, this transition is also reflected by the shift from a roof-spall rich sediment during MIS5 to an aeolian-dominated sediment (Karkanas et al., 2015) followed by a shift to microlithic technology and an emphasis on the use of silcrete for stone tool production (Brown et al., 2012). The phytolith assemblage dating to the beginning of MIS4 (SADBS and ALBS StratAggs) showed a slight increase in C_4 grasses in comparison with the dominance of C_3 grasses in the LBSR (Fig. 35 and Fig. 41). And together with an increase in C_4 grasses, irregular and indeterminate phytoliths abounded and mostly in SADBS deposits (~72ka) (Fig. 35 and Fig. 41). This phytolith record, when compared with the modern soil phytolith record from extant habitats occurring in the south coast, shows great similarity with the phytolith assemblage observed in samples from the coastal thicket vegetation that occurred on the slopes of the Pinnacle Point cliffs. The presence of irregular morphologies has been here interpreted as indicative of large amounts of wood. Both paleoenvironmental and foraging practices interpretations fit well as thicket vegetation presents dense shrubby/low tree vegetation and this would have been the source for the wood fuel used. Nevertheless, restio phytoliths were also detected in the deposits dating to this period and this might be indicative of the presence of some sort of fynbos vegetation in the surrounding areas of Pinnacle Point.

The pollen record from Vankervelsvlei detected the dominance of Ericaceae and the *Stoebe*-type pollen (probably *Elytropappus* spp.) during MIS4, which was interpreted by Quick et al. (2015) as an increase in drought stress and rainfall seasonality under cool conditions. And at 67 ka the authors observed a spike in *Stoebe*-type pollen

interpreted as the reduction in moisture availability that could be the reflection of a slight aridification during what was generally a period of relatively humid conditions. Westwards from Pinnacle Point, at Die Kelders Cave 1, the MSA micro- and macromammalian and sedimentological records showed a general tendency towards cooler and moister conditions at the end of MIS5 and along MIS4 (Avery, 1982; Feathers and Bush, 2000; Klein and Cruz-Uribe, 2000). The wood anatomy study at Boomplaas, in the interior parts of the Southern Cape, from deposits dating to MIS4, was also suggestive of a cold and dry climate. During cooler periods the increase in C_4 grasses was interpreted by Bar-Matthews et al. (2010) to indicate the presence of grassy fynbos or thicket vegetation characterized by an abundance of C_4 grasses. During MIS4 the combined abundance of large plains animals and rich intertidal beds made Pinnacle Point extremely attractive for lengthy hunter–gatherer occupation (Karkanas et al., 2015). Thus, the phytolith assemblage from PP5-6 together with the speleothem record from Crevice Cave, and supported by the archives recorded from the south coast here reported, indicates the presence of a fynbos-thicket mosaic vegetation where C_3 grasses dominated although C_4 grasses were also well represented.

MIS3 is a relatively unexplored period in comparison to MIS 4 (Mitchell, 2008; Wurz, 2013). In Boomplas the charcoal and pollen record seemed to be indicative of cold and dry conditions (Scholtz, 1986; Deacon and Lancaster, 1988). During this period of time (~50 ka ago), sea levels arose together with the increased of sea surface temperatures (Vimeux et al., 1999; Ramsay and Cooper, 2002). The values of the δ18Occ and δ13Ccc from Pinnacle Point dating from ~66 to ~50 ka suggested more summer-rain and C_4 grass than today (Bar-Matthews et al., 2010). This was suggestive to Bar-Matthews et al. (2010) of the occurrence in the surrounding areas of Pinnacle Point of grassy fynbos and thicket, and probably a mosaic of the two, because only these vegetation types of the Cape are found in summer rain and have the substantial C_4 grass components that would accommodate the ∂13Ccc. At Vankervelsvlei the pollen record showed high proportions of Ericaceae and other fynbos taxa from 59 to 37 ka what might indicate cool conditions (Quick et al., 2015). Unfortunately, only one sample dating to MIS3 contained enough phytoliths for a reliable morphological interpretation of the data and the spectra detected differed greatly from that detected in older moments of occupation of the site. Here grasses and restios were absent while eudicot plants, mostly from the leaves, together with spheroids and elongates with

decorated margins phytolith morphotypes dominated (Fig. 35 and Fig. 41). And despite the interpretation is tentative it could be indicative of shrubby/forest vegetation occurring in the vicinity areas of Pinnacle Point. Whereas other vegetation types might be also present, this was the area preferred for plant foraging practices by the inhabitants of Pinnacle Point. Nevertheless, further work on the uppermost StratAggs of PP5-6 is needed in order to have a much broader vision of the paleoclimate and paleoenvironment during MIS3.

VII. Conclusions

The main outcomes obtained through the study of South African phytolith assemblages from the three essential elements of this study, which are modern plants, modern surface soil samples and archaeological sediment samples from the GCFR and Pinnacle Point cave 5-6 respectively, are summarized below:

VII. 1. GCFR plant identification through phytolith assemblages

The research into the quantitative and morphological production of phytoliths of modern plants from the GCFR establishes criteria for the identification of plants that might have been exploited by past hunter-gatherers inhabiting the south coast of South Africa. This study contributes to the phytolith and the paleoanthropological research community through four main outcomes:

1. Through optical microscopical identification, thin sections, SEM microscopy and EDAX analysis, it has been reinforced the hypothesis that characteristic restio phytoliths (large spheroids, showing protuberances, with verrucate and granulate ornamentation and most probably also spheroids showing spiraling ornamentation) characterize Restionaceae plants. Since the Restionaceae family is also present in other austral regions, such as New Zealand, New Guinea, Aru Islands, Malesia, Hainan Island, Chile and Madagascar, these results might also be useful for research conducted in these regions.

2. This study presents the first phytolith reference collection conducted from modern species of geophytes from South Africa. The observation that geophytes do not produce diagnostic phytolith morphotypes that can be used for taxonomic identification, make difficult their identification in the paleoanthropological record. Nevertheless, we observed that the leaves of geophytes, and mostly from the genera *Moraea*, are characterized by the high presence of elongate morphologies without decorated margins.

3. The results here reported confirmed the patterns previously recorded elsewhere (e.g Piperno, 1988; Albert and Weiner, 2001; Tsartsidou et al., 2007), with Poaceae plants being the highest phytolith producers and thus they might be overrepresented in the phytolith record.

4. C_3 and C_4 grasses and restio plants can be differentiated from one another and from other plants in South Africa through the phytolith morphological production and this is an important result when studying fossil phytolith assemblages.

5. Despite rondels, bilobates and saddles were mainly detected in C_3, C_4 and C_4 Chloridoideae grasses, some multiplicity and redundancy occurred. And this was revealed through ANOVA as GSSC distribution among C_3 and C_4 grasses was not clearly detected and this stresses the importance to further extend the reference collection on grasses in order to obtain more reliable statistical results.

6. Following previous studies on eudicot plants, we observed that trees and shrubs from the GCFR are characterized and differed from other plant parts by the high presence of spheroids with psilate textures, ellipsoid morphologies, epidermal ground mass, tracheids and sclereid cells.

VII. 2. GCFR vegetation reconstruction through modern surface soil phytolith assemblages

This study shows the potential and limitations for using phytolith assemblages from modern soils to reconstruct GCFR vegetation. Our results also provided key details on identifying specific GCFR vegetation types through phytolith analysis. The results provided in this study might contribute to the understanding of past environments and climate changes on the south coast of South Africa.

The grass phytolith assemblage detected in each of the vegetation types studied is consistent with a mix of grass subfamilies from the C_3 and the C_4 photosynthetic pathway, which is consistent with the distribution of grasses in the Southern Cape.

The co-occurrence of restio phytoliths, high presence of spheroid morphotypes, and a high presence of rondel GSSCs from C_3 grasses are the characteristic feature for the identification of fynbos vegetation, mainly limestone and sand fynbos.

We demonstrated that the new phytolith index (Fy) developed here is a useful tool to detect fynbos vegetation. However, if grass plants are present in the vegetation, it is not possible to identify fynbos vegetation accurately. The D/Pº index was useful in identifying limestone fynbos vegetation, but it was not able to characterize forest and shrubland/thicket vegetation types.

Coastal forest vegetation appears to be related to the dominance of GSSC lobates though a larger number of samples are needed to corroborate this association. Similarly, saddles from the C_4 Chloridoideae grass subfamily may be used to identify riparian and coastal thicket vegetation when studying fossil phytolith assemblages. However, we contend that further studies focused on the vegetation types occurring in Western (C_3 dominance) and Eastern Cape (C_4 dominance) are needed to fully understand the phytolith morphological distribution along different South African habitats with different environmental and climatic conditions.

VII. 3. The archaeological phytolith assemblage at Pinnacle Point 5-6 during the MSA

PP5-6 represents the continuation of the occupation of the area (by moving from PP13B to PP5-6) and thus the results presented here extend the previously published record from cave PP13B (Albert and Marean, 2012) and now covers the termination of MIS5 until MIS3.

Phytoliths in archaeological sediments are a product of both the selection habits of people and the vegetation within the collection radius of the people inhabiting the site. We expect that the phytoliths deposited in the site were brought there primarily as plant foods, wood fuel for fires, and also probably bedding as well as other functions. So the relative abundance of phytoliths can be a merged product of human behavior and local vegetation. In this thesis the archaeological phytolith assemblage has been interpreted by focusing on interpreting the behavioral implications on the one hand and the climate and vegetation signal on the other.

VII. 3.1. Plant foraging strategies

This study was set out to explore the strategies of exploitation of vegetal resources by past hunter-gatherers inhabiting Pinnacle Point. The main results of this study shed light on the patterns of plant deposition and phytolith preservation, fire fuel used, mode of occupation of PP5-6 and changes in the strategies of plant exploitation over 120,000 years.

We observed that plant phytoliths at PP5-6 were introduced into the site via anthropogenic input. We also demonstrated the well state of preservation of the phytolith assemblage and thus it can be considered representative of the original phytolith input. And even though some partial dissolution might have affected some phytoliths in some of the samples, this was not extensive enough to bias the correct interpretation of the whole data set.

The joint study of phytoliths and FTIR helped us to understand the mode of occupation and the intensity in the human activities along the different occupation

periods of PP5-6. Similarly, this study reaffirms the usefulness of phytoliths and FTIR in identifying changes in the fuel used for fires and its relation with the different living strategies and modes of occupation of the site.

This study reports evidence of the intentional gathering and introduction into living areas of restio plants by MSA hunter-gatherers inhabiting the south coast of South Africa. It is likely that people inhabiting the Cape during the Middle and Late Pleistocene used them for other different purposes such as fire (for example fire maintenance) or as sleeping mats and these could have been placed close by the fires so they could have been burned at some point and mixed with the rest of the plant fuel and that could be why restio phytoliths have been identified in combustion features. Nevertheless, the reason for the gathering and introduction into the cave needs also further research, as well as the study of phytoliths in other MSA archaeological sites for comparison.

Our study supports evidence for changes in foraging strategies in relation to changes in modern human behavior in regards of lithic tool activities and climate change. Together with the development of complex technologies such as heat treatment during MIS4, it is observed that people also changed foraging strategies by gathering large amounts of dry wood, perhaps to improve combustion and create the proper conditions for the continuous practice of heating silcrete.

On the basis of the elongate morphologies without decorated margins presence, which has been documented in high frequencies in the two *Moraea* species analyzed in this modern plant phytolith reference collection, we hypothesized that the higher frequencies of these morphologies detected at PP13B might be related to other plants aside from grasses such as geophytes, and particularly from the *Moraea* genus. However, this possibility needs to be further explored.

VII. 3.2. Paleoscape reconstruction from MIS5 to MIS3

The Pinnacle Point sites have provided a wide range of proxy data on paleoenvironments and paleoclimates, including speleothem records, macro- and micromammal taxonomic data, sedimentary observations, marine geophysics of the

offshore platform, and a coastaline model. In this research work it has been integrated the observations of phytoliths with these other proxies and largely found concordance, and also that by utilizing this multi-proxy approach we were able to provide an enriched picture of the changing environments at the Pinnacle Point locality from MIS5 to MIS3.

This study demonstrated that phytolith assemblages from the Pinnacle Point archaeological deposits are a useful tool for the reconstruction of the paleoenvironmental and paleovegetation though some limitations exist. This is the first attempt at using phytolith indices to reconstruct the paleoclimate and paleovegetation from the South African archaeological record. Differences in the phytolith index values were detected in samples among StratAggs and thus showing differences in the C_3 and C_4 grass distribution as well as in the fynbos vegetation signal.

The paleoscape reconstruction of Pinnacle Point area during a period of time associated with glacial cycling and sea level change covers from MIS5 to MIS3. For the latter phases of MIS5 the paleoscape at Pinnacle Point was here reconstructed using phytoliths analysis as a mosaic of habitats that might have occurred through time where fynbos, thicket/forests and some sort of vegetation with high grass content as could be grassy fynbos or renosterveld occurred. During MIS4 the phytolith record at PP5-6 was indicative of the presence of a fynbos-thicket mosaic vegetation where C_3 grasses dominated although C_4 grasses were also well represented and this is also supported by previous archives recorded from the south coast. Thus, the changes observed in the phytolith record from Pinnacle Point deposits might be indicative of vegetation movements accordingly to climate changes and sea level fluctuations, in a continuous regional mosaic of habitats.

VII. 4. Future perspectives

The work conducted in this thesis it is a first attempt to understand modern human plant exploitation and paleoenvironmental changes in South Africa along MIS5-3. In spite of the positive results of this study, it is evident that further research is needed. This section presents research questions and future plan built on this thesis.

The phytolith evidence from the archaeological deposits of PP5-6 showed that changes in the plants used by PP5-6 inhabitants are in association to changes in cultural material and intensity of human occupation of the site. We also showed that the phytolith assemblage from PP5-6 was interpreted, in terms of paleoclimate and paleoenvironment, as indicative of a mosaic of habitats that might have occurred through time where fynbos, thicket/forests and some sort of vegetation with high grass content as could be grassy fynbos or renosterveld.

In order to compare this landscape reconstruction to other South African regions, future work might include the study of other archaeological sites from the south coast of the Southern Cape. Furthermore, future research might also focus on the expansion of the study area to three other South African geo-climatic regions (western Cape, eastern Cape and interior parts of the southern Cape), where the archaeological record also shows evidences of modern human cultural material dating to the Middle and Late Pleistocene. Presently, these regions occur under the influence of different climate and environmental conditions and present different vegetation types: i) western Cape, occurring in the WRZ, where pure fynbos vegetation and C_3 grasses dominate, ii) eastern Cape, occurring in the SRZ with four main vegetation biomes -Albany Thicket, Grassland, Savannah and the Indian Ocean Coastal Belt (IOCB)- and where C_4 grasses dominate, iii) the interior parts of the southern Cape, which present mesic and similar climate conditions and vegetation types to Pinnacle Point but without ocean influences both in terms of environment and human resources. Thus, we will be able to compare whether changes in the cultural material occurring along South Africa correlate with changes in the exploitation of plant resources characteristic of each particular region.

Furthermore, in order to identify past climate, climate changes and past environmental conditions along South Africa, paleosoils might be study from at least two of the above mentioned study areas. Special attention should be paid to the southern

and eastern Cape because of its importance for the study of past climate shifts that might have influenced vegetation distribution during the Pleistocene. Lacustrine and terrestrial records have been successfully used in paleoenvironmental studies through phytolith analysis since they offer a continuous record on the vegetation and climate. However, only two phytolith studies of paleosols have been conducted in South Africa, in the Pondoland region from a terrestrial sediment core (Fisher et al., 2013), and the Tswaing Crater– the Pretoria Saltpan from a lake sedimentary core (Maclean and Scott, 1996), and only the latter is dated from the Middle to the Late Pleistocene.

Following the methodological procedures followed in this thesis, the fossil phytolith record will be compared with modern phytolith assemblages from plants and surface soils from extant habitats. In this thesis we have developed a modern phytolith reference collection of surface soils from extant habitats occurring in our study area (the CGFR of the south coast of South Africa) in order to identify phytolith assemblages with the potential to be used as proxies for the paleoenvironment, paleoclimate and paleovegetation reconstruction at Pinnacle Point and other south coast sites. The evidence from this study showed that phytoliths are a useful tool for the reconstruction of fynbos vegetation. Furthermore, our results from the GSSCs provided key details on identifying coastal forest and coastal thicket vegetation types. However, we contend that further studies focused on the vegetation types occurring in western (C_3 dominance) and eastern Cape (C_4 dominance) are needed, and focusing not only in GSSCs (Cordova and Scott, 2010; Cordova, 2013) but on the whole phytolith assemblage, to fully understand the phytolith morphological distribution along different South African habitats with different environmental and climatic conditions. The research strategy might focus on the sampling of a variety of vegetation units within the vegetation biomes/vegetation types related to the three geo-climatic regions mentioned above and particularly to the GCFR. The sampling will be based on those vegetation types that are present in the surrounding areas of both the paleosoils and the archaeological sites. Similarly, following the methodological procedures followed in this thesis, the sampled areas will be described in terms of geology, type of soils, dominant plants, vegetation types and season of collection.

The work carried out on modern plants was the first attempt to understand the phytolith production from eudicot plants and geophytes from the GCFR. We also showed through thin sections and SEM that the characteristic restio phytoliths, firstly

identified in Cordova's works (Cordova and Scott, 2010; Cordova, 2013), belong to and characterize the Restionaceae family and that are produced in the parenchyma sheath of the culms. It was observed that grass phytolihs were also detected in other plants types and thus some contamination from other plants such as wood can occur in the archaeological record. And these have been reported elsewhere. In this thesis we tried to determine that, in terms of phytolith concentration, the grass phytolith input from other plants might be very small (Table 9 in section VI.1.). However, more systematic research is needed to establish an appropriate approach to detect differences and bias in the plant phytolith input in the archaeological record in South Africa. Despite of the positive results reported in this thesis, we are aware that the sample is very small in comparison to the high species richness in the GCFR so further work is needed on expanding the plant list and on characterizing the phytolith morphological production and distribution among plant types and plants in order to better identify foraging strategies of past hunter-gatherers and to reconstruct past climate and vegetation on the south coast of South Africa. Morphometric analysis might be a suitable tool in order to accomplish this purpose.

References

Acocks, J.P.H., 1953. Veld Types of South Africa. Memoirs of the Botanical Survey of South Africa, 28, 1-192.

Albert, R.M., 2000. Study of ash layers through phytolith analyses from the Middle Palaeolithic levels of Kebara and Tabun caves. Unpublished PhD Thesis, Universitat de Barcelona, Barcelona.

Albert, R.M., 2010. Hearths and plant uses during the Upper Palaeolithic period at Klissoura Cave 1 (Greece): the results from phytolith analyses. Eurasian Prehistory, 7(2), 71-85.

Albert, R.M., Weiner, S., 2001. Study of phytoliths in prehistoric ash layers using a quantitative approach. In: Meunier, J.D., Coline, F. (Eds.), Phytoliths: Applications in Earth Sciences and Human History. A.A. Balkema Publishers, Lisse.

Albert, R.M., Cabanes D., 2009. Fire in prehistory: an experimental approach to combustion processes and phytolith remains. Israel Journal of Earth Science 56:175-189.

Albert, R.M., Bamford, M., 2012. Vegetation during UMBI and deposition of Tuff IF at Olduvai Gorge, Tanzania (ca. 1.8 Ma) based on phytoliths and plant remains. Journal of Human Evolution 63, 342-350.

Albert, R.M., Marean, C.W., 2012. The exploitation of plant resources by early Homo sapiens: the phytolith record from pinnacle point 13B Cave, South Africa. Geoarchaeology 27 (4), 363-384.

Albert, R.M., Tsatskin, A., Ronen, A., Lavi, O., Estroff, L., Lev-Yadun, S., Weiner, S., 1999. Mode of occupation of Tabun Cave, Mt Carmel Israel during the Mousterian period: a study of the sediments and the phytoliths. Journal of Archaeological Science 26, 1249-1260.

Albert, R.M., Weiner, S., Bar-Yosef, O., Meignen, L., 2000. Phytoliths in the Middle Palaeolithic deposits of Kebara Cave, Mt Carmel, Israel: study of the plant materials used for fuel and other purposes. Journal of Archaeological Science 27, 931-947.

Albert, R.M., Bar-Yosef, O., Meignen, L., Weiner, S., 2003. Phytolith and mineralogical study of hearths from the Middle Palaeolithic levels of Hayonim Cave (Galilee, Israel). Journal of Archaeological Science 30, 461-480

Albert, R.M., Bamford, M.K., Cabanes, D., 2006. Taphonomy of phytoliths and macroplants in different soils from Olduvai Gorge (Tanzania) and the application to Plio-Pleistocene palaeoanthropological samples. Quaternary International 148, 78-94.

Albert, R.M., Shahack-Gross, R., Cabanes, D., Gilboa, A., Lev-Yadun, S., Portillo, M., Sharon, I., Boaretto, E., Weiner, S., 2008. Phytolith-rich layers from the Late Bronze and Iron Ages at Tel Dor (Israel): mode of formation and archaeological significance, Journal of Archaeological Science 35(1), 57-75.

Albert, R.M., Bamford, M.K., Cabanes, D., 2009. Palaeoecological significance of palms at Olduvai Gorge, Tanzania, based on phytolith remains. Quaternary International 193, 41-48.

Albert, R.M., Bamford, M.K., Esteban, I., 2015. Reconstruction of ancient palm vegetation landscapes using a phytolith approach. Quaternary International 369, 51-66.

Albert, R.M., Ruíz, J.A., Sans, A., 2016. PhytCore ODB: a new tool to improve efficiency in the management and exchange of information on phytoliths. Journal of Archaeological Science 68, 98-105.

Aleman, J. C., Saint-Jean, A., Leys, B., Carcaillet, C., Favier, C., Bremond, L. 2013. Estimating phytolith influx in lake sediments. Quaternary Research, 80(2), 341-347.

Aleman, J.C., Canal-Subitani, S., Favier, C., Bremond, L., 2014. Influence of the local environment on lacustrine sedimentary phytolith records. Palaeogeography, Palaeoclimatology, Palaeoecology 414, 273-283.

Alexandre, A., Meunier, J.-D., Le_zine, A.-M., Vincens, A., Schwartz, D., 1997. Phytoliths indicators of grasslands dynamics during the late Holocene in intertropical Africa. Palaeogeography, Palaeoclimatology, Palaeoecology 136, 213-219.

Ambrose, S.H., 1998. Late Pleistocene human population bottlenecks, volcanic winter, and differentiation of modern humans. Journal of Human Evolution, 34(6), 623-651.

Ashley, G., Barboni, D., Dominguez-Rodrigo, M., Bunn, H.T., Mabulla, A.Z.P., Diez-Martin, F., Barba, R., Baquedano, E., 2010a. A spring and wooded habitat at FLK Zinj and their relevance to origins of human behavior. Quaternary Research 74, 304-314.

Ashley, G., Barboni, D., Dominguez-Rodrigo, M., Bunn, H.T., Mabulla, A.Z.P., Diez-Martin, F., Barba, R., Baquedano, E., 2010b. Paleoenvironmental and paleoecological reconstruction of a freshwater oasis in savannah grassland at FLK North, Olduvai Gorge, Tanzania. Quaternary Research 74, 333-343.

Avery, D.M. 1982. Micromammals as palaeoenviromnental indicators and an interpretation of the late Quaternary in the southern Cape Province, South Africa. Annals of the South African Museum 85,183-374.

Backwell, L., d'Errico, F., Wadley, L. 2008. Middle Stone Age bone tools from the Howiesons Poort layers, Sibudu Cave, South Africa. Journal of Archaeological Science 35(6), 1566-1580.

Backwell, L. R., McCarthy, T. S., Wadley, L., Henderson, Z., Steininger, C. M., Barré, M., Lamothe, M., Chase, B.M., Woodborne, S., Susino, G.J., Bamford, M.K., Sievers, C., Brink, J.S., Rossouw, L., Pollarolo, L., Trower, G., Scott, L., d'Errico, F., 2014. Multiproxy record of late Quaternary climate change and Middle Stone Age human occupation at Wonderkrater, South Africa. Quaternary Science Reviews, 99, 42-59.

Ball, T.B., Brotherson, J.D., Gardner, J.S., 1993. A typologic and morphometric study of variation in phytoliths from einkorn wheat (Triticum monococcum). Canadian Journal of Botany 71(9), 1182-1192.

Ball, T., Gardner, J.S., Brotherson, J.D., 1996. Identifying Phytoliths Produced by the Inflorescence Bracts of Three Species of Wheat (*Triticum monococcum* L., *T. dicoccon* Schrank., and *T. aestivum* L.) Using Computer-Assisted Image and Statistical Analyses. Journal of Archaeological Science 23(4), 619-632.

Ball, T.B., Gardner, J.S., Anderson, N., 1999. Identifying inflorescence phytoliths from selected species of wheat (*Triticum monococcum*, *T. dicoccon*, *T. dicoccoides*, and *T. aestivum*) and barley (*Hordeum vulgare* and *H. spontaneum*)(Gramineae). American Journal of Botany 86(11), 1615-1623.

Ball, T., Vrydaghs, L., Van Den Hauwe, I., Manwaring, J., De Langhe, E. 2006. Differentiating banana phytoliths: wild and edible Musa acuminata and Musa balbisiana. Journal of archaeological science 33(9), 1228-1236.

Ball, T., Chandler-Ezell, K., Dickau, R., Duncan, N., Hart, T. C., Iriarte, J., Lentferg, C., Logani, A., Lu, H., Madella, M., Pearsall, D., Piperno, D., Rosen, A., Vrydaghs, L., Weisskopf, A., Zhang, J., 2016. Phytoliths as a tool for investigations of agricultural origins and dispersals around the world. Journal of Archaeological Science 68, 32-45.

Bamford, M.K., Albert, R.M., Cabanes, D., 2006. Assessment of the lowermost Bed II Plio-Pleistocene vegetation in the eastern palaeolake margin of Olduvai Gorge (Tanzania) and preliminary results from fossil macroplant and phytolith re- mains. Quaternary International 148, 95-112.

Bamford, M.K., Stanistreet, I.G., Stollhofen, H., Albert, R.M., 2008. Late Pliocene grassland from Olduvai Gorge, Tanzania. Palaeogeogry, Palaeoclimatology, Palaeoecology 257, 280-293.

Bar-Matthews, M., Marean, C.W., Jacobs, Z., Karkanas, P., Fisher, E.C., Herries, A.I.R., Brown, K., Williams, H.M., Bernatchez, J., Ayalon, A., Nilssen, P.J., 2010. A high resolution and continuous isotopic speleothem record of paleoclimate and paleoenvironment from 90 to 53 ka from Pinnacle point on the south coast of South Africa. Quaternary Science Review 29, 2131-2145.

Barboni, D., 2014. Vegetation of Northern Tanzania during the Plio-Pleistocene: A synthesis of the paleobotanical evidences from Laetoli, Olduvai, and Peninj hominin sites. Quaternary International 322-323, 264-276.

Barboni, D., Bremond, L., 2009. Phytoliths of East African grasses: an assessment of their environmental and taxonomic significance based on floristic data. Review of Palaeobotany and Palynology 158 (1e2), 29-41.

Barboni, D., Bonnefille, R., Alexandre, A., Meunier, J., 1999. Phytoliths as paleoenvironmental indicators, west side Middle Awash Valley, Ethiopia. Palaeogeography, Palaeoclimatology, Palaeoecology 152, 87-100.

Barboni, D., Bremond, L., Bonnefille, R., 2007. Comparative study of modern phytolith assemblages from inter-tropical Africa. Palaeogeography, Palaeoclimatology, Palaeoecology 246(2), 454-470.

Barboni, D., Ashley, G.M., Dominguez-Rodrigo, M., Bunn, H.T., Mabulla, A.Z.P., Baquedano, E., 2010. Phytoliths infer locally dense and heterogeneous paleo-vegetation at FLK North and surrounding localities during upper Bed I time, Olduvai Gorge, Tanzania. Quaternary Research 74, 344-354.

Barham, L. 2002. Systematic Pigment Use in the Middle Pleistocene of South□Central Africa1. Current anthropology, 43(1), 181-190.

Barham, L.S., Smart, P.L., 1996. Current events: An early date for the Middle Stone Age of central Zambia. Journal of Human Evolution 30(3), 287-290.

Basell, L.S. 2008. Middle Stone Age (MSA) site distributions in eastern Africa and their relationship to Quaternary environmental change, refugia and the evolution of Homo sapiens. Quaternary Science Reviews 27(27), 2484-2498.

Beaumont, P.B., 1978. Border Cave University of Cape Town. Unpublished M.A. thesis.

Beaumont, P.B, 1980. On the age of Border Cave hominids 1–5. Palaeontol. Afr. 23, 21-33.

Beck, R. B. 2015. Hazel Crampton, Jeff Peires and Carl Vernon, eds. Into the Hitherto Unknown: Ensign Beutler's Expedition to the Eastern Cape, 1752. Cape Town, South Africa: Van Riebeeck Society, 2013. 209 pp. ISBN: 9780981426440. Itinerario 39(01), 183-185.

Benvenuto, M.L., Honaine, M.F., Osterrieth, M.L., Morel, E., 2015. Differentiation of globular phytoliths in Arecaceae and other monocotyledons: morphological description for paleobotanical application. Turkish Journal of Botany 39(2), 341.

Bergh, N.G., Verboom, G.A., Rouget, M., Cowling, R.M., 2014. Vegetation types of the greater cape floristic region. In: Allsopp, N., Colville, J.F., Verboom, T. (Eds.), Fynbos: Ecology, Evolution, and Conservation of a Megadiverse Region. Oxford University Press, Oxford, pp. 1-25.

Berlin, A.M., Ball, T., Thompson, R., Herbert, S.C., 2003. Ptolemaic agriculture, ''Syrian wheat'', and *Triticum aestivum*. Journal of Archaeological Science 30, 115-121.

Berna, F., Behar, A., Shahack-Gross, R., Berg, J., Boaretto, E., Gilboa, A., Sharon, I., Shalev, S., Shilshtein, S., Yahalom-Mack, N., Zorn, J.R., Weiner, S., 2007. Sediments exposed to high temperatures: reconstructing pyrotechnological processes in Late Bronze and Iron Age Strata at Tel Dor (Israel). Journal of Archaeological Science 34(3), 358-373.

Bernatchez, J., Marean, C.W., 2011. Total station archaeology and the use of digital photography. SAA Archaeological Record, 11(3), 16-21.

Blinnikov, M.S., 2005. Phytoliths in plants and soils of the interior Pacific Northwest, USA. Review of Palaeobotany and Palynology 135(1), 71-98.

Blinnikov, M., Busacca, A., Whitlock, C., 2002. Reconstruction of the late Pleistocene grassland of the Columbia basin, Washington, USA, based on phytolith records in loess. Palaeogeography, Palaeoclimatology, Palaeoecology 177(1), 77-101.

Born, J., Linder, H. P., Desmet, P., 2007. The greater cape floristic region. Journal of Biogeography 34(1), 147-162.

Bozarth, S.R., 1992. Classification of opal phytoliths formed in selected dicotyledons native to the Great Plains. In: Rapp Jr., G., Mulholland, C.S. (Eds.), Phytolith Systematics. Emerging Issues, Advances in Archaeological and Museum Science. Plenum Press, New York.

Bozarth, S., 1993. Maize (*Zea mays*) cob phytoliths from a central Kansas Great Bend Aspect archaeological site. The Plains Anthropologist 279-286.

Bräuer, G., Singer, R., 1996. The Klasies zygomatic bone: archaic or modern?. Journal of Human Evolution 30(2), 161-165.

Braun, K., Bar-Matthews, M., Zahn, Z., Matthews, A., Ayalona, A., Cowling, R.M., Karkanas, P., Fisher E., Zilbermana T., Dyez, K., Marean, C.W., (submitted). A record of climate and environment between 463 and 41 ka from speleothem stable isotopic compositions at Pinnacle Point on the South African south coast. Quaternary Science Review.

Bremond, L., Alexandre, A., Véla, E., Guiot, J., 2004. Advantages and disadvantages of phytolith analysis for the reconstruction of Mediterranean vegetation: an assessment based on modern phytolith, pollen and botanical data (Luberon, France). Review of Palaeobotany and Palynology 129(4), 213-228.

Bremond, L., Alexandre, A., Hely, C., Peyron, O., Guiot, J., 2005a. Grass water stress estimated from phytoliths in West Africa. Journal of Biogeography 32 (2), 311-327.

Bremond, L., Alexandre, A., Hely, C., Guiot, J., 2005b. A phytolith index as a proxy of tree cover density in tropical areas: calibration with leaf area index along a forestesavanna transect in southeastern Cameroon. Global and Planetary Change 45 (4), 277-293.

Bremond, L., Alexandre, A., Wooller, M.J., Hely, C., Williamson, D., Scheafer, P.A., Majule, A., Guiot, J., 2008. Phytolith indices as proxies of grass subfamilies on East African tropical mountains. Global and Planetary Change 61 (3), 209-224.

Brown, D.A., 1984. Prospects and limits of a phytolith key for grasses in the Central United States. Journal of Archaeological Science 11, 345–368.

Brown, K.S., Marean, C.W., Herries, A.I., Jacobs, Z., Tribolo, C., Braun, D., Roberts, D.L., Meyer, M.C., Bernatchez, J., 2009. Fire as an engineering tool of early modern humans. Science 325, 859-862.

Brown, K.S., Marean, C.W., Jacobs, Z., Schoville, B.J., Oestmo, S., Fisher, E.C., Bernatchez, J., Karkanas, P., Matthews, T., 2012. An early and enduring advanced technology originating 71000 years ago in South Africa. Nature 491, 590-593.

Cabanes, D., Shahack-Gross, R., 2015. Understanding Fossil phytolith preservation: the role of partial dissolution in paleoecology and archaeology. PLoS One 10(5), e0125532.

Cabanes, D., Allué, E., Vallverdú, J., Cáceres, I., Vaquero, M., Pastó, I., 2007. Hearth structure and function at level J (50 kyr, BP) from Abric Romaní (Capellades, Spain): phytoliths, charcoal, bones and stone-tools. In: Madella M, Zurro D (eds) Plant, people and places—recent studies in phytolith analysis. Oxbow Books, Oxford, pp. 98–106

Cabanes, D., Mallol, C., Expósito, I., Baena, J., 2010. Phytolith evidence for hearths and beds in the late Mousterian occupations of Esquilleu cave (Cantabria, Spain). Journal of Archaeological Science 37(11), 2947-2957.

Cabanes, D., Weiner, S., Shahack-Gross, R., 2011. Stability of phytoliths in the archaeological record: a dissolution study of modern and fossil phytoliths.Journal of Archaeological Science 38(9), 2480-2490.

Cabanes, D., Gadot, Y., Cabanes, M., Finkelstein, I., Weiner, S., Shahack-Gross, R., 2012. Human impact around settlement sites: a phytolith and mineralogical study for assessing site boundaries, phytolith preservation, and implications for spatial reconstructions using plant remains. Journal of Archaeological Science 39(8), 2697-2705.

Caley, T., Kim, J.-H., Malaize, B., Giraudeau, J., Laepple, T., Caillon, N., et al. 2011. High-latitude obliquity forcing drives the Agulhas leakage. Climates of the Past, 7, 2193–2215.

Campbell, M.C., Tishkoff, S.A. 2008. African genetic diversity: implications for human demographic history, modern human origins, and complex disease mapping. Annual review of genomics and human genetics 9, 403.

Campbell, B.M., Cowling, R.M., Bond, W., Kruger, F.J., 1981. Structural characterization of vegetation in the Fynbos Biome. South African National Scienttfk Programmes Report 52.

Carnelli, A. L., Theurillat, J. P., Madella, M., 2004. Phytolith types and type-frequencies in subalpine–alpine plant species of the European Alps. Review of Palaeobotany and Palynology 129(1), 39-65.

Carter, P.L., Mitchell, P.J., Vinnicombe, P., 1988. Sehonghong: the Middle and Later Stone Age industrial sequence at a Lesotho rock-shelter. Oxford: British Archaeological Reports International Series 406,1-258.

Cawthra, H.C., Compton, J.S., Fisher, E.C., MacHutchon, M.R., Marean, C.W., 2016. Submerged shorelines and landscape features offshore of Mossel Bay, South Africa. Geological Society, London, Special Publications 411(1), 219-233.

Charrié-Duhaut, A., Porraz, G., Cartwright, C.R., Igreja, M., Connan, J., Poggenpoel, C., Texier, P.J., 2013. First molecular identification of a hafting adhesive in the late Howiesons Poort at Diepkloof Rock Shelter (Western Cape, South Africa). Journal of Archaeological Science 40(9), 3506-3518.

Chase, B.M., 2010. South African palaeoenvironments during marine oxygen isotope stage 4: a context for the Howiesons Poort and Still Bay industries. Journal of Archaeological Science 37(6), 1359-1366.

Chase, B.M., Meadows, M.E., 2007. Late Quaternary dynamics of southern Africa's winter rainfall zone. Earth-Science Reviews 84(3), 103-138.

Clark, J.D., Beyene, Y., WoldeGabriel, G., Hart, W.K., Renne, P.R., Gilbert, H., Defleur, A., Suwa, G., Katoh, S., Ludwig, K.R., Boisserie, J.R., Asfaw, B., White, T.D.,

2003. Stratigraphic, chronological and behavioural contexts of Pleistocene Homo sapiens from Middle Awash, Ethiopia. Nature 423, 747-752.

Collura, L. V., Neumann, K., (in press). Wood and bark phytoliths of West African woody plants. Quaternary International.

Colville, J.F., Potts, A.J., Bradshaw, P.L., Measey, G.J., Snijman, D., Picker, M.D., Proches, S., Bowie, R.C.K., Manning, J.C., 2014. Floristic and faunal Cape biochoria: do they exist?. In: Allsopp, N., Colville, J.F., Verboom, G.A., (Eds.), Fynbos: Ecology, Evolution, and Conservation of a Megadiverse Region. Oxford University Press United Kingdom, pp. 73-92.

Compton, J.S., 2011. Pleistocene sea-level fluctuations and human evolution on the southern coastal plain of South Africa. Quaternary Science Reviews 30(5), 506-527.

Cook, S.F., 1964. The nature of charcoal excavated at archaeological sites. Am. Antiquity 29(4), 514-517.

Copeland, S.R., Cawthra, H.C., Fisher, E.C., Lee-Thorp, J.A., Cowling, R.M., le Roux, P.J., Hodgkins, J., Marean, C.W., 2016. Strontium isotope investigation of ungulate movement patterns on the Pleistocene Paleo-Agulhas Plain of the Greater Cape Floristic Region, South Africa. Quaternary Science Reviews 141, 65-84.

Cordova, C.E., Scott, L., 2010. The Potential of Poaceae, Cyperaceae, and Restionaceae Phytoliths to Reflect Past Environmental Conditions in South Africa. Palaeoecology of Africa. CRC Press Taylor and Francis Group, Boca Raton, Florida, pp. 107-133.

Cordova, C.E., 2013. C3 Poaceae and Restionaceae phytoliths as potential proxies for reconstructing winter rainfall in South Africa. Quaternary International 287, 121-140.

Cowling, R.M., 1983. The occurrence of C3 and C4 grasses in fynbos and allied shrublands in the South Eastern Cape, South Africa. Oecologia 58(1), 121-127.

Cowling, R.M., 1990. Diversity components in a species- rich area of the Cape Floristic Region. Journal of Vegetation Science 1, 699-710.

Cowling, R.M., Rundel, P.W., Lamont, B.B., Kalin Arroyo, M., Arianoutsou, M., 1996. Plant diversity in mediterranean-climate regions. Trends in Ecology and Evolution 11, 362-366.

Cowling, R.M., Cartwright, C.R., Parkington, J.E., Allsopp, J.C., 1999. Fossil wood charcoal assemblages from Elands Bay Cave, South Africa: implications for Late Quaternary vegetation and climates in the winter-rainfall fynbos biome. Journal of Biogeography 26(2), 367-378.

Cowling, R.M., Ojeda, F., Lamont, B. B., Rundel, P.W., Lechmere-Oertel, R., 2005. Rainfall reliability, a neglected factor in explaining convergence and divergence of plant traits in fire-prone Mediterranean-climate ecosystems. Global Ecology and Biogeography 14(6), 509-519.

d'Errico, F., Henshilwood, C.S., 2007. Additional evidence for bone technology in the southern African Middle Stone Age. Journal of Human Evolution 52, 142-163.

d'Errico, F., Stringer, C.B., 2011. Evolution, revolution or saltation scenario for the emergence of modern cultures?. Philosophical Transactions of the Royal Society of London B: Biological Sciences 366(1567), 1060-1069.

d'Errico, F., Henshilwood, C., Nilssen, P., 2001. An engraved bone fragment from c. 70,000-year-old Middle Stone Age levels at Blombos Cave, South Africa: implications for the origin of symbolism and language. Antiquity 75(288), 309-318.

d'Errico, F., Henshilwood, C.S., Vanhaeren, M., van Niekerk, K., 2005. Nassarius kraussianus shell beads from Blombos Cave: evidence for symbolic behaviour in the Middle Stone Age. Journal of Human Evolution 48, 3-24.

d'Errico, F., Backwell, L., Villa, P., Degano, I., Lucejko, J. J., Bamford, M. K., Thomas F. G. Highamh, Colombinig, M.P., Beaumont, P.B., 2012. Early evidence of San material culture represented by organic artifacts from Border Cave, South Africa. Proceedings of the National Academy of Sciences 109(33), 13214-13219.

Day, M.H, 1969. Omo human skeletal remains. Nature 222, 1135-1138.

De Villiers, H., 1973. Human skeletal remains from Border Cave, Ingwavuma District, KwaZulu, South Africa.

De Vynck, J.C., Van Wyk, B.E., Cowling, R.M., 2015. Indigenous edible plant use by contemporary Khoe-San descendants of South Africa's Cape South Coast. South African Journal of Botany 102, 60-69.

De Vynck, J.C., Van Wyk, B.E., Cowling, R.M., 2016. Indigenous edible plant use by contemporary Khoe-San descendants of South Africa's Cape South Coast. South African Journal of Botany 102, 60-69.

Deacon, H.J., 1976. Where hunters gathered: a study of Holocene Stone Age people in the eastern Cape (No. 1). South African Archaeological Society.

Deacon, H.J., 1983. Another look at the Pleistocene climates of South Africa. South African Journal of Science 79, 325-328.

Deacon, H.J., 1989. Late Pleistocene palaeoecology and archaeology in the southern Cape, South Africa. In P. Mellars and C. Stringer, (Eds.), The human revolution. Princeton University Press, Princeton, pp. 547–64.

Deacon, H.J., 1993. Planting an idea: an archaeology of Stone Age gatherers in South Africa. The South African Archaeological Bulletin, 86-93.

Deacon, H.J., 1995. Two late Pleistocene-Holocene archaeological depositories from the southern Cape, South Africa. The South African Archaeological Bulletin, 121-131.

Deacon, H.J., Jury, M.R., Ellis, F., 1992. Selective regime and time. In: Cowling, R.M. (Ed.), The Ecology of Fynbos: Nutrients, Fire and Diversity. Oxford University Press, Cape Town, South Africa, pp. 6-22.

Deacon, J., 1984. Later Stone Age people and their descendants in southern Africa. In R.G. Klein, ed. Southern African prehistory and paleoenvironments, pp. 221-328. Balkema, Rotterdam.

Deacon, J., Lancaster, N., 1988. Late Quaternary palaeoenvironments of southern Africa. Clarendon press.

Deino, A. L., McBrearty, S., 2002. 40 Ar/39 Ar dating of the Kapthurin Formation, Baringo, Kenya. Journal of Human Evolution 42(1), 185-210.

Delhon, C., Alexandre, A., Berger, J.F., Thiébault, S., Brochier, L., J.L., Meunier, J.D. 2003. Phytolith assemblages as a promising tool for reconstructing Mediterranean Holocene vegetation. Quaternary Research 59(1), 48-60.

Derry, L.A., Kurtz, A.C., Ziegler, K., Chadwick, O.A., 2005. Biological control of terrestrial silica cycling and export fluxes to watersheds. Nature 433, 728-731.

Devos, Y., Nicosia, C., Vrydaghs, L., Speleers, L., van der Valk, J., Marinova, E., Britt Claesc, Albert, R.M., Esteban, I., Ball, T.B., Court-Piconb, M., Court-Picon, M, in press. An integrated study of Dark Earth from the alluvial valley of the Senne river (Brussels, Belgium). Quaternary International.

Dibble, H.L., Marean, C.W., McPherron, S.P., 2007. The use of barcodes in excavation projects: examples from Mossel Bay (South Africa) and Roc de Marsal (France). The SAA Archaeological Record 7(1), 33-38.

Diester-Haass, L., Schrader, H.J., Thiede, J., 1973. Sedimentological and Paleoclimatological investigations of two Pelagic Ooze cores off cape Barbas, North-West Africa. Meteor Forsh-Ergebnisse C 16, 19-66.

Dusseldorp, G.L., 2010. Prey choice during the South African Middle Stone Age: avoiding dangerous prey or maximising returns?. African Archaeological Review 27(2), 107-133.

Dwyer, P. D., Minnegal, M., 1990. Yams and megapode mounds in the lowland rain forest of Papua New Guinea. Human Ecology 18(2), 177-185.

Engelbrecht, C.J., Landman, W.A., Engelbrecht, F.A., Malherbe, J., 2014. A synoptic decomposition of rainfall over the Cape south coast of South Africa. Climate Dynamics 44 (9-10), 2589-2607.

EPICA Community Members, 2006. One-to-one coupling of glacial climate variability in Greenland and Antarctica. Nature 444, 195–8.

Esteban, I., De Vynck, J.C., Singels, E., Vlok, J., Marean, C.W., Cowling, R.M., Fisher, E., Cabanes, D., Albert, R.M., in press-a. Modern soil phytolith assemblages used as proxies for Paleoscape reconstruction on the south coast of South Africa. Quaternary International.

Esteban, I., Albert, R. M., Eixea, A., Zilhão, J., Villaverde, V., in press-b. Neanderthal use of plants and past vegetation reconstruction at the Middle Paleolithic site of Abrigo

de la Quebrada (Chelva, Valencia, Spain). Archaeological and Anthropological Sciences.

Fagundes, N.J.R., Ray, N., Beaumont, M., Neuenschwander, S., Salzano, F.M., Bonatto, S.L., Excoffier, L., 2007. Statistical evaluation of alternative models of human evolution. Proceedings of the National Academy of Sciences 104, 17614.

Fahmy, A.G., 2008. Diversity of lobate phytoliths in grass leaves from the Sahel region, west tropical Africa: tribe Paniceae. Plant Systematics and Evolution 270, 1-23.

Faith, J.T., 2008. Eland, buffalo, and wild pigs: were Middle Stone Age humans ineffective hunters?. Journal of Human Evolution 55(1), 24-36.

Farmer, V.C., 2005. Forest vegetation does recycle substantial amounts of silicon from and back to the soil solution with phytoliths as an intermediate phase, contrary to recent reports. European journal of soil science 56(2), 271-272.

Feathers, J.K., Bush, D.A., 2000. Luminescence dating of middle stone age deposits at Die Kelders. Journal of Human Evolution 38(1), 91-119.

Fisher, E.C., Bar-Matthews, M., Jerardino, A., Marean, C.W., 2010. Middle and Late Pleistocene paleoscape modeling along the southern coast of South Africa. Quaternary Science Reviews 29(11), 1382-1398.

Fisher, E.C., Albert, R.M., Botha, G., Cawthra, H.C., Esteban, I., Harris, J., Jacobs, Z., Jerardino, A., Marean, C.W., Neumann, F.H., Pargeter, J., Poupart, M., Venter, J., 2013. Archaeological reconnaissance for Middle Stone Age sites along the Pondoland coast, South Africa. PaleoAnthropology 104-137.

Fishkis, O., Ingwersen, J., Streck, T., 2009. Phytolith transport in sandy sediment: experiments and modeling. Geoderma 151(3), 168-178.

Fiskish, O., Ingwersena, J., Lamers, M., Denysenko, D., Streck, T., 2010. Phytolith transport in soil: a laboratory study on intact soil cores. European Journal of Soil Science 61, 445-455.

Fox, F.W., Norwood Young, M.E., 1983. Food from the veld. Edible wild plants of southern Africa. Johannesburg, Delta Books.

Franceschini, G., Compton, J.S., 2006. Holocene evolution of the sixteen mile beach complex, Western Cape, South Africa. Journal of Coastal Research 1158-1166.

Fraysse, F., Cantais, F., Pokrovsky, O.S., Schott, J., Meunier, J.D., 2006. Aqueous reactivity of phytoliths and plant litter: physico-chemical constraints on terrestrial biogeochemical cycle of silicon. Journal of Geochemical Exploration 88(1), 202-205.

Fredlund, G.G., Tieszen, L.T., 1994. Modern phytolith assemblages from the North American Great Plains. Journal of Biogeography 21, 321-335.

Gallego, L., Distel, R.A., 2004. Phytolith assemblages in grasses native to Central Argentina. Annals of Botany 94(6), 865-874.

Gallego, L., Distel, R.A., Camina, R., Rodríguez Iglesias, R.M., 2004. Soil phytoliths as evidence for species replacement in grazed rangelands of central Argentina. Ecography 27(6), 725-732.

García-Granero, J.J., Lancelotti, C., Madella, M., Ajithprasad, P., 2016. Millets and Herders: The Origins of Plant Cultivation in Semiarid North Gujarat (India). Current Anthropology 257:2, 149-173.

Geis, J.W., 1973. Biogenic silica in selected species of deciduous angiosperms. Soil science 116(2), 113-130.

Goldberg, P., Miller, C. E., Schiegl, S., Ligouis, B., Berna, F., Conard, N. J., Wadley, L. 2009. Bedding, hearths, and site maintenance in the Middle Stone age of Sibudu cave, KwaZulu-Natal, South Africa. Archaeological and Anthropological Sciences 1(2), 95-122.

Goldblatt, P., Manning, J.C., 2002. Plant diversity of the Cape region of southern Africa. Annals of the Missouri Botanical Garden, 281-302.

Gonder, M.K., Mortensen, H.M., Reed, F.A., de Sousa, A., Tishkoff, S.A., 2007. Whole- mtDNA Genome Sequence analysis of ancient African lineages. Molecular Biology and Evolution 24, 757-768.

Gould, R.A., 1980. Living archaeology. CUP Archive.

Grass Phylogeny Working Group II 2012 New grass phylogeny resolves deep evolutionary relationships and discovers C4 origins. New Phytol 193(2):304–312.

Gregg, M.L., Grybush, R.J., 1976. Thermally altered siliceous stone from prehistoric contexts: intentional versus unintentional alteration. American Antiquity, 189-192.

Grine, F.E., 2000. Middle Stone Age human fossils from Die Kelders Cave 1, Western Cape Province, South Africa. Journal of human evolution 38(1), 129-145.

Grine, F.E., Klein, R. G., Volman, T.P., 1991. Dating, archaeology and human fossils from the Middle Stone Age levels of Die Kelders, South Africa.Journal of Human Evolution 21(5), 363-395.

Harpending, H., Rogers, A., 2000. Genetic perspectives on human origins and differentiation. Annual review of genomics and human genetics 1(1), 361-385.

Harpending, H.C., Sherry, S.T., Rogers, A.R., Stoneking, M., 1993. The genetic structure of ancient human populations. Current Anthropology 34(4), 483-496.

Hart, D.M., Humphreys, G.S., 2003. Phytolith depth functions in surface regolith materials. In: Roach, I.C. (Ed.), Advances in regolith: Proceedings of the CRC LEME Regional Regolith Symposia. Adelaide, Canberra, and Perth, pp. 159-163.

Hart, J.P., Thompson, R.G., Brumbach, H.J., 2003. Phytolith evidence for early maize (Zea mays) in the northern Finger Lakes region of New York.American Antiquity, 619-640.

Heizer, R.F., 1963. Domestic fuel in primitive society. Journal of the Royal Anthropological Institute of Great Britain and Ireland 93, 186-194.

Henn, B. M., Gignoux, C. R., Jobin, M., Granka, J. M., Macpherson, J. M., Kidd, J. M., Rodríguez-Botigué, L., Ramachandran, S., Hon, L., Brisbin, A., Lin, A.A., Underhill, P.A., Comas, D., Kidd, K.K., Norman, P.J., Parham, P., Bustamante, C.D., Mountain, J.L., Lin, A.A., 2011. Hunter-gatherer genomic diversity suggests a southern African origin for modern humans. Proceedings of the National Academy of Sciences 108(13), 5154-5162.

Henry, D.O., Hietala, H.J., Rosen, A.M., Demidenko, Y.E., Usik, V. I., Armagan, T. L. 2004. Human behavioral organization in the Middle Paleolithic: were Neanderthals different?. American Anthropologist 106(1), 17-31.

Henshilwood, C.S., 2012. Late Pleistocene techno-traditions in southern Africa: A review of the Still Bay and Howiesons Poort, c. 75–59 ka. Journal of World Prehistory 25(3-4), 205-237.

Henshilwood, C.S., Marean, C.W., 2003. The origin of modern human behavior. Current anthropology 44(5), 627-651.

Henshilwood, C.S., d'Errico, F., 2011. Middle Stone Age engravings and their significance to the debate on the emergence of symbolic material culture.Homo symbolicus: The dawn of language, imagination and spirituality, 75-96.

Henshilwood, C.S., Dubreuil, B., 2011. The Still Bay and Howiesons Poort, 77–59 ka. Current Anthropology 52(3), 361-400.

Henshilwood, C.S., Sealy, J.C., Yates, R., Cruz-Uribe, K., Goldberg, P., Grine, F.E., Klein, R.G., Poggenpoel, C., van Niekerk, K., Watts, I., 2001a. Blombos Cave, southern Cape, South Africa: preliminary report on the 1992–1999 excavations of the Middle Stone Age levels. Journal of Archaeological Science 28(4), 421-448.

Henshilwood, C.S., d'Errico, F., Marean, C.W., Milo, R.G., Yates, R.J., 2001b. An early bone tool industry from the Middle Stone Age, Blombos Cave, South Africa: implications for the origins of modern human behaviour, symbolism and lan- guage. Journal of Human Evolution 41, 631-678.

Henshilwood, C.S., d'Errico, F., Yates, R., Jacobs, Z., Tribolo, C., Duller, G.A.T., Mercier, N., Sealy, J.C., Valladas, H., Watts, I., Wintle, A.G., 2002. Emergence of modern human behavior: Middle Stone Age engravings from South Africa. Science 295, 1278-1280.

Henshilwood, C., d'Errico, F., Vanhaeren, M., van Niekerk, K., Jacobs, Z., 2004. Middle Stone Age shell beads from South Africa. Science 304, 404.

Henshilwood, C.S., d'Errico, F., Watts, I., 2009. Engraved ochres from the middle stone age levels at Blombos Cave, South Africa. Journal of human evolution 57(1), 27-47.

Henshilwood, C.S., d'Errico, F., Van Niekerk, K.L., Coquinot, Y., Jacobs, Z., Lauritzen, S.E., Menu M., García-Moreno, R., 2011. A 100,000-year-old ochre-processing workshop at Blombos Cave, South Africa. Science 334(6053), 219-222.

Herries, A.I., 2011. A chronological perspective on the Acheulian and its transition to the Middle Stone Age in southern Africa: the question of the Fauresmith. International Journal of Evolutionary Biology, 2011.

Hladik, C.M., Linares, O.F., Hladik, A., Pagezy, H., Semple, A., 1993. Tropical forests, people and food: an overview. In : Hladik, C.M., Hladik, A., Linares, O.F., PAGEZY, H, Semple, A. et Hadley, M., (Eds). Tropical Forests, People and Food: Biocultural interactions and applications to development. UNESCO-Parthenon, Paris, pp. 3-14.

Humphreys, G.S., Shakesby, R.A., Doerr, S.H., Blake, W.H., Wallbrink, P., Hart, D.M., 2003. Some effects of fire on the regolith. In Advances in regolith. CRC LEME Symposium, pp. 216-220.

Iriarte, J., 2003. Assessing the feasibility of identifying maize through the analysis of cross-shaped size and three-dimensional morphology of phytoliths in the grasslands of southeastern South America. Journal of Archaeological Science 30(9), 1085-1094.

Iriarte, J., Paz, E.A., 2009. Phytolith analysis of selected native plants and modern soils from southeastern Uruguay and its implications for paleoenvironmental and archeological reconstruction. Quaternary International 193(1), 99-123.

Jacobs, Z., 2010. An OSL chronology for the sedimentary deposits from Pinnacle Point Cave 13B—a punctuated presence. Journal of Human Evolution 59(3), 289-305.

Jacobs, Z., Roberts, R.G., Lachlan, T.J., Karkanas, P., Marean, C.W., Roberts, D.L. 2011. Development of the SAR TT-OSL procedure for dating Middle Pleistocene dune and shallow marine deposits along the southern Cape coast of South Africa. Quaternary Geochronology 6(5), 491-513.

Jerardino, A. 2016. Shell density as proxy for reconstructing prehistoric aquatic resource exploitation, perspectives from southern Africa. Journal of Archaeological Science: Reports 6, 637-644.

Jerardino, A., Marean, C.W., 2010. Shellfish gathering, marine palaeoecology and modern human behavior: perspectives from Cave PP13B, Pinnacle point, South Africa. Journal of Human Evolution 59, 412-429.

Johnson, C.R., McBrearty, S., 2010. 500,000 year old blades from the Kapthurin Formation, Kenya. Journal of Human Evolution 58(2), 193-200.

Johnson, T.C., Brown, E.T., McManus, J., Barry, S., Barker, P., Gasse, F., 2002. A high-resolution paleoclimate record spanning the past 25,000 years in southern East Africa. Science 296(5565), 113-132.

Jones, L.H.P., Handreck, K.A., 1965. The relation between the silica content of the diet and the excretion of silica by sheep. The Journal of Agricultural Science 65(01), 129-134.

Karkanas, P., 2010. Preservation of anthropogenic materials under different geochemical processes: A mineralogical approach. Quaternary International 214(1), 63-69.

Karkanas, P., Goldberg, P., 2010. Site formation processes at Pinnacle point Cave 13B (Mossel Bay, Western Cape Province, South Africa): resolving stratigraphic and depositional complexities with micromorphology. Journal of Human Evolution 59(3), 256-273.

Karkanas, P., Bar-Yosef, O., Goldberg, P., Weiner, S., 2000. Diagenesis in prehistoric caves: the use of minerals that form in situ to assess the completeness of the archaeological record. Journal of Archaeological Science 27(10), 915-929.

Karkanas, P., Rigaud, J. P., Simek, J. F., Albert, R. M., Weiner, S. 2002. Ash bones and guano: a study of the minerals and phytoliths in the sediments of Grotte XVI, Dordogne, France. Journal of Archaeological Science 29(7), 721-732.

Karkanas, P., Brown, K.S., Fisher, E.C., Jacobs, Z., Marean, C.W., 2015. Interpreting human behavior from depositional rates and combustion features through the study of sedimentary microfacies at site Pinnacle Point 5-6, South Africa. Journal of Human Evolution 85, 1-21.

Katz, O., Cabanes, D., Weiner, S., Maeir, A., Boaretto, E., Shahack-Gross, R., 2010. Rapid phytolith extraction for analysis of phytolith concentrations and assemblages during an excavation: an application at Tell es-Safi/Gath, Israel. Journal of Archaeological Science 37 (7), 1557-1563.

Kelly, E.F., Amundson, R.G., Marino, B.D., Deniro, M.J., 1991a. Stable isotope ratios of carbon in phytoliths as a quantitative method of monitoring vegetation and climate change. Quaternary Research 35(2), 222-233.

Kelly, E.F., Amundson, R.G., Marino, B.D., DeNiro, M.J., 1991b. Stable carbon isotopic composition of carbonate in Holocene grassland soils. Soil Science Society of America Journal, 55(6), 1651-1658.

Kelly, R.L., 1995. The Foraging Spectrum: Diversity in Hunter-Gatherer Lifeways. Washington: The Smithsonian Institution Press.

Kemper, J., Cowling, R.M., Richardson, D.M., Forsyth, G.G., McKelly, D.H., 2000. Landscape fragmentation in South Coast Renosterveld, South Africa, in relation to rainfall and topography. Austral Ecology 25 (2), 179e186.

Kerns, B.K., Moore, M. M., Hart, S.C., 2001. Estimating forest-grassland dynamics using soil phytolith assemblages and d13C of soil organic matter. Ecoscience 8(4), 478-488.

Klein, R.L., Geiss, K.W., 1978. Biogenic silica in the pinaceae. Soil Science 126, 145-156.

Klein, R.G., Cruz-Uribe, K., 2000. Middle and later stone age large mammal and tortoise remains from Die Kelders Cave 1, Western Cape Province, South Africa. Journal of Human Evolution 38(1), 169-195.

Kondo, R., 1977. Opal phytoliths, inorganic, biogenic particles in plants and soils. Japan Agricultural Research Quarterly 11, 198-203.

Kondo, R., Pearson, T., 1981. Opal phytoliths in tree leaves (part 2): opal phytoliths in dicotyledonous angiosperm trees. Research Bulletin of Obihiro University 12, 217-230 (in Japanese).

Kondo, R., Childs, C., Atkinson, I., 1994. Opal phytoliths of New Zealand. Canterbury: Manaaki Whenua Press.

Kuman, K., Inbar, M., Clarke, R.J., 1999. Palaeoenvironments and cultural sequence of the Florisbad Middle Stone Age hominid site, South Africa. Journal of Archaeological Science 26, 1409-1426.

Lancelotti, C., 2010. Fuelling Harappan Hearths: HumaneEnvironment Interactions as Revealed by Fuel Exploitation and Use. Unpublished PhD Dissertation, Department of Archaeology, University of Cambridge, Cambridge.

Lee, R.B., 1979. The !Kung San: Men, Women, and Work in a Foraging Society. Cambridge: Cambridge University Press.

Lee, R. B., DeVore, I., 1968. Man the hunter. Aldine Publishing Company, Chicago.

Li, X., Dodson, J., Zhou, X., Zhang, H., Masutomoto, R., 2007. Early cultivated wheat and broadening of agriculture in Neolithic China. The Holocene 17(5), 555-560.

Liengme, C.A., 1983. A survey of ethnobotanical research in southern Africa. Bothalia14, 621–629.

Linder, H.P., Ellis, R.P., 1990. A revision of Pentaschistis (Arundineae: poaceae). Contributions from the Bolus Herbarium 12, 1-124.

Linder, H.P., Vlok, J.H., 1991. The morphology, taxonomy and evolution of Rhodocoma (Restionaceae). Plant Systematics and Evolution 175, 139-160.

Linder, H.P., Caddick, L.R., 2001. Restionaceae seedlings: morphology, anatomy and systematic implications. Feddes Repertorium 112(-2), 59-80.

Linton, S. 1971. Woman the Gatherer: Male Bias in Anthropology. In: Jacob, S.E. (Ed), Women in Cross- Cultural Perspective: A Preliminary Sourcebook. University of Illinois Press: Champaign, IL.

Lippmann, F., 1973. Sedimentary carbonate minerals. New York: Springer-Verlag.

Lombard, M., Phillipson, L. 2010. Indications of bow and stone-tipped arrow use 64,000 years ago in KwaZulu-Natal, South Africa. Antiquity 84, 635–648.

Lombard, M., Pargeter, J., 2008. Hunting with Howiesons Poort segments: Pilot experimental study and the functional interpretation of archaeological tools. Journal of Archaeological Science 35, 26–41.

Low, A.B., Rebelo, A.G., 1998. Vegetation of South Africa, Lesotho and Swaziland. Department of Environmental Affairs and Tourism, Pretoria, South Africa.

Lu, H., Zhang, J., Liu, K. B., Wu, N., Li, Y., Zhou, K., Yed, M., Zhang, T., Zhang, H., Yang, X., Shen, L., Xu, D., Li, Q., 2009. Earliest domestication of common millet (Panicum miliaceum) in East Asia extended to 10,000 years ago. Proceedings of the National Academy of Sciences 106(18), 7367-7372.

Mackay, A., Stewart, B.A., Chase, B.M., 2014 Coalescence and fragmentation in the late Pleistocene archaeology of southernmost Africa. Journal of Human Evolution 72, 26–51.

Madella, M., 2003. Investigating agriculture and environment in South Asia: present and future contributions from opal phytoliths. 2003) Indus Ethnobiology: New Perspectives from the Field. Lanham: Lexington Books, 199-249.

Madella, M., Lancelotti, C., 2012. Taphonomy and phytoliths: a user manual.Quaternary International 275, 76-83.

Madella, M., Jones, M.K., Goldberg, P., Goren, Y., Hovers, E., 2002. The exploitation of plant resources by Neander- thals in Amud Cave (Israel): the evidence from phytolith studies. Journal of Archaeological Science 29, 703-719.

Madella, M., Alexandre, A., Ball, T., 2005. International code for phytolith nomen-clature 1.0. Annals of Botany 96, 253-260.

Madella, M., García-Granero, J. J., Out, W. A., Ryan, P., Usai, D., 2014. Microbotanical evidence of domestic cereals in Africa 7000 years ago. PloS one 9(10), e110177.

Mallol, C., Hernandez, C.M., Cabanes, D., Sistiaga, A., Machado, J., Rodríguez, A., Perez, L., Galvan, B., 2013. The black layer of Middle Palaeolithic combustion structures. Interpretation and archaeostratigraphic implications. Journal of Archaeological Science 40 (5), 2515-2537.

Manning, J.C., Goldblatt, P., 2012. Plants of the Greater Cape Floristic Region 1: the Core Cape Region. Strelitzia 29. South African National Biodiversity Institute, Pretoria.

Marean, C.W., 2008. The African Origins of Modern Human Behavior. Nobel Conference 44. Available from: http://gustavus.edu/events/nobelconference/2008/.

Marean, C.W., 2010. Pinnacle point Cave 13B (Western Cape Province, South Africa) in context: the Cape Floral kingdom, shellfish, and modern human origins. Journal of Human Evolution 59 (3-4), 425-443.

Marean, C.W., Assefa, Z., 2005. The Middle and Upper Pleistocene African record for the biological and behavioral origins of modern humans, In: Stahl, A.B. (Ed), African Archaeology. New York (NY): Blackwell, pp. 93-129.

Marean, C.W., Nilssen, P. J., Brown, K., Jerardino, A., Stynder, D., 2004. Paleoanthropological investigations of Middle Stone Age sites at Pinnacle Point, Mossel Bay (South Africa): archaeology and hominid remains from the 2000 field season. Paleoanthropology 2(1).

Marean, C.W., Bar-Matthews, M., Bernatchez, J., Fisher, E.C., Goldberg, P., Herries, A.I., Jacobs, Z., Jerardino, A., Karkanas, P., Minichillo, T., 2007. Early human use of marine resources and pigment in South Africa during the Middle Pleistocene. Nature 449, 905-908.

Marean, C.W., Bar-Matthews, M., Fisher, E., Goldberg, P., Herries, A.I.R., Jacobs, Z., Jerardino, A., Karkanas, P., Nilssen, P.J., 2008. The life history of Pinnacle Point Cave 13B (Mossel Bay, South Africa): Setting the context for human occupation. The Annual Meeting of the Paleoanthropology Society, Vancouver, British Columbia.

Marean, C.W., Bar-Matthews, M., Fisher, E., Goldberg, P., Herries, A., Karkanas, P., Nilssen, P.J., Thompson, E., 2010. The stratigraphy of the Middle Stone Age sediments at Pinnacle Point Cave 13B (Mossel Bay, Western Cape Province, South Africa). Journal of Human Evolution 59 (3-4), 234-255.

Marean, C.W., Cawthra, H.C., Cowling, R.M., Esler, K.L., Fisher, E., Milewski, A., Potts, A.J., Singels, E., De Vynck, J., 2014. Stone Age people in a changing South African Greater Cape floristic region. In: Allsopp, N., Colville, J.F., Verboom, G.A. (Eds.), Fynbos: Ecology, Evolution, and Conservation of a Megadiverse Region. Oxford University Press, pp. 164-199.

Marlowe, F.W., 2005. Hunter-gatherers and human evolution. Evolutionary Anthropology 14, 54-67.

Marth, G., Schuler, G., Yeh, R., Davenport, R., Agarwala, R., Church, D., Wheelan, S., Baker, J., Ward, M., Kholodov, M., Phan, L., Czabarka, E., Murvai, J., Cutler, D., Wooding, S., Rogers, A., Chakravarti, A., Harpending, H.C., Kwok, P.Y., Sherry, S.T., 2003. Sequence variations in the public human genome data reflect a bottlenecked population history. Proceedings of the National Academy of Sciences 100, 376-381.

Matthews, T., Marean, C.W., Nilssen, P.J., 2009. Micromammals from the Middle Stone Age (92-167 ka) at Cave PP13B, Pinnacle Point, south coast, South Africa. Paleontological Africa 44, 112-120.

Matthews, T., Rector, A., Jacobs, Z., Herries, A.I.R., Marean, C.W., 2011. Environmental implications of micromammals accumulated close to the MIS 6 to MIS 5 transition at Pinnacle point cave 9 (Mossel Bay, western Cape province, South Africa). Palaeogeography, Palaeoclimatology, Palaeoecology 302, 213-229.

McBrearty, S., Brooks, A.S., 2000. The revolution that wasn't: a new interpretation of the origin of modern human behavior. Journal of Human Evolution 39, 453-563.

McDougall, I., Brown, F.H., Fleagle, J.G., 2005. Stratigraphic placement and age of modern humans from Kibish, Ethiopia. Nature 433, 733-736.

McGrath, J.R., Cleghorn, N., Gennari, B., Henderson, S., Kyriacou, K., Nelson-Viljoen, C., Nilssen, P., Richardson, L., Shelton, C., Wilkins, J., Marean, C.W., 2015. The Pinnacle Point shell midden complex: A high resolution Mid- to Late Holocene record of Later Stone Age coastal foraging along the southern Cape coast of South Africa. South African Archaeological Bulletin 70, 209.

McInerney, F.A., Strömberg, C.A.E. White, J.W.C., 2011. The Neogene transition from C3 to C4 grasslands in North America: stable carbon isotope ratios of fossil phytoliths. Paleobiology 37(1), 23–49.

McLean, B., Scott, L., 1999. Phytoliths in sediments of the Pretoria Saltpan (Tswaing Crater) and their potential as indicators of the environmental history at the site. Investigations into the origin, age and paleoenvironments of the Pretoria Saltpan. Council for Geosciences, Pretoria.

Menge, B.A., Branch, G.M., 2001. Rocky intertidal communities. In: Bertness, M.D., Gaines, S.D., Hay, M.E. (Eds.), Marine Community Ecology. Sinauer Associates, Sunderland, pp. 221-251.

Mercader, J., Runge, F., Vrydaghs, L., Doutrelepont, H., Ewango, C. E., Juan-Tresseras, J., 2000. Phytoliths from archaeological sites in the tropical forest of Ituri, Democratic Republic of Congo. Quaternary Research 54(1), 102-112.

Mercader, J., Bennett, T., Esselmont, C., Simpson, S., Walde, D., 2009. Phytoliths in woody plants from the miombo woodlands of Mozambique. Annals of Botany 104, 91-113.

Mercader, J., Bennett, T., Esselmont, C., Simpson, S., Walde, D., 2011. Soil phytoliths from miombo woodlands in Mozambique. Quaternary Research 75 (1), 138-150.

Messager, E., Lordkipanidze, D., Delhon, C., Ferring, C.R., 2010. Palaeoecological implications of the Lower Pleistocene phytolith record from the Dmanisi Site (Georgia). Palaeogeography, Palaeoclimatology, Palaeoecology 288(1), 1-13.

Metcalfe, C.R., 1960. Anatomy of Monocotyledons: I. Gramineae Claredon Press, Oxford.

Metcalfe, C.R., 1971. Anatomy of the Monocotyledons: II. Cyper- aceae Claredon Press, Oxford.

Metcalfe, C. R., Chalk, L. 1979. Anatomy of the dicotyledons. v. 1: Systematic anatomy of leaf and stem; with a brief history of the subject. v. 2: Wood structure and conclusion of the general introduction. Clarendon Press, Oxford.

Milton, K., 2000. Hunter-gatherer diets, a different perspective. American Journal of Clinical Nutrition 71(3), 665–667

Mitchell,P.J., 2008. Developing the archaeology of Marine Isotope Stage 3. South African Archaeological Society Goodwin Series 10, 52-65.

Moll, E.J., Campbell, B.M., Cowling R.M., Bossi, L., Jarman, ML., Boucher, C., 1984. A description of the major vegetation categories in and adjacent to the Fynbos Biome. South African National Scientific Programmes Report 83. CSIR, Pretoria

Morgan, L.E., Renne, P.R., 2008. Diachronous dawn of Africa's Middle Stone Age: new 40 Ar/39 Ar ages from the Ethiopian Rift. Geology 36(12), 967-970.

Mourre, V., Villa, P., Henshilwood, C.S., 2010. Early use of pressure flaking on lithic artifacts at Blombos Cave, South Africa. Science 330(6004), 659-662.

Mucina, L., Geldenhuys, C.J., 2006. Afrotemperate, subtropical and azonal forests. In: Mucina, L., Rutherford, M.C., (Eds.), The Vegetation Map of South Africa, Lesotho and Swaziland. SANBI, Pretoria, pp. 584-614.

Mucina, L., Rutherford, M.C., 2006. The Vegetation Map of South Africa, Lesotho and Swaziland. SANBI, Pretoria.

Mucina, L., Adams, J.B., Knevel, I.C., Rutherford, M.C., Powrie, L.W., Bolton, J.J., van der Merwe, J.H., Anderson, R.J., Bornman, T.G., le Roux, A., Janssen, J.A.M., 2006. Coastal vegetation of South Africa. In: Mucina, L., Rutherford, M.C., (Eds.), The Vegetation Map of South Africa, Lesotho and Swaziland. SANBI, Pretoria, pp. 658-697.

Mulholland, S.C., 1989. Phytolith shape frequencies in North Dakota grasses: a comparison to general patterns. Journal of Archaeological Science 16, 489-511.

Mulholland, S.C., Rapp Jr., C., 1992. A morphological classification of grass silica-bodies. In: Rapp Jr., G., Mulholland, C.S. (Eds.), Phytolith Systematics. Emerging Issues, Advances in Archaeological and Museum Science. Plenum Press, New York, pp. 65-89.

Neumann, K., Fahmy, A.G., Müller-Scheeßel, N., Schmidt, M., in press. Taxonomic, ecological and palaeoecological significance of leaf phytoliths in West African grasses, Quaternary International.

Neuwinger, H.D., 1996. African ethnobotany: poisons and drugs: chemistry, pharmacology, toxicology. Chapman and Hall, Germany.

North Greenland Ice Core Project Members. 2004. High- resolution record of Northern Hemisphere climate extending into the last interglacial period. Nature 431, 147–51.

Novello, A., Barboni, D., Berti-Equille, L., Mazur, J.C., Poilecot, P., Vignaud, P., 2012. Phytolith signal of aquatic plants and soils in Chad, Central Africa. Review of Palaeobotany and Palynology 178, 43-58.

Novello, A., Lebatard, A.E., Moussa, A., Barboni, D., Sylvestre, F., Bourles, D.L., Pailles, C., Buchet, G., Decarreau, A., Duringer, P., Ghienne, J.F., Maley, J., Mazur, J.C., Roquin, C., Schuster, M., Vignaud, P., 2015. Diatom, phytolith, and pollen records from a 10Be/9Be dated lacustrine succession in the Chad basin: insight on the MioceneePliocene paleoenvironmental changes in Central Africa. Palaeogeography, Palaeoclimatology, Palaeoecology 430, 85-103.

O'Dea, K., 1991. Westernisation, insulin resistance and diabetes in Australian aborigines. The Medical Journal of Australia 155(4), 258-264.

Oakley, K. 1970. On man's use of fire, with comments on tool-making and hunting. Viking Fund Publications in Anthropology 31, 176–93

Oestmo, S., Marean, C.W., 2014. Pinnacle Point: Excavation and Survey Methods. In M. B. Carver, B. Gaydarska, S. Monton-Subias (Eds.), Field Archaeology from Around the World. New York: Springer, pp. 5955-5959.

Ollendorf, A.L., 1992. Toward a classification scheme of sedge (Cyperaceae) phytoliths. In Phytolith Systematics. Springer US, pp. 91-111.

Opperman, H., 1996. Strathalan Cave B, north-eastern Cape Province, South Africa: evidence for human behaviour 29 000–26 000 years ago. Quaternary International 33, 45-53.

Osterrieth, M., Madella, M., Zurro, D., Alvarez, M.F., 2009. Taphonom- ical aspects of silica phytoliths in the loess sediments of the Argentinean Pampas. Quaternary International 193, 70-79.

Out, W.A., Pertusa Grau, J.F., Madella, M., 2014. A new method for morphometric analysis of opal phytoliths from plants. Microsocopy Microanalysis 20 (6), 1876-1887.

Pargeter, J., 2007. Howiesons Poort segments as hunting weapons: experiments with replicated projectiles. South African Archaeological Bulletin 62,147-153.

Parkington, J.E., 1972. Seasonal mobility in the Later Stone Age. African Studies 31, 223-243.

Parkington, J., 1980. Time and place: some observations on spatial and temporal patterning in the Later Stone Age sequence in southern Africa. South African Archaeological Bulletin 35, 73-83.

Parkington, J., 1981. The effects of environmental change on the scheduling of visits to the Elands Bay Cave, Cape Province, S.A. In: Hodder, I., Isaac, G., Hammond, N. (Eds.), Pattern of The Past. Cambridge University Press, Cambridge, pp. 341-359.

Parr, J.F., Dolic, V., Lancaster, G., Boyd, W.E., 2001. A microwave digestion method for the extraction of phytoliths from herbarium specimens. Review of Palaeobotany and Palynology 116 (3), 203-212.

Parsons, N., 1993. A New History of Southern Africa (2nd edn.) MacMillan, London.

Pearsall, D., Piperno, D., Dinan, E.H., Umlauf, M., Zhao, Z., Benfer, R.A., 1995 Distinguishing rice (*Oryza sativa*, Poaceae) from wild *Oryza* species through phytolith analysis: results of preliminary research. Economic Botany 49, 183-96.

Perlès, C., 1977. Préhistoire du feu. Masson, Paris.

Petö, A., Gyulai, F., Popity, D., Kenez, A., 2013. Macro- and micro-archaeobotanical study of a vessel content from a Late Neolithic structured deposition from southeastern Hungary. Journal of Archaeological Science 40 (1), 58-71.

Pickering, R., Jacobs, Z., Herries, A. I.R., Karkanas, P., Bar- Matthews, M., Woodhead, J.D., Kappen, P., Erich Fisher, E., and Marean, C.W., 2013. Paleoanthropologically Significant South African Sea Caves dated to 1.0 Million Years using a combination of U-Pb, TT-OSL and palaeomagnetism. Quaternary Science Reviews 65, 39-52.

Piperno, D.R., 1985. Phytolith taphonomy and distributions in archeological sediments from Panama. Journal of Archaeological Science 12(4), 247-267.

Piperno, D.R., 1988. Phytolith Analysis: an Archaeological and Geological Perspective. Academic Press, San Diego.

Piperno, D.R., 2006. Phytoliths: a Comprehensive Guide for Archaeologists and Paleoecologists. AltaMira Press, Lanham, MD.

Piperno, D. R., Becker, P. 1996. Vegetational history of a site in the central Amazon basin derived from phytolith and charcoal records from natural soils. Quaternary Research 45(2), 202-209.

Piperno, D.R., Flannery, K.V., 2001. The earliest archaeological maize (*Zea mays* L.) from highland Mexico: new accelerator mass spectrometry dates and their implications. Proceedings of the National Academy of Sciences 98(4), 2101-2103.

Piperno, D.R., Stothert, K.E., 2003. Phytolith evidence for early Holocene Cucurbita domestication in southwest Ecuador. Science 299(5609), 1054-1057.

Piperno, D.R., Pearsall, D.M., 1998. The Silica Bodies of Tropical American Grasses: Morphology, Taxonomy, and Implications for Grass Systematics and Fossil Phytolith Identification. In: Smithonian Contributions to Botany 85. Smithsonian Institution Press, Washington, D.C.

Piperno, D.R., Andres, T.C., Stothert, K. E. 2000. Phytoliths in Cucurbita and other Neotropical Cucurbitaceae and their occurrence in early archaeological sites from the lowland American tropics. Journal of Archaeological Science 27(3), 193-208.

Porat, N., Chazan, M., Grün, R., Aubert, M., Eisenmann, V., Horwitz, L. K. 2010. New radiometric ages for the Fauresmith industry from Kathu Pan, southern Africa: Implications for the Earlier to Middle Stone Age transition. Journal of Archaeological Science 37(2), 269-283.

Portillo, M., 2006. La mòlta i triturat d'aliments vegetals durant la Protohistòria en la Catalunya Oriental. Ph.D. Thesis. University of Barcelona, Barcelona.

Portillo, M., Ball, T., Manwaring, J., 2006. Morphometric analysis of inflorescence phytoliths produced by *Avena sativa* L. and *Avena strigosa* Schreb. Economic Botany 60,121-129.

Portillo, M., Albert, R.M., Henry, D.O., 2009. Domestic activities and spatial distribution in Ain Abu¯Nukhayla (Wadi Rum, Southern Jordan): the use of phytoliths and spherulites studies. Quaternary International 193 (1), 174-183.

Portillo, M., Albert, R. M., Kadowaki, S., Nishiaki, Y., 2010. Domestic activities at early Neolithic Tell Seker al-Aheimar (Upper Khabur, Northeastern Syria) through phytoliths and spherulites studies. Des hommes et des plantes: exploitation du milieu et gestion des ressources végétales de la Préhistoire à nos jours. Éditions ADPCA, Antibes, 19-30.

Portillo, M., Bofill, M., Molist, M., Albert, R.M., 2013. Phytolith and use-wear functional evidence for grinding stones from the Near East. In: Anderson, P.C., Cheval, C., Durand, A., (Eds), Regards croisés sur les outils liés au travail des végétaux. An interdisciplinary focus on plant working tools. APDCA, Antibes, pp 161-174

Potts, R., 1998. Environmental hypotheses of hominin evolution. American journal of physical anthropology 107(27), 93-136.

Procheş, Ş., Cowling, R.M., du Preez, D., 2005. Patterns of geophyte diversity and storage organ size in the winter rainfall region of southern Africa. Diversity and Distributions 11, 101-9.

Procheş, Ş., Cowling, R.M., Goldblatt, P., Manning, J.M., and Snijman, D.A. 2006. An overview of the Cape geophytes. Biological Journal of the Linnean Society, 87, 27-43.

Quick, L.J., Meadows, M.E., Bateman, M.D., Kirsten, K.L., Mäusbacher, R., Haberzettl, T., Chase, B.M., 2015. Vegetation and climate dynamics during the last glacial period in the fynbos-afrotemperate forest ecotone, southern Cape, South Africa. Quaternary International 404, 136–149.

Radomski, K.U., Neumann, K., 2011. Grasses and grinding stones: inflorescence phytoliths from modern West African Poaceae and archaeological stone arte- facts. In: Fahmy, A.G., Kahlheber, S., D'Andrea, A.C. (Eds.), Windows on the African Past. Current Approaches to African Archaeobotany. Africa Magna Verlag, Frankfurt am Main, pp. 153-166.

Ramsay, P.J., Andrew, J., Cooper, G., 2002. Late Quaternary sea-level change in South Africa. Quaternary Research 57(1), 82-90.

Rebelo, A.G., Cowling, R.M., Campbell, B.M., Meadows, M.E., 1991. Plant communities of the Riversdale Plain. South African Journal of Botany 57, 10-18.

Rebelo, A.G., Boucher, C., Helme, N., Mucina, L., Rutherford, M.C., 2006. Fynbos Biome. In L. Mucina and M.C. Rutherford, eds. The vegetation of South Africa, Lesotho and Swaziland, Strelitzia 19. South African National Biodiversity Institute, Pretoria, pp. 53-219.

Rector, A.L., Reed, K.E., 2010 Middle and late Pleistocene faunas of Pinnacle Point and their paleoecological implications. Journal of Human Evolution 59, 340-357.

Regev, L., Poduska, K.M., Addadi, L., Weiner, S., Boaretto, E., 2010. Distinguishing between calcites formed by different mechanisms using infrared spectrometry: archaeological applications. Journal of Archaeological Science 37, 3022-3029.

Rightmire, G.P., Deacon, H.J, 1991. Comparative studies of late Pleistocene human remains from Klasies River mouth, South Africa. Journal of Human Evolution 20(2), 131-156.

Rightmire, G.P., 1976. Relationships of middle and upper Pleistocene hominids from sub-Saharan Africa. Nature 260, 238-240.

Rightmire, G.P., 1984. Homo sapiens in sub-Saharan Africa. The origins of modern humans: A world survey of the fossil evidence, 295-325.

Rodríguez-Cintas, A., Cabanes, D., in press. Phytolith and FTIR studies applied to combustion structures: The case of the Middle Paleolithic site of El Salt (Alcoy, Alicante). Quaternary International.

Rogers, A.R., Jorde, L.B. 1995. Genetic evidence on modern human origins. Human biology, 1-36.

Rosen, A.M., 2003. Middle Paleolithic Plant Exploitation: The Microbotanical Evidence. In: Henry, D.O., (Ed), Neanderthals in the Levant: Behavioral Organization and the Beginning of Human Modernity. London: Continuum International Publishing Group, pp. 156-171.

Rosen, A.M., Weiner, S., 1994. Identifying ancient irrigation e a new method using opaline phytoliths from Emmer Wheat. Journal of Archaeological Science 21, 125-132.

Rossouw, L., 2009. The Application of Fossil Grass-phytolith Analysis in the Reconstruction of Late Cainozoic Environments in the South African Interior. Doctoral dissertation. University of the Free State.

Rourke, J., 1974. On restios and roofs. Veld and Flora, 4, 57-59.

Rovner, I., 1971. Potential of opal phytoliths for use in paleoecological reconstruction. Quaternary Research 1, 343-359.

Rovner, I, 1983. Plant opal phytolith analysis: major advances in archaeobotanical research. In: Schiffer, M.B.E., (Ed.), Advances in archaeological method and theory. Academic Press, London.

Runge, F., 1996. Leaf Phytoliths and Silica Skeletons from East African Plants. CD-Rom Database. Germany, Department of Physical Geography. University of Paderborn.

Runge, F., 1999. The opal phytolith inventory of soils in central Africadquantities, shapes, classification, and spectra. Review of Palaeobotany and Palynology 107(1), 23-53.

Rutherford, M.C., 1997. Categorization of biomes. In: Cowling, R.M., Richardson, D.M. and Pierce, S.M., (Ed.), Vegetation of southern Africa, Cambridge University Press, Cambridge, pp. 91-98.

Rutherford, M.C., Westfall, R.H., 1986. Biomes of southern Africa- an objective classification. Memoirs of the Botanical Survey of South Africa, 54, 1-98.

Rutherford, M.C., Westfall, R.H., 1994. Biomes of southern Africa: an objective characterization. Memoirs of the Botanical Survey of South Africa, 63.

Rutherford, M.C, Mucina, L., Powrie, L.W., 2006. Biomes and Bioregions of Southern Africa. In: Mucina, L., Rutherford, M.C., 2006. The Vegetation Map of South Africa, Lesotho and Swaziland. SANBI, Pretoria.

Sangster, A.G., Parry, D.W., 1969. Some factors in relation to bulliform cell silicification in the grass leaf. Annals of Botany 33, 315-323.

Schefuß, E., Kuhlmann, H., Mollenhauer, G., Prange, M., Pätzold, J., 2011. Forcing of wet phases in southeast Africa over the past 17,000 years. Nature 480(7378), 509-512.

Schiegl, S., Stockhammer, P., Scott, C., Wadley, L., 2004. A mineralogical and phytolith study of the Middle Stone Age hearths in Sibudu Cave, Kwazulu-Natal, South Africa. South African Journal of Science 100, 185-194.

Schmidt, P., Porraz, G., Slodczyk, A., Bellot-Gurlet, L., Archer, W., Miller, C.E., 2013. Heat treatment in the South African Middle Stone Age: temperature induced transformations of silcrete and their technological implications. Journal of Archaeological Science 40(9), 3519-3531.

Scholtz, A., 1986. Palynological and palaeobotanical studies in the southern Cape. Unpublished MA thesis, University of Stellenbosch.

Shi, N., Schneider, R., Beug, H.J., Dupont, L.M., 2001. Southeast trade wind variations during the last 135 kyr: evidence from pollen spectra in eastern South Atlantic sediments. Earth and Planetary Science Letters 187(3), 311-321.

Singer, R., Wymer, J.J., 1982. The middle stone age at Klasies river Mouth in South Africa. University of Chicago Press.

Stahl, A.B., Dunbar, R.I.M., Homewood, K., Ikawa-Smith, F., Kortlandt, A., McGrew, W.C., Milton, K., Paterson, J.D., Poirier, F.E., Sugardjito, J., Tanner, N.M., Wrangham, R.W., 1984. Hominid dietary selection before fire. Current Anthropology 25 (2), 151-168.

Stoneking, M., Soodyall, H., 2006. Genetic evidence for our recent African ancestry. The Prehistory of Africa: Tracing the Lineage of Modern Man. Jonathan Ball Publishers, Cape Town, pp. 21-30.

Story, R., 1958. Some Plants Used by the Bushmen in Obtaining Food and Water. Memoirs of the Botanical Survey of South Africa 30. Department of Agriculture, Pretoria.

Story, R., 1964. Plant lore of the Bushmen. In: Davies, D.H.S., (Ed.), Ecological Studies in Southern Africa. W. Junk, The Hague, pp. 87-99.

Strömberg, C.A.E., 2003. The origin and spread of grass-dominated habitats in North America during the Tertiary and how it relates to the evolution of hypsodonty in equids. Ph.D. thesis, University of California at Berkeley.

Strömberg C.A.E., Werdelin, L., Friis, E.M., Saraç, G., 2007. The spread of grass-dominated habitats in Turkey and surrounding areas during the Cenozoic: phytolith evidence. Palaeogeography, Palaeoclimatology, Palaeoecology 250 (1-4), 18-49.

Strömberg, C.A.E., McInerney, F.A., 2011. TheNeogenetransitionfromC3toC4 grasslands in North America: assemblage analysis of fossil phytoliths. Paleobiology 37 (1), 50-71.

Stuut, J. B. W., Prins, M. A., Schneider, R. R., Weltje, G. J., Jansen, J. F., Postma, G., 2002. A 300-kyr record of aridity and wind strength in southwestern Africa: inferences from grain-size distributions of sediments on Walvis Ridge, SE Atlantic. Marine Geology 180(1), 221-233.

Tanaka, J., 1976. Subsistence Ecology of Central Kalahari San. In: Lee, R.B., DeVore, I., (Eds), Kalahari Hunter-Gatherers. Harvard University Press, pp. 98-119.

Tanaka, J., 1978. A study of the comparative ecology of African gatherer-hunters with special reference to San (Bushman-speaking people) and Pygmies. Senri Ethnological Studies 1, 189-212.

Taylor, H.C., 1978 Capensis. In: M.J.A., Werger (Ed.), Biogeography and ecology ofsouthem Africa. Junk, The Hague, pp. 171-229.

Taylor, H.C., 1980. Phytogeography of fynbos. Bothalia 13, 231-235.

Texier, P.J., Porraz, G., Parkington, J., Rigaud, J.P., Poggenpoel, C., Miller, C., Tribolo, C., Cartwright, C., Coudenneau, A., Klein, R., Steele, T., Verna, C., 2010. A Howiesons Poort tradition of engraving ostrich eggshell containers dated to 60,000 years ago at Diepkloof Rock Shelter, South Africa. Proceedings National Academy of Science 107, 6180-6185.

Thwaites, R.N., Cowling, R.M., 1988. Soil-vegetation relationships on the Agulhas plain, South Africa. Catena 15 (3), 333-345.

Tieszen, L.L., Senyimba, M.M., Imbamba, S.K., Troughton, J.H., 1979. The distribution of C3 and C4 grasses and carbon isotope discrimination along an altitudinal and moisture gradient in Kenya. Oecologia 37 (3), 337-350.

Tryon, C.A., McBrearty, S., 2002. Tephrostratigraphy and the Acheulian to Middle Stone Age transition in the Kapthurin formation, Kenya. Journal of Human Evolution 42(1), 211-235.

Tsartsidou, G., Lev-Yadun, S., Albert, R.M., Miller-Rosen, A., Efstratiou, N., Weiner, S., 2007. The phytolith archaeological record: strengths and weaknesses evaluated based on a quantitative modern reference collection from Greece. Journal of Archaeological Science 34 (8), 1262-1275.

Tsartsidou, G., Karkanas, P., Marshall, G., Kyparissi-Apostolika, N., 2015. Palaeoenvironmental reconstruction and flora exploitation at the Palaeolithic cave of Theopetra, central Greece: the evidence from phytolith analysis.Archaeological and Anthropological Sciences 7(2), 169-185.

Twiss, P.C., 1987. Grass-opal phytoliths as climatic indicators of the Great Plains Pleistocene. Quaternary Environments of Kansas 5, 179-188.

Twiss, P.C., 1992. Predicted world distribution of C3 and C4 grass phytoliths. In: Rapp Jr., G., Mulholland, S.C. (Eds.), Phytolith Systematics: Emerging Issues, Advances in Archaeological and Museum Science. Plenum Press, New York, pp. 113-128.

Twiss, P.C., Suess, E., Smith, R.M., 1969. Morphological classification of grass phytoliths. Soil Science Society of America Journal 33, 109-115.

Tyson, P.D., Preston-Whyte, R.A., 2000. The Weather and Climate of Southern Africa. Oxford University Press, Cape Town.

van Campo, E., Duplessy, J. C., Prell, W. L., Barratt, N., Sabatier, R., 1990. Comparison of terrestrial and marine temperature estimates for the past 135 kyr off Southeast Africa: A test for GCM simulations of palaecoclimate. Nature 348(6298), 209-212.

Van Wyk, B.E., 2002. A review of ethnobotanical research in South Africa. South African Journal of Botany 68(1),1-13.

Van Wyk, B.E., Gericke, N., 2000. People's plants: a guide to useful plants of southern Africa. Johannesburg: Briza Publications.

Villa, P., Soriano, S., Tsanova, T., Degano, I., Higham, T.F.G., d'Errico, F., Backwell, L., Lucejko, J.J., Colombini, M.P., Beaumont, P.B., 2012. Border Cave and the beginning of the Later Stone Age in South Africa. Proceedings National Academy of Science 109, 13208-13213.

Vimeux, F., Masson, V., Jouzel, J., Stievenard, M., Petit, J.R., 1999. Glacial and interglacial changes in ocean surface conditions in the Southern Hemisphere. Nature 398, 410–413.

Vlok, J.H.J., De Villiers, M.E., 2007. Vegetation Map for the Riversdale Domain. Unpublished 1:50 000 maps and report supported by the CAPE Fine Scale Planning Task Team and Cape Nature.

Vlok, J.H., Euston-Brown, D.I.W., Cowling, R.M., 2003. Acocks' Valley Bushveld 50 years on: new perspectives on the delimitation, characterisation and origin of subtropical thicket vegetation. South African Journal of Botany 69, 27-51.

Vogel, J.C., Fuls, A., Ellis, R.P., 1978. Geographical distribution of Kranz grasses in South Africa. South African Journal of Science 74, 209-215.

Von Koenen, E., 2001. Medicinal Poisonous and Edible Plants in Namibia. Klaus Hess Publishers, Windhoek and Göttingen, ISBN: Namibia 99916-747-4-8; Germany 3-9804518-7-9.

Vrydaghs, L., Ball, T., Volkaert, H., Van den Houwe, I., Manwaring, J., De Langhe, E., 2009. Differentiating the volcaniform phytoliths of bananas: *Musa acuminate*. Ethnobotany Research and Applications 7, 239-246.

Wadley, L., 2001. What is cultural modernity? A general view and a South African perspective from Rose Cottage Cave. Cambridge Archaeological Journal 11, 201-221.

Wadley, L., 2010. Were snares and traps used in the Middle Stone Age and does it matter? A review and a case study from Sibudu, South Africa. J. Hum. Evol. 58 (2), 179-192.

Wadley, L., 2012. Some combustion features at Sibudu, South Africa, between 65,000 and 58,000 years ago. Quaternary International 247, 341-349.

Wadley, L., 2015. Those marvellous millennia: the Middle Stone Age of Southern Africa. Azania: Archaeological Research in Africa 50 (2), 155-226.

Wadley, L., Hodgskiss, T., Grant, M., 2009. Implications for complex cognition from the hafting of tools with compound adhesives in the Middle Stone Age, South Africa. Proceedings National Academy of Science 106 (24), 9590-9594.

Wadley, L., Sievers, C., Bamford, M., Goldberg, P., Berna, F., Miller, C., 2011. Middle Stone Age bedding construction and settlement patterns at Sibudu, South Africa. Science 334(6061), 1388-1391.

Watkeys, M.K., 1999. Soils of the arid south-western zone of Africa. In: Dean, W.R.J., Milton, S.J. (Eds), The Karoo: Ecological Patterns and Processes. Cambridge University Press, Cambridge.

Watling, J., Iriarte, J., 2013. Phytoliths from the coastal savannas of French Guiana. Quaternary International 287, 162-180.

Watts, I., 2002. Ochre in the Middle Stone Age of southern Africa: ritualized display or hide preservative? South African Arcaheological Bulletin 57, 64-74.

Watts, I., 2010. The pigments from Pinnacle point cave 13B, western Cape, South Africa. Journal of Human Evolution 59 (3), 392-411.

Watts, I., 2009. Red ochre, body-painting, and language: interpreting the Blombos ochre. In: Botha, R., Knight, C. (Eds.), The Cradle of Language, vol. 2. Oxford University Press, Oxford, pp. 93-129.

Weiner, S., 2010. Microarchaeology. Beyond the Visible Archaeological Record. New York: Cambridge University Press

Wells, M.J., 1965. An analysis of plant remains from Scott's Cave in the Gamtoos Valley. The South African Archaeological Bulletin 20(78), 79-84.

White, T.D., Asfaw, B., DeGusta, D., Gilbert, H., Richard, G.D., Suwa, G., Howell, F.C., 2003. Pleistocene Homo sapiens from Middle Awash, Ethiopia. Nature 423, 742-747.

Wilding, L.P., Drees, L.R., 1971. Biogenic opal in Ohio soils. Soil Science Society of America Journal, 35(6), 1004-1010.

Wilkins, J., Chazan, M., 2012. Blade production~ 500 thousand years ago at Kathu Pan 1, South Africa: support for a multiple origins hypothesis for early Middle Pleistocene blade technologies. Journal of Archaeological Science 39(6), 1883-1900.

Wilkins, J., Schoville, B.J., Brown, K.S., Chazan, M., 2012. Evidence for early hafted hunting technology. Science, 338(6109), 942-946.

Wolde Gabriel, G., Ambrose, S.H., Barboni, D., Bonnefille, R., Bremond, L., Currie, B., DeGusta, D., Hart, W. K., Murray, A. M., Renne, P. R., Jolly-Saad, M. C., Stewart, K.M., White, T.D., 2009. The geological, isotopic, botanical, invertebrate and lower vertebrate surroundings of Ardipithecus ramidus. Science 326, 5949, 65 65e1-65e5

Woodburn, J., 1968. An introduction to Hadza ecology. In: Lee, R.B., DeVore, I. (Eds.) Man the Hunter. Chicago: Aldine

Wrangham, R.W., Holland Jones, J., Laden, G., Pilbeam, D., Conklin-Brittain, N.L., 1999. The raw and the stolen: cooking and the ecology of human origins. Current Anthropology 40, 567-94

Wu, Y., Wang, C., Hill, D.V., 2012. The transformation of phytolith morphology as the result of their exposure to high temperature. Microscopy Research and Technique 75 (7), 852-855.

Wurz, S., 2013. Technological trends in the Middle Stone Age of South Africa between MIS 7 and MIS 3. Current Anthropology 54(S8), 305-319.

Yoshioka, S., Kitano, Y., 1985. Transformation of aragonite to calcite through heating. Geochemical Journal 19, 245-249.

Zhang, J., Lu, H., Wu, N., Yang, X., Diao, X., 2011. Phytolith analysis for differentiating between Foxtail millet (*Setaria italica*) and Green Foxtail (*Setaria viridis*). PLoS One 6 (5), e19726.

Zhao, Z., Pearsall, D.M., Benefer Jr., A.B., Piperno, D.R., 1998. Distinguishing rice (*Oryza sativa* Poaceae) from wild *Oryza* species through phytolith analysis, II: finalized method. Econ. Bot. 52, 134-135.

Ziegler, M., Simon, M.H., Hall, I.R., Barker, S., Stringer, C., Zahn, R., 2013. Development of Middle Stone Age innovation linked to rapid climate change. Nat. Commun. 4, 1905.

Zucol, A.F., 1998. Microfitolitos de las Poaceae Argentinas: II. Microfitolitos foliares de algunas especies del genero Panicum (Poaceae, Paniceae) de la provincia de Entre Ríos. Darwinia 36(1– 4), 29–50

Zurro, D., García-Granero, J.J., Lancelotti, L., Madella, M., 2016. Directions in current and future phytolith research. Journal of Archaeological Science 68, 112-117.

Appendices

Table A1. Frequencies of the phytolith morphotypes identified in the different parts analyzed from the modern plant specimens. EGM = epidermal ground mass. GSSC = grass silica short cell.

Plant species	***Elytropappus rhinocerotis***	***Protea repens***	***Acacia karoo***	***Sideroxylon inerme***	***Celtis africana***	***Leucospermum praecox***	***Pterocelastrus tricaspidatus***	***Searsia crenata***	***Searsia pterota***	***Protea lanceolata***	***Vepris undulata***	***Olea europaea sub. Africana***	***Cassine peragua***	***Eriocephalus africanus***	***Euclea racemosa***
Sample description	**Eudicot - Wood/bark**	**Eudicot - Wood/bark**	**Eudicot - Wood/bark**	**Eudicot - Wood/bark**	**Eudicot - Wood/bark**	**Eudicot - Wood/bark**	**Eudicot - Wood/bark**	**Eudicot - Wood/bark**	**Eudicot - Wood/bark**	**Eudicot - Wood/bark**	**Eudicot - Wood/bark**	**Eudicot - Wood/bark**	**Eudicot - Wood/bark**	**Eudicot - Wood/bark**	**Eudicot - Wood/bark**
Bulliform	10.71	0.00	1.45	0.00	0.00	0.00	50.00	0.00	0.00	0.00	0.00	10.00	0.00	0.00	0.00
Blocky Polyhedral	0.00	0.00	0.00	0.00	0.00	0.00	0.00	0.00	0.00	0.00	0.00	0.00	0.00	0.00	0.00
Cone-shape	0.00	0.00	0.00	0.00	0.00	0.00	0.00	0.00	0.00	0.00	0.00	0.00	2.04	0.00	0.00
Cystolith	0.00	0.00	0.00	0.00	0.00	0.00	0.00	0.00	0.00	0.00	0.00	0.00	0.00	0.00	0.00
Ellipsoid	0.00	0.00	8.70	0.00	0.00	13.79	0.00	0.00	28.57	0.00	0.00	10.00	0.00	12.50	33.33
Ellipsoid echinate	0.00	0.00	0.00	0.00	0.00	0.00	0.00	0.00	0.00	0.00	0.00	0.00	0.00	0.00	0.00
Elongate	0.00	0.00	8.70	92.44	0.00	3.45	0.00	0.00	0.00	6.25	100.00	20.00	2.04	12.50	0.00
Elongate blocky	0.00	0.00	5.80	0.17	0.00	0.00	0.00	0.00	0.00	0.00	0.00	0.00	2.04	0.00	0.00
Elongate blocky echinate	0.00	0.00	0.00	0.00	0.00	0.00	0.00	0.00	0.00	0.00	0.00	0.00	0.00	0.00	0.00
Elongate blocky striate	0.00	0.00	0.00	0.00	0.00	0.00	0.00	0.00	0.00	0.00	0.00	0.00	0.00	0.00	0.00
Elongate bulbous	0.00	0.00	0.00	0.00	0.00	0.00	0.00	0.00	0.00	0.00	0.00	0.00	0.00	0.00	0.00
Elongate curved	0.00	0.00	0.00	0.00	0.00	0.00	0.00	0.00	0.00	0.00	0.00	0.00	0.00	0.00	0.00
Elongate facetate	0.00	0.00	0.00	0.00	0.00	0.00	0.00	0.00	0.00	0.00	0.00	0.00	0.00	0.00	0.00
Elongate striate	0.00	0.00	0.00	0.00	0.00	0.00	0.00	0.00	0.00	0.00	0.00	0.00	0.00	0.00	0.00
Elongate tuberculate	0.00	0.00	0.00	0.00	0.00	0.00	0.00	0.00	0.00	0.00	0.00	0.00	0.00	0.00	0.00

Elongate verrucate	0.00	0.00	0.00	0.00	0.00	0.00	0.00	0.00	0.00	0.00	0.00	0.00	0.00	0.00	0.00
Elongate dendritic	0.00	0.00	0.00	0.00	0.00	0.00	0.00	0.00	0.00	0.00	0.00	0.00	0.00	0.00	0.00
Elongate echinate	0.00	0.00	1.45	0.00	0.00	0.00	0.00	0.00	0.00	0.00	0.00	0.00	0.00	0.00	0.00
Elongate sinuate	0.00	0.00	0.00	0.00	0.00	0.00	0.00	0.00	0.00	0.00	0.00	0.00	0.00	0.00	0.00
Elongate polylobate	0.00	0.00	0.00	0.00	0.00	0.00	0.00	0.00	0.00	0.00	0.00	0.00	0.00	0.00	0.00
EGM	0.00	0.00	0.00	0.00	0.00	0.00	0.00	0.00	0.00	0.00	0.00	0.00	0.00	0.00	0.00
EGM elongate	0.00	0.00	0.00	0.00	0.00	0.00	0.00	0.00	0.00	0.00	0.00	0.00	0.00	0.00	0.00
EGM polyhedral	0.00	0.00	0.00	0.17	44.14	0.00	0.00	0.00	0.00	0.00	0.00	0.00	0.00	0.00	0.00
EGM sinuous	0.00	0.00	0.00	0.00	0.00	0.00	0.00	0.00	0.00	0.00	0.00	0.00	0.00	0.00	0.00
EGM rings	0.00	0.00	0.00	0.00	0.00	0.00	0.00	0.00	0.00	0.00	0.00	0.00	0.00	0.00	0.00
EGM dots	0.00	0.00	0.00	0.00	0.00	0.00	0.00	0.00	0.00	0.00	0.00	0.00	0.00	0.00	0.00
Hair cell (trichomes)	0.00	0.00	1.45	0.00	0.00	5.17	0.00	0.00	0.00	0.00	0.00	10.00	0.00	0.00	0.00
Hair cell (prickle)	7.14	0.00	4.35	0.67	0.00	3.45	50.00	11.11	0.00	12.50	0.00	0.00	0.00	0.00	0.00
Hair cell aciculate	0.00	0.00	0.00	0.00	0.00	0.00	0.00	0.00	0.00	0.00	0.00	0.00	0.00	0.00	0.00
Hair cell armed	0.00	0.00	0.00	0.00	0.00	0.00	0.00	0.00	0.00	0.00	0.00	0.00	0.00	0.00	0.00
Hair cell with protuberances	0.00	0.00	0.00	0.00	0.00	0.00	0.00	0.00	0.00	0.00	0.00	0.00	0.00	0.00	0.00
Hair cell curved	0.00	0.00	0.00	0.00	0.00	0.00	0.00	0.00	0.00	0.00	0.00	0.00	0.00	0.00	0.00
Hair cell unciform	0.00	0.00	0.00	0.00	0.00	0.00	0.00	0.00	0.00	0.00	0.00	0.00	0.00	0.00	0.00
Hair base	0.00	0.00	0.00	0.00	0.00	0.00	0.00	0.00	0.00	0.00	0.00	0.00	0.00	0.00	0.00
Hair base sinuous shape	0.00	0.00	0.00	0.00	0.00	0.00	0.00	0.00	0.00	0.00	0.00	0.00	0.00	0.00	0.00
Indetermined	10.71	0.00	0.00	0.00	0.00	0.00	0.00	0.00	0.00	0.00	0.00	0.00	0.00	0.00	0.00
Irregular	3.57	0.00	23.19	1.34	0.00	0.00	0.00	0.00	14.29	12.50	0.00	0.00	0.00	0.00	0.00
Irregular echinate	0.00	0.00	0.00	0.00	0.00	0.00	0.00	0.00	0.00	0.00	0.00	0.00	0.00	0.00	0.00
Irregular facetate	0.00	0.00	0.00	0.00	0.00	0.00	0.00	0.00	0.00	0.00	0.00	0.00	0.00	0.00	0.00
Papillae	0.00	0.00	0.00	0.00	0.00	0.00	0.00	0.00	0.00	0.00	0.00	0.00	0.00	0.00	0.00

Parallelepiped thin	0.00	0.00	2.90	0.34	0.00	1.72	0.00	11.11	0.00	0.00	0.00	10.00	0.00	0.00	0.00
Parenchyma strand	0.00	0.00	0.00	3.70	55.86	0.00	0.00	0.00	0.00	0.00	0.00	0.00	0.00	0.00	0.00
Platelet	0.00	0.00	0.00	0.00	0.00	0.00	0.00	0.00	0.00	0.00	0.00	0.00	0.00	0.00	0.00
Sclereid	0.00	0.00	0.00	0.00	0.00	0.00	0.00	0.00	0.00	0.00	0.00	0.00	0.00	0.00	0.00
GSSC bilobate tabular flattened-concave lobes	3.57	0.00	2.90	0.00	0.00	0.00	0.00	11.11	0.00	0.00	0.00	0.00	0.00	12.50	0.00
GSSC bilobate tabular flattened lobes	0.00	0.00	0.00	0.00	0.00	0.00	0.00	0.00	0.00	0.00	0.00	0.00	0.00	0.00	0.00
GSSC bilobate tabular rounded lobes, short shank	0.00	0.00	0.00	0.00	0.00	0.00	0.00	0.00	0.00	0.00	0.00	0.00	0.00	0.00	0.00
GSSC bilobate tabular rounded lobes, long shank	0.00	0.00	0.00	0.00	0.00	0.00	0.00	0.00	0.00	0.00	0.00	0.00	0.00	0.00	0.00
GSSC bilobate trapeziform notched lobes	0.00	0.00	0.00	0.00	0.00	0.00	0.00	0.00	0.00	0.00	0.00	0.00	0.00	0.00	0.00
GSSC bilobate tabular angulate lobes	0.00	0.00	0.00	0.00	0.00	0.00	0.00	0.00	0.00	0.00	0.00	0.00	0.00	0.00	0.00
GSSC bilobate tabular angulate asymmetrical lobes	0.00	0.00	0.00	0.00	0.00	0.00	0.00	0.00	0.00	0.00	0.00	0.00	0.00	0.00	0.00
GSSC bilobate tabular segmented angulate/planar lobes	0.00	0.00	0.00	0.00	0.00	0.00	0.00	0.00	0.00	0.00	0.00	0.00	0.00	0.00	0.00
GSSC bilobate trapezoid	0.00	0.00	0.00	0.00	0.00	0.00	0.00	0.00	0.00	0.00	0.00	0.00	0.00	0.00	0.00
GSSC bilobate trapezoid wavy top	0.00	0.00	0.00	0.00	0.00	0.00	0.00	0.00	0.00	0.00	0.00	0.00	0.00	0.00	0.00
GSSC cross trapeziform	0.00	0.00	0.00	0.00	0.00	0.00	0.00	0.00	0.00	0.00	0.00	0.00	0.00	0.00	0.00
GSSC cross tabular	0.00	0.00	0.00	0.00	0.00	0.00	0.00	0.00	0.00	0.00	0.00	0.00	0.00	0.00	0.00
GSSC trilobate	0.00	0.00	0.00	0.00	0.00	0.00	0.00	0.00	0.00	0.00	0.00	0.00	0.00	0.00	0.00
GSSC polylobate	0.00	0.00	0.00	0.00	0.00	0.00	0.00	0.00	0.00	0.00	0.00	0.00	0.00	0.00	0.00
GSSC rondel cilyndric	10.71	0.00	0.00	0.00	0.00	0.00	0.00	0.00	0.00	6.25	0.00	0.00	0.00	0.00	0.00
GSSC rondel conical	0.00	0.00	4.35	0.00	0.00	0.00	0.00	0.00	0.00	6.25	0.00	20.00	2.04	12.50	0.00
GSSC rondel conical wavy top	0.00	0.00	0.00	0.00	0.00	0.00	0.00	0.00	0.00	0.00	0.00	0.00	0.00	0.00	0.00

GSSC rondel keeled	0.00	0.00	0.00	0.00	0.00	0.00	0.00	0.00	0.00	0.00	0.00	0.00	0.00	0.00	0.00
GSSC long tower	0.00	0.00	0.00	0.00	0.00	0.00	0.00	0.00	0.00	0.00	0.00	0.00	0.00	0.00	0.00
GSSC long tower wavy top	0.00	0.00	0.00	0.00	0.00	0.00	0.00	0.00	0.00	0.00	0.00	0.00	0.00	0.00	0.00
GSSC trapeziform	0.00	0.00	0.00	0.00	0.00	0.00	0.00	0.00	0.00	0.00	0.00	0.00	0.00	0.00	0.00
GSSC oblong tabular	0.00	0.00	0.00	0.00	0.00	0.00	0.00	0.00	0.00	0.00	0.00	10.00	0.00	0.00	0.00
GSSC oblong trapeziform sinuous	0.00	0.00	0.00	0.00	0.00	1.72	0.00	0.00	0.00	0.00	0.00	0.00	0.00	0.00	0.00
GSSC round tabular	0.00	0.00	0.00	0.00	0.00	0.00	0.00	0.00	0.00	0.00	0.00	0.00	0.00	0.00	0.00
GSSC saddle	0.00	0.00	4.35	0.00	0.00	3.45	0.00	11.11	0.00	0.00	0.00	0.00	2.04	0.00	0.00
GSSC collapsed saddle	0.00	0.00	0.00	0.00	0.00	0.00	0.00	0.00	0.00	0.00	0.00	0.00	0.00	0.00	0.00
Spheroid psilate	39.29	100.00	24.64	0.67	0.00	55.17	0.00	33.33	57.14	43.75	0.00	0.00	0.00	50.00	66.67
Semi spheroids	3.57	0.00	0.00	0.00	0.00	0.00	0.00	11.11	0.00	0.00	0.00	0.00	2.04	0.00	0.00
Small spheroids	0.00	0.00	0.00	0.17	0.00	0.00	0.00	0.00	0.00	12.50	0.00	0.00	0.00	0.00	0.00
Large spheroid	0.00	0.00	0.00	0.00	0.00	0.00	0.00	0.00	0.00	0.00	0.00	0.00	0.00	0.00	0.00
Large spheroid facetate	0.00	0.00	0.00	0.00	0.00	0.00	0.00	0.00	0.00	0.00	0.00	0.00	0.00	0.00	0.00
Large spheroid granulate and verrucate	7.14	0.00	0.00	0.34	0.00	1.72	0.00	11.11	0.00	0.00	0.00	10.00	0.00	0.00	0.00
Spheroid spiraling decorations	0.00	0.00	0.00	0.00	0.00	0.00	0.00	0.00	0.00	0.00	0.00	0.00	0.00	0.00	0.00
Spheroid rugulate	3.57	0.00	5.80	0.00	0.00	10.34	0.00	0.00	0.00	0.00	0.00	0.00	87.76	0.00	0.00
Stomata	0.00	0.00	0.00	0.00	0.00	0.00	0.00	0.00	0.00	0.00	0.00	0.00	0.00	0.00	0.00
Tracheid	0.00	0.00	0.00	0.00	0.00	0.00	0.00	0.00	0.00	0.00	0.00	0.00	0.00	0.00	0.00

Table A1. continued

Plant species	*Morella cardifolia*	*Passerina vulgaris*	*Tarchonanthus camphoratus*	*Acacia karoo*	*Vepris undulata*	*Searsia crenata*	*Celtis africana*	*Searsia pterota*	*Pterocelastrus tricaspidatus*	*Sideroxylon inerme*	*Olea europaeae sub. Africana*	*Passerina vulgaris*	*Grewia occidentalis*	*Cassine peragua*	*Morella cardifolia*
Sample description	**Eudicot - Wood/bark**	**Eudicot - Wood/bark**	**Eudicot - Wood/bark**	**Eudicot - Leaves**	**Eudicot - Leaves**	**Eudicot - Leaves**	**Eudicot - Leaves**	**Eudicot - Leaves**	**Eudicot - Leaves**	**Eudicot - Leaves**	**Eudicot - Leaves**	**Eudicot - Leaves**	**Eudicot - Leaves**	**Eudicot - Leaves**	**Eudicot - Leaves**
Bulliform	0.00	0.00	0.00	0.85	0.00	0.62	0.00	0.00	0.00	0.00	0.00	5.66	0.09	0.37	0.00
Blocky Polyhedral	0.00	0.00	0.00	1.71	0.00	0.00	0.00	0.00	0.00	0.07	0.00	1.89	0.00	0.00	0.00
Cone-shape	0.00	0.00	0.00	0.00	0.00	0.00	0.00	0.00	0.00	0.00	0.00	0.00	0.00	0.00	0.00
Cystolith	0.00	0.00	0.00	0.00	0.16	0.00	10.50	0.00	0.00	0.00	0.00	0.00	0.00	60.49	0.00
Ellipsoid	50.00	0.00	2.33	0.00	0.00	5.88	0.00	0.00	0.00	0.76	0.00	1.89	0.00	0.00	1.45
Ellipsoid echinate	0.00	0.00	0.00	0.00	0.00	0.00	0.00	0.00	0.00	0.00	0.00	0.00	0.00	0.00	0.00
Elongate	0.00	0.00	2.33	17.95	0.00	0.00	0.00	0.00	0.00	0.21	0.00	3.77	0.00	0.37	2.17
Elongate blocky	0.00	50.00	0.00	0.85	0.00	0.00	0.00	0.00	0.00	0.00	0.00	1.89	0.00	0.00	0.00
Elongate blocky echinate	0.00	0.00	0.00	0.00	0.00	0.00	0.00	0.00	0.00	0.00	0.00	0.00	0.00	0.00	0.00
Elongate blocky striate	0.00	0.00	0.00	0.00	0.00	0.00	0.00	0.00	0.00	0.00	0.00	0.00	0.00	0.00	0.00
Elongate bulbous	0.00	0.00	0.00	0.00	0.00	17.34	0.00	0.00	0.00	0.00	0.00	0.00	0.00	0.00	0.00
Elongate curved	0.00	0.00	0.00	0.00	0.00	0.00	0.00	0.00	0.00	0.00	0.00	0.00	0.00	0.00	0.00
Elongate facetate	0.00	0.00	0.00	1.71	0.00	0.00	0.00	0.00	0.00	0.00	0.00	0.00	0.00	0.00	0.00
Elongate striate	0.00	0.00	0.00	0.00	0.72	0.00	0.00	0.00	0.00	0.00	0.00	0.00	0.00	0.00	0.00
Elongate tuberculate	0.00	0.00	0.00	0.00	0.00	0.00	0.00	0.00	0.00	0.00	0.00	0.00	0.00	0.00	0.00

Elongate verrucate	0.00	0.00	0.00	0.00	0.00	0.00	0.00	0.00	0.00	0.00	0.00	0.00	0.00	0.00	0.00
Elongate dendritic	0.00	0.00	0.00	0.00	0.00	0.00	0.00	0.00	0.00	0.00	0.00	0.00	0.00	0.00	0.00
Elongate echinate	0.00	0.00	0.00	4.27	0.00	0.00	0.00	0.00	0.00	0.28	0.00	0.00	0.00	0.00	0.00
Elongate sinuate	0.00	0.00	0.00	0.00	0.00	0.00	0.00	0.00	0.00	0.00	0.00	0.00	0.00	0.00	0.00
Elongate polylobate	0.00	0.00	0.00	0.85	0.00	0.00	0.00	0.00	0.00	0.00	0.00	0.00	0.00	0.00	0.00
EGM	0.00	0.00	0.00	0.00	0.96	0.00	7.75	7.40	5.34	0.00	0.00	0.00	0.00	1.31	0.00
EGM elongate	0.00	0.00	0.00	0.00	0.00	0.00	0.00	0.00	0.00	0.00	0.00	0.00	0.00	0.00	0.00
EGM polyhedral	0.00	0.00	0.00	0.00	76.93	0.00	3.25	0.63	73.91	58.51	22.83	0.00	73.68	0.00	0.00
EGM sinuous	0.00	0.00	0.00	0.00	0.00	0.00	0.00	0.00	0.00	0.00	0.00	0.00	0.00	0.00	0.00
EGM rings	0.00	0.00	0.00	0.00	0.00	0.00	0.00	0.00	0.00	0.00	0.00	0.00	0.00	0.00	0.00
EGM dots	0.00	0.00	0.00	0.00	0.00	0.00	0.00	0.00	0.00	0.00	0.00	0.00	0.00	0.00	0.00
Hair cell (trichomes)	0.00	0.00	2.33	1.71	0.00	0.31	64.00	0.42	0.00	1.45	0.54	0.00	0.00	0.75	0.00
Hair cell (prickle)	0.00	0.00	2.33	6.84	0.00	0.00	0.00	0.00	0.00	0.00	0.00	0.00	0.00	0.00	0.72
Hair cell aciculate	0.00	0.00	0.00	1.71	0.00	0.00	0.00	0.00	0.00	0.00	0.00	0.00	0.00	0.00	0.00
Hair cell armed	0.00	0.00	0.00	0.00	0.00	0.00	0.00	0.00	0.00	0.35	3.26	0.00	0.00	0.00	0.00
Hair cell with protuberances	0.00	0.00	0.00	0.00	0.00	0.00	2.50	0.00	0.00	0.00	0.00	0.00	0.00	0.00	0.00
Hair cell curved	0.00	0.00	0.00	0.00	0.00	0.00	0.00	0.00	0.00	0.21	0.00	0.00	0.00	0.00	0.00
Hair cell unciform	0.00	0.00	0.00	0.00	0.00	0.00	0.00	0.00	0.00	0.00	0.00	0.00	0.00	0.00	0.00
Hair base	0.00	0.00	0.00	0.00	1.05	0.31	6.50	2.96	0.00	0.90	0.54	0.00	9.47	0.00	0.72
Hair base sinuous shape	0.00	0.00	0.00	0.00	0.00	0.00	5.25	0.00	0.00	0.00	0.00	0.00	0.00	0.00	0.00
Indetermined	0.00	0.00	2.33	5.13	0.00	5.57	0.00	0.00	0.00	0.00	0.00	0.00	0.00	0.00	2.90
Irregular	0.00	50.00	20.93	6.84	0.00	0.00	0.00	0.00	0.00	0.69	3.26	9.43	0.00	0.00	0.72
Irregular echinate	0.00	0.00	0.00	0.00	0.00	0.00	0.00	0.00	0.00	0.00	0.00	0.00	0.00	0.00	0.00
Irregular facetate	0.00	0.00	0.00	0.00	0.00	0.00	0.00	0.00	0.00	0.00	0.00	0.00	0.00	0.00	0.00
Papillae	0.00	0.00	0.00	0.00	0.00	0.00	0.00	0.00	0.00	0.00	0.00	0.00	0.00	0.00	0.00

Parallelepiped thin	0.00	0.00	0.00	0.00	0.00	0.00	0.00	0.00	0.00	0.00	0.00	1.89	0.00	0.00	0.00
Parenchyma strand	0.00	0.00	0.00	0.00	0.16	0.00	0.00	0.00	0.00	4.36	0.00	0.00	1.32	0.00	0.00
Platelet	0.00	0.00	0.00	0.85	0.96	0.00	0.25	0.00	0.27	0.21	0.00	0.00	0.00	0.00	0.00
Sclereid	0.00	0.00	0.00	0.85	0.00	0.00	0.00	0.00	0.09	0.35	0.00	0.00	0.00	0.19	0.00
GSSC bilobate tabular flattened-concave lobes	0.00	0.00	2.33	7.69	0.00	0.00	0.00	0.00	0.00	0.00	0.00	3.77	0.00	0.00	0.00
GSSC bilobate tabular flattened lobes	0.00	0.00	0.00	0.00	0.00	0.00	0.00	0.00	0.00	0.00	0.00	0.00	0.00	0.00	0.00
GSSC bilobate tabular rounded lobes, short shank	0.00	0.00	0.00	0.00	0.00	0.00	0.00	0.00	0.00	0.00	0.00	0.00	0.00	0.00	0.00
GSSC bilobate tabular rounded lobes, long shank	0.00	0.00	0.00	0.00	0.00	0.00	0.00	0.00	0.00	0.00	0.00	0.00	0.00	0.00	0.00
GSSC bilobate trapeziform notched lobes	0.00	0.00	0.00	0.00	0.00	0.00	0.00	0.00	0.00	0.00	0.00	0.00	0.00	0.00	0.00
GSSC bilobate tabular angulate lobes	0.00	0.00	0.00	0.00	0.00	0.00	0.00	0.00	0.00	0.00	0.00	0.00	0.00	0.00	0.00
GSSC bilobate tabular angulate asymmetrical lobes	0.00	0.00	0.00	0.00	0.00	0.00	0.00	0.00	0.00	0.00	0.00	0.00	0.00	0.00	0.00
GSSC bilobate tabular segmented angulate/planar lobes	0.00	0.00	0.00	0.00	0.00	0.00	0.00	0.00	0.00	0.00	0.00	0.00	0.00	0.00	0.00
GSSC bilobate trapezoid	0.00	0.00	0.00	0.00	0.00	0.00	0.00	0.00	0.00	0.00	0.00	0.00	0.00	0.00	0.00
GSSC bilobate trapezoid wavy top	0.00	0.00	0.00	0.00	0.00	0.00	0.00	0.00	0.00	0.00	0.00	0.00	0.00	0.00	0.00
GSSC cross trapeziform	0.00	0.00	0.00	0.00	0.00	0.00	0.00	0.00	0.00	0.00	0.00	0.00	0.00	0.00	0.00
GSSC cross tabular	0.00	0.00	0.00	0.00	0.00	0.00	0.00	0.00	0.00	0.00	0.00	0.00	0.00	0.00	0.00
GSSC trilobate	0.00	0.00	0.00	0.00	0.00	0.00	0.00	0.00	0.00	0.00	0.00	0.00	0.00	0.00	0.00
GSSC polylobate	0.00	0.00	0.00	0.00	0.00	0.00	0.00	0.00	0.00	0.00	0.00	0.00	0.00	0.00	0.00
GSSC rondel cilyndric	0.00	0.00	0.00	0.00	0.00	0.00	0.00	0.00	0.00	0.00	0.00	7.55	0.09	0.00	2.17
GSSC rondel conical	0.00	0.00	0.00	15.38	0.00	0.00	0.00	0.00	0.00	0.00	0.00	0.00	0.00	0.00	0.00
GSSC rondel conical wavy top	0.00	0.00	0.00	0.00	0.00	0.00	0.00	0.00	0.00	0.00	0.00	0.00	0.00	0.00	0.00

GSSC rondel keeled	0.00	0.00	0.00	0.00	0.00	0.00	0.00	0.00	0.00	0.00	0.00	0.00	0.00	0.00	0.00
GSSC long tower	0.00	0.00	0.00	0.00	0.00	0.00	0.00	0.00	0.00	0.00	0.00	0.00	0.00	0.00	0.00
GSSC long tower wavy top	0.00	0.00	0.00	0.00	0.00	0.00	0.00	0.00	0.00	0.00	0.00	0.00	0.00	0.00	0.00
GSSC trapeziform	0.00	0.00	0.00	0.00	0.00	0.00	0.00	0.00	0.00	0.00	0.00	7.55	0.00	0.00	0.00
GSSC oblong tabular	0.00	0.00	0.00	4.27	0.00	0.00	0.00	0.00	0.00	0.00	0.00	0.00	0.00	0.00	0.72
GSSC oblong trapeziform sinuous	0.00	0.00	0.00	0.00	0.00	0.00	0.00	0.00	0.00	0.00	0.00	0.00	0.00	0.00	0.00
GSSC round tabular	0.00	0.00	0.00	0.00	0.00	0.00	0.00	0.00	0.00	0.00	0.00	0.00	0.00	0.00	0.00
GSSC saddle	0.00	0.00	2.33	3.42	0.00	0.00	0.00	0.00	0.00	0.00	0.00	3.77	0.00	0.00	0.00
GSSC collapsed saddle	0.00	0.00	0.00	0.00	0.00	0.00	0.00	0.00	0.00	0.00	0.00	0.00	0.00	0.00	0.00
Spheroid psilate	25.00	0.00	23.26	15.38	0.48	57.59	0.00	37.84	8.10	10.86	32.61	7.55	0.00	2.43	1.45
Semi spheroids	0.00	0.00	4.65	1.71	0.88	0.00	0.00	0.00	0.00	0.62	0.54	0.00	0.00	0.00	0.00
Small spheroids	0.00	0.00	34.88	0.00	0.00	0.00	0.00	0.00	0.00	0.00	0.54	0.00	0.00	0.00	0.00
Large spheroid	0.00	0.00	0.00	0.00	0.00	4.02	0.00	0.00	0.00	0.00	0.00	0.00	0.00	0.00	0.00
Large spheroid facetate	25.00	0.00	0.00	0.00	0.00	0.00	0.00	0.00	0.00	0.00	0.00	0.00	0.00	0.00	0.00
Large spheroid granulate and verrucate	0.00	0.00	0.00	0.00	0.00	0.00	0.00	0.00	0.00	0.00	0.00	0.00	0.00	0.00	0.00
Spheroid spiraling decorations	0.00	0.00	0.00	0.00	0.00	0.00	0.00	0.00	0.00	0.00	0.00	0.00	0.00	0.00	0.00
Spheroid rugulate	0.00	0.00	0.00	0.00	0.00	0.00	0.00	0.00	0.00	0.41	1.63	0.00	0.00	0.00	0.00
Stomata	0.00	0.00	0.00	0.00	16.88	2.79	0.00	38.48	0.00	0.90	0.00	3.77	6.23	8.80	0.00
Tracheid	0.00	0.00	0.00	0.00	0.80	5.57	0.00	12.26	12.29	18.88	34.24	39.62	9.12	25.28	86.96

Table A1. Continued

Plant species	*Elytropappus rhinocerotis*	*Tarchonanthus camphoratus*	*Protea repens*	*Eriocephalus africanus*	*Protea lanceolata*	*Stoebe plumosa*	*HelIcrisum pandurifolium*	*Rhoicissus digitata*	*Metalasia muricata*	*Babiana fourcadei*	*Trachyandra sp*	*Tritonia crocata*	*Pelargonium triste*	*Watsonia laccata*	*Moraea unguiculata*
Sample description	**Eudicot - Leaves**	**Eudicot - Leaves**	**Eudicot - Leaves**	**Eudicot - Leaves**	**Eudicot - Leaves**	**Eudicot - Whole plant**	**Eudicot - Whole plant**	**Eudicot - Whole plant**	**Eudicot - Whole plant**	**Geophyte - Leaves**	**Geophyte - Leaves**	**Geophyte - Leaves**	**Geophyte - Leaves**	**Geophyte - Leaves**	**Geophyte - Leaves**
Bulliform	0.00	0.00	0.00	0.00	0.00	0.00	0.00	0.00	0.09	0.62	0.31	0.00	0.32	0.00	0.00
Blocky Polyhedral	3.64	0.00	0.49	0.00	0.00	0.00	0.00	0.00	0.00	4.32	4.00	3.56	5.71	6.79	1.95
Cone-shape	0.00	0.00	0.00	0.00	0.00	0.00	0.00	0.00	0.00	0.00	0.00	0.00	0.00	0.00	0.00
Cystolith	0.00	0.00	0.00	0.00	0.00	0.00	0.00	0.00	0.00	0.00	0.00	0.00	0.00	0.00	0.00
Ellipsoid	0.00	0.00	0.00	11.11	0.00	1.84	10.96	0.00	1.46	0.62	0.00	0.00	0.32	0.75	0.00
Ellipsoid echinate	0.00	0.00	0.00	0.00	0.00	0.00	0.00	0.00	0.00	1.85	0.00	0.00	0.00	0.00	0.00
Elongate	18.18	0.00	2.67	25.93	0.00	10.29	21.23	0.00	2.91	12.35	19.08	7.56	14.60	15.85	64.94
Elongate blocky	0.00	0.00	0.00	0.00	0.00	0.00	0.00	0.00	0.00	3.09	0.62	2.22	1.90	1.13	0.65
Elongate blocky echinate	0.00	0.00	0.00	0.00	0.00	0.00	0.00	0.00	0.00	0.00	0.00	0.00	0.00	0.00	0.00
Elongate blocky striate	0.00	0.00	0.00	0.00	0.00	0.00	4.11	0.00	0.64	0.00	0.00	0.00	0.00	0.00	0.00
Elongate bulbous	0.00	0.00	0.00	0.00	0.00	0.00	0.00	0.00	0.00	0.62	0.00	0.44	0.00	0.00	0.00
Elongate curved	0.00	0.00	0.00	0.00	0.00	0.00	0.00	0.00	0.00	0.00	0.00	0.00	0.00	0.00	0.00
Elongate facetate	0.00	0.00	0.00	0.00	3.85	0.00	4.11	0.00	0.55	0.00	5.85	0.89	2.86	1.51	4.87
Elongate striate	0.00	0.00	0.00	0.00	0.00	0.00	0.00	0.00	0.00	0.00	0.00	0.00	0.00	0.00	0.00
Elongate tuberculate	0.00	0.00	0.00	0.00	0.00	0.00	0.00	0.00	0.00	0.00	0.00	0.00	0.00	0.00	0.00
Elongate verrucate	0.00	0.00	0.00	0.00	0.00	0.00	0.00	0.00	0.00	0.00	0.00	0.00	0.00	0.00	0.00
Elongate dendritic	0.00	0.00	0.00	0.00	0.00	0.00	0.00	0.00	0.00	0.00	0.00	0.00	0.00	0.00	0.00

Elongate echinate	1.82	0.00	0.00	0.00	0.00	0.00	0.68	0.18	0.18	0.00	3.08	0.89	0.95	3.40	0.32
Elongate sinuate	0.00	0.00	0.00	0.00	0.00	0.00	0.00	0.00	0.00	0.00	0.00	0.00	0.00	0.00	0.65
Elongate polylobate	0.00	0.00	0.00	0.00	0.00	0.00	0.00	0.00	0.00	0.00	0.00	0.00	0.00	0.00	0.00
EGM	0.00	0.00	76.46	0.93	55.77	0.00	1.37	3.78	0.18	0.00	0.31	0.00	0.63	0.00	0.00
EGM elongate	0.00	0.00	0.00	0.00	0.00	27.21	0.00	0.00	81.71	0.00	0.00	0.00	0.00	0.00	0.00
EGM polyhedral	0.00	87.20	0.00	0.00	0.00	0.00	0.68	55.14	0.36	0.00	0.31	0.00	0.00	0.00	0.00
EGM sinuous	0.00	0.00	0.00	0.00	0.00	0.00	0.00	30.09	0.00	0.00	0.00	0.00	0.00	0.00	0.00
EGM rings	0.00	3.61	0.00	0.00	0.00	0.00	0.00	0.00	0.00	0.00	0.00	0.00	0.00	0.00	0.00
EGM dots	0.00	0.00	4.85	0.00	9.62	0.00	0.00	0.00	0.00	0.00	0.00	0.00	0.00	0.00	0.00
Hair cell (trichomes)	0.00	0.00	0.24	0.93	0.00	0.74	1.37	0.00	0.27	0.00	0.00	3.56	4.44	7.17	0.00
Hair cell (prickle)	0.00	0.00	0.00	6.48	0.00	0.00	2.05	0.00	0.36	1.23	3.69	3.11	3.49	4.91	0.00
Hair cell aciculate	0.00	0.00	0.00	0.00	0.00	0.00	0.00	0.00	0.00	0.00	0.92	0.00	0.00	0.00	0.00
Hair cell armed	0.00	0.00	0.00	0.00	0.00	0.00	0.00	0.00	0.00	0.00	0.00	0.00	0.00	0.00	0.00
Hair cell with protuberances	0.00	0.00	0.00	0.00	0.00	0.00	0.00	0.00	0.00	0.00	0.00	0.00	0.00	0.00	0.00
Hair cell curved	0.00	0.00	0.00	0.00	0.00	0.00	0.00	0.00	0.00	0.00	0.00	0.00	0.00	0.00	0.00
Hair cell unciform	0.00	0.00	0.00	0.00	0.00	0.00	0.00	0.00	0.00	0.00	0.00	0.00	0.00	0.00	0.00
Hair base	0.00	1.20	0.00	0.00	0.00	0.74	0.00	0.72	0.18	0.00	0.00	0.00	0.00	0.00	0.00
Hair base sinuous shape	0.00	0.00	0.00	0.00	0.00	0.00	0.00	0.00	0.00	0.00	0.00	0.00	0.00	0.00	0.00
Indetermined	0.00	0.00	0.00	0.00	0.00	0.00	0.68	0.00	0.09	0.00	0.31	0.00	0.00	0.00	0.32
Irregular	7.27	0.75	0.00	3.70	0.00	0.00	1.37	0.00	0.36	4.32	5.23	0.44	1.27	1.51	3.90
Irregular echinate	0.00	0.00	0.00	0.00	0.00	0.00	0.00	0.00	0.00	0.00	0.00	0.00	0.00	0.00	0.00
Irregular facetate	0.00	0.00	0.00	0.00	0.00	0.00	0.00	0.00	0.00	0.00	0.00	0.00	0.00	0.00	0.32
Papillae	0.00	0.00	0.00	0.00	0.00	0.00	0.00	0.00	0.00	1.23	0.31	0.00	0.95	0.75	0.00
Parallelepiped thin	0.00	0.00	0.00	0.00	0.00	0.00	0.00	0.00	0.00	0.00	0.00	0.00	0.32	0.75	2.27
Parenchyma strand	0.00	0.00	0.00	0.00	0.00	0.00	0.68	0.00	0.09	0.00	0.00	0.89	0.32	0.00	8.44

Platelet	1.82	0.00	0.00	0.00	0.00	0.00	0.00	0.00	0.00	0.00	0.00	0.00	0.00	0.00	0.00
Sclereid	0.00	0.30	0.00	0.00	0.00	16.91	0.68	0.00	0.09	0.00	0.00	0.00	0.00	0.00	0.00
GSSC bilobate tabular flattened-concave lobes	5.45	0.00	0.00	1.85	0.00	0.00	0.00	0.00	0.18	16.67	14.46	52.44	16.51	11.32	3.57
GSSC bilobate tabular flattened lobes	0.00	0.00	0.00	0.00	0.00	0.00	1.37	0.00	0.00	0.00	0.00	0.00	0.00	0.00	0.00
GSSC bilobate tabular rounded lobes, short shank	0.00	0.00	0.00	0.00	0.00	0.00	0.00	0.00	0.00	0.00	0.00	0.00	0.00	0.00	0.00
GSSC bilobate tabular rounded lobes, long shank	0.00	0.00	0.00	0.00	0.00	0.00	0.00	0.00	0.00	0.00	0.00	0.00	0.00	0.00	0.00
GSSC bilobate trapeziform notched lobes	0.00	0.00	0.00	0.00	0.00	0.00	0.00	0.00	0.00	0.00	0.00	0.00	0.00	0.00	0.00
GSSC bilobate tabular angulate lobes	0.00	0.00	0.00	0.00	0.00	0.00	0.00	0.00	0.00	0.00	0.00	0.00	0.00	0.00	0.00
GSSC bilobate tabular angulate asymmetrical lobes	0.00	0.00	0.00	0.00	0.00	0.00	0.00	0.00	0.00	0.00	0.00	0.00	0.00	0.00	0.00
GSSC bilobate tabular segmented angulate/planar lobes	0.00	0.00	0.00	0.00	0.00	0.00	0.00	0.00	0.00	0.00	0.00	0.00	0.00	0.00	0.00
GSSC bilobate trapezoid	0.00	0.00	0.00	0.00	0.00	0.00	0.00	0.00	0.00	0.00	0.31	0.00	0.00	0.00	0.00
GSSC bilobate trapezoid wavy top	0.00	0.00	0.00	0.00	0.00	0.00	0.00	0.00	0.00	0.00	0.00	0.00	0.00	0.00	0.00
GSSC cross trapeziform	0.00	0.00	0.00	0.00	0.00	0.00	0.68	0.00	0.09	0.00	0.00	0.00	0.00	0.00	0.00
GSSC cross tabular	0.00	0.00	0.00	0.00	0.00	0.00	0.00	0.00	0.00	2.47	1.23	0.44	0.32	0.38	0.00
GSSC trilobate	0.00	0.00	0.00	0.00	0.00	0.00	0.00	0.00	0.00	0.00	0.00	0.00	0.00	0.00	0.00
GSSC polylobate	0.00	0.00	0.00	0.00	0.00	0.00	0.00	0.00	0.00	0.00	0.00	0.00	0.00	0.00	0.00
GSSC rondel cilyndric	18.18	0.00	0.00	7.41	0.00	0.37	3.42	0.00	0.00	0.00	0.00	0.00	0.00	0.00	0.00
GSSC rondel conical	0.00	0.00	0.00	0.00	0.00	0.00	0.00	0.00	0.55	24.07	22.15	9.33	28.25	25.28	2.60
GSSC rondel conical wavy top	0.00	0.00	0.00	0.00	0.00	0.00	0.68	0.00	0.09	0.00	0.00	0.00	0.32	0.00	0.00
GSSC rondel keeled	0.00	0.00	0.00	0.00	0.00	0.00	0.00	0.00	0.00	0.00	0.00	0.00	0.00	0.00	0.00
GSSC long tower	0.00	0.00	0.00	0.00	0.00	0.00	0.00	0.00	0.00	0.00	0.31	0.00	0.00	0.38	0.00

GSSC long tower wavy top	0.00	0.00	0.00	0.00	0.00	0.00	0.00	0.00	0.00	0.00	0.00	0.00	0.00	0.00	0.00
GSSC trapeziform	0.00	0.00	0.00	0.00	0.00	0.00	1.37	0.00	0.18	1.23	0.92	0.00	1.27	1.89	0.65
GSSC oblong tabular	0.00	0.00	0.00	1.85	0.00	0.00	2.05	0.00	0.27	4.94	1.54	0.89	2.86	1.51	0.00
GSSC oblong trapeziform sinuous	0.00	0.00	0.00	0.00	0.00	0.00	0.00	0.00	0.00	0.00	0.92	0.00	0.00	0.00	0.00
GSSC round tabular	0.00	0.00	0.00	0.00	0.00	0.00	0.00	0.00	0.00	0.00	0.00	0.00	0.32	0.00	0.00
GSSC saddle	1.82	0.00	0.00	0.00	0.00	0.74	0.00	0.00	0.00	0.62	3.08	1.33	3.81	5.28	0.00
GSSC collapsed saddle	0.00	0.00	0.00	0.00	0.00	0.00	0.00	0.00	0.00	1.23	0.00	0.00	0.00	0.00	0.00
Spheroid psilate	20.00	0.00	6.07	19.44	3.85	23.53	36.30	0.54	5.10	14.81	3.38	0.44	0.32	7.92	1.30
Semi spheroids	1.82	0.00	0.00	0.00	0.00	0.74	0.00	0.00	0.00	0.00	0.00	0.00	0.00	0.00	0.00
Small spheroids	0.00	0.00	0.00	18.52	0.00	0.00	0.00	0.00	0.00	0.00	0.00	0.00	0.00	0.00	0.00
Large spheroid	0.00	0.00	0.00	0.00	0.00	3.68	0.00	0.00	0.00	0.00	0.00	0.00	0.00	0.00	0.00
Large spheroid facetate	0.00	0.00	0.00	0.00	0.00	0.00	0.00	0.00	0.00	0.00	0.00	0.00	0.00	0.00	0.00
Large spheroid granulate and verrucate	0.00	0.00	0.00	0.00	0.00	0.00	0.00	0.00	0.00	1.23	5.54	1.78	6.35	0.38	1.95
Spheroid spiraling decorations	0.00	0.00	0.00	0.00	0.00	0.00	0.00	0.00	0.00	0.00	0.00	0.00	0.00	0.00	0.00
Spheroid rugulate	0.00	0.00	0.00	0.00	0.00	0.00	0.00	0.00	0.00	0.62	1.54	3.11	1.27	1.13	0.00
Stomata	0.00	0.00	0.00	0.00	0.00	0.74	0.00	0.90	3.09	0.00	0.00	0.00	0.00	0.00	0.00
Tracheid	20.00	6.93	9.22	1.85	26.92	12.50	4.11	8.65	0.91	1.85	0.62	6.67	0.32	0.00	1.30

Table A1. continued

Plant species	*Moraea sp*	*Freesia alba*	*Gladiolus rogersii*	*Cynella hyacinthoides*	*Albuca maxima*	*Tritoniopsis antholyza*	*Watsonia fourcadei*	*Babiana fourcadei*	*Tritonia crocata*	*Pelargonium triste*	*Watsonia laccata*	*Moraea unguiculata*	*Moraea sp*	*Freesia alba*	*Cynella hyacinthoides*
Sample description	**Geophyte - Leaves**	**Geophyte - Leaves**	**Geophyte - Leaves**	**Geophyte - Leaves**	**Geophyte - Leaves**	**Geophyte - Leaves**	**Geophyte - Leaves**	**Geophyte - Bulb**	**Geophyte - Bulb**	**Geophyte - Bulb**	**Geophyte - Bulb**	**Geophyte - Bulb**	**Geophyte - Bulb**	**Geophyte - Bulb**	**Geophyte - Bulb**
Bulliform	0.00	0.00	0.00	0.72	0.00	0.00	0.00	0.00	0.00	7.92	0.00	0.00	0.00	0.00	0.00
Blocky Polyhedral	2.67	13.64	0.00	1.44	0.00	3.73	0.00	0.00	25.00	0.00	0.00	0.00	18.18	0.00	0.00
Cone-shape	0.00	0.00	0.00	0.00	0.00	0.00	0.00	11.11	0.00	0.00	0.00	0.00	0.00	0.00	0.00
Cystolith	0.00	0.00	0.00	0.00	0.00	0.00	0.00	0.00	0.00	0.00	0.00	0.00	0.00	0.00	0.00
Ellipsoid	1.21	0.00	0.00	0.72	0.00	1.24	0.00	0.00	0.00	0.00	0.00	0.00	0.00	0.00	0.00
Ellipsoid echinate	0.00	0.00	0.00	0.00	0.00	0.00	0.00	0.00	0.00	0.00	0.00	0.00	0.00	0.00	0.00
Elongate	53.64	9.09	63.64	17.27	6.90	25.73	14.81	0.00	0.00	22.77	8.33	0.00	18.18	0.00	8.33
Elongate blocky	0.49	0.00	4.55	0.00	0.00	2.49	3.70	11.11	0.00	0.00	0.00	0.00	0.00	0.00	0.00
Elongate blocky echinate	0.00	0.00	0.00	0.00	0.00	0.00	0.00	0.00	0.00	0.00	0.00	0.00	0.00	0.00	0.00
Elongate blocky striate	0.00	0.00	0.00	0.00	0.00	0.00	0.00	0.00	0.00	0.00	0.00	0.00	0.00	0.00	0.00
Elongate bulbous	0.00	0.00	0.00	0.00	0.00	0.00	0.00	0.00	0.00	0.00	0.00	0.00	0.00	0.00	0.00
Elongate curved	0.00	0.00	0.00	1.44	0.00	0.00	0.00	0.00	0.00	0.00	0.00	0.00	0.00	0.00	0.00
Elongate facetate	0.24	0.00	0.00	0.72	0.00	0.00	0.00	0.00	0.00	0.99	0.00	0.00	0.00	0.00	0.00
Elongate striate	0.00	0.00	0.00	0.00	0.00	0.00	3.70	0.00	0.00	0.00	0.00	0.00	0.00	0.00	0.00
Elongate tuberculate	0.00	0.00	0.00	0.00	0.00	0.00	0.00	0.00	0.00	0.00	0.00	0.00	0.00	0.00	0.00
Elongate verrucate	0.00	0.00	0.00	0.00	0.00	0.00	0.00	0.00	0.00	0.00	0.00	0.00	0.00	0.00	0.00
Elongate dendritic	0.00	0.00	0.00	0.00	0.00	0.00	0.00	0.00	0.00	0.00	0.00	0.00	0.00	0.00	0.00

Elongate echinate	0.49	4.55	0.00	2.88	3.45	1.66	0.00	0.00	0.00	2.97	0.00	0.00	4.55	0.00	0.00
Elongate sinuate	0.00	0.00	0.00	0.00	0.00	0.00	0.00	0.00	0.00	0.00	0.00	0.00	0.00	0.00	0.00
Elongate polylobate	0.00	0.00	0.00	0.72	0.00	0.00	0.00	0.00	0.00	0.00	0.00	0.00	0.00	0.00	0.00
EGM	0.00	0.00	2.27	1.44	0.00	2.90	0.00	0.00	0.00	0.00	0.00	0.00	0.00	0.00	0.00
EGM elongate	12.86	0.00	0.00	0.00	0.00	0.00	0.00	0.00	0.00	0.00	0.00	0.00	0.00	0.00	0.00
EGM polyhedral	0.00	0.00	0.00	0.00	0.00	0.00	0.00	0.00	0.00	0.00	0.00	0.00	0.00	0.00	0.00
EGM sinuous	0.00	0.00	0.00	0.00	0.00	0.00	0.00	0.00	0.00	0.00	0.00	0.00	0.00	0.00	0.00
EGM rings	0.00	0.00	0.00	0.00	0.00	0.00	0.00	0.00	0.00	0.00	0.00	0.00	0.00	0.00	0.00
EGM dots	0.00	0.00	0.00	0.00	0.00	0.00	0.00	0.00	0.00	0.00	0.00	0.00	0.00	0.00	0.00
Hair cell (trichomes)	0.73	4.55	2.27	0.72	0.00	0.00	0.00	0.00	0.00	0.99	8.33	0.00	0.00	0.00	0.00
Hair cell (prickle)	0.49	0.00	0.00	2.16	3.45	2.49	0.00	22.22	25.00	4.95	0.00	0.00	4.55	0.00	8.33
Hair cell aciculate	0.00	0.00	0.00	0.00	0.00	0.00	0.00	0.00	0.00	0.00	0.00	0.00	0.00	0.00	0.00
Hair cell armed	0.00	0.00	0.00	0.00	0.00	0.00	0.00	0.00	0.00	0.00	0.00	0.00	0.00	0.00	0.00
Hair cell with protuberances	0.00	0.00	0.00	0.00	0.00	0.00	0.00	0.00	0.00	0.00	0.00	0.00	0.00	0.00	0.00
Hair cell curved	0.00	0.00	0.00	0.00	0.00	0.00	0.00	0.00	0.00	0.00	0.00	0.00	0.00	0.00	0.00
Hair cell unciform	0.00	0.00	0.00	0.00	0.00	0.00	0.00	0.00	0.00	0.00	0.00	0.00	0.00	0.00	0.00
Hair base	0.00	0.00	0.00	0.00	0.00	0.00	0.00	0.00	0.00	0.00	0.00	0.00	0.00	0.00	0.00
Hair base sinuous shape	0.00	0.00	0.00	0.00	0.00	0.00	0.00	0.00	0.00	0.00	0.00	0.00	0.00	0.00	0.00
Indetermined	0.00	0.00	0.00	0.00	0.00	0.00	7.41	0.00	0.00	0.00	0.00	0.00	0.00	0.00	0.00
Irregular	0.73	13.64	0.00	3.60	3.45	5.81	25.93	33.33	0.00	4.95	8.33	0.00	13.64	0.00	41.67
Irregular echinate	0.00	0.00	0.00	0.00	0.00	0.00	0.00	0.00	0.00	0.00	0.00	0.00	0.00	0.00	0.00
Irregular facetate	0.00	0.00	0.00	0.00	0.00	0.00	0.00	0.00	0.00	0.00	0.00	0.00	0.00	0.00	0.00
Papillae	0.00	0.00	0.00	0.00	0.00	0.41	0.00	0.00	0.00	0.99	0.00	0.00	0.00	0.00	0.00
Parallelepiped thin	0.00	0.00	0.00	0.00	0.00	0.00	0.00	0.00	0.00	0.00	0.00	0.00	0.00	0.00	0.00
Parenchyma strand	0.49	9.09	4.55	3.60	0.00	0.00	0.00	0.00	0.00	0.00	0.00	0.00	0.00	0.00	0.00

Platelet	0.00	0.00	0.00	0.00	0.00	0.00	0.00	0.00	50.00	0.00	0.00	0.00	0.00	0.00	0.00
Sclereid	0.00	0.00	0.00	0.00	0.00	0.41	0.00	0.00	0.00	0.00	0.00	0.00	0.00	0.00	0.00
GSSC bilobate tabular flattened-concave lobes	2.43	4.55	2.27	10.79	41.38	9.54	3.70	0.00	0.00	13.86	0.00	0.00	4.55	0.00	0.00
GSSC bilobate tabular flattened lobes	0.00	0.00	0.00	0.00	0.00	0.00	0.00	0.00	0.00	0.00	0.00	0.00	0.00	0.00	0.00
GSSC bilobate tabular rounded lobes, short shank	0.00	0.00	0.00	0.00	0.00	0.00	0.00	0.00	0.00	0.00	0.00	0.00	0.00	0.00	0.00
GSSC bilobate tabular rounded lobes, long shank	0.00	0.00	0.00	0.00	0.00	0.00	0.00	0.00	0.00	0.00	0.00	0.00	0.00	0.00	0.00
GSSC bilobate trapeziform notched lobes	0.00	0.00	0.00	0.00	0.00	0.00	0.00	0.00	0.00	0.00	0.00	0.00	0.00	0.00	0.00
GSSC bilobate tabular angulate lobes	0.00	0.00	0.00	0.00	0.00	0.00	0.00	0.00	0.00	0.00	0.00	0.00	0.00	0.00	0.00
GSSC bilobate tabular angulate asymmetrical lobes	0.00	0.00	0.00	0.00	0.00	0.00	0.00	0.00	0.00	0.00	0.00	0.00	0.00	0.00	0.00
GSSC bilobate tabular segmented angulate/planar lobes	0.00	0.00	0.00	0.00	0.00	0.00	0.00	0.00	0.00	0.00	0.00	0.00	0.00	0.00	0.00
GSSC bilobate trapezoid	0.00	0.00	0.00	0.00	0.00	0.41	0.00	0.00	0.00	0.00	0.00	0.00	0.00	0.00	0.00
GSSC bilobate trapezoid wavy top	0.00	0.00	0.00	0.00	0.00	0.00	0.00	0.00	0.00	0.00	0.00	0.00	0.00	0.00	0.00
GSSC cross trapeziform	0.00	0.00	0.00	0.00	0.00	0.00	0.00	0.00	0.00	0.00	0.00	0.00	0.00	0.00	0.00
GSSC cross tabular	0.00	0.00	0.00	0.00	0.00	0.00	0.00	0.00	0.00	0.00	0.00	0.00	0.00	0.00	0.00
GSSC trilobate	0.00	0.00	0.00	0.00	0.00	0.00	0.00	0.00	0.00	0.00	0.00	0.00	0.00	0.00	0.00
GSSC polylobate	0.00	0.00	0.00	0.00	0.00	0.00	0.00	0.00	0.00	0.00	0.00	0.00	0.00	0.00	0.00
GSSC rondel cilyndric	0.00	0.00	0.00	0.00	0.00	0.00	0.00	0.00	0.00	0.00	0.00	0.00	0.00	0.00	0.00
GSSC rondel conical	10.68	4.55	2.27	22.30	17.24	26.14	14.81	22.22	0.00	23.76	0.00	0.00	9.09	4.17	0.00
GSSC rondel conical wavy top	0.00	0.00	0.00	0.00	0.00	0.00	0.00	0.00	0.00	0.00	0.00	0.00	0.00	0.00	0.00
GSSC rondel keeled	0.00	0.00	0.00	0.00	0.00	0.00	0.00	0.00	0.00	0.00	0.00	0.00	0.00	0.00	0.00
GSSC long tower	0.00	0.00	0.00	0.00	0.00	1.24	0.00	0.00	0.00	2.97	0.00	0.00	0.00	0.00	0.00

GSSC long tower wavy top	0.00	0.00	0.00	0.00	0.00	0.00	0.00	0.00	0.00	0.00	0.00	0.00	0.00	0.00	0.00
GSSC trapeziform	1.46	0.00	0.00	0.72	3.45	0.83	0.00	0.00	0.00	4.95	0.00	0.00	0.00	0.00	0.00
GSSC oblong tabular	0.49	0.00	0.00	2.16	3.45	2.07	0.00	0.00	0.00	0.00	0.00	0.00	0.00	0.00	0.00
GSSC oblong trapeziform sinuous	0.00	0.00	0.00	0.72	0.00	0.00	0.00	0.00	0.00	0.00	0.00	0.00	0.00	0.00	0.00
GSSC round tabular	0.00	0.00	0.00	0.00	3.45	0.41	0.00	0.00	0.00	0.00	0.00	0.00	0.00	0.00	0.00
GSSC saddle	0.73	0.00	0.00	2.88	3.45	0.41	0.00	0.00	0.00	1.98	0.00	0.00	18.18	0.00	0.00
GSSC collapsed saddle	0.00	0.00	0.00	0.00	0.00	0.00	0.00	0.00	0.00	0.00	0.00	0.00	0.00	0.00	0.00
Spheroid psilate	4.85	4.55	6.82	10.79	0.00	4.15	25.93	0.00	0.00	4.95	58.33	0.00	0.00	95.83	33.33
Semi spheroids	0.00	0.00	0.00	0.00	0.00	0.00	0.00	0.00	0.00	0.00	8.33	0.00	4.55	0.00	0.00
Small spheroids	0.00	0.00	0.00	0.00	0.00	0.00	0.00	0.00	0.00	0.00	0.00	100.00	4.55	0.00	0.00
Large spheroid	0.00	0.00	0.00	0.00	0.00	0.00	0.00	0.00	0.00	0.00	8.33	0.00	0.00	0.00	0.00
Large spheroid facetate	0.00	0.00	0.00	0.00	0.00	0.00	0.00	0.00	0.00	0.00	0.00	0.00	0.00	0.00	0.00
Large spheroid granulate and verrucate	0.73	0.00	2.27	2.16	3.45	1.24	0.00	0.00	0.00	0.00	0.00	0.00	0.00	0.00	8.33
Spheroid spiraling decorations	0.00	0.00	0.00	0.00	0.00	0.00	0.00	0.00	0.00	0.00	0.00	0.00	0.00	0.00	0.00
Spheroid rugulate	0.73	4.55	4.55	1.44	0.00	5.81	0.00	0.00	0.00	0.00	0.00	0.00	0.00	0.00	0.00
Stomata	0.00	0.00	0.00	0.00	0.00	0.00	0.00	0.00	0.00	0.00	0.00	0.00	0.00	0.00	0.00
Tracheid	3.88	27.27	4.55	8.63	6.90	0.83	0.00	0.00	0.00	0.99	0.00	0.00	0.00	0.00	0.00

Table A1. continued

Plant species	*Tritoniopsis antholyza*	*Babiana fourcadei*	*Tritonia crocata*	*Watsonia laccata*	*Moraea unguiculata*	*Moraea sp*	*Cynella hyacinthoides*	*Albuca maxima*	*Tritoniopsis antholyza*	*Watsonia fourcadei*	*Boophaene disticha*	*Setaria sphacelata*	*Tristachya leucotrix*	*Stenotaphrum secundatum*	*Heteropogon contortus*
Sample description	**Geophyte - Bulb**	**Geophyte - Bulb scale leaves**	**Geophyte - Bulb scale leaves**	**Geophyte - Bulb scale leaves**	**Geophyte - Bulb scale leaves**	**Geophyte - Bulb scale leaves**	**Geophyte - Bulb scale leaves**	**Geophyte - Bulb scale leaves**	**Geophyte - Bulb scale leaves**	**Geophyte - Bulb scale leaves**	**Leaves medicinal plant**	**Poaceae C4**	**Poaceae C4**	**Poaceae C4**	**Poaceae C4**
Bulliform	0.00	0.00	0.35	0.00	0.59	0.00	0.00	4.14	1.03	0.00	0.00	0.45	0.00	9.90	0.12
Blocky Polyhedral	0.00	3.72	4.56	5.60	6.80	0.00	0.00	0.69	5.15	0.00	8.00	0.00	0.00	0.19	0.00
Cone-shape	0.00	0.00	0.00	0.00	0.00	0.00	0.00	0.00	0.00	3.45	0.00	0.00	0.00	0.00	0.00
Cystolith	0.00	0.00	0.00	0.00	0.00	0.00	0.00	0.00	0.00	0.00	0.00	0.00	0.00	0.00	0.00
Ellipsoid	0.00	0.00	0.70	0.00	0.00	0.00	0.00	0.00	0.00	0.00	0.00	0.00	0.00	0.00	0.00
Ellipsoid echinate	0.00	0.00	0.00	0.00	0.00	0.00	0.00	0.00	0.00	0.00	0.00	0.00	0.00	0.00	0.00
Elongate	0.00	16.53	17.19	13.81	20.41	27.27	22.58	22.07	37.63	13.79	16.80	5.87	1.31	3.30	1.45
Elongate blocky	2.78	3.31	1.05	0.37	0.59	0.00	0.00	0.00	4.12	0.00	2.40	0.00	0.00	0.00	0.00
Elongate blocky echinate	0.00	0.83	0.00	0.00	0.00	0.00	0.00	0.00	0.00	0.00	0.00	0.00	0.00	0.00	0.00
Elongate blocky striate	0.00	0.00	0.00	0.00	0.00	0.00	0.00	0.00	0.00	0.00	0.00	0.00	0.00	0.00	0.00
Elongate bulbous	0.00	0.00	0.00	0.00	0.00	0.00	0.00	0.00	0.00	0.00	0.80	0.00	0.00	0.00	0.00
Elongate curved	0.00	0.00	0.00	0.00	0.00	0.00	0.00	0.00	0.00	0.00	0.00	0.00	0.00	0.00	0.00
Elongate facetate	0.00	1.65	1.05	3.73	0.00	0.00	0.00	0.00	1.03	6.90	0.80	0.00	0.00	0.00	0.00
Elongate striate	0.00	0.00	0.00	0.00	0.00	0.00	0.00	0.00	0.00	0.00	0.00	0.00	0.00	0.00	0.00
Elongate tuberculate	0.00	0.00	0.00	0.00	0.00	0.00	0.00	0.00	0.00	0.00	0.00	0.00	0.00	0.00	0.00
Elongate verrucate	0.00	0.00	0.00	0.00	0.00	0.00	0.00	0.00	0.00	0.00	0.00	0.00	0.00	0.00	0.00

Elongate dendritic	0.00	0.00	0.00	0.37	0.00	0.00	0.00	0.00	0.00	0.00	0.00	0.00	0.00	0.00	0.00
Elongate echinate	0.00	1.24	1.40	1.49	0.00	0.00	3.23	2.76	0.52	0.00	1.60	0.00	1.31	2.52	2.30
Elongate sinuate	0.00	0.00	0.00	0.00	0.00	0.00	0.00	0.00	0.00	0.00	0.00	29.42	21.44	0.00	41.07
Elongate polylobate	0.00	0.00	0.35	0.00	0.00	0.00	0.00	0.69	0.00	0.00	1.60	0.00	0.00	0.58	0.00
EGM	0.00	0.00	0.00	0.00	0.00	0.00	0.00	0.00	0.00	0.00	0.00	0.00	0.00	0.00	0.00
EGM elongate	0.00	0.00	0.00	0.00	0.00	0.00	0.00	0.00	0.00	0.00	0.00	0.00	0.00	0.00	0.00
EGM polyhedral	0.00	0.00	0.00	0.00	0.00	0.00	0.00	0.00	0.00	3.45	0.80	0.00	0.00	0.00	0.00
EGM sinuous	0.00	0.00	0.00	0.00	0.00	0.00	0.00	0.00	0.00	0.00	0.00	0.00	0.00	0.00	0.00
EGM rings	0.00	0.00	0.00	0.00	0.00	0.00	0.00	0.00	0.00	0.00	0.00	0.00	0.00	0.00	0.00
EGM dots	0.00	0.00	0.00	0.00	0.00	0.00	0.00	0.00	0.00	0.00	0.00	0.00	0.00	0.00	0.00
Hair cell (trichomes)	0.00	0.41	1.05	5.60	0.00	0.00	0.00	2.76	0.00	0.00	2.40	2.71	8.83	0.78	2.42
Hair cell (prickle)	0.00	7.02	4.21	7.46	5.92	0.00	1.61	6.90	3.09	3.45	1.60	0.00	0.29	0.19	0.12
Hair cell aciculate	0.00	0.00	0.00	0.00	0.00	0.00	0.00	0.00	0.00	0.00	0.00	0.00	0.00	0.00	0.00
Hair cell armed	0.00	0.00	0.00	0.00	0.00	0.00	0.00	0.00	0.00	0.00	0.00	0.00	0.00	0.00	0.00
Hair cell with protuberances	0.00	0.00	0.00	0.00	0.00	0.00	0.00	0.00	0.00	0.00	0.00	0.00	0.00	0.00	0.00
Hair cell curved	0.00	0.00	0.00	0.00	0.00	0.00	0.00	0.00	0.00	0.00	0.00	0.00	0.00	0.00	0.00
Hair cell unciform	2.78	0.00	0.00	0.00	0.00	0.00	0.00	0.00	0.00	0.00	0.00	0.00	0.00	0.00	0.00
Hair base	0.00	0.00	0.00	0.00	0.00	0.00	0.00	0.00	0.00	0.00	0.00	0.00	0.00	0.00	0.00
Hair base sinuous shape	0.00	0.00	0.00	0.00	0.00	0.00	0.00	0.00	0.00	0.00	0.00	0.00	0.00	0.00	0.00
Indetermined	47.22	0.41	0.00	0.00	0.00	0.00	0.00	1.38	0.52	0.00	0.00	0.00	0.80	0.00	0.48
Irregular	47.22	1.65	5.26	2.24	10.36	18.18	12.90	11.03	0.52	27.59	0.00	0.00	0.00	0.00	0.00
Irregular echinate	0.00	0.00	0.00	0.00	1.48	4.55	0.00	0.00	0.00	0.00	0.00	0.00	0.00	0.00	0.00
Irregular facetate	0.00	0.00	0.00	0.00	0.00	0.00	0.00	0.00	0.00	0.00	0.00	0.00	0.00	0.00	0.00
Papillae	0.00	0.41	0.00	0.37	0.30	0.00	0.00	0.00	0.00	0.00	0.00	0.00	0.00	0.00	0.00
Parallelepiped thin	0.00	0.00	0.00	0.37	0.00	0.00	0.00	0.00	0.00	0.00	0.00	0.00	0.00	0.00	0.00

Parenchyma strand	0.00	0.00	0.00	0.00	0.00	0.00	0.00	0.00	0.00	0.00	0.00	0.00	0.00	0.00	0.00
Platelet	0.00	0.00	0.00	0.00	0.00	0.00	1.61	0.00	0.00	0.00	0.00	0.00	0.00	0.00	0.00
Sclereid	0.00	0.00	0.00	0.00	0.00	0.00	0.00	0.00	0.52	0.00	0.00	0.00	0.00	0.00	0.00
GSSC bilobate tabular flattened-concave lobes	0.00	16.94	12.28	12.69	9.76	0.00	4.84	9.66	7.22	3.45	12.80	4.60	1.39	67.77	34.89
GSSC bilobate tabular flattened lobes	0.00	0.00	0.00	0.00	0.00	0.00	0.00	0.00	0.00	0.00	0.00	22.20	40.18	0.00	10.18
GSSC bilobate tabular rounded lobes, short shank	0.00	0.00	0.00	0.00	0.00	0.00	0.00	0.00	0.00	0.00	0.00	13.90	9.19	0.00	0.00
GSSC bilobate tabular rounded lobes, long shank	0.00	0.00	0.00	0.00	0.00	0.00	0.00	0.00	0.00	0.00	0.00	0.00	0.00	0.00	2.06
GSSC bilobate trapeziform notched lobes	0.00	0.00	0.00	0.00	0.00	0.00	0.00	0.00	0.00	0.00	0.00	0.99	11.82	0.00	0.48
GSSC bilobate tabular angulate lobes	0.00	0.00	0.00	0.00	0.00	0.00	0.00	0.00	0.00	0.00	0.00	0.00	0.00	0.00	0.00
GSSC bilobate tabular angulate asymmetrical lobes	0.00	0.00	0.00	0.00	0.00	0.00	0.00	0.00	0.00	0.00	0.00	0.00	0.00	0.00	0.00
GSSC bilobate tabular segmented angulate/planar lobes	0.00	0.00	0.00	0.00	0.00	0.00	0.00	0.00	0.00	0.00	0.00	0.00	0.00	0.00	0.00
GSSC bilobate trapezoid	0.00	0.00	0.00	0.00	0.59	0.00	0.00	0.00	0.52	0.00	0.80	2.26	0.00	13.01	0.00
GSSC bilobate trapezoid wavy top	0.00	0.00	0.00	0.00	0.00	0.00	0.00	0.00	0.00	0.00	0.00	0.00	0.00	0.00	0.00
GSSC cross trapeziform	0.00	0.00	0.00	0.00	0.00	0.00	0.00	0.00	0.00	0.00	0.80	1.44	0.22	0.00	0.24
GSSC cross tabular	0.00	0.41	0.00	0.00	0.89	0.00	1.61	0.00	0.00	0.00	0.00	0.00	0.00	0.00	0.00
GSSC trilobate	0.00	0.00	0.00	0.00	0.00	0.00	0.00	0.00	0.00	0.00	0.00	0.00	1.02	0.00	0.12
GSSC polylobate	0.00	0.00	0.00	0.00	0.00	0.00	0.00	0.00	0.00	0.00	0.00	0.00	0.00	0.00	0.00
GSSC rondel cilyndric	0.00	0.00	0.00	0.00	0.00	0.00	0.00	0.00	0.00	0.00	0.00	0.00	0.00	0.00	0.00
GSSC rondel conical	0.00	28.93	33.33	30.97	26.04	18.18	25.81	26.90	21.65	10.34	32.00	0.00	0.00	1.55	0.55
GSSC rondel conical wavy top	0.00	0.00	0.35	0.00	0.00	0.00	0.00	0.00	0.00	0.00	0.00	0.00	0.00	0.00	0.00
GSSC rondel keeled	0.00	0.00	0.00	0.00	0.00	0.00	0.00	0.00	0.00	0.00	0.00	0.00	0.00	0.00	0.00

GSSC long tower	0.00	0.83	0.70	0.37	0.59	0.00	0.00	0.00	0.00	0.00	0.00	0.00	0.00	0.00	0.00
GSSC long tower wavy top	0.00	0.00	0.00	0.00	0.00	0.00	0.00	0.00	0.00	0.00	0.00	0.00	0.00	0.00	0.00
GSSC trapeziform	0.00	0.41	2.11	2.61	5.33	4.55	9.68	3.45	0.00	6.90	0.80	0.00	0.00	0.00	0.00
GSSC oblong tabular	0.00	3.31	1.40	2.24	2.66	0.00	0.00	0.00	0.52	0.00	3.20	0.00	0.00	0.00	0.00
GSSC oblong trapeziform sinuous	0.00	0.00	0.00	0.00	0.00	0.00	0.00	0.00	0.00	0.00	0.00	0.00	0.00	0.00	0.00
GSSC round tabular	0.00	0.41	0.00	0.00	0.00	0.00	0.00	0.00	0.00	0.00	0.00	0.00	0.00	0.00	0.00
GSSC saddle	0.00	8.26	2.46	5.60	0.59	9.09	0.00	2.07	1.55	0.00	7.20	0.00	0.00	0.00	0.00
GSSC collapsed saddle	0.00	0.00	0.00	0.00	0.00	0.00	0.00	0.00	0.00	0.00	0.00	0.00	0.00	0.00	0.00
Spheroid psilate	0.00	0.41	6.67	0.37	3.55	0.00	0.00	0.00	2.06	20.69	0.00	16.16	0.00	0.00	0.00
Semi spheroids	0.00	0.00	0.00	0.00	0.00	0.00	1.61	0.00	0.00	0.00	0.00	0.00	0.00	0.00	0.00
Small spheroids	0.00	0.00	0.00	0.37	0.00	0.00	0.00	2.07	0.00	0.00	0.00	0.00	0.00	0.00	0.00
Large spheroid	0.00	0.00	0.00	0.00	0.00	0.00	0.00	0.00	0.00	0.00	0.00	0.00	0.00	0.00	0.00
Large spheroid facetate	0.00	0.00	0.00	0.00	0.00	0.00	0.00	0.00	0.00	0.00	0.00	0.00	0.00	0.00	0.00
Large spheroid granulate and verrucate	0.00	1.65	2.81	2.24	2.96	13.64	12.90	3.45	3.09	0.00	2.40	0.00	0.00	0.00	0.00
Spheroid spiraling decorations	0.00	0.00	0.00	0.00	0.00	0.00	0.00	0.00	0.00	0.00	0.00	0.00	0.00	0.00	0.00
Spheroid rugulate	0.00	1.24	0.70	0.75	0.00	4.55	1.61	0.00	9.28	0.00	3.20	0.00	0.00	0.00	0.00
Stomata	0.00	0.00	0.00	0.00	0.00	0.00	0.00	0.00	0.00	0.00	0.00	0.00	2.19	0.19	3.51
Tracheid	0.00	0.00	0.00	0.37	0.59	0.00	0.00	0.00	0.00	0.00	0.00	0.00	0.00	0.00	0.00

Table A1. continued

Plant species	*Panicum deustum*	*Themeda trianda*	*Stipagrostis zeyheri*	*Eragrostis curvula*	*Eragrostis capensis*	*Pentachistis pallida*	*Pentachistis colorata*	*Tribolium uniolae*	*Festuca scabra*	*Ehrharta bulbosa*	*Stipa dgregeana*	*Elegia juncea*	*Thamnochortus rigidus*	*Restio triticeus*	*Thamnocortus insignis*
Sample description	**Poaceae C4**	**Poaceae C4**	**Poaceae C4**	**Poaceae C4**	**Poaceae C4**	**Poaceae C3**	**Poaceae C3**	**Poaceae C3**	**Poaceae C3**	**Poaceae C3**	**Poaceae C3**	**Restionaceae**	**Restionaceae**	**Restionaceae**	**Restionaceae**
Bulliform	0.18	0.00	0.07	0.12	0.35	0.18	0.00	0.44	1.16	5.85	0.00	0.00	0.00	0.40	0.00
Blocky Polyhedral	0.00	0.00	0.00	0.00	0.00	0.00	0.32	0.15	0.00	0.00	0.00	0.00	0.00	0.00	0.00
Cone-shape	0.00	0.00	0.00	0.00	0.00	0.00	0.00	0.00	0.00	0.00	0.00	0.00	0.00	0.00	0.00
Cystolith	0.00	0.00	0.00	0.00	0.00	0.00	0.00	0.00	0.00	0.00	0.00	0.00	0.00	0.00	0.00
Ellipsoid	0.00	0.00	0.00	0.00	0.00	0.00	0.00	0.00	0.00	0.00	0.00	0.41	9.09	0.00	2.92
Ellipsoid echinate	0.00	0.00	0.00	0.00	0.00	0.00	0.00	0.00	0.00	0.00	0.00	0.00	0.00	0.00	0.00
Elongate	2.40	0.24	0.52	0.41	1.22	6.18	0.32	1.61	8.24	2.20	1.92	4.55	9.09	15.94	26.30
Elongate blocky	0.00	0.00	0.26	0.00	0.00	0.27	0.00	0.00	0.00	0.00	0.00	0.00	0.00	0.80	0.00
Elongate blocky echinate	0.00	0.00	0.00	0.00	0.00	0.00	0.00	0.00	0.00	0.00	0.00	0.00	0.00	0.00	0.00
Elongate blocky striate	0.00	0.00	0.00	0.00	0.00	0.00	0.00	0.00	0.00	0.00	0.00	0.00	1.14	0.00	0.00
Elongate bulbous	0.00	0.00	0.00	0.00	0.00	0.00	0.00	0.00	0.00	0.00	0.00	84.71	4.55	5.18	2.60
Elongate curved	0.00	0.00	0.00	0.00	0.00	0.00	0.00	0.00	0.00	0.00	0.00	0.00	0.00	0.00	0.00
Elongate facetate	0.00	0.24	0.07	0.00	0.00	1.09	0.00	2.20	0.11	0.00	0.00	0.00	1.14	9.96	0.32
Elongate striate	0.00	0.00	0.00	0.00	0.00	0.09	0.00	0.00	0.00	1.71	0.00	0.00	0.00	0.00	0.00
Elongate tuberculate	0.12	8.84	0.00	0.00	0.00	0.00	0.00	0.00	0.00	0.00	0.00	0.00	0.00	0.00	0.00
Elongate verrucate	45.92	0.00	0.00	0.00	0.00	0.00	0.00	0.00	0.00	0.00	0.00	0.00	0.00	0.00	0.00

Elongate dendritic	0.00	0.00	0.00	0.00	0.00	0.00	0.00	0.00	0.00	0.00	0.00	0.00	0.00	0.00	0.00
Elongate echinate	0.42	0.96	3.67	0.35	30.03	9.45	1.84	0.73	1.06	0.24	0.00	1.24	2.27	4.78	0.00
Elongate sinuate	0.00	28.20	63.39	37.09	0.95	0.45	21.84	26.65	11.40	8.78	41.07	0.00	0.00	0.00	0.00
Elongate polylobate	0.00	0.00	0.00	0.00	0.00	0.27	0.11	0.00	0.00	0.00	0.00	0.00	0.00	0.00	0.00
EGM	0.00	0.00	0.00	0.00	0.00	0.00	0.00	0.00	0.00	0.00	0.00	0.00	0.00	0.00	0.00
EGM elongate	0.00	0.00	0.00	0.00	0.00	0.00	0.00	0.00	0.00	0.00	0.00	0.00	0.00	0.00	0.00
EGM polyhedral	0.00	0.00	0.00	0.00	0.00	0.00	0.00	0.00	0.00	0.00	0.00	0.00	0.00	0.00	0.00
EGM sinuous	0.00	0.00	0.00	0.00	0.00	0.00	0.00	0.00	0.00	0.00	0.00	0.00	0.00	0.00	0.00
EGM rings	0.00	0.00	0.00	0.00	0.00	0.00	0.00	0.00	0.00	0.00	0.00	0.00	0.00	0.00	0.00
EGM dots	0.00	0.00	0.00	0.00	0.00	0.00	0.00	0.00	0.00	0.00	0.00	0.00	0.00	0.00	0.00
Hair cell (trichomes)	12.83	12.66	7.14	4.83	2.69	3.09	7.14	6.15	6.44	7.07	3.25	0.00	0.00	1.20	0.32
Hair cell (prickle)	0.30	1.08	0.00	0.06	0.35	0.27	0.22	0.00	0.63	2.20	0.20	0.00	0.00	1.59	0.00
Hair cell aciculate	0.00	0.00	0.00	0.00	0.00	0.00	0.00	0.00	0.00	0.00	0.00	0.00	0.00	0.00	0.00
Hair cell armed	0.00	0.00	0.00	0.00	0.00	0.00	0.00	0.00	0.00	0.00	0.00	0.00	0.00	0.00	0.00
Hair cell with protuberances	0.00	0.00	0.00	0.00	0.00	0.00	0.00	0.00	0.00	0.00	0.00	0.00	0.00	0.00	0.00
Hair cell curved	0.00	0.00	0.00	0.00	0.00	0.00	0.00	0.00	0.00	0.00	0.00	0.00	0.00	0.00	0.00
Hair cell unciform	0.00	0.00	0.00	0.00	0.00	0.00	0.00	0.00	0.00	0.00	0.00	0.00	2.27	0.00	0.00
Hair base	0.00	0.00	0.00	0.00	0.00	0.00	0.00	0.00	0.00	0.00	0.00	0.00	0.00	0.00	0.00
Hair base sinuous shape	0.00	0.00	0.00	0.00	0.00	0.00	0.00	0.00	0.00	0.00	0.00	0.00	0.00	0.00	0.00
Indetermined	0.00	0.00	0.00	0.00	0.00	0.00	0.00	0.00	0.00	0.00	0.00	0.00	0.00	0.40	0.00
Irregular	0.00	0.00	0.00	0.00	0.00	0.00	0.00	0.00	0.00	0.00	0.00	0.00	3.41	0.00	0.00
Irregular echinate	0.00	0.00	0.00	0.00	0.00	0.00	0.00	0.00	0.00	0.00	0.00	0.00	0.00	0.00	0.00
Irregular facetate	0.00	0.00	0.00	0.00	0.00	0.00	0.11	0.00	0.00	0.00	0.00	0.00	0.00	0.00	0.00
Papillae	0.00	1.55	0.00	0.00	0.00	3.91	0.00	0.00	10.35	8.05	0.00	0.00	4.55	0.00	0.00
Parallelepiped thin	0.00	0.00	0.00	0.00	0.00	0.00	0.00	0.00	0.00	0.00	0.00	0.00	1.14	0.00	0.00

Parenchyma strand	0.00	0.00	0.00	0.00	0.00	0.00	0.00	0.00	0.00	0.00	0.00	0.00	0.00	0.00	0.00
Platelet	0.00	0.00	0.00	0.00	0.00	0.00	0.00	0.00	0.00	0.00	0.00	0.00	0.00	0.00	0.00
Sclereid	0.00	0.00	0.00	0.00	0.00	0.00	0.00	0.00	0.00	0.00	0.00	0.00	0.00	0.00	0.00
GSSC bilobate tabular flattened-concave lobes	6.00	32.74	0.00	0.35	3.99	4.82	34.38	0.00	0.00	2.93	11.64	0.00	4.55	11.95	0.32
GSSC bilobate tabular flattened lobes	1.19	0.00	0.00	0.00	0.00	0.00	5.84	0.00	0.00	8.29	0.00	0.00	0.00	0.00	0.00
GSSC bilobate tabular rounded lobes, short shank	0.00	0.00	0.00	0.00	0.00	52.27	5.41	0.00	0.00	7.56	0.00	0.00	0.00	0.00	0.00
GSSC bilobate tabular rounded lobes, long shank	0.00	0.00	0.00	0.00	0.00	10.91	0.00	0.00	0.00	0.00	0.00	0.00	0.00	0.00	0.00
GSSC bilobate trapeziform notched lobes	24.46	0.00	0.00	0.00	0.00	0.00	0.00	0.00	0.00	0.00	0.00	0.00	0.00	0.00	0.00
GSSC bilobate tabular angulate lobes	0.00	0.36	0.00	0.00	0.00	0.00	3.14	0.00	0.00	2.20	3.80	0.00	0.00	0.00	0.00
GSSC bilobate tabular angulate asymmetrical lobes	0.00	0.00	0.00	0.00	0.00	0.00	4.65	0.00	0.00	0.00	0.00	0.00	0.00	0.00	0.00
GSSC bilobate tabular segmented angulate/planar lobes	0.00	0.00	0.00	0.00	0.00	0.00	2.81	0.00	0.00	0.00	0.00	0.00	0.00	0.00	0.00
GSSC bilobate trapezoid	0.06	5.14	0.00	0.00	0.00	0.00	2.38	0.00	0.00	0.00	0.00	0.00	0.00	0.00	0.00
GSSC bilobate trapezoid wavy top	0.00	2.39	0.00	0.00	0.00	0.00	0.00	0.00	0.00	0.00	0.00	0.00	0.00	0.00	0.00
GSSC cross trapeziform	0.30	3.46	0.00	0.00	0.00	6.18	1.19	0.00	0.00	0.00	0.20	0.00	0.00	0.00	0.00
GSSC cross tabular	0.00	0.00	0.00	0.00	0.00	0.00	0.54	0.00	0.00	5.12	0.00	0.00	0.00	0.00	0.00
GSSC trilobate	0.00	0.36	0.00	0.00	0.00	0.18	6.81	1.02	0.00	0.24	1.68	0.00	0.00	0.00	0.00
GSSC polylobate	3.24	0.00	0.00	0.00	0.00	0.00	0.00	0.00	0.00	0.00	0.00	0.00	0.00	0.00	0.00
GSSC rondel cilyndric	0.00	0.00	0.00	0.00	28.82	0.00	0.00	0.29	17.11	11.95	0.00	0.83	0.00	0.00	0.00
GSSC rondel conical	0.00	0.00	13.95	3.72	9.29	0.18	0.00	36.16	1.69	15.85	30.28	0.83	19.32	20.32	0.00
GSSC rondel conical wavy top	0.00	0.00	5.83	0.06	8.68	0.00	0.00	0.00	0.00	0.73	0.00	0.41	0.00	0.00	0.00
GSSC rondel keeled	0.00	0.00	0.00	0.00	0.00	0.00	0.11	22.11	0.11	0.00	0.00	0.00	0.00	0.00	0.00

GSSC long tower	0.00	0.00	0.00	0.06	5.38	0.00	0.00	0.73	0.00	1.71	0.00	0.83	3.41	0.00	0.00
GSSC long tower wavy top	0.00	0.00	0.00	0.00	0.00	0.00	0.00	0.00	0.00	0.98	0.00	0.00	0.00	0.00	0.00
GSSC trapeziform	0.00	0.00	0.00	0.00	0.00	0.00	0.00	0.00	1.90	0.00	1.68	0.00	0.00	0.00	0.00
GSSC oblong tabular	0.00	0.00	0.00	0.00	0.00	0.00	0.00	0.15	38.23	3.41	0.00	0.41	0.00	0.40	0.00
GSSC oblong trapeziform sinuous	0.00	0.00	0.00	0.00	0.00	0.00	0.00	0.00	1.58	0.49	0.00	0.00	0.00	0.00	0.00
GSSC round tabular	0.00	0.00	0.00	0.00	0.00	0.00	0.00	0.00	0.00	0.00	0.00	0.00	0.00	0.00	0.00
GSSC saddle	0.00	0.00	0.00	45.87	7.03	0.00	0.11	0.15	0.00	0.00	0.00	0.41	3.41	14.74	0.00
GSSC collapsed saddle	0.00	0.00	0.00	0.12	0.00	0.00	0.00	0.00	0.00	0.00	0.00	0.00	0.00	0.00	0.00
Spheroid psilate	0.00	0.00	0.00	0.93	0.00	0.00	0.00	0.00	0.00	2.44	0.00	0.00	0.00	0.00	0.00
Semi spheroids	0.00	0.00	0.00	0.00	0.00	0.00	0.00	0.00	0.00	0.00	0.00	0.00	6.82	0.00	0.00
Small spheroids	0.00	0.00	0.00	0.00	0.00	0.00	0.00	0.00	0.00	0.00	0.00	2.07	0.00	0.00	0.00
Large spheroid	0.00	0.00	0.00	0.00	0.00	0.00	0.00	0.00	0.00	0.00	0.00	0.00	0.00	0.00	0.00
Large spheroid facetate	0.00	0.00	0.00	0.00	0.00	0.00	0.00	0.00	0.00	0.00	0.00	0.00	0.00	0.00	0.00
Large spheroid granulate and verrucate	0.00	0.00	0.00	0.00	0.00	0.00	0.00	0.00	0.00	0.00	0.00	0.00	2.27	7.57	48.38
Spheroid spiraling decorations	0.00	0.00	0.00	0.00	0.00	0.00	0.00	0.00	0.00	0.00	0.00	2.89	0.00	0.80	13.64
Spheroid rugulate	0.00	0.00	0.00	0.00	0.00	0.00	0.00	0.00	0.00	0.00	0.00	0.41	21.59	0.80	3.57
Stomata	2.58	1.79	5.11	6.05	1.13	0.18	0.76	1.46	0.00	0.00	4.29	0.00	0.00	0.00	0.00
Tracheid	0.00	0.00	0.00	0.00	0.09	0.00	0.00	0.00	0.00	0.00	0.00	0.00	0.00	3.19	1.62

Table A2. ANOVA results of the phytolith morphotypes from the different vegetation types. *P-values* in bold indicate those phytolith morphotypes that are statistically representative of specific vegetation types (retrieved from Esteban et al., in press).

Phytolith Morphotypes	**Limestone fynbos**		**Sand fynbos**		**Grassy fynbos**		**Renosterveld**		**Subtropical ticket**		**Coastal thicket**		**Strandveld**		**Riparian**		**ANOVA results**		
	Mean	SD	Mean	SD	Mean	SD	Mean	SD	Mean	SD	Mean	SD	Mean	SD	Mean	SD	*df*	F	*p value*
Bulliform	1.68	1.46	3.56	0.84	7.00	1.46	4.49	0.61	1.62	1.46	1.50	1.27	7.30	1.46	4.83	0.96	7	2.86	**0.016**
Sclereid	0.37	0.32	0.27	0.18	0.00	0.32	0.43	0.13	0.26	0.32	0.00	0.28	0.58	0.32	0.49	0.20	7	0.64	0.7205
Elongate	9.16	4.24	17.36	2.45	26.60	4.24	16.42	1.78	18.12	4.24	8.57	3.67	16.58	4.24	13.74	2.77	7	2.03	0.0736
Ellipsoid	1.02	0.40	0.61	0.23	0.75	0.40	0.13	0.17	1.53	0.40	0.00	0.35	0.00	0.40	0.07	0.26	7	2.59	**0.026**
Hat shape	0.65	0.54	1.29	0.31	0.00	0.54	0.03	0.23	0.00	0.54	0.00	0.47	0.00	0.54	0.15	0.36	7	1.90	0.0947
Hair cell (trichome)	5.95	1.76	5.81	1.02	8.08	1.76	6.44	0.74	12.79	1.76	3.80	1.52	12.79	1.76	4.81	1.15	7	2.83	**0.0167**
Hair Base	0.00	0.08	0.00	0.05	0.00	0.08	0.00	0.03	0.35	0.08	0.00	0.07	0.00	0.08	0.00	0.05	7	2.75	**0.0195**
Stomata	0.00	0.13	0.14	0.07	0.00	0.13	0.00	0.05	0.00	0.13	0.00	0.11	0.00	0.13	0.18	0.08	7	0.79	0.5962
Elongate with decorated margins	2.94	1.06	2.48	0.61	2.03	1.06	2.71	0.45	1.11	1.06	0.78	0.92	2.81	1.06	2.80	0.70	7	0.85	0.5558
Parallelepiped blocky	3.59	0.87	2.17	0.50	2.20	0.87	1.62	0.37	0.71	0.87	0.41	0.76	1.21	0.87	0.16	0.57	7	2.39	**0.0378**
Parallelepiped thin	2.74	1.25	1.68	0.72	0.56	1.25	1.23	0.52	3.15	1.25	2.40	1.08	2.92	1.25	2.10	0.82	7	0.74	0.6386
GSSC trapeziform	22.60	7.24	30.14	4.18	29.80	7.24	42.46	3.04	29.56	7.24	27.54	6.27	34.99	7.24	32.84	4.74	7	1.84	0.1056
GSSC bilobate	8.52	2.38	7.97	1.37	12.73	2.38	8.15	1.00	7.29	2.38	7.25	2.06	5.87	2.38	8.70	1.56	7	0.73	0.6479
GSSC saddle	2.19	6.19	3.79	3.57	3.38	6.19	6.27	2.60	6.26	6.19	26.39	5.36	5.01	6.19	22.42	4.05	7	3.91	**0.0024**
Spheroid psilate and rugulate	22.00	2.79	11.56	1.61	0.93	2.79	4.39	1.17	5.55	2.79	4.30	2.42	5.99	2.79	1.87	1.83	7	7.90	**<.0001**
Spheroid echinate	0.00	0.25	0.00	0.15	0.00	0.25	0.03	0.11	0.00	0.25	1.07	0.22	0.58	0.25	0.00	0.17	7	3.53	**0.0046**

Restio phytolith	12.96	1.92	7.11	1.11	2.22	1.92	0.95	0.81	0.00	1.92	0.00	1.66	6.63	1.92	0.45	1.26	7	8.66	**<.0001**
Tracheid	0.37	0.19	0.07	0.11	0.00	0.19	0.00	0.08	0.00	0.19	0.00	0.16	0.00	0.19	0.35	0.12	7	1.27	0.2899
Fiber	0.00	0.06	0.00	0.04	0.00	0.06	0.03	0.03	0.00	0.06	0.00	0.05	0.00	0.06	0.08	0.04	7	0.41	0.8917
Epidermal ground mass polyhedral	0.00	0.53	0.82	0.31	0.18	0.53	0.21	0.22	0.00	0.53	0.00	0.46	2.04	0.53	0.58	0.35	7	2.03	0.0736
Fruit phyotliths	0.00	0.04	0.00	0.03	0.00	0.04	0.00	0.02	0.00	0.04	0.00	0.04	0.00	0.04	0.08	0.03	7	0.84	0.5634
Irregular/Indeterminate	3.26	2.35	3.15	1.35	3.53	2.35	4.02	0.99	11.70	2.35	15.99	2.03	2.50	2.35	3.31	1.54	7	6.22	**<.0001**

Table A3. ANOVA results of the phytolith morphotypes from the different vegetation biomes. *P-values* in bold indicate those phytolith morphotypes that are statistically representative of specific vegetation biomes (retrieved from Esteban et al., in press).

Phytolith Morphotypes	**Fynbos biome**		**Renosterveld biome**		**Thicket biome**		**Azonal vegetation**		**ANOVA results**		
	Mean	SD	Mean	SD	Mean	SD	Mean	SD	*df*	F	*p value*
Bulliform	3.87	0.75	4.49	0.70	3.27	0.92	4.83	1.09	3.00	0.56	0.646
Sclereid	0.23	0.14	0.43	0.13	0.25	0.17	0.49	0.21	3.00	0.62	0.6074
Elongate	17.57	2.06	16.42	1.93	13.84	2.52	13.74	3.01	3.00	0.64	0.5944
Ellipsoid	0.72	0.19	0.13	0.18	0.46	0.24	0.07	0.28	3.00	2.11	0.1126
Hat shape	0.91	0.24	0.03	0.23	0.00	0.30	0.15	0.36	3.00	2.89	**0.0456**
Hair cell (trichome)	6.30	0.90	6.44	0.85	6.85	1.10	4.81	1.32	3.00	0.51	0.6764
Epidermal appendage Hair Base	0.00	0.04	0.00	0.04	0.11	0.05	0.00	0.06	3.00	1.33	0.2775
Stomata	0.09	0.06	0.00	0.05	0.00	0.07	0.18	0.08	3.00	1.44	0.2441
Elongate with decorated margins	2.48	0.47	2.71	0.44	1.49	0.57	2.80	0.69	3.00	1.13	0.3469
Parallelepiped blocky	2.46	0.38	1.62	0.36	0.74	0.47	0.16	0.56	3.00	4.88	**0.005**
Parallelepiped thin	1.67	0.54	1.23	0.51	2.78	0.67	2.10	0.80	3.00	1.20	0.3199
GSSC trapeziform	28.57	3.15	42.46	2.96	30.38	3.85	32.84	4.61	3.00	4.03	**0.0128**
GSSC bilobate	9.03	1.05	8.15	0.99	6.85	1.29	8.70	1.54	3.00	0.61	0.6144
GSSC saddle	3.39	2.92	6.27	2.74	13.94	3.58	22.42	4.27	3.00	5.47	**0.0027**
Spheroid psilate and rugulate	11.52	1.55	4.39	1.46	5.18	1.90	1.87	2.27	3.00	5.72	**0.0021**
Spheroid echinate	0.00	0.12	0.03	0.11	0.60	0.15	0.00	0.18	3.00	4.23	0.0103
Restio phytolith	7.30	1.03	0.95	0.97	0.95	0.97	0.95	0.97	3.00	8.43	**0.0001**
Tracheid	0.12	0.08	0.00	0.08	0.00	0.10	0.35	0.12	3.00	2.28	0.0923
Fiber	0.00	0.03	0.03	0.02	0.00	0.03	0.08	0.04	3.00	1.05	0.3817
Epidermal ground mass polyhedral	0.53	0.26	0.21	0.24	0.61	0.32	0.58	0.38	3.00	0.49	0.6925
Fruit phyotliths	0.00	0.02	0.00	0.02	0.00	0.02	0.08	0.03	3.00	2.14	0.108
Irregular/Indeterminate	3.25	1.21	4.02	1.14	10.66	1.49	3.31	1.78	3.00	6.07	**0.0015**

Table A4. List of the one hundred eighty-three samples analyzed from the PP5-6 sequence giving sample location and description, and the main phytolith, relative number of phytoliths per gram of sediment (/g sed) and FT-IR results. Cl = clay, Qz = quartz, Dah = dahllite (carbonate-hydroxylapatite), Cal = calcite, Arg = aragonite, b = burnt, nb = no burnt, n? = probably burnt.

Sample Number	StratAgg	Sample description	Phyt g/sed	FT-IR
418164	RBSR	Black layer	0	Cl (b?), Qz, Dah
418165	RBSR	Yellowish Brown - geogenic	0	Qz, Cl (traces)
418166	RBSR	Yellowish Brown - geogenic	0	Qz, Cl (traces)
418167	RBSR	Greyish	0	Qz, Cl
418168	RBSR	Yellowish Brown - geogenic	0	Qz, Cl
418169	RBSR	Greyish	7,000	Qz, Cl
418170	RBSR	Yellowish Brown - geogenic	0	Qz, Cl (b?)
418171	RBSR	Black layer	7,000	Qz, Cl
418173	RBSR	Yellowish Brown - geogenic	0	Qz, Cl
418174	RBSR	Black layer	0	Cl, Qz
418175	RBSR	Yellowish Brown - geogenic	0	Qz, Cl, few Cal
418176	RBSR	Greyish light	0	Qz, Cl
418177	RBSR	Yellowish Brown	0	Qz, few Cl
418178	RBSR	Black layer	0	Qz, Cl
418179	RBSR	Blackish brown	0	Cl, Qz
418180	RBSR	Yellowish Brown	0	Qz, Cl
110578	RBSR	Black light	22,000	Clay, Qz, organic matter, some Cal
110579	RBSR	Yellowish Brown - geogenic	0	Qz, Cl na (not altered)
110580	RBSR	Reddish	2,000	Cl na, few Qz
110581	RBSR	Reddish	500	Cl, Qz
110582	RBSR	Reddish	6,000	Cl, Qz, Cal, some organic matter
110584	RBSR	Reddish	5,200	Cl, Qz, some Cal, organic matter?
110585	RBSR	Yellowish Brown - geogenic	1,000	Cl, Qz
110599	RBSR		0	Cl, Qz
418152	BBCSR	Greyish	21,500	Cal, Cl, Qz
418153	BBCSR	White layer	41,000	Cal, Cl (b), Qz?, Dah
418154	BBCSR	dark	13,200	Cal, Cl (b?), Qz, Dah?

418155	BBCSR	White layer	135,100	Ca, Cl (b), Qz, Dah
418156	BBCSR	Yellowish Brown - geogenic	0	?
162688	BBCSR	Yellowish Brown - geogenic	0	Qz, Cl
162773	BBCSR	Yellow Light	0	?
162774	BBCSR	Yellow	0	Qz, Cl (b)
162683	DBCS	Yellowish Brown - geogenic	0	Qz, Cl
162682	SGS	Yellowish Brown - geogenic	13,000	Qz, Cl, some Cal
162473	OBS1	Greyish	22,400	Qz, Cal, Cl
162474	OBS1	Black layer	0	Qz, Cl, Cal
162475	OBS1	Red Layer	0	Qz, Cl, Cal (traces)
418157	OBS2	General archaeologiCall layer	13,500	Cl (b??), Qz, Cal?, Dah?
418158	OBS2	Yellowish Brown - geogenic	0	Qz, Cl (b?)
418159	OBS2	Yellowish Brown - geogenic	0	Qz, few Cl
418160	OBS2	General archaeologiCall layer	13,500	Cl, Qz, Cal (traces)
418161	OBS2	Yellowish Brown - geogenic	0	Qz, few Cl and Cal
418162	OBS2	General archaeologiCall layer	0	Qz , Cl
418163	OBS2	Yellowish Brown - geogenic	0	Qz, few Cl
356480	SADBS	Greyish brown light	33,200	Cal, Qz, Cl some Dah, few Arg
356481	SADBS	White layer	166,600	Cal, few Cl and Qz, Dah, Arg
356482	SADBS	Black layer	8,000	Cal, few Cl and Qz, Dah
356483	SADBS	Greyish light	308,600	Cal, Qz, Cl, some Dah
356484	SADBS	Black light	39,200	Cal, few Cl and Qz, few Dah
162466	SADBS	White layer	300,000	Ca, Qz, Cl (b), Dah
162467	SADBS	Black layer	69,000	Ca, Qz, Cl (b), few Dah
46682	SADBS	Dark Grey	67,000	Ca, Qz, Cl (nb), some Dah
46681	SADBS	Greyish light	30,300	Cal, Qz, Cl, some Dah
46680	SADBS	Mixed layer	0	Cal, Qz, Cl (b), Dah
356485	SADBS	Black layer	54,400	Cal, few Cl and Qz, Dah, few Arg
356486	SADBS	Black layer	0	Cal, few Cl and Qz, Dah

356487	SADBS	White layer	75,100	Ca, Qz, Cl (b?), few Dah
356488	SADBS	Blackish brown light	7,000	Cal, Qz, Cl, some Dah
162684	SADBS	Geogenic	51,800	Cal, Cl (b?), Qz, Dah
356489	SADBS	Whitish grey	15,300	Cal, few Cl and Qz, few Dah, Arg?
356490	SADBS	Whitish grey	72,200	Cal (b), few Cl and Qz, Dah
356491	SADBS	Greyish brown light	78,900	Cal, Qz, Cl (b), some Dah
356492	SADBS	Whitish grey	68,500	Cal, Qz, Cl, few Dah
356493	SADBS	Greyish brown light	26,100	Cal, Qz, Cl, few Dah
356494	SADBS	White layer	45,785	Cal, few Cl and Qz, Dah
162800	SADBS	White layer	0	Cal, Qz, Cl (nb), Dah
162801	SADBS	Dark Grey	7,000	Cal, Qz, Cl (b?)
356495	ALBS	Brown - Orange	0	Qz, Cl, Cal, Arg
356496	ALBS	Whitish grey	7,500	Qz, Cal, Cl
357372	ALBS	Whitish grey	28,000	Cal, Qz, Cl
357373	ALBS	Dark Grey	35,700	Cal, Qz, Cl
357375	ALBS	White layer	237,700	Cal, Qz, Cl, Dah
357374	ALBS	Dark Grey	58,200	Ca, Qz, Cl (nb)
357376	ALBS	Brown grey	42,500	Cal, Qz, Cl
357385	ALBS	Dark Grey	0	Cal, few Qz and Cl
357383	ALBS	Greyish	284,100	Ar transforming to Ca, Qz, Cl (nb)
357377	ALBS	Orange Brown	0	Qz, few Cl, few Cal, some Arg
357380	ALBS	Dark Grey	230,300	Ca, Qz, Cl (nb)
357381	ALBS	Lightly Grey	35,900	Ca, Qz, Cl (nb)
357378	ALBS	Yellowish Brown - geogenic	0	Qz, few Cl
357382	ALBS	Yellowish Brown - geogenic	0	Qz, Cl, Cal?, Arg
157212	ALBS	Black layer	0	Qz, Cl, few Cal
157211	ALBS	Above Hearth	6,500	Qz, Cl, few Cal
157213	ALBS	Red Layer	0	Qz, Cl, few Cal
162490	ALBS	Black layer	0	Qz, Cl, few Cal, some Arg?
162489	ALBS	White layer	0	Cal, Q, Cl
357379	ALBS	Greyish	0	Qz, Cl, few Cal
357384	ALBS	Yellowish Brown - geogenic	8,100	Qz, Cl, few Cal, Arg
162480	ALBS	Above Hearth	0	Qz, Cl, few Cal, Arg

162482	ALBS	Outside Hearth	110,600	Ca, Qz, Cl (nb)
162483	ALBS	Red layer	123,700	Ca, Qz, Cl (nb)
162481	ALBS	Black layer	314,600	Ca, Qz, Cl (nb)
157181	LBSR	Black layer	38,700	Cal, few Qz and Cl
157182	LBSR	Red layer	13,300	Qz, Cl, Cal
157180	LBSR	White layer	31,700	Cal, Cl, Qz
157207	LBSR	Outside Hearth	6,000	Qz, Cl, few Cal
157208	LBSR	White layer	82,000	Cal, Qz, Cl
157209	LBSR	Black layer	122,000	Cal, few Qz and Cl, some Arg
162477	LBSR	Red layer	8,500	Arg, Qz, Cl, some Cal
162478	LBSR	Red layer	13,200	Arg, Cal, Qz, Cl
162476	LBSR	Black layer	36,700	Arg, Cal, Qz, Cl
162494	LBSR	Outside Hearth	87,600	Qz, Cl (nb), few Ca, few Ar, some Dah
162493	LBSR	Red layer	107,000	Qz, Cl (nb), Ca, few Ar
162491	LBSR	Above Hearth	12,500	Arg, Qz, Cl, Cal
162492	LBSR	Black layer	239,600	Ar transforming into Ca, Qz, Cl (nb), few dah
356476	LBSR	Black layer	117,400	Ca, Cl (nb), Qz, Dah
162558	LBSR	Black layer	108,800	Cl (nb), Qz, Ca, few Dah?
162559	LBSR	Outside Hearth	17,700	Cl, Qz, few Cal
162557	LBSR	Red layer	320,100	Ca, Qz, Cl (nb), few Dah
162556	LBSR	Above Hearth	35,600	Qz, Cl, few Cal
162551	LBSR	Outside Hearth	6,300	Qz, Cl, few Cal
162549	LBSR	Red layer	416,000	Cl (nb), Qz, Ca
162550	LBSR	Black layer	355,500	Ca, Cl (nb), Qz
162548	LBSR	Above Hearth	122,600	Qz, Cl (nb), Ca
356475	LBSR	Grey Brown	1,117,500	Qz, Cl (nb), few Ca
356474	LBSR	Black layer	392,700	Cl (nb), Qz, Ca, few Dah
357368	LBSR	Black layer	833,200	Ca, Cl (nb), Qz, Dah
357369	LBSR	Black layer	404,900	Ca, Cl (nb), Qz, Dah
357370	LBSR	Lightly Black	855,350	Ca, few Cl (nb), few Qz, Dah
356472	LBSR	Above Hearth	7,000	Qz, Cl, Cal?
356470	LBSR	White layer	161,100	Ca, Qz, Cl (nb), few Dah
356471	LBSR	Blackish brown	354,000	Ca, Cl (nb), Qz, Dah
356473	LBSR	Red layer	7,000	Qz, Cl, Cal?

357363	LBSR	Grey - Ashes	3,780,500	Ca, Cl (nb), Qz, Dah
357362	LBSR	Black layer	887,900	Cl (nb), Qz, Ca, Dah
357364	LBSR	Black layer	310,800	Ca, Cl (nb), Qz, Dah
357365	LBSR	Black layer	362,700	Qz, Cl (nb), some Ca, few Dah
357366	LBSR	Black layer	185,600	Ca, Qz, Cl (nb), Dah
356454	LBSR	Black layer	558,700	Cl (nb), Qz
356453	LBSR	Black layer	866,200	Cl (nb), Qz
356455	LBSR	Black layer	372,500	Cl (nb), Qz, some Ca, Dah
162778	LBSR	Black layer	1,237,700	Qz, Cl (nb), few Ca
162779	LBSR	Red layer	7,000	Qz, Cl
162777	LBSR	Geogenic	0	Qz, Cl
356465	LBSR	Brown light	0	Qz, Cl
356464	LBSR	Black layer	364,500	Ca, Cl (nb), Qz, few Dah
356466	LBSR	Brown light	19,500	Qz, Cl, few Cal
356467	LBSR	Reddish	15,000	Qz, Cl, Cal?
356468	LBSR	Brown light	0	Qz, Cl, Cal?
356469	LBSR	Black layer	220,500	Qz, Cl (nb), few Ca, some Dah
356462	LBSR	Black layer	135,500	Cl (nb), Qz, some Dah
356456	LBSR	Black layer	225,000	Cl (nb), Qz, few Dah
162781	LBSR	Black layer	1,185,500	Cl (nb), Qz, Ca, some Dah
356457	LBSR	Black layer	771,000	Cl (nb), Qz few Ca, Dah
356458	LBSR	Black layer	539,800	Cl (nb), Qz, few Ca, Dah
356459	LBSR	Black layer	491,300	Ca, Cl (nb), Qz, Dah
162782	LBSR	Black layer	255,300	Ca, few Cl (nb) and Qz, Dah
356463	LBSR	Whitish grey	155,100	Ca, few Qz and Cl (b), Dah
356460	LBSR	Black layer	216,600	Ca, Cl (nb), Qz, few Dah
356461	LBSR	Black layer	174,200	Ca, Cl (nb), Qz, some Dah
162780	LBSR	Geogenic	6,200	Qz, Cl
162714	LBSR	Black layer	0	Qz, Cl, Cal
162716	LBSR	Above Hearth	0	Qz, Cl, Cal
162715	LBSR	Outside Hearth	7,600	Cal, Qz, Cl
162717	LBSR	Red layer	75,100	Ca, Cl (nb), Qz, some Dah
162729	LBSR	Reddish	74,900	Cal, Qz, Cl, Dah

162728	LBSR	Reddish	212,500	Ca, Qz, Cl (nb), Dah
162749	LBSR	White layer	141,900	Ar transfoming into Ca, Qz, Cl (b?), some Dah
162750	LBSR	Black layer	117,100	Ar, Qz, Cl (nb), some Ca, some Dah
162785	LBSR	Mixed layer	0	Qz, Cl, Cal (traces)
162812	LBSR	White layer	115,700	Cal, traces of silicates
162813	LBSR	Black layer	82,300	Qz, Cl, Cal
162783	YBSR	Mixed layer mostly red with some black and ashy material	115,700	Qz, Cl (nb)
356479	YBSR	Greyish	935,700	Ca, Qz, Cl (nb), few Dah
388612	YBSR	White layer	1,165,700	Qz, Ca, Cl (nb)
388613	YBSR	Red layer	289,400	Qz, Cl (nb), Ca
388614	YBSR	Grey - Ashes	350,900	Ca, Qz, Cl (b), Dah
388615	YBSR	Black layer	482,500	Qz, Ca, Cl (nb)
388626	YBSR	Yellowish Brown	54,900	Cl, Qz, Cal
388586	YBSR	Above Hearth	0	Qz, Cl, Cal
388587	YBSR	Red layer	76,000	Cal, Qz, Cl (b)
388588	YBSR	Black layer	210,600	Ca, Cl (nb), Qz
388589	YBSR	Outside Hearth	35,800	Cal, Qz, Cl
356478	YBSR	Black layer	106,000	Qz, Cl (nb), few calcite
162784	YBSR	Yellowish Brown - geogenic	13,000	Qz, Cl
162710	YBSR	Black layer	117,600	Qz, Cl (nb)
162711	YBSR	Outside Hearth	33,800	Qz, few Cl, few Cal
162712	YBSR	Above Hearth	61,800	Qz, few Cl, Cal
162713	YBSR	Red layer	0	Qz, few Cl, Cal
356414	YBSR	Black layer	143,400	Ar transforming into Ca, Qz, Cl (nb)
356415	YBSR	Red layer	35,500	Qz, Cl, few Cal
356417	YBSR	Red layer	134,000	Qz, Cl (nb), Ca
356418	YBSR	Brown light	19,500	Qz, Cl

Table A5. List of morphotypes identified and their frequencies in samples from the PP5-6 sequence, giving the stratigraphic location and sample information.

	Sample Number	418155	162466	162467	46682	356487	356491	162483	162481	357374	357380	357383
	StratAgg	BCSR	SADBS	SADBS	SADBS	SADBS	SADBS	ALBS	ALBS	ALBS	ALBS	ALBS
Morphotypes	Sample Type	White layer	White layer	Black layer	Black layer	White layer	Grey color	Grey color	Grey color	Grey color	Red layer	Black layer
Bulliform		0.00	3.36	0.00	0.00	2.86	1.61	7.00	1.71	0.00	0.00	2.08
Blocky Polyhedral		0.00	0.00	12.50	4.26	1.43	0.00	0.00	0.00	0.00	2.53	0.00
Ellipsoid		1.67	0.00	0.00	0.00	1.43	1.61	1.00	0.57	0.00	1.27	0.00
Elongate without decoration margin		0.00	10.07	12.50	31.91	14.29	24.19	15.00	5.14	4.26	9.49	12.50
Elongate blocky		0.00	0.67	0.00	2.13	0.00	0.00	1.00	0.00	0.00	0.00	0.00
Elongate blocky echinate		0.00	0.00	0.00	0.00	0.00	0.00	0.00	0.00	0.00	0.00	0.00
Elongate bulbous		0.00	0.00	0.00	0.00	0.00	0.00	0.00	0.00	0.00	0.63	0.00
Elongate curved		0.00	0.00	0.00	0.00	0.00	1.61	0.00	0.00	0.00	0.00	0.00
Elongate facetate		0.00	0.67	0.00	2.13	2.86	0.00	1.00	2.29	8.51	0.63	0.00
Elongate striate		0.00	0.00	0.00	0.00	0.00	0.00	0.00	0.00	0.00	0.63	0.00
Elongate dendritic		0.00	0.00	0.00	0.00	0.00	0.00	0.00	0.00	0.00	0.00	0.00
Elongate echinate		0.00	2.01	0.00	4.26	4.29	6.45	2.00	3.43	2.13	7.59	4.17

Elongate echinate (one side)	0.00	0.00	0.00	0.00	0.00	0.00	0.00	0.00	0.00	0.00	0.00
Elongate sinuate	5.00	0.00	0.00	0.00	0.00	0.00	0.00	0.00	0.00	0.00	1.39
Elongate polylobate	0.00	0.67	0.00	0.00	0.00	0.00	0.00	0.00	0.00	0.00	0.00
Epidermal ground-mass	55.00	0.00	0.00	0.00	0.00	0.00	1.00	0.00	6.38	6.96	0.69
Epidermal ground-mass polyhedral	0.00	0.67	0.00	2.13	1.43	0.00	0.00	0.00	4.26	0.00	0.69
Epidermal ground-mass polyhedral elongate	0.00	0.00	0.00	0.00	0.00	0.00	0.00	0.00	0.00	0.00	0.00
Epidermal ground-mass elongate	0.00	0.00	0.00	0.00	0.00	0.00	0.00	0.00	0.00	0.00	0.00
Epidermal ground-mass jigsaw puzzle	0.00	0.00	0.00	0.00	0.00	0.00	0.00	0.00	0.00	0.00	0.00
Epidermal ground-mass sinuate	0.00	0.00	0.00	0.00	0.00	0.00	0.00	0.00	0.00	0.63	0.00
Epidermal ground-mass octogonal	0.00	0.00	0.00	0.00	0.00	0.00	0.00	0.00	0.00	0.00	0.00
Hair cell (trichomes)	0.00	1.34	0.00	0.00	1.43	0.00	0.00	0.00	2.13	1.27	0.69
Hair cell (prickles)	1.67	0.67	0.00	0.00	5.71	4.84	2.00	1.14	0.00	1.27	1.39
Hair aciculate	0.00	0.00	0.00	0.00	0.00	0.00	0.00	0.00	0.00	0.00	0.69
Hair unciform	0.00	0.00	0.00	0.00	0.00	0.00	0.00	0.00	0.00	0.00	0.00
Hair base	0.00	0.00	0.00	0.00	0.00	0.00	0.00	0.00	0.00	0.00	0.00
Hat-shape	0.00	0.00	0.00	0.00	0.00	0.00	1.00	0.00	0.00	0.00	0.00
Indetermined	6.67	2.68	0.00	6.38	2.86	3.23	2.00	1.71	4.26	1.90	0.00
Irregular	8.33	11.41	56.25	12.77	4.29	6.45	1.00	5.14	25.53	10.76	8.33
Irregular facetate	0.00	0.00	0.00	0.00	0.00	0.00	0.00	0.00	0.00	0.00	0.00
Irregular protuberances (fruit eudicot)	0.00	0.00	0.00	0.00	0.00	0.00	0.00	0.00	0.00	0.00	0.00
Irregular verrucate	0.00	0.67	0.00	0.00	0.00	0.00	0.00	0.00	0.00	0.00	0.00
Papillae	0.00	0.00	0.00	0.00	0.00	0.00	0.00	0.00	0.00	0.00	0.00
Parallelepiped blocky	0.00	0.00	0.00	0.00	0.00	0.00	2.00	0.00	0.00	0.63	0.69
Parallelepiped blocky echinate	0.00	0.00	0.00	0.00	1.43	0.00	0.00	0.00	0.00	0.63	0.00

Parallelepiped thin	0.00	0.00	0.00	0.00	1.43	0.00	0.00	0.57	0.00	3.80	3.47
Parenchyma strand	0.00	0.00	0.00	0.00	0.00	0.00	0.00	0.00	0.00	0.00	0.00
Platelet	3.33	3.36	0.00	2.13	1.43	8.06	0.00	22.86	2.13	0.00	0.00
Polyhedral	0.00	1.34	0.00	0.00	0.00	4.84	0.00	0.00	0.00	3.80	0.00
Sclereids	0.00	0.67	0.00	0.00	1.43	0.00	0.00	0.00	0.00	0.00	0.00
Seed sedge	0.00	0.00	0.00	0.00	0.00	0.00	0.00	0.00	0.00	0.00	0.00
GSSC bilobate	0.00	2.01	0.00	0.00	4.29	1.61	10.00	2.86	0.00	6.33	4.86
GSSC cross	0.00	1.34	0.00	0.00	0.00	1.61	0.00	0.00	0.00	0.00	1.39
GSSC polylobate	0.00	0.00	0.00	0.00	0.00	0.00	0.00	0.00	0.00	0.00	0.00
GSSC rondel	0.00	44.97	6.25	17.02	34.29	17.74	29.00	37.14	25.53	31.01	38.19
GSSC rondel wavy top	0.00	0.00	0.00	0.00	0.00	0.00	0.00	0.00	0.00	0.00	0.00
GSSC saddle	0.00	1.34	0.00	0.00	1.43	1.61	5.00	2.29	0.00	0.63	2.78
GSSC long tower	0.00	6.71	0.00	0.00	0.00	0.00	10.00	2.86	0.00	0.63	7.64
GSSC oblong tabular	0.00	2.01	0.00	2.13	2.86	1.61	7.00	5.14	0.00	0.00	2.78
GSSC oblong trapeziform sinuous	0.00	0.00	0.00	0.00	0.00	1.61	0.00	0.00	2.13	4.43	0.69
GSSC tabular round	0.00	0.00	0.00	0.00	1.43	0.00	0.00	0.00	0.00	0.00	0.00
Spheroid echinate	0.00	0.00	0.00	0.00	0.00	0.00	0.00	0.00	0.00	0.00	0.00
Spheroid psilate	8.33	0.67	0.00	4.26	1.43	0.00	0.00	0.00	0.00	0.00	2.08
Semi spheroid	1.67	0.00	0.00	0.00	0.00	0.00	0.00	0.00	0.00	0.00	0.00
Small spheroid	0.00	0.00	0.00	2.13	0.00	1.61	0.00	0.00	0.00	0.00	0.00
Large spheroid	0.00	0.00	0.00	0.00	1.43	0.00	0.00	0.00	0.00	0.00	0.00
Restio morphotypes	0.00	0.00	6.25	6.38	1.43	1.61	1.00	2.29	4.26	0.63	1.39
Spheroid rugulate	8.33	0.67	0.00	0.00	2.86	8.06	2.00	2.86	4.26	1.27	1.39
Stomata	0.00	0.00	0.00	0.00	0.00	0.00	0.00	0.00	0.00	0.63	0.00

Tracheid (vascular tissue)	0.00	0.00	0.00	0.00	0.00	0.00	0.00	0.00	0.00	0.00	0.00
Trapeziform	0.00	0.00	6.25	0.00	0.00	0.00	0.00	0.00	4.26	0.00	0.00

Table A5. continued

	Sample Number	162728	162717	162782	162749	162750	356453	356454	162778	356455	356462	356456
	StratAgg	LBSR	LBSR	LBSR	LBSR	LBSR	LBSR	LBSR	LBSR	LBSR	LBSR	LBSR
Morphotypes	Sample Type	Outside Hearth	Red layer	Black layer	Black layer	Black layer	Red layer	Red layer	Black layer	Above Hearth	White layer	Black layer
Bulliform		0.54	3.08	0.00	0.97	1.92	1.02	2.01	0.00	3.74	0.00	0.00
Blocky Polyhedral		1.08	0.00	0.00	3.88	0.00	0.00	0.00	0.00	0.00	3.57	0.00
Ellipsoid		0.00	0.00	0.00	0.00	0.00	0.34	2.01	0.00	0.47	0.00	0.00
Elongate without decoration margin		8.11	10.77	11.11	23.30	19.23	57.34	20.81	22.54	12.15	26.79	17.95
Elongate blocky		0.00	1.54	0.00	0.00	0.00	0.00	0.00	0.00	0.00	0.00	0.00
Elongate blocky echinate		0.00	0.00	0.00	0.00	0.00	0.00	0.00	0.00	0.00	0.00	0.00
Elongate bulbous		0.00	0.00	0.00	0.00	1.92	0.34	0.00	4.23	0.47	0.00	0.00
Elongate curved		0.00	0.00	0.00	0.00	0.00	0.34	0.00	0.00	0.00	0.00	0.00
Elongate facetate		0.54	0.00	0.00	0.00	5.77	0.68	1.34	0.00	0.47	1.79	0.00
Elongate striate		0.00	1.54	0.00	0.00	0.00	0.00	0.00	0.00	0.00	0.00	0.00
Elongate dendritic		0.00	0.00	0.00	0.00	0.00	0.00	0.00	0.00	0.00	0.00	0.00
Elongate echinate		1.08	0.00	0.58	2.91	0.00	2.39	2.68	2.82	0.00	2.68	1.28

Elongate echinate (one side)	0.00	0.00	0.00	0.00	0.00	0.00	0.00	0.00	0.00	0.00	0.00
Elongate sinuate	0.00	3.08	0.00	0.00	0.00	0.34	0.00	0.00	0.00	0.00	0.00
Elongate polylobate	0.00	1.54	0.00	0.00	0.00	0.00	0.00	0.00	0.00	0.00	0.00
Epidermal ground-mass	0.00	0.00	0.00	0.00	0.00	0.00	0.00	0.00	0.00	0.00	0.00
Epidermal ground-mass polyhedral	0.00	0.00	11.70	0.00	0.00	0.68	0.00	8.45	0.00	1.79	0.00
Epidermal ground-mass polyhedral elongate	0.00	0.00	0.00	0.00	0.00	0.00	0.00	0.00	0.00	0.00	0.00
Epidermal ground-mass elongate	0.00	0.00	0.58	0.00	0.00	0.00	0.00	1.41	0.00	0.00	0.00
Epidermal ground-mass jigsaw puzzle	0.00	0.00	0.00	0.00	0.00	0.00	0.00	0.00	0.00	0.00	0.00
Epidermal ground-mass sinuate	0.00	0.00	0.00	0.00	0.00	0.00	0.00	0.00	0.00	0.00	0.00
Epidermal ground-mass octogonal	0.00	0.00	0.00	0.00	0.00	0.00	0.00	0.00	0.00	0.00	0.00
Hair cell (trichomes)	0.00	0.00	0.00	0.00	0.00	2.39	0.00	9.86	0.00	0.00	1.28
Hair cell (prickles)	1.08	1.54	2.34	0.97	3.85	1.02	0.67	1.41	3.74	2.68	5.13
Hair aciculate	0.00	0.00	0.00	0.00	0.00	0.00	0.00	0.00	0.00	0.00	0.00
Hair unciform	0.00	0.00	0.00	0.00	0.00	0.00	0.00	0.00	0.00	0.00	0.00
Hair base	0.00	0.00	0.00	0.00	0.00	0.00	0.00	0.00	0.00	0.00	0.00
Hat-shape	0.00	0.00	0.00	0.00	0.00	0.00	0.00	1.41	0.00	0.00	0.00
Indetermined	12.97	3.08	0.58	0.00	1.92	1.37	2.68	0.00	1.40	0.00	3.85
Irregular	8.65	3.08	20.47	8.74	19.23	0.00	1.34	8.45	2.34	1.79	5.13
Irregular facetate	0.00	0.00	0.00	0.00	0.00	0.00	0.00	0.00	0.00	0.00	0.00
Irregular protuberances (fruit eudicot)	0.00	0.00	0.00	0.00	0.00	0.00	0.00	0.00	0.00	0.00	0.00

Irregular verrucate	0.00	0.00	0.00	0.00	0.00	0.00	0.00	0.00	0.00	0.00	0.00
Papillae	0.00	0.00	0.00	0.00	0.00	0.00	0.00	0.00	0.00	0.00	0.00
Parallelepiped blocky	3.24	12.31	0.00	0.00	0.00	1.02	2.68	0.00	0.00	0.00	1.28
Parallelepiped blocky echinate	0.00	0.00	0.00	0.00	0.00	0.00	0.00	0.00	0.00	0.00	0.00
Parallelepiped thin	4.86	0.00	0.58	0.97	0.00	0.00	0.00	0.00	1.40	0.00	0.00
Parenchyma strand	0.00	0.00	0.00	0.00	0.00	0.00	0.00	0.00	0.00	0.00	0.00
Platelet	2.70	0.00	0.00	0.97	0.00	0.00	0.00	1.41	0.00	0.00	0.00
Polyhedral	0.54	0.00	0.00	0.97	0.00	0.00	0.00	0.00	0.00	0.00	0.00
Sclereids	1.08	0.00	1.17	0.00	0.00	0.00	0.00	0.00	0.00	0.89	0.00
Seed sedge	0.00	0.00	0.00	0.00	0.00	0.00	0.00	0.00	0.00	0.00	0.00
GSSC bilobate	1.08	3.08	0.00	2.91	0.00	2.73	4.03	2.82	1.87	0.89	7.69
GSSC cross	0.00	0.00	0.00	0.00	1.92	0.00	0.00	0.00	0.00	0.00	0.00
GSSC polylobate	0.00	0.00	0.00	0.00	0.00	0.00	0.00	0.00	0.47	0.89	0.00
GSSC rondel	38.38	33.85	39.18	34.95	28.85	22.87	30.87	29.58	56.07	46.43	46.15
GSSC rondel wavy top	0.00	0.00	0.00	0.00	0.00	0.00	0.00	0.00	0.00	0.00	0.00
GSSC saddle	0.00	0.00	0.00	0.00	0.00	0.68	1.34	0.00	1.40	0.00	1.28
GSSC long tower	7.03	1.54	5.26	1.94	0.00	1.37	6.04	0.00	2.34	3.57	1.28
GSSC oblong tabular	1.62	6.15	4.09	1.94	0.00	1.37	4.03	1.41	7.48	3.57	5.13
GSSC oblong trapeziform sinuous	0.00	0.00	0.00	0.00	1.92	0.00	0.00	0.00	0.93	0.89	0.00
GSSC tabular round	0.00	0.00	0.00	0.00	0.00	0.00	0.00	0.00	0.00	0.00	0.00
Spheroid echinate	0.00	0.00	0.58	0.00	0.00	0.00	0.00	0.00	0.47	0.00	0.00
Spheroid psilate	0.00	0.00	0.00	0.00	1.92	0.34	10.74	0.00	0.00	0.00	0.00
Semi spheroid	0.00	0.00	0.00	0.00	0.00	0.00	0.00	0.00	0.00	0.00	0.00

Small spheroid	0.00	6.15	0.00	0.97	0.00	0.00	0.00	0.00	0.00	0.89	0.00
Large spheroid	0.00	1.54	0.00	0.00	0.00	0.00	2.68	0.00	0.00	0.00	0.00
Restio morphotypes	0.00	3.08	0.00	7.77	3.85	0.00	0.00	0.00	1.87	0.00	1.28
Spheroid rugulate	3.78	1.54	1.75	5.83	5.77	1.02	2.68	2.82	0.93	0.89	1.28
Stomata	0.00	0.00	0.00	0.00	0.00	0.00	0.67	0.00	0.00	0.00	0.00
Tracheid (vascular tissue)	0.00	1.54	0.00	0.00	0.00	0.34	0.00	1.41	0.00	0.00	0.00
Trapeziform	1.62	0.00	0.00	0.00	1.92	0.00	0.67	0.00	0.00	0.00	0.00

Table A5. continued

	Sample Number	162781	356457	356458	356459	356460	356461	356463	357368	357369	357370	357364
	StratAgg	LBSR	LBSR	LBSR	LBSR	LBSR	LBSR	LBSR	LBSR	LBSR	LBSR	LBSR
Morphotypes	Sample Type	Black layer	Black layer	Black layer	White layer	Black layer	White layer	Black layer	Black layer	Black layer	Black layer	Black layer
Bulliform		5.64	1.02	0.00	0.97	0.56	0.00	0.00	3.70	1.54	0.47	0.00
Blocky Polyhedral		0.00	0.00	0.00	0.00	0.56	0.97	0.00	2.47	0.00	0.47	0.00
Ellipsoid		0.00	0.00	0.00	0.48	0.56	0.97	0.00	0.00	0.00	0.95	0.00
Elongate without decoration margin		13.65	7.65	24.12	13.53	16.20	16.50	0.00	23.46	24.62	18.01	25.44
Elongate blocky		0.00	0.00	0.00	0.00	0.56	0.00	0.00	0.00	0.00	0.00	0.00
Elongate blocky echinate		0.00	0.00	0.00	0.00	0.00	0.00	0.00	0.00	0.00	0.00	0.00
Elongate bulbous		0.00	0.00	0.00	0.00	0.56	0.00	0.00	0.62	0.00	0.47	0.00
Elongate curved		0.00	0.00	0.00	0.00	0.00	0.00	0.00	0.00	0.00	0.47	0.00
Elongate facetate		0.89	0.00	0.00	0.00	0.00	0.00	0.00	4.32	0.00	0.47	0.88
Elongate striate		0.00	0.00	0.00	0.00	0.00	0.00	0.00	0.00	0.00	0.00	0.00
Elongate dendritic		0.00	0.00	0.00	0.00	0.00	0.00	0.00	0.00	0.00	0.00	0.00
Elongate echinate		2.97	0.00	2.94	2.42	1.12	0.97	0.00	9.26	6.15	6.16	2.63

Elongate echinate (one side)	0.00	0.00	1.18	0.00	0.00	0.00	0.00	1.23	0.00	0.00	0.00
Elongate sinuate	0.00	0.00	0.00	0.00	0.00	0.00	0.00	0.00	0.00	0.47	0.00
Elongate polylobate	0.00	0.00	0.00	0.00	0.00	0.00	0.00	0.00	0.00	0.00	0.00
Epidermal ground-mass	0.00	0.00	0.00	0.00	0.00	0.00	16.67	0.00	0.00	0.00	0.00
Epidermal ground-mass polyhedral	0.89	0.00	0.00	0.00	0.00	0.00	4.17	0.62	0.00	0.00	1.75
Epidermal ground-mass polyhedral elongate	0.00	0.00	0.00	0.00	0.00	0.00	0.00	0.00	0.00	0.00	0.00
Epidermal ground-mass elongate	0.00	0.00	0.00	0.00	0.00	0.00	0.00	0.00	0.00	0.00	0.00
Epidermal ground-mass jigsaw puzzle	0.00	0.00	0.00	0.00	0.00	0.00	0.00	0.00	0.00	0.00	0.00
Epidermal ground-mass sinuate	0.00	0.00	0.00	0.00	0.00	0.00	0.00	0.00	0.00	0.00	0.00
Epidermal ground-mass octogonal	0.00	0.00	0.00	0.00	0.00	0.00	0.00	0.00	0.00	0.00	0.00
Hair cell (trichomes)	0.59	1.02	0.59	0.48	0.56	0.00	0.00	0.00	0.51	0.00	1.75
Hair cell (prickles)	2.37	2.04	1.18	0.97	2.79	2.91	4.17	4.32	1.54	2.37	0.00
Hair aciculate	0.00	0.00	0.00	0.00	0.00	0.00	0.00	0.00	0.00	0.00	0.00
Hair unciform	0.00	0.00	0.00	0.00	0.00	0.00	0.00	0.00	0.00	0.00	0.00
Hair base	0.00	0.00	0.00	0.00	0.00	0.00	0.00	0.00	0.00	0.00	0.00
Hat-shape	0.00	0.00	1.76	0.00	0.00	0.00	0.00	0.00	0.00	0.00	0.00
Indetermined	1.48	0.00	0.00	1.93	1.12	0.00	8.33	1.23	0.00	0.00	0.88
Irregular	3.56	0.00	0.00	0.48	0.56	4.85	33.33	0.00	1.54	0.00	6.14
Irregular facetate	0.00	0.00	0.00	0.00	0.00	0.00	0.00	0.00	0.00	0.00	0.00
Irregular protuberances (fruit eudicot)	0.00	0.00	0.00	0.00	0.00	0.00	0.00	0.00	0.00	0.00	0.00

Irregular verrucate	0.00	0.00	0.00	0.00	0.00	0.00	0.00	0.00	0.00	0.00	0.00
Papillae	0.30	0.00	0.00	0.97	0.00	0.00	0.00	0.00	0.00	0.00	0.00
Parallelepiped blocky	0.00	2.04	2.35	0.48	0.00	1.94	0.00	0.00	0.00	0.00	0.00
Parallelepiped blocky echinate	0.00	0.00	0.00	0.00	0.00	0.00	0.00	0.00	0.00	0.00	0.00
Parallelepiped thin	1.48	1.53	0.00	0.00	0.00	0.00	4.17	1.23	1.54	0.00	1.75
Parenchyma strand	0.00	0.00	0.00	0.00	0.00	0.00	0.00	0.00	0.00	0.00	0.00
Platelet	0.00	0.00	0.00	0.00	0.00	0.97	0.00	1.23	1.03	1.90	1.75
Polyhedral	0.00	0.00	0.00	0.48	0.00	0.00	0.00	0.00	0.51	0.47	0.00
Sclereids	0.30	0.00	0.00	0.97	3.35	0.97	0.00	0.00	1.03	0.00	0.00
Seed sedge	0.00	0.00	0.00	0.00	0.00	0.00	0.00	0.00	0.00	0.00	0.00
GSSC bilobate	2.37	0.51	3.53	4.83	1.12	1.94	4.17	1.85	2.05	0.47	3.51
GSSC cross	0.00	0.00	0.00	0.00	0.00	0.00	0.00	0.00	0.00	0.00	0.00
GSSC polylobate	0.30	0.00	0.00	0.00	0.00	0.00	0.00	0.00	0.00	0.00	0.00
GSSC rondel	59.05	77.04	49.41	50.72	60.34	42.72	16.67	27.16	47.18	43.13	28.95
GSSC rondel wavy top	0.00	0.00	0.00	0.00	0.00	0.00	0.00	0.00	0.00	0.00	0.00
GSSC saddle	0.30	0.00	3.53	4.35	0.00	0.00	0.00	0.62	0.00	0.00	0.00
GSSC long tower	0.59	5.61	4.71	6.76	1.68	7.77	0.00	5.56	3.59	6.16	0.88
GSSC oblong tabular	1.78	1.02	1.76	2.42	4.47	8.74	4.17	2.47	1.54	2.84	4.39
GSSC oblong trapeziform sinuous	0.30	0.00	0.00	0.00	1.12	0.00	0.00	0.00	0.00	0.00	0.00
GSSC tabular round	0.00	0.00	0.00	0.00	0.00	1.94	0.00	0.00	0.00	0.00	0.00
Spheroid echinate	0.00	0.00	0.00	0.48	0.00	0.00	0.00	0.00	0.00	0.00	0.00
Spheroid psilate	0.00	0.51	0.00	0.00	0.00	0.00	0.00	0.00	0.00	0.00	0.00
Semi spheroid	0.00	0.00	0.00	0.00	0.00	0.00	0.00	0.00	0.00	0.00	0.00

Small spheroid	0.00	0.00	0.59	0.00	0.00	0.00	0.00	2.47	0.51	10.90	14.91
Large spheroid	0.00	0.00	0.00	0.00	0.00	0.00	0.00	0.00	0.00	0.47	0.00
Restio morphotypes	0.89	0.00	0.59	0.00	0.00	1.94	0.00	0.00	0.00	0.00	0.00
Spheroid rugulate	0.30	0.00	0.59	1.45	2.79	3.88	4.17	5.56	4.10	3.32	4.39
Stomata	0.00	0.00	0.00	0.00	0.00	0.00	0.00	0.00	0.00	0.00	0.00
Tracheid (vascular tissue)	0.00	0.00	0.00	0.00	0.00	0.00	0.00	0.62	0.00	0.00	0.00
Trapeziform	0.00	0.00	1.18	4.83	0.00	0.00	0.00	0.00	1.03	0.00	0.00

Table A5. continued

	Sample Number	357365	357366	356474	356475	356476	356464	356469	356470	356471	357362	357363
	StratAgg	LBSR	LBSR	LBSR	LBSR	LBSR	LBSR	LBSR	LBSR	LBSR	LBSR	LBSR
Morphotypes	Sample Type	Black layer	Black layer	Black layer	Black layer	Black layer	Black layer	Black layer	Black layer	Black layer	Black layer	Black layer
Bulliform		0.00	0.82	7.61	6.25	2.00	2.90	2.68	0.00	0.57	7.41	3.49
Blocky Polyhedral		0.00	0.00	0.00	0.00	0.00	0.00	0.00	0.00	0.00	0.00	0.00
Ellipsoid		0.00	0.00	0.54	0.00	3.00	0.00	0.00	0.00	0.00	2.22	0.00
Elongate without decoration margin		10.20	21.31	14.67	14.06	29.00	15.94	21.43	16.00	13.79	14.81	13.95
Elongate blocky		0.00	1.64	0.00	0.00	1.00	0.00	0.00	2.67	0.00	0.00	0.00
Elongate blocky echinate		0.00	0.00	0.00	0.00	1.00	0.00	0.00	0.00	0.00	0.00	0.00
Elongate bulbous		0.00	0.00	0.00	0.00	0.00	0.00	0.00	1.33	0.00	0.00	0.00
Elongate curved		0.00	0.00	0.00	0.00	0.00	0.00	0.00	0.00	0.00	0.00	0.00
Elongate facetate		0.00	2.46	5.98	0.00	1.00	3.62	0.00	0.00	6.32	10.37	4.65
Elongate striate		0.00	0.00	0.00	0.00	0.00	0.00	0.00	0.00	0.00	0.00	0.00
Elongate dendritic		0.00	0.00	0.00	0.00	0.00	0.00	0.00	0.00	0.00	0.00	0.00
Elongate echinate		24.49	0.82	3.26	1.56	4.00	0.00	0.89	0.00	2.30	4.44	2.33

Elongate echinate (one side)	0.00	0.00	0.54	0.00	0.00	0.00	0.00	0.00	0.00	0.00	0.00
Elongate sinuate	0.00	0.82	0.00	1.56	1.00	0.00	0.00	0.00	0.00	0.74	2.33
Elongate polylobate	0.00	0.00	0.00	0.00	0.00	0.00	0.00	1.33	0.00	0.00	0.00
Epidermal ground-mass	10.20	0.82	0.00	0.00	0.00	0.00	0.00	0.00	1.72	0.74	3.49
Epidermal ground-mass polyhedral	0.00	0.82	0.54	0.00	0.00	0.00	0.00	0.00	0.57	0.00	1.16
Epidermal ground-mass polyhedral elongate	0.00	0.00	0.00	0.00	0.00	0.00	0.00	0.00	0.00	0.00	0.00
Epidermal ground-mass elongate	6.12	0.00	0.00	0.00	0.00	0.00	0.00	0.00	0.00	0.00	0.00
Epidermal ground-mass jigsaw puzzle	0.00	0.00	0.00	0.00	0.00	0.00	0.00	0.00	0.00	0.00	0.00
Epidermal ground-mass sinuate	0.00	0.00	0.00	0.00	0.00	0.00	0.00	0.00	0.00	0.00	0.00
Epidermal ground-mass octogonal	0.00	0.00	0.00	0.00	0.00	0.00	0.00	0.00	0.00	0.00	0.00
Hair cell (trichomes)	2.04	0.00	1.09	0.00	0.00	2.90	0.00	1.33	0.00	0.00	3.49
Hair cell (prickles)	0.00	4.10	3.26	4.69	4.00	2.90	4.46	2.67	2.30	2.96	3.49
Hair aciculate	0.00	0.00	0.00	0.00	0.00	0.00	0.00	0.00	0.00	0.00	0.00
Hair unciform	0.00	0.00	0.54	0.00	0.00	0.00	0.00	0.00	0.00	0.74	0.00
Hair base	0.00	0.00	0.54	0.00	0.00	0.00	0.00	0.00	0.00	0.00	0.00
Hat-shape	0.00	0.00	0.54	0.00	0.00	0.72	0.00	0.00	0.00	0.00	0.00
Indetermined	0.00	0.82	3.80	0.00	4.00	3.62	1.79	0.00	1.72	2.96	1.16
Irregular	6.12	6.56	1.63	10.94	1.00	2.90	0.89	0.00	1.15	11.85	3.49
Irregular facetate	0.00	0.00	0.00	0.00	0.00	0.00	0.00	0.00	0.00	0.00	0.00
Irregular protuberances (fruit eudicot)	0.00	0.82	0.54	0.00	0.00	0.72	0.00	0.00	0.00	0.00	0.00

Irregular verrucate	0.00	0.00	0.00	0.00	0.00	0.00	0.00	0.00	0.00	0.00	0.00
Papillae	0.00	0.00	0.00	0.00	0.00	0.00	0.00	0.00	0.00	0.00	0.00
Parallelepiped blocky	2.04	0.82	2.72	0.00	3.00	4.35	8.04	2.67	1.15	1.48	3.49
Parallelepiped blocky echinate	0.00	0.00	0.00	0.00	0.00	0.00	0.00	0.00	0.00	0.00	0.00
Parallelepiped thin	0.00	0.00	0.54	0.00	0.00	0.00	6.25	2.67	1.15	3.70	1.16
Parenchyma strand	0.00	0.00	0.00	0.00	0.00	0.00	0.00	0.00	0.00	0.00	0.00
Platelet	0.00	0.82	2.17	1.56	0.00	0.00	1.79	0.00	0.00	0.00	1.16
Polyhedral	0.00	0.00	1.63	0.00	2.00	0.00	0.00	0.00	1.15	0.00	0.00
Sclereids	2.04	0.00	0.00	0.00	0.00	0.00	0.00	0.00	0.57	0.74	1.16
Seed sedge	0.00	0.00	0.00	0.00	0.00	0.00	0.00	0.00	0.00	0.00	0.00
GSSC bilobate	4.08	4.10	5.43	3.13	11.00	4.35	2.68	0.00	2.30	2.22	2.33
GSSC cross	0.00	0.00	0.54	0.00	0.00	0.00	0.00	0.00	0.00	0.00	0.00
GSSC polylobate	0.00	0.00	0.00	0.00	0.00	0.00	0.00	0.00	0.00	0.00	0.00
GSSC rondel	26.53	35.25	25.00	42.19	22.00	39.13	25.89	53.33	47.70	15.56	26.74
GSSC rondel wavy top	0.00	0.00	0.00	0.00	0.00	0.00	0.00	0.00	0.00	0.00	0.00
GSSC saddle	0.00	0.82	3.80	3.13	2.00	0.72	2.68	0.00	0.00	2.22	3.49
GSSC long tower	0.00	0.82	0.00	0.00	1.00	5.80	4.46	4.00	6.90	2.22	1.16
GSSC oblong tabular	0.00	2.46	4.35	9.38	1.00	1.45	7.14	6.67	4.02	2.96	9.30
GSSC oblong trapeziform sinuous	0.00	0.82	0.00	0.00	1.00	0.00	0.00	0.00	0.57	0.00	0.00
GSSC tabular round	0.00	0.00	0.00	0.00	0.00	0.00	0.00	0.00	0.00	0.00	0.00
Spheroid echinate	0.00	0.00	0.00	0.00	0.00	0.00	0.00	0.00	0.00	0.00	0.00
Spheroid psilate	0.00	0.82	1.09	0.00	0.00	0.00	0.00	0.00	0.00	0.00	0.00
Semi spheroid	0.00	0.00	0.00	0.00	0.00	0.00	0.00	0.00	0.00	0.00	0.00

Small spheroid	0.00	0.00	0.00	0.00	0.00	0.00	0.00	0.00	0.00	0.00	0.00
Large spheroid	0.00	0.00	0.00	0.00	0.00	0.00	0.00	0.00	0.00	0.00	0.00
Restio morphotypes	0.00	0.00	3.80	0.00	3.00	2.90	4.46	2.67	2.87	3.70	4.65
Spheroid rugulate	4.08	7.38	3.80	1.56	2.00	5.07	4.46	2.67	1.15	5.93	1.16
Stomata	0.00	0.00	0.00	0.00	0.00	0.00	0.00	0.00	0.00	0.00	0.00
Tracheid (vascular tissue)	0.00	0.00	0.00	0.00	1.00	0.00	0.00	0.00	0.00	0.00	1.16
Trapeziform	2.04	4.10	0.00	0.00	0.00	0.00	0.00	0.00	0.00	0.00	0.00

Table A5. continued

	Sample Number	162548	162549	162550	162557	162558	162492	162493	162494	356478	356479	162710
	StratAgg	LBSR	LBSR	LBSR	LBSR	LBSR	LBSR	LBSR	LBSR	YBSR	YBSR	YBSR
Morphotypes	Sample Type	Black layer	White layer	Black layer	Black layer	Red layer	Black layer	White layer	Black layer	Red layer	White layer	White layer
Bulliform		0.00	10.87	4.69	0.00	11.25	4.60	3.57	19.23	1.14	0.00	2.63
Blocky Polyhedral		2.94	0.00	3.91	6.06	0.00	0.00	3.57	0.00	1.14	0.00	0.00
Ellipsoid		0.00	0.00	0.78	0.00	1.25	0.00	1.19	0.00	0.00	3.77	0.00
Elongate without decoration margin		20.59	15.22	25.78	19.19	26.25	10.34	34.52	15.38	27.27	19.81	7.89
Elongate blocky		0.00	0.00	0.78	3.03	2.50	0.00	0.00	0.00	1.14	0.00	0.00
Elongate blocky echinate		0.00	0.00	0.00	0.00	0.00	0.00	0.00	0.00	0.00	0.00	0.00
Elongate bulbous		0.00	0.00	0.00	0.00	0.00	0.00	0.00	0.00	0.00	0.00	0.00
Elongate curved		0.00	0.00	0.78	0.00	0.00	0.00	0.00	0.00	0.00	0.00	0.00
Elongate facetate		2.94	0.00	0.78	1.01	3.75	0.00	0.00	1.92	1.14	0.94	5.26
Elongate striate		0.00	0.00	0.00	0.00	0.00	0.00	0.00	0.00	0.00	0.00	0.00
Elongate dendritic		0.00	0.00	0.00	2.02	0.00	0.00	0.00	0.00	0.00	0.00	0.00
Elongate echinate		5.88	2.17	0.78	2.02	0.00	3.45	0.00	1.92	2.27	2.83	0.00

Elongate echinate (one side)	0.00	0.00	0.00	0.00	0.00	0.00	0.00	0.00	0.00	0.00	0.00
Elongate sinuate	0.00	0.00	4.69	0.00	0.00	0.00	0.00	0.00	0.00	0.00	0.00
Elongate polylobate	0.00	0.00	0.00	0.00	0.00	0.00	0.00	0.00	0.00	0.00	0.00
Epidermal ground-mass	0.00	6.52	0.00	0.00	3.75	12.64	0.00	1.92	0.00	0.00	0.00
Epidermal ground-mass polyhedral	0.00	2.17	0.78	0.00	1.25	1.15	0.00	0.00	0.00	0.00	0.00
Epidermal ground-mass polyhedral elongate	0.00	0.00	0.00	0.00	0.00	0.00	0.00	0.00	0.00	0.00	0.00
Epidermal ground-mass elongate	0.00	0.00	0.00	0.00	0.00	0.00	0.00	0.00	0.00	0.00	0.00
Epidermal ground-mass jigsaw puzzle	0.00	0.00	0.00	0.00	0.00	0.00	0.00	0.00	0.00	0.00	0.00
Epidermal ground-mass sinuate	0.00	2.17	0.00	0.00	0.00	1.15	0.00	0.00	0.00	0.00	0.00
Epidermal ground-mass octogonal	0.00	0.00	0.00	0.00	0.00	0.00	0.00	0.00	0.00	0.00	0.00
Hair cell (trichomes)	5.88	0.00	2.34	2.02	0.00	0.00	1.19	0.00	1.14	0.00	0.00
Hair cell (prickles)	0.00	6.52	4.69	2.02	1.25	1.15	5.95	9.62	4.55	1.89	2.63
Hair aciculate	0.00	0.00	0.00	0.00	0.00	0.00	0.00	0.00	0.00	0.00	0.00
Hair unciform	0.00	0.00	0.00	0.00	0.00	0.00	0.00	0.00	0.00	0.00	0.00
Hair base	0.00	0.00	0.00	0.00	0.00	0.00	0.00	0.00	0.00	0.00	0.00
Hat-shape	0.00	0.00	0.00	0.00	0.00	0.00	0.00	0.00	1.14	0.00	0.00
Indetermined	2.94	15.22	1.56	0.00	2.50	5.75	2.38	5.77	0.00	0.00	0.00
Irregular	17.65	4.35	4.69	2.02	2.50	2.30	0.00	19.23	7.95	8.49	2.63
Irregular facetate	0.00	0.00	0.00	0.00	0.00	0.00	0.00	0.00	0.00	0.00	0.00
Irregular protuberances (fruit eudicot)	0.00	0.00	0.00	0.00	1.25	0.00	0.00	0.00	0.00	0.00	0.00

Irregular verrucate	0.00	0.00	0.78	0.00	0.00	0.00	0.00	0.00	0.00	0.00	0.00
Papillae	0.00	0.00	0.00	0.00	0.00	0.00	0.00	0.00	0.00	0.00	0.00
Parallelepiped blocky	0.00	0.00	4.69	2.02	0.00	2.30	1.19	0.00	5.68	0.00	0.00
Parallelepiped blocky echinate	0.00	0.00	0.00	0.00	0.00	0.00	0.00	0.00	0.00	0.00	0.00
Parallelepiped thin	0.00	0.00	0.00	1.01	0.00	0.00	0.00	0.00	1.14	0.00	3.95
Parenchyma strand	0.00	0.00	0.00	0.00	0.00	0.00	0.00	0.00	0.00	0.00	0.00
Platelet	0.00	4.35	0.00	1.01	3.75	1.15	2.38	0.00	2.27	4.72	0.00
Polyhedral	0.00	0.00	2.34	0.00	2.50	1.15	0.00	1.92	0.00	0.00	1.32
Sclereids	0.00	0.00	0.78	0.00	0.00	0.00	0.00	1.92	0.00	0.00	0.00
Seed sedge	0.00	0.00	0.00	0.00	1.25	0.00	0.00	0.00	0.00	0.00	0.00
GSSC bilobate	5.88	4.35	1.56	7.07	7.50	2.30	5.95	0.00	3.41	7.55	3.95
GSSC cross	0.00	0.00	0.00	0.00	0.00	0.00	0.00	0.00	0.00	0.00	0.00
GSSC polylobate	0.00	0.00	0.00	0.00	0.00	0.00	0.00	0.00	0.00	0.00	0.00
GSSC rondel	14.71	15.22	19.53	27.27	15.00	32.18	21.43	13.46	12.50	16.98	30.26
GSSC rondel wavy top	0.00	0.00	0.00	0.00	0.00	0.00	0.00	0.00	0.00	0.00	0.00
GSSC saddle	2.94	0.00	0.78	0.00	0.00	3.45	0.00	1.92	0.00	0.94	0.00
GSSC long tower	0.00	2.17	0.78	0.00	0.00	1.15	2.38	0.00	1.14	1.89	26.32
GSSC oblong tabular	8.82	2.17	0.78	1.01	0.00	6.90	3.57	1.92	0.00	2.83	5.26
GSSC oblong trapeziform sinuous	0.00	0.00	0.00	0.00	0.00	0.00	0.00	0.00	0.00	0.00	0.00
GSSC tabular round	0.00	0.00	0.00	0.00	1.25	0.00	0.00	0.00	0.00	0.00	0.00
Spheroid echinate	0.00	0.00	0.00	0.00	0.00	0.00	0.00	0.00	0.00	0.00	0.00
Spheroid psilate	0.00	0.00	0.00	0.00	1.25	1.15	0.00	0.00	0.00	6.60	0.00
Semi spheroid	0.00	0.00	0.00	0.00	0.00	0.00	0.00	0.00	0.00	0.00	0.00

Small spheroid	0.00	0.00	0.00	2.02	0.00	0.00	1.19	0.00	3.41	0.00	0.00
Large spheroid	0.00	0.00	0.00	1.01	2.50	0.00	0.00	0.00	1.14	2.83	0.00
Restio morphotypes	2.94	2.17	5.47	3.03	2.50	1.15	8.33	0.00	10.23	6.60	5.26
Spheroid rugulate	5.88	4.35	5.47	11.11	3.75	2.30	1.19	3.85	9.09	10.38	2.63
Stomata	0.00	0.00	0.00	0.00	0.00	0.00	0.00	0.00	0.00	0.00	0.00
Tracheid (vascular tissue)	0.00	0.00	0.00	1.01	1.25	2.30	0.00	0.00	0.00	0.00	0.00
Trapeziform	0.00	0.00	0.00	3.03	0.00	0.00	0.00	0.00	1.14	0.94	0.00

Table A5. continued

	Sample Number	356414	356417	388615	388613	388614	388612	388588	162783
	Strat-Agg	YBSR	YBSR	YBSR	YBSR	YBSR	YBSR	YBSR	YBSR
Morphotypes	Sample Type	Red layer	Grey color	Black layer	Black layer	Black layer	Black layer	Black layer	Red layer
Bulliform									
Blocky Polyhedral		0.99	0.00	7.55	4.17	2.44	0.81	6.52	0.95
Ellipsoid		1.98	0.00	0.00	4.17	0.00	0.00	2.17	4.76
Elongate without decoration margin		0.99	0.00	0.00	0.00	0.00	0.00	0.00	0.00
Elongate blocky		15.84	28.00	20.75	29.17	8.54	8.94	19.57	19.05
Elongate blocky echinate		0.00	0.00	0.00	0.00	0.00	0.00	0.00	0.00
Elongate bulbous		0.00	0.00	0.00	0.00	0.00	0.00	0.00	0.00
Elongate curved		0.00	0.00	0.00	0.00	0.00	0.00	0.00	0.00
Elongate facetate		1.98	0.00	0.00	0.00	0.00	0.00	0.00	0.00
Elongate striate		3.96	2.00	0.00	0.00	4.88	3.25	2.17	0.00
Elongate dendritic		0.00	0.00	0.00	0.00	0.00	0.00	0.00	0.00
Elongate echinate		0.00	0.00	0.00	0.00	0.00	0.00	0.00	0.00
Elongate echinate (one side)		0.00	0.00	0.00	0.00	0.00	0.00	0.00	1.90
Elongate sinuate		0.00	0.00	0.00	0.00	0.00	0.00	0.00	0.00

Elongate polylobate	0.99	0.00	0.00	0.00	6.10	0.00	0.00	0.00
Epidermal ground-mass	0.00	0.00	0.00	0.00	0.00	0.00	0.00	0.00
Epidermal ground-mass polyhedral	1.98	6.00	3.77	2.08	41.46	5.69	4.35	0.00
Epidermal ground-mass polyhedral elongate	0.00	0.00	0.00	0.00	0.00	3.25	0.00	0.00
Epidermal ground-mass elongate	0.00	0.00	0.00	0.00	1.22	0.00	0.00	0.00
Epidermal ground-mass jigsaw puzzle	0.00	0.00	0.00	0.00	0.00	0.00	0.00	0.00
Epidermal ground-mass sinuate	0.00	0.00	0.00	0.00	1.22	0.00	0.00	0.00
Epidermal ground-mass octogonal	0.00	0.00	0.00	0.00	0.00	0.00	0.00	0.00
Hair cell (trichomes)	0.00	0.00	0.00	0.00	0.00	0.00	0.00	0.00
Hair cell (prickles)	0.99	0.00	1.89	4.17	7.32	0.00	4.35	0.00
Hair aciculate	0.00	6.00	1.89	0.00	1.22	0.81	0.00	7.62
Hair unciform	0.00	0.00	0.00	0.00	0.00	0.00	0.00	0.00
Hair base	0.00	0.00	0.00	0.00	0.00	0.00	0.00	0.00
Hat-shape	0.00	0.00	0.00	0.00	0.00	0.00	0.00	0.00
Indetermined	0.00	0.00	0.00	2.08	0.00	1.63	0.00	0.00
Irregular	0.00	0.00	0.00	0.00	1.22	0.00	0.00	0.00
Irregular facetate	0.00	0.00	0.00	0.00	4.88	0.00	4.35	1.90
Irregular protuberances (fruit eudicot)	0.00	0.00	0.00	2.08	0.00	0.00	0.00	0.00
Irregular verrucate	0.00	0.00	0.00	2.08	0.00	0.00	0.00	0.00
Papillae	0.00	0.00	0.00	0.00	0.00	0.00	0.00	0.00
Parallelepiped blocky	0.00	0.00	1.89	0.00	0.00	0.00	0.00	0.00
Parallelepiped blocky echinate	0.00	4.00	0.00	2.08	0.00	0.81	0.00	1.90
Parallelepiped thin	0.00	0.00	0.00	0.00	0.00	0.00	0.00	0.00
Parenchyma strand	1.98	4.00	0.00	0.00	0.00	0.00	0.00	0.00

Platelet	0.00	0.00	0.00	0.00	8.54	0.00	2.17	0.00
Polyhedral	0.00	0.00	0.00	2.08	0.00	1.63	2.17	0.00
Sclereids	1.98	0.00	1.89	0.00	0.00	0.00	0.00	0.00
Seed sedge	0.99	0.00	0.00	0.00	0.00	0.00	0.00	0.00
GSSC bilobate	0.00	0.00	0.00	0.00	0.00	0.00	0.00	0.00
GSSC cross	6.93	6.00	7.55	0.00	0.00	0.81	4.35	4.76
GSSC polylobate	0.00	0.00	0.00	0.00	0.00	0.00	0.00	0.00
GSSC rondel	0.00	0.00	0.00	0.00	0.00	0.00	0.00	0.00
GSSC rondel wavy top	37.62	30.00	41.51	12.50	8.54	65.85	23.91	40.00
GSSC saddle	2.97	0.00	0.00	0.00	0.00	0.00	0.00	0.00
GSSC long tower	1.98	0.00	1.89	0.00	0.00	0.00	2.17	0.95
GSSC oblong tabular	0.99	0.00	0.00	2.08	0.00	0.00	2.17	0.00
GSSC oblong trapeziform sinuous	7.92	0.00	1.89	2.08	0.00	0.81	2.17	5.71
GSSC tabular round	0.00	0.00	1.89	2.08	0.00	0.00	0.00	0.95
Spheroid echinate	0.00	0.00	0.00	0.00	0.00	0.00	0.00	0.00
Spheroid psilate	0.00	0.00	0.00	0.00	0.00	0.00	0.00	0.00
Semi spheroid	0.00	0.00	0.00	0.00	0.00	1.63	0.00	0.00
Small spheroid	0.00	0.00	0.00	0.00	0.00	0.00	0.00	0.00
Large spheroid	0.00	0.00	0.00	0.00	0.00	0.00	0.00	0.00
Restio morphotypes	0.00	0.00	0.00	0.00	0.00	0.00	0.00	6.67
Spheroid rugulate	2.97	8.00	0.00	4.17	0.00	3.25	10.87	0.00
Stomata	2.97	6.00	0.00	14.58	2.44	0.81	4.35	2.86
Tracheid (vascular tissue)	0.00	0.00	0.00	0.00	0.00	0.00	0.00	0.00
Trapeziform	0.99	0.00	0.00	0.00	0.00	0.00	2.17	0.00